Electronic Supplementary Information

Fluorescent Organo-Antimony Compounds as Precursors for Syntheses of Redox-Active Trimeric and Dimeric Alkali Metal Antimonides: An Insight into Electron Transfer Reduction Processes

Ekta Nag, [a] Aditya Kulkarni, [a] Sai Manoj N. V. T. Gorantla, [b] Nico Graw, [c] Maria Francis, [a] Regine Herbst-Irmer, [c] Dietmar Stalke,*[c] Herbert W. Roesky, *[c] Kartik Chandra Mondal *[b] and Sudipta Roy *[a]

[a]Department of Chemistry, Indian Institute of Science Education and Research (IISER), Tirupati 517507, India. Email: roy.sudipta@iisertiruapti.ac.in

[b]Department of Chemistry, Indian Institute of Technology Madras, Chennai 600036, India. Email: csdkartik@iitm.ac.in

[c]Institut für Anorganische Chemie, Georg-August-Universität, Tammannstraβe 4, 37077-Göttingen, Germany. Email: dstalke@chemie.uni-goettingen; hroesky@gwdg.de

Contents:

S1. General Remarks

All manipulations were carried out using standard Schlenk line techniques under inert argon atmosphere or in an argon-filled MBraun Eco Plus glove box, where O_2 and H_2O levels were kept below 0.1 ppm at all times. Solvents obtained from MBraun Solvent Purification System were further dried by refluxing with Na/K alloy for two days, followed by distillation and collection over 4 Å molecular sieves. All deuterated solvents, e.g., C_6D_6 and THF-D_8 were purchased from Sigma-Aldrich and further purified by stirring over Na/K alloy for two days, followed by 6 h of reflux and vacuum distillation under argon atmosphere. ^{1}H, ^{13}C, ^{7}Li, ^{31}P and ^{1}H-^{15}N HMBC NMR spectra were recorded on Bruker Avance 500 MHz and Bruker Neo Avance 400 MHz NMR spectrometers. Elemental analysis for the new compounds were not reported because of their very high air and moisture sensitive nature. However, EI-MS spectra were obtained with a Finnigan MAT 8230 or a Varian MAT CH5 instrument (70 eV) by EI-MS methods. HRMS data were recorded for the majority of the reported compounds by isolating the pure crystals. Melting points were measured in sealed glass tubes on a Büchi B-540 melting point apparatus. Cyclic voltammetry studies were performed on a Metrohm Multi-Autolab PGSTAT204.

S2. Detailed syntheses of 1, 4, 6 and 14-21

S2.1. Synthesis of TipMgBr:

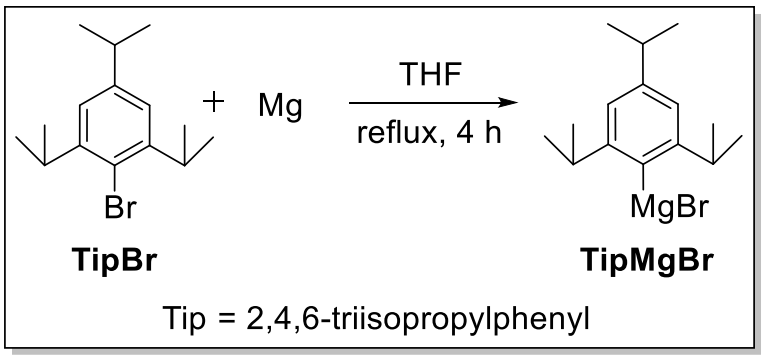

Scheme S1: Synthesis of TipMgBr.

TipBr (40 mmol, 10.13 mL) was added into a 100 mL Schlenk flask containing 1.4 equivalents of freshly activated Mg metal (1.35 g, 56 mmol). To this 50 mL of anhydrous THF was added. The resulting mixture was then refluxed for 3 h to obtain

a pale yellow solution of TipMgBr which was then allowed to cool to room temperature (rt) and directly used for the subsequent reactions without further characterization.

S2.2. Synthesis of $(Tip)_2SbCl$ (1):

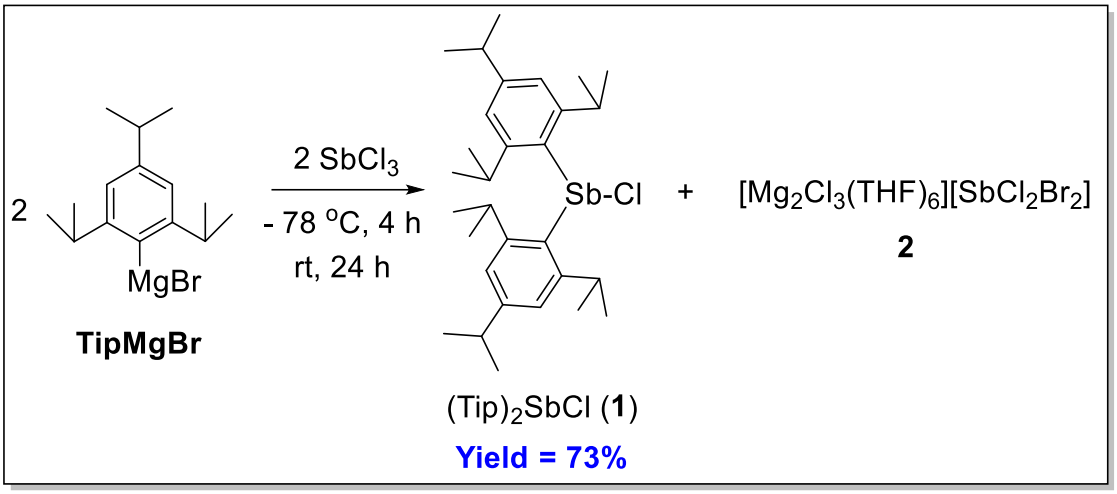

Scheme S2: Synthesis of $(Tip)_2SbCl$ (**1**). One equivalent of $SbCl_3$ was utilized for the formation of **1** and the other equivalent was utilized for the formation of **2**.

The colorless crystals of $SbCl_3$ (9.12 g, 40 mmol) were dissolved in diethyl ether (100 mL) and cooled to -78 °C by using an isopropanol bath. To this, THF solution of TipMgBr (12.3 g, 40 mmol) was added through a cannula. The temperature of the solution was slowly raised to -30 °C over 2-3 h to obtain a pale yellow solution with the formation of a dense colorless precipitate. The reaction mixture was then slowly brought to rt over 1 h and allowed to stir for 24 h. The colorless precipitate of $[Mg_2Cl_3(THF)_6][SbCl_2Br_2]$ (**2**) was then filtered, and the filtrate was evaporated close to dryness (2-3 mL) under high vacuum to obtain a mixture of $(Tip)_2SbCl$ (**1**) and $[Mg_2Cl_3(THF)_6][SbCl_2Br_2]$ (**2**). Complex **2** is a highly crystalline solid due to the ionic character, while compound **1** is a pale yellow, low melting solid. Compound **1** was separated by extracting in toluene (70 mL). The pale yellow, rod-shaped crystals of **1** were obtained from the concentrated toluene solution at rt in 73% yield (8.23 g, based on the equation given in Scheme 2). The crystals of **1** were found to be stable at rt under inert atmosphere for more than a year and highly soluble in organic solvents (e.g., THF, toluene, *n*-hexane).

Complex **2** $[Mg_2Cl_3(THF)_6][SbCl_2Br_2]$ was separated as highly crystalline white powder which was insoluble in toluene. The yield of **2** was 97% (18.2 g, based on the equation given in Scheme 2). **2** was crystallized from a 1:1 volume mixture of THF and diethyl ether at rt as colourless blocks. The crystals of **2** were moderately soluble in THF but only partially soluble in the mixture of THF and diethyl ether.

Both **1** and **2** were characterized by X-ray single crystal diffraction. Compound **1** underwent dissociation under ESI mass ionisation and $(Tip)_2Sb^+$ cation was characterized by the ESI mass spectrometry.

Compound **1** [$(Tip)_2SbCl$]: **MP:** 104-105 ^oC

^{1}H NMR (300 MHz, THF-D_8, 298 K) δ: 7.04 (s, 4H, Ar*H*), 3.35 (p, *J* = 6.6 Hz, 4H, *o*-C*H*Me_2), 2.83 (p, *J* = 6.9 Hz, 2H, *p*-C*H*Me_2), 1.18 (d, *J* = 6.9 Hz, 12H, *p*-CH*Me*$_2$), 1.06 (d, *J* = 1.8 Hz, 12H, *o*-CH*Me*$_2$), 1.03 (d, *J* = 1.8 Hz, 12H, *o*-CH*Me*$_2$) ppm.

^{13}C NMR (75 MHz, THF-D_8, 298 K) δ: 152.0, 148.5, 140.3, 120.8, 33.5, 32.3, 22.4, 21.6, 21.6, 21.3 ppm.

EI-MS for $[C_{30}H_{46}Sb]^+$, m/z (%): predicted 527.2632 (100%); obtained 527.2627 (100%).

S2.3. Synthesis of $(Tip)_2Sb$-$Sb(Tip)_2$ (4):

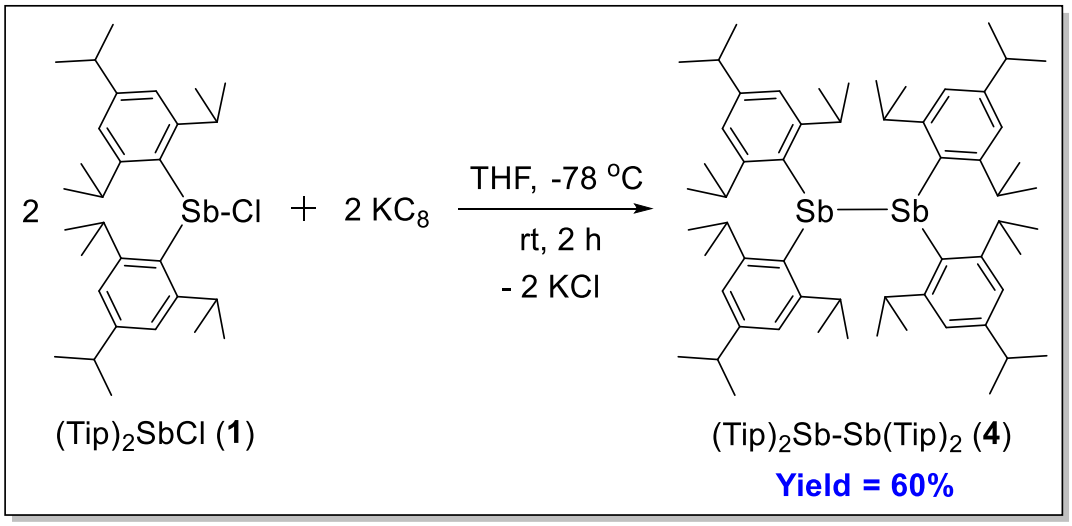

Scheme S3: Synthesis of $(Tip)_2Sb$-$Sb(Tip)_2$ (**4**).

A 1:1 molar mixture of $(Tip)_2SbCl$ (**1**) (564 mg, 1 mmol) and KC_8 (135 mg, 1 mmol) were taken in a 100 mL Schlenk flask and precooled (-78 ^oC) THF (20 mL) was added through a cannula. The temperature of the reaction mixture was then slowly raised to rt over 30 min and then allowed to stir for another 2 h to obtain a yellow solution of Tip_4Sb_2. The reaction mixture was then filtered to remove graphite and the filtrate was concentrated under vacuum. Compound **4** was extracted in *n*-hexane (30 mL). The light yellow, rod-shaped crystals of compound **4** were obtained from the concentrated *n*-hexane solution, kept at -32 ^0C freezer in 60% yield after a week. The crystals of compound **4** were found to be stable at rt under an inert atmosphere for more than a year.

Compound **4** $[(Tip)_2Sb\text{-}Sb(Tip)_2]$: **MP:** 95-96 ^oC

^{1}H NMR (400 MHz, C_6D_6, 298 K) *δ*: 7.06 (d, 8H, -Ar*H*), 3.66-3.60 (m, 8H, -C*H*$(CH_3)_2$), 2.71 (p, *J* = 6.9 Hz, 4H, -C*H*$(CH_3)_2$), 1.25-0.87 (m, 72H, -CH(C*H*$_3)_2$) ppm.

^{13}C NMR (101 MHz, C_6D_6, 298 K) *δ*: 153.7, 153.3, 148.1, 122.0, 121.9, 121.2, 66.6, 34.8, 33.2, 28.9, 24.6, 24.0, 23.0, 23.0, 22.9, 22.8 ppm.

EI-MS for $[C_{60}H_{92}Sb_2]^{+1}$, observed m/z [predicted] (%): 1056.5269 [1056.5282] (100%).

EI-MS for $[C_{60}H_{92}Sb_2]^{+2}$, observed m/z [predicted] (%): 527.2623 [527.2632] (100%).

S2.4. Synthesis of $[K_3((Tip)_2Sb)_3(THF)_5]$ (6):

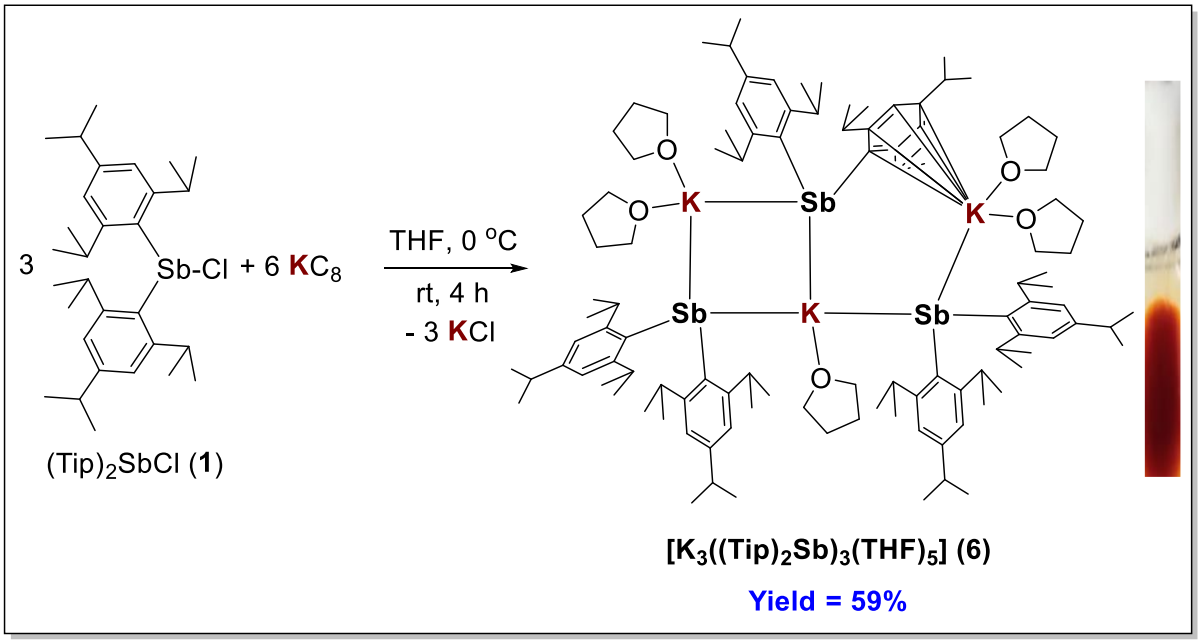

Scheme S4: Synthesis of $[K_3(THF)_5((Tip)_2Sb)_3]$ (**6**).

Method 1: A 1:2 molar mixture of $(Tip)_2SbCl$ (**1**) (1.128 g, 2 mmol) and KC_8 (540 mg, 4 mmol) was taken in a 100 mL Schlenk flask and precooled (at around 10 °C) THF (45 mL) was added through a cannula. The temperature of the reaction mixture was then slowly raised to rt over 10-15 min to obtain an initial dark green solution. The reaction mixture was then stirred for another 2.5 h to obtain a dark red solution which was filtered to remove graphite. THF was removed under vacuum to obtain a dark red solid, which was then extracted with toluene (60 mL). The bright red, rod-shaped crystals of $[K_3((Tip)_2Sb)_3(THF)_5]$ (**6**) were obtained in 59% yield (based on the equation given in Scheme 4) after a week from the concentrated toluene solution kept at -32 °C freezer. **6** was found to decompose to a black solid at 130 °C.

Method 2: To a pale yellow solution of $(Tip)_2SbCl$ (**1**) (564 mg, 1 mmol) in THF (20 mL), freshly prepared K-Naphthalenide ($KC_{10}H_8$) solution (2.1 mmol in 5 mL THF) was added at rt leading to the formation of an immediate dark red color. The reaction mixture was then stirred for 1 h. Afterwards, THF was evaporated under vacuum to produce a dark red crystalline solid which was then extracted with toluene and filtered. The dark red filtrate was concentrated up to 2 ml to obtain the bright red, rod-shaped crystals of complex **6** from -40 °C freezer with an improved yield of 70%.

^{1}H NMR (300 MHz, C_6D_6, 298 K) *δ*: 7.11 (s, 10H, Ar*H*), 7.09 (s, 2H, Ar*H*), 4.32 (quintet, *J* = 6.7 Hz, 12H, *o*-C*H*Me$_2$), 3.50-3.40 (m, 16H), 2.93-2.83 (m, 6H), 1.42-1.34 (m, 16H), 1.30 (s, 18H), 1.27 (d, *J* = 3.1 Hz, 36H), 1.25 (s, 3H), 1.24 (s, 24H), 1.23 (s, 3H), 1.22 (s, 3H), 1.19 (s, 3H), 1.13 (dd, *J* = 10.6, 6.7 Hz, 18H) ppm.

^{13}C NMR (300 MHz, C_6D_6, 298 K) *δ*: 155.1, 154.6, 149.6, 148.9, 146.3, 142.1, 134.3, 122.2, 121.7, 120.1, 67.6, 40.8, 38.3, 37.9, 34.6, 34.4, 34.4, 34.2, 31.7, 25.5, 25.3, 24.5, 24.5, 24.2, 24.1, 24.0, 14.1 ppm.

S2.5. Synthesis of $[Li_2((Tip)_2Sb)_2(THF)_4]$ (14):

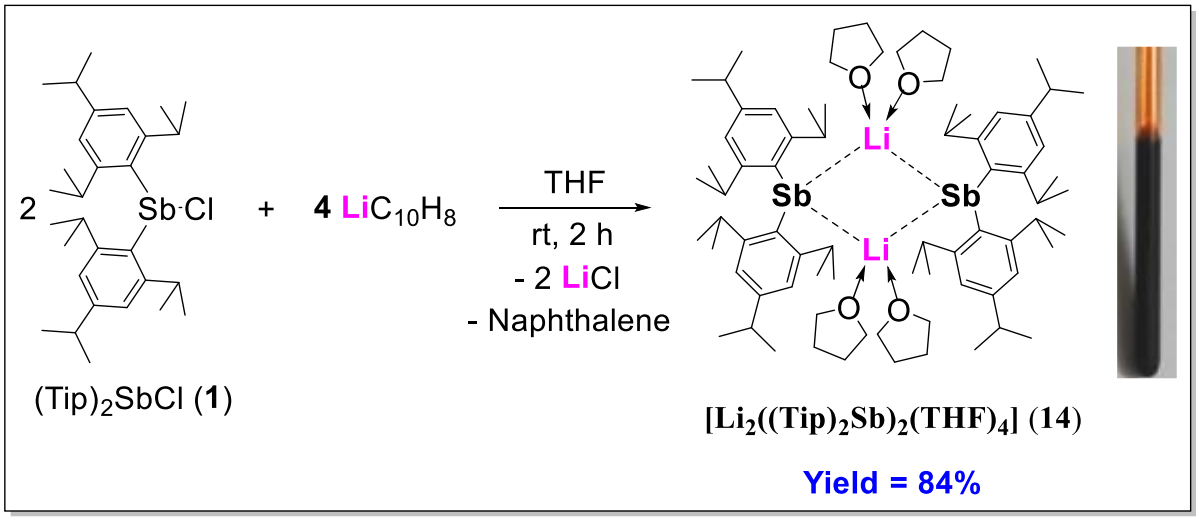

Scheme S5: Synthesis of $[Li_2((Tip)_2Sb)_2(THF)_4]$ (**14**).

To a pale yellow THF solution (20 mL) of $(Tip)_2SbCl$ (**1**) (564 mg, 1 mmol), freshly prepared $LiC_{10}H_8$ (2.1 mmol) solution was added at rt leading to the formation of an immediate dark red color. The reaction mixture was then stirred for 1 h. Afterwards, THF was evaporated under vacuum to produce a dark red crystalline solid which was then extracted with toluene and filtered. The dark red filtrate was concentrated upto 1 ml to obtain the bright red, block-shaped crystals of complex **14** at rt in 84% yield.

^{1}H NMR (400 MHz, THF-D_8, 298 K) *δ*: 6.69 (s, 8H), 4.51 (septet *J* = 6.9 Hz, 8H), 2.75 (septet, *J* = 6.9 Hz, 4H), 1.21 (d, *J* = 6.9 Hz, 24H), 0.96 (d, *J* = 6.9 Hz, 48H) ppm.

^{13}C NMR (101 MHz, THF-D_8, 298 K) δ: 154.6, 147.2, 142.8, 117.9, 40.3, 34.2, 24.3, 24.0, 23.6 ppm (Naphthalene peaks at 133.6, 127.6, 124.5 ppm).

^{7}Li NMR (156 MHz, THF-D_8, 298 K) δ: 0.30 ppm.

S2.6. Synthesis of $[Na_2((Tip)_2Sb)_2(THF)_2(tol)_2]\cdot Tol$ (15) and observed solvatochromism:

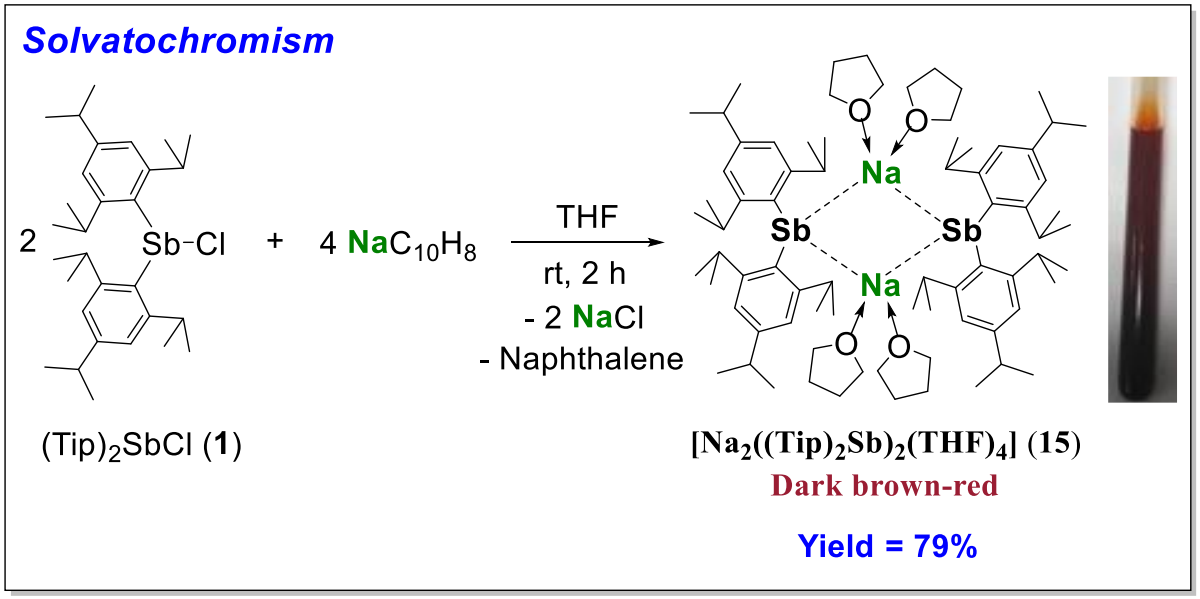

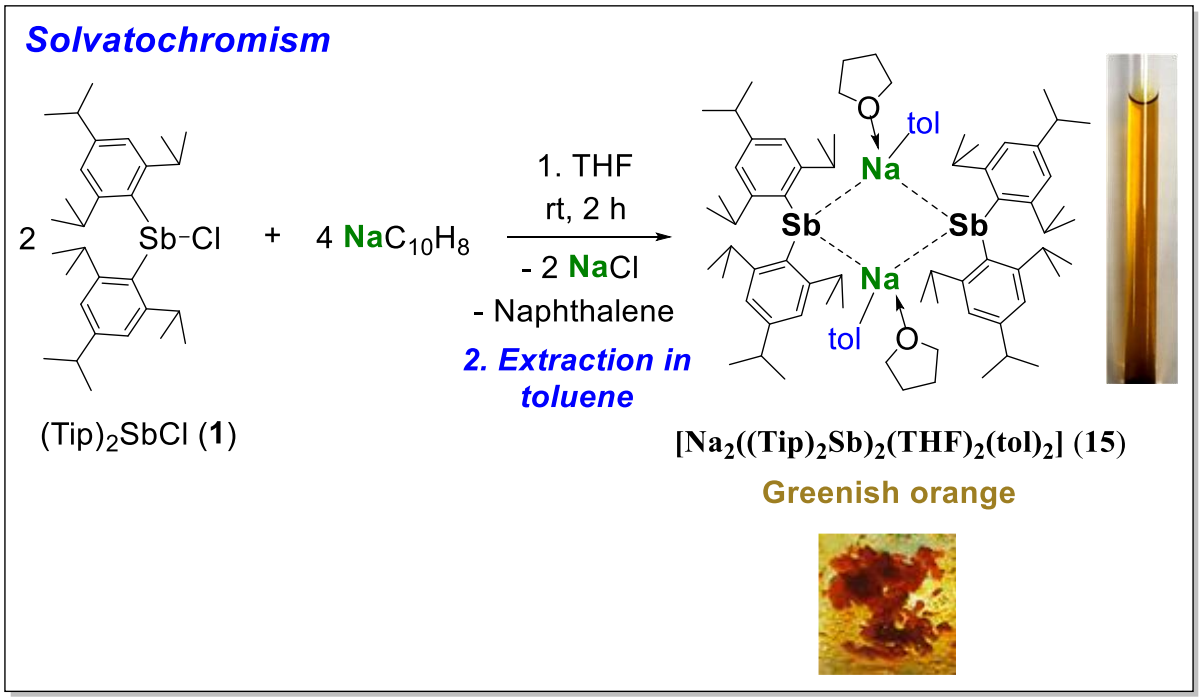

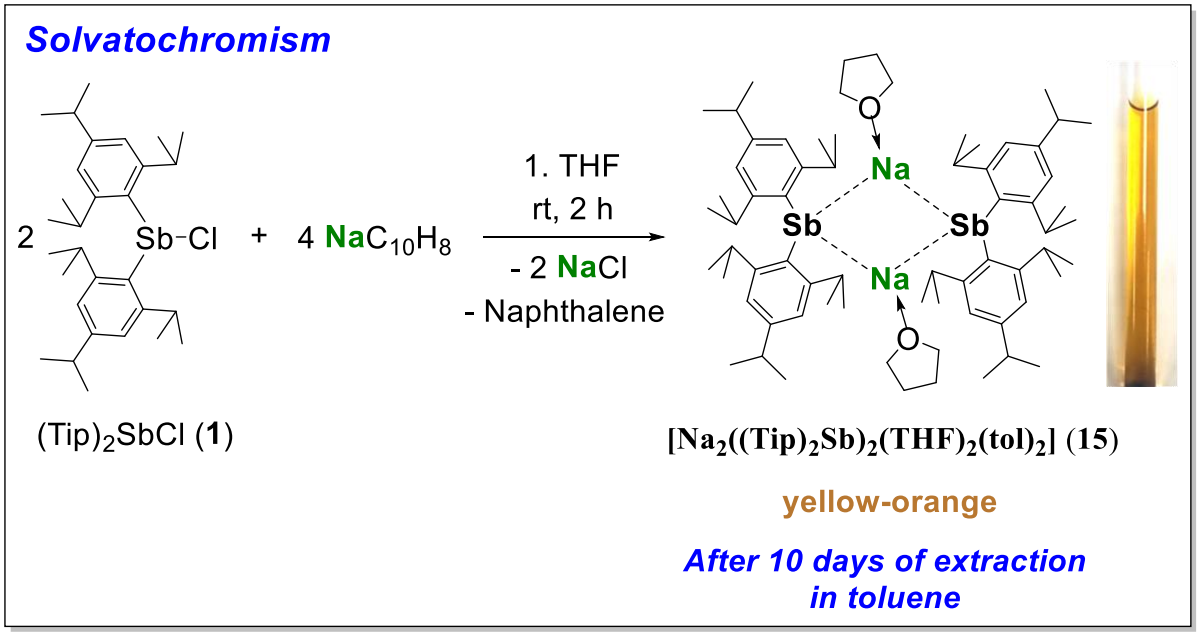

Scheme S6: Synthesis of $[Na_2((Tip)_2Sb)_2(THF)_2(tol)_2]\cdot Tol$ (**15**). ***Solvatochromism:*** The color of Complex **15** is dark red in THF (top), greenish orange in toluene (middle), yellow-orange after 10 days of extraction in toluene (bottom). Coordinated toluene molecules get released from the metal centers, which is also evident from the ^{1}H NMR spectrum of complex **15** (see Figure S75).

To a pale yellow THF solution (10 mL) of $(Tip)_2SbCl$ (**1**) (564 mg, 1 mmol), freshly prepared $NaC_{10}H_8$ (2.1 mmol) solution was added at rt leading to the formation of an immediate dark red color. The reaction mixture was then stirred for 1 h. Afterwards, THF was evaporated under vacuum to produce a dark greenish-red crystalline solid which was then extracted with toluene and filtered. The dark green filtrate was concentrated upto 2 ml to obtain the bright orange-red, block-shaped crystals of complex **15** at rt in 79% yield.

^{1}H NMR (400 MHz, C_6D_6, 298 K) δ: 6.95 (s, 6H), 6.93 (d, J = 2.6 Hz, 8H), 6.81 (s, 2H), 6.79 (d, J = 3.2 Hz, 2H), 4.07 (septet, J = 6.6 Hz, 8H), 2.70 (septet, J = 13.7, 6.9 Hz, 4H), 1.90 (s, 6H), 1.11 (s, 12H), 1.10 (d, J = 1.9 Hz, 12H), 1.05 (s, 24H), 1.04 (d, J = 2.4 Hz, 24H).

^{13}C NMR (101 MHz, C_6D_6, 298 K) δ: 153.7, 145.5, 138.3, 119.2, 66.8, 39.8, 33.4, 24.3, 24.1, 23.4, 23.2, 20.2 ppm.

^{1}H NMR spectrum of pure crystals of complex 15 after 7-10 days of extraction in toluene: This shows the removal of coordinated toluene molecule along with the change in color from dark-red to dark-yellow.

^{1}H NMR (400 MHz, C_6D_6, 298 K) δ: 7.13 (s, 8H), 4.27 (m, 8H), 2.89 (quintet, J = 6.9 Hz, 4H), 1.31 (d, J = 6.9 Hz, 24H), 1.24 (d, J = 6.9 Hz, 48H) ppm.

Solvatochromism effect of Complex 15:

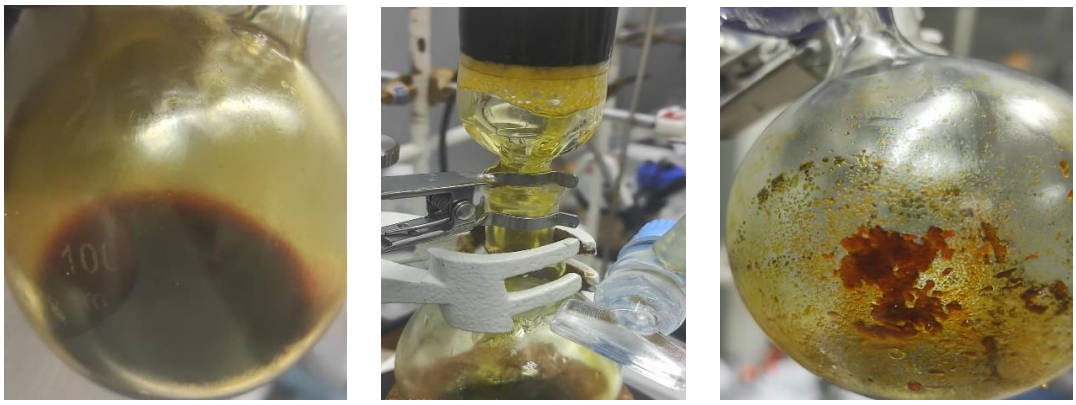

Figure S1: Complex **15** in THF: brown-red solution (left), in toluene: dark green solution (middle), solid state: orange-red (right).

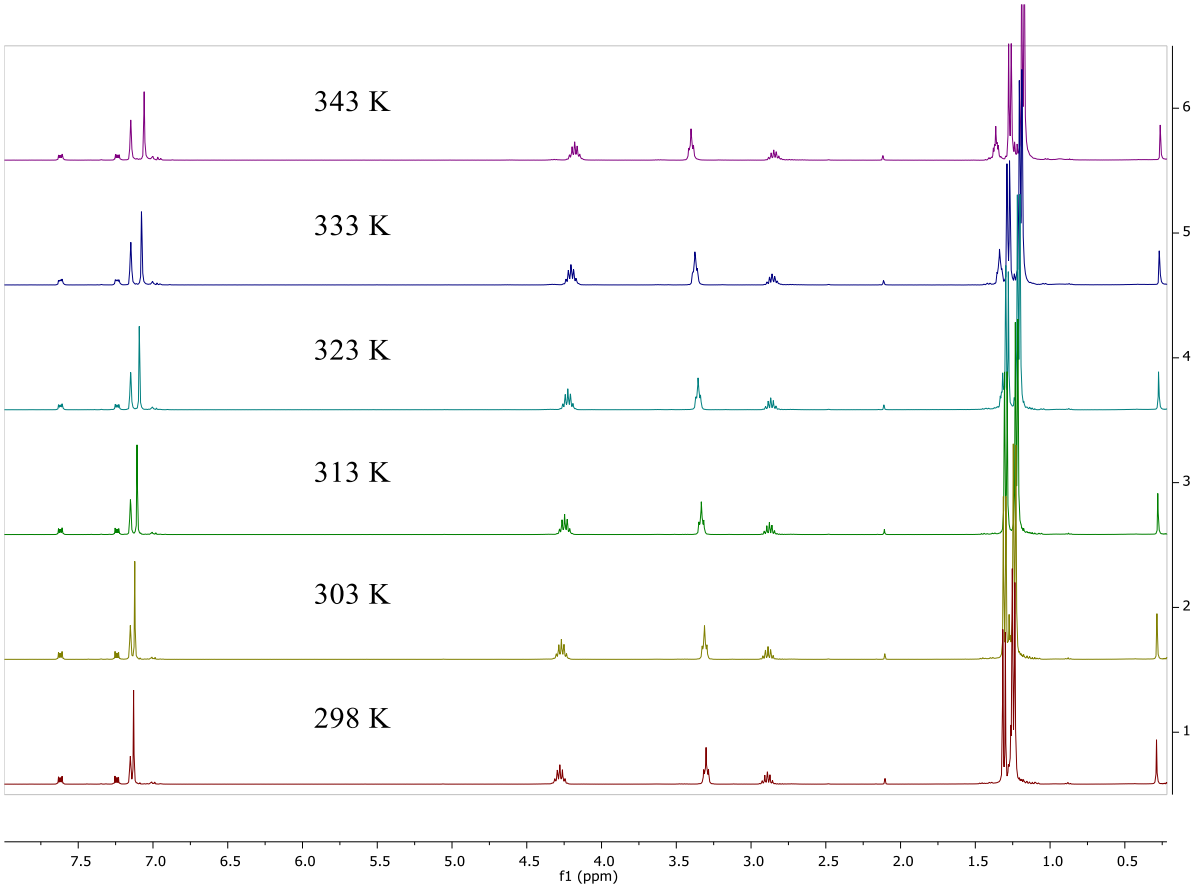

Figure S2. Temperature dependent ^{1}H NMR spectra of complex **15** in C_6D_6.

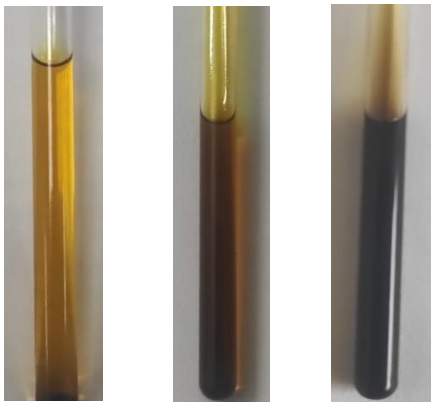

Figure S3: Complex **15** in C_6D_6 at rt (left), at 55 ^{0}C (middle), at 70 ^{0}C (right).

S2.8. Synthesis of $[Cs_2((Tip)_2Sb)_2]$ (16):

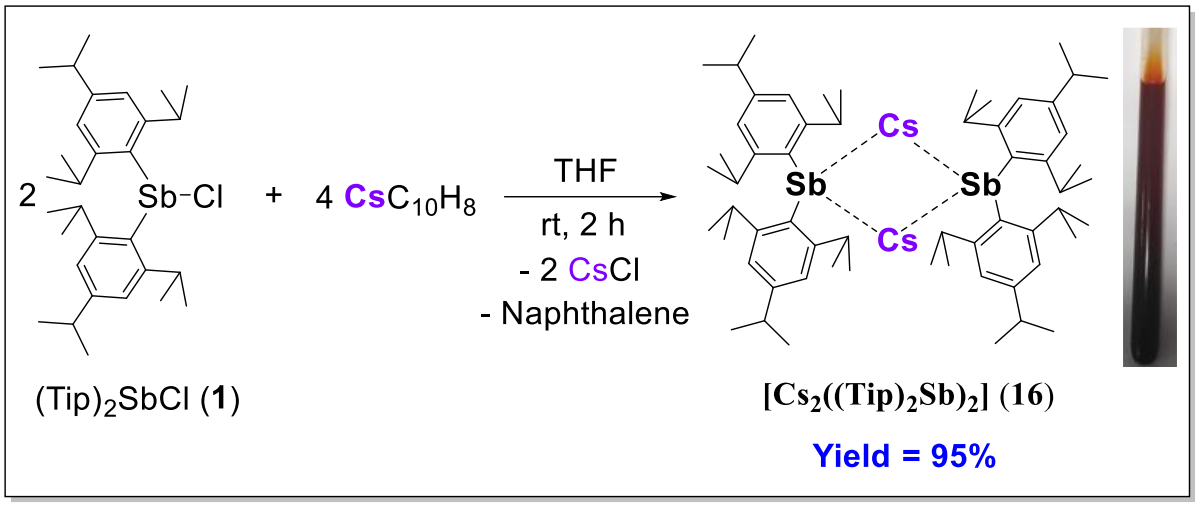

Scheme S7: Synthesis of $[Cs_2((Tip)_2Sb)_2]$ (**16**).

To a pale yellow THF solution (20 mL) of $(Tip)_2SbCl$ (**1**) (564 mg, 1 mmol), freshly prepared Cs-Naphthalenide ($CsC_{10}H_8$) (2.1 mmol) solution was added at rt leading to the formation of an immediate dark red color. The reaction mixture was then stirred for 2 h. Afterwards, THF was evaporated under vacuum to produce a dark red crystalline solid, which was then extracted with toluene and filtered. The dark red filtrate was concentrated upto 2 ml to obtain the bright orange-red, block-shaped crystalline precipitate of complex **16** at -40 ^{0}C in 95% yield.

^{1}H NMR (400 MHz, THF-D_8, 298 K) *δ*: 6.59 (d, *J* = 3.0 Hz, 8H), 4.30 (septet, *J* = 6.7 Hz, 8H), 2.62 (septet, *J* = 6.8 Hz, 4H), 1.07 (d, *J* = 6.4 Hz, 24H), 0.85 (d, *J* = 2.8 Hz, 24H), 0.83 (d, *J* = 2.9 Hz, 24H) ppm.

^{13}C NMR (101 MHz, THF-D_8, 298 K) *δ*: 155.6, 148.3, 144.4, 122.7, 119.4, 41.2, 35.1, 25.2, 24.9, 24.6 ppm.

S2.9. Synthesis of $(Tip)_2Sb^+$ NTf_2^- (19):

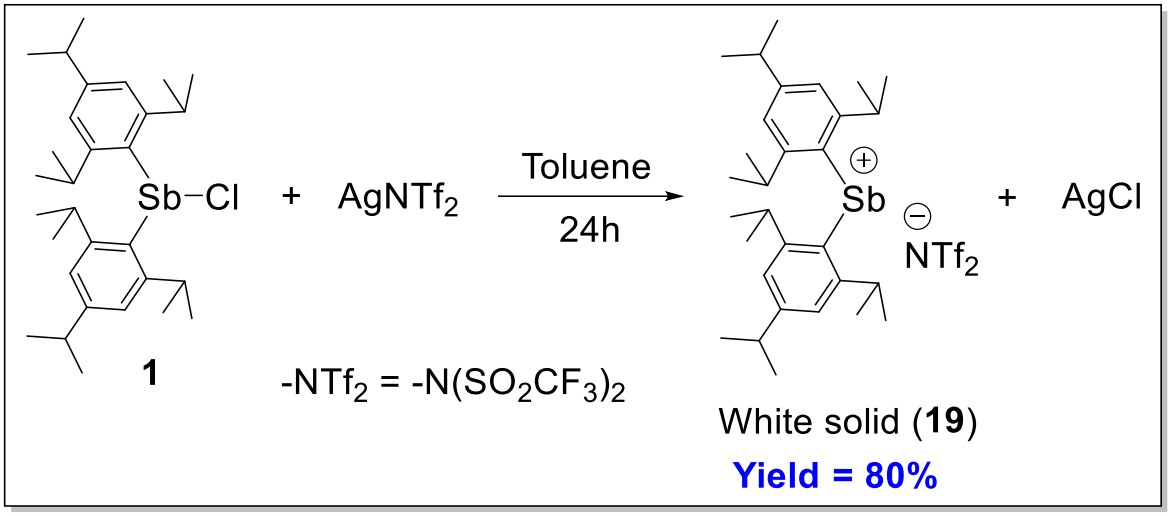

Scheme S8: Synthesis of the cation $(Tip)_2Sb^+$ NTf_2^- (**19**).

A 1:1 molar ratio of Tip_2SbCl (**1**) (100 mg, 0.17 mmol) and $AgNTf_2$ (68 mg, 0.17 mmol) was taken in a 50 ml Schlenk flask and added 10 ml of toluene. The reaction mixture was stirred overnight at rt and then filtered to remove the AgCl. Afterwards, the filtrate was concentrated up to complete dryness to obtain a grey-white solid of the cation **19** The cation (**19**) was then recrystallized from a concentrated toluene solution to obtain the colorless crystalline solid (110 mg, 80% yield). **M.P.** 108-110 ^oC.

^{1}H NMR (400 MHz, C_6D_6, 298 K) δ: 7.06 (s, 4H, -Ar*H*), 3.47 (septet, *J* = 6.5 Hz, 4H, *o*-C*H*$(CH_3)_2$), 2.68 (septet, *J* = 6.9 Hz, 2H, *p*-C*H*$(CH_3)_2$)), 1.14 (d, *J* = 6.9 Hz, 12H, *p*-$(CH_3)_2$), 1.11 (d, *J* = 6.6 Hz, 24H, *o*-$(CH_3)_2$) ppm.

^{13}C NMR (101 MHz, C_6D_6, 298 K) δ: 154.4, 151.4, 141.3, 123.4, 36.2, 34.5, 25.1, 24.2, 23.9 ppm.

^{19}F NMR (377 MHz, C_6D_6, 298 K) δ: -76.84 ppm.

HRMS (ESI): m/z calculated for $C_{30}H_{46}Sb^+$: 527.2632, found 527.2638.

3: Reactivity of the cation 19 with Lewis Bases

S3.1. Synthesis of the adduct 20:

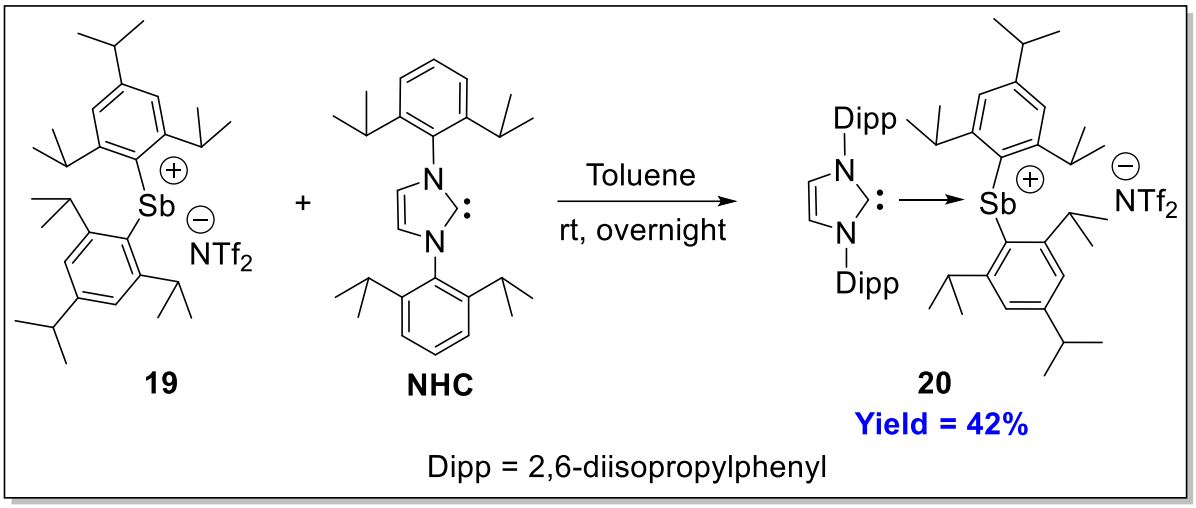

Scheme S9: Reactivity of the cation $(Tip)_2Sb^+$ NTf_2^- (**19**) with free NHC to generate the adduct **20**.

A 1:1.1 molar ratio of the cation $(Tip)_2Sb^+$ NTf_2^- (**19**) (123 mg, 0.15 mmol) and free NHC (67 mg, 0.17 mmol) were taken in a 50 ml Schlenk flask and added 10 ml of toluene. The reaction mixture was stirred overnight at rt and then filtered. After the filtration, the obtained white residue was washed with *n*-hexane to remove the unreacted starting materials and then dried completely under vacuum. The adduct **20** was obtained as a white solid (77 mg, 42% yield). **Decomposition Point:** 230-232 °C.

^{1}H NMR (400 MHz, THF-D_8, 298 K) *δ*: 7.52 (d, *J* = 7.7 Hz, 2H, CH=CH_{NHC}), 7.49 (s, 4H, -ArH_{Tip}), 7.22 (d, *J* = 7.8 Hz, 6H, -ArH_{Dipp}), 2.35 (td, *J* = 11.9, 5.2 Hz, 10H, -CH(CH_3)$_2$), 1.36-1.29 (m, 3H, -C$H_{3Tip-Me}$), 1.25-1.10 (m, 4H, -C$H_{2Tip-Me}$), 1.07 (d, *J* = 6.7 Hz, 18H, -*(*CH_3*)$_{2Tip}$), 1.04-1.00 (m, 4H, -C$H_{2Tip-Me}$), 0.96-0.89 (m, 6H, -C$H_{3Tip-Me}$ and -C$H_{3NHC-Dipp}$), 0.85 (d, *J* = 6.8 Hz, 18H, -*(*CH_3*)$_{2NHC-Dipp}$), 0.81-0.77 (m, 3H, -C$H_{3NHC-Dipp}$).

^{13}C NMR (101 MHz, THF-D_8, 298 K) *δ*: ^{13}C NMR (101 MHz, THF- D_8, 298 K) *δ*: 184.3 (C_{NHC}), 182.3 (C_{NHC}), 146.3, 136.0, 131.7, 129.8, 129.0, 126.5, 126.5, 126.2, 125.4, 32.7, 29.6, 25.3, 24.2, 14.6 ppm.

^{19}F NMR (377 MHz, THF-D_8, 298 K) *δ*: -79.92 ppm.

^{1}H-^{15}N HMBC (400 MHz, THF-D_8, 298 K) *δ*: -196.85 ppm.

HRMS (ESI): m/z calculated for $[C_{57}H_{82}N_2Sb - 2CH4]^+$ 883.4885, found 883.4890.

S3.2. Synthesis of the adduct 21:

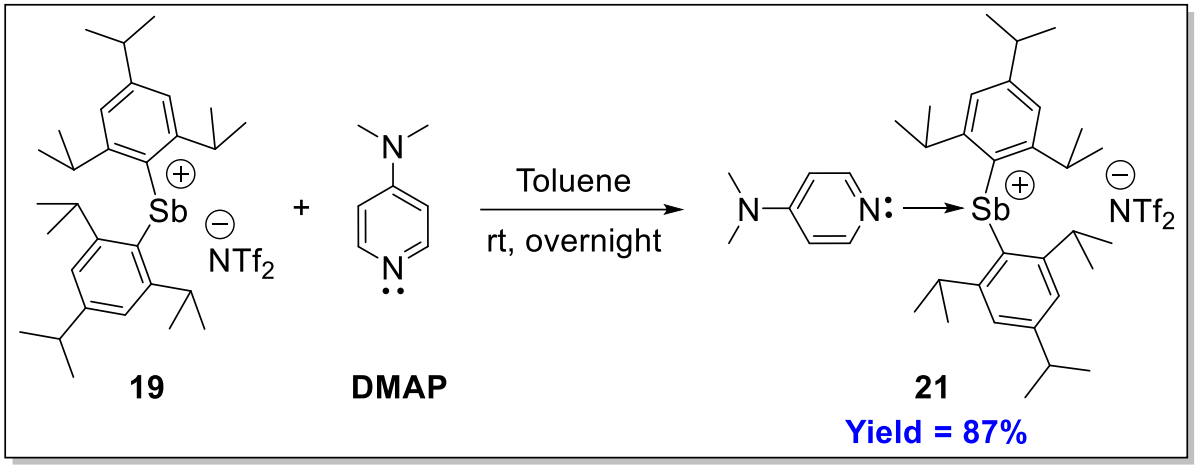

Scheme S10: Reactivity of the cation $(Tip)_2Sb^+$ NTf_2^- (**19**) with 4-dimethylaminopyridine to generate the adduct **21**.

A 1:1 molar ratio of the cation $(Tip)_2Sb^+$ NTf_2^- (**19**) (120 mg, 0.14 mmol) and 4-dimethylaminopyridine (DMAP) (17 mg, 0.14 mmol) was taken in a 50 ml Schlenk flask and added 10 ml of toluene. The reaction mixture was stirred overnight at rt and then filtered. Afterwards, the filtrate was concentrated up to 1-2 ml to obtain the colorless crystals of desired adduct **21** (120 mg, 87% yield). **M.P.** 130-135 ^{o}C

^{1}H NMR (400 MHz, C_6D_6, 298 K) *δ*: 7.83 (d, *J* = 5.2 Hz, 2H, -Ar*H*), 7.13 (s, 4H, -Ar*H*), 6.16-6.08 (m, 2H, -Ar*H*), 3.01 (quintet, *J* = 6.6 Hz, 4H, -C*H*$(CH_3)_2$), 2.72 (quintet, *J* = 6.8 Hz, 2H, -C*H*$(CH_3)_2$), 2.44 (s, 6H, -CH_3), 1.17 (dd, *J* = 6.8, 3.4 Hz, 14H, -(CH_3)$_2$), 1.05 (d, *J* = 6.6 Hz, 22H, -(CH_3)$_2$) ppm.

^{13}C NMR (101 MHz, C_6D_6, 298 K) *δ*: 156.5, 155.3, 154.9, 153.1, 140.5, 124.3, 123.5, 39.5, 36.6, 36.4, 34.9, 25.5, 24.9, 24.2 ppm.

^{19}F NMR (377 MHz, C_6D_6, 298 K) *δ*: -78.76 ppm.

HRMS (ESI): m/z calculated for $C_{37}H_{56}N_2Sb^+$: 649.3476, found 649.3482.

S4. UV-vis and fluorescence studies of compounds 1, 4

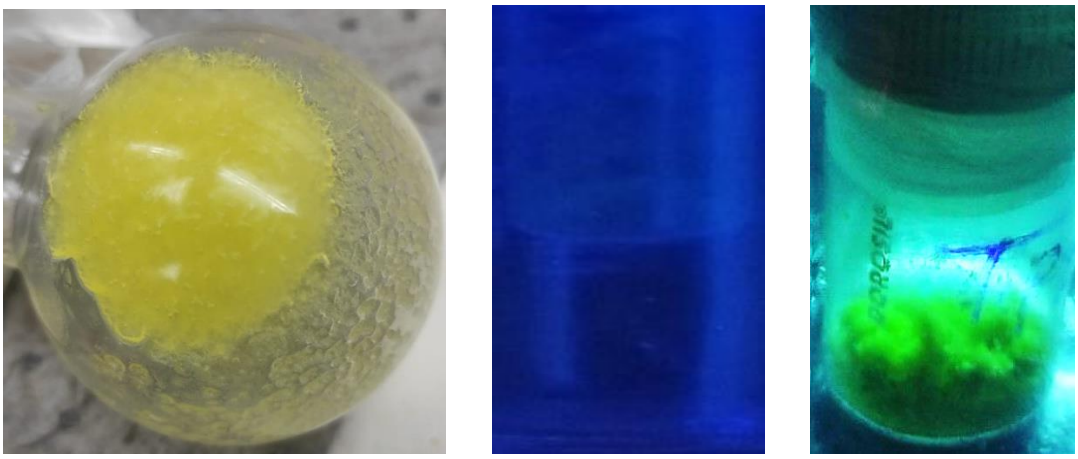

Figure S4: Crystals of compound **1** under white light (left), under long-UV (middle), under short-UV (right).

S4.1. UV-vis absorption spectrum of $(Tip)_2SbCl$ (1) in toluene

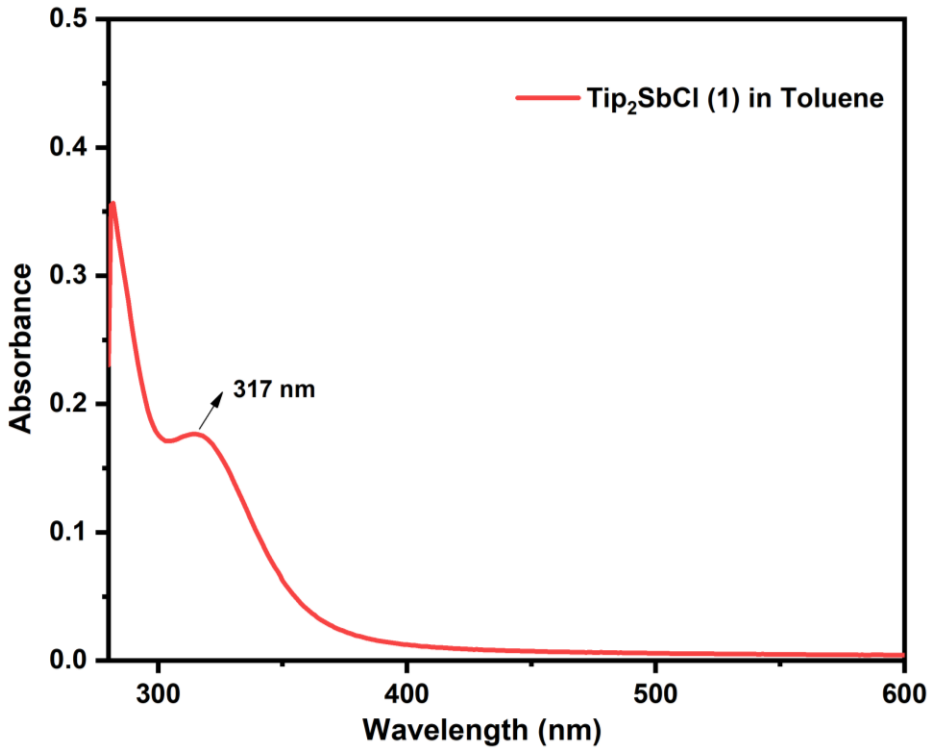

Figure S5: UV-Vis absorption spectrum of $(Tip)_2SbCl$ (**1**) in toluene.

S4.2. Emission spectra of $(Tip)_2SbCl$ (1) in toluene

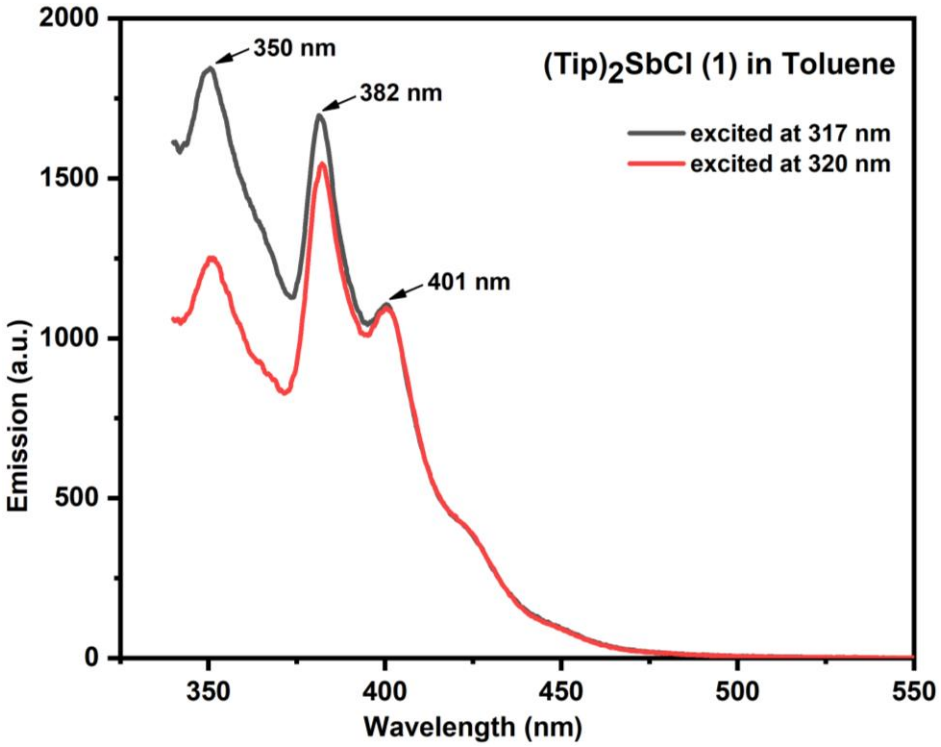

Figure S6: Emission spectra of $(Tip)_2SbCl$ (**1**) in toluene.

S4.3. Absorption and emission spectra of $(Tip)_2SbCl$ (1) in *n*-hexane

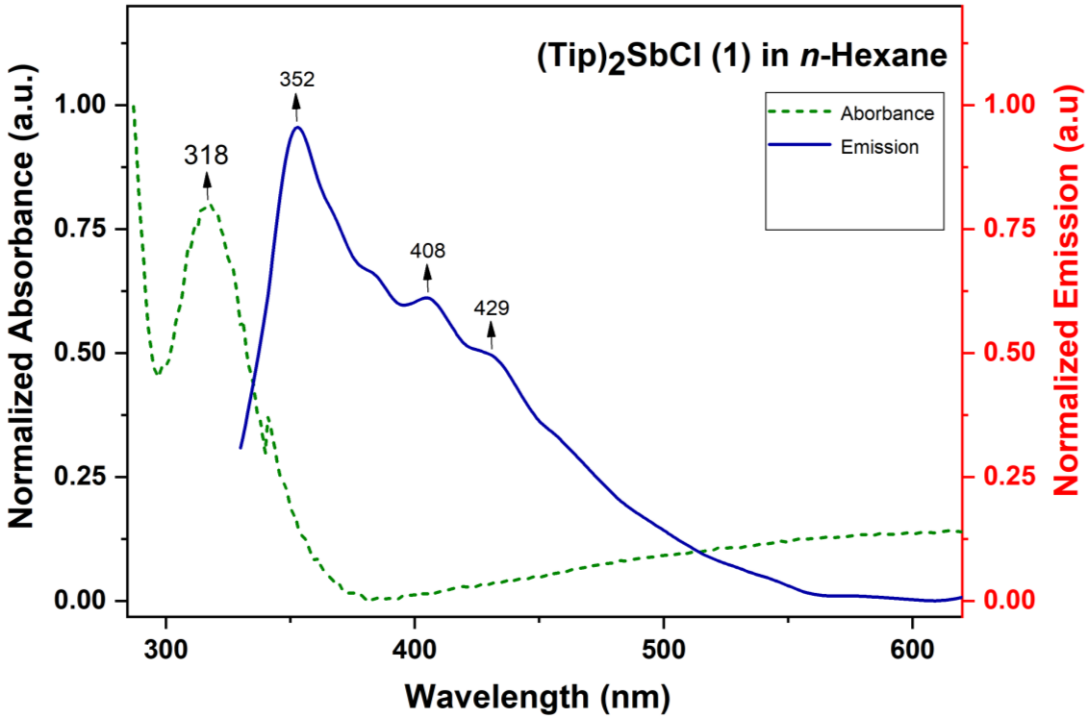

Figure S7: Absorption and emission spectra of $(Tip)_2SbCl$ (**1**) in *n*-hexane.

S4.4. Solid state absorption and emission spectra of $(Tip)_2SbCl$ (1)

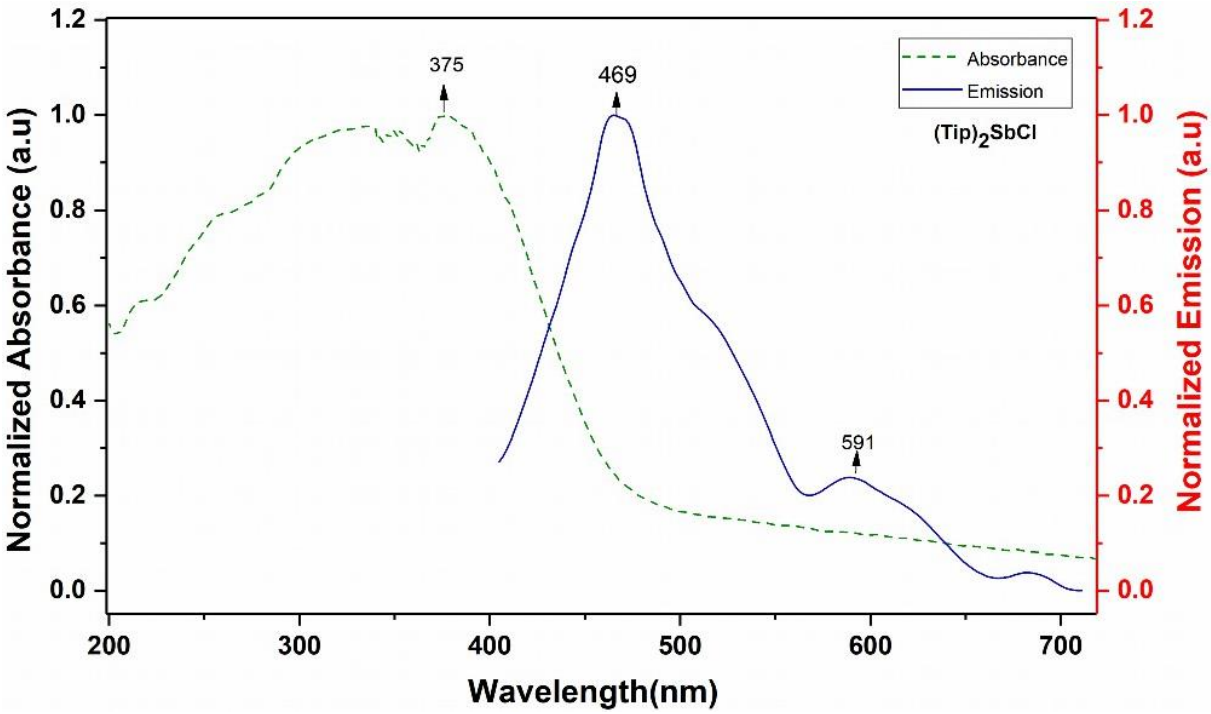

Figure S8: Solid state absorption and emission spectra of $(Tip)_2SbCl$ (**1**).

S4.5. Lifetime measurement of compound 1 in toluene

The photoluminescence decay of compound **1** was measured by JOBIN-VYON M/S instrument using quartz cuvettes with path lengths of 10 mm in diluted solutions (1 mg in 3 ml of dry toluene) at room temperature. All the samples were measured under an inert atmosphere by using a glove box. The exponential decay of a sample was measured twice to get the two Lifetime (τ) values. Then calculated the average lifetime value of a sample by substituting the values in the given equation:

$$Average\ life\ time\ (\tau) = \frac{(t_1B_1 + t_2B_2)}{B_1 + B_2}$$

B_1 = Population of the molecules having t_1 life time

B_2 = Population of the molecules having t_2 life time.

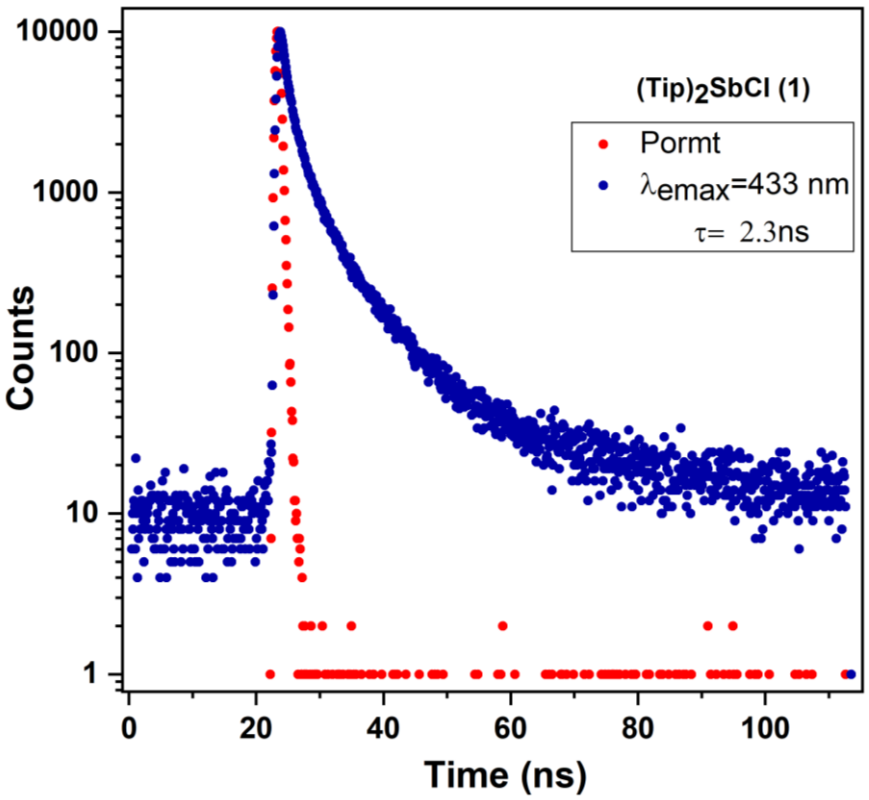

Figure S9: Fluorescence decay of $(Tip)_2SbCl$ (**1**) in solution state (toluene) at room temperature (λ_{ex} = 313 nm). The sharp profile is the Excitation lamp profile (Red color). The compound exciting pulsed and emission in blue color. (τ_s = 2.3 ns at 433 nm during the excitation light source LED 320 nm).

S4.6. Quantum yield calculation for compound 1 in toluene *n*-hexane

The fluorescence quantum yield of compound **1** was measured using quartz cuvettes with path lengths of 10 mm at room temperature in highly diluted solutions (with an absorption intensity below 0.1). All the samples for measurement were prepared under argon atmosphere using a glove box. Initially, the UV-vis absorbance of the standard reference (2-aminopyridine) and unknown fluorophore were recorded to maintain the absorption intensity of samples below 0.1. The fluorescence spectrum of the same solutions was recorded afterwards. Integrated fluorescence intensity (the area of the fluorescence spectrum) of the standard reference and unknown fluorophore was calculated from the fully corrected fluorescence spectrum. Then, the Quantum yield (ϕ) was calculated by substituting the values in the given equation:

$$\boldsymbol{\phi_F} = \phi_R \frac{I_F}{I_R} \frac{A_R}{A_R} \frac{\eta_F^2}{\eta_R^2}$$

Where subscript R and F refers to standard reference and unknown fluorophore.

ϕ_F = Quantum yield of an unknown fluorophore.

ϕ_R = Quantum yield of standard reference (2-aminopyridine has been used as the standard).

I_F/I_R = ratio of peak area under the emission curve of unknown fluorophore and reference.

A_R/A_F = ratio of absorbance values of the reference and the unknown fluorophore.

η_F^2/η_R^2 = ratio of the refractive index of solvent used for the unknown fluorophore (*n*-hexane) and the reference (0.1 M H_2SO_4).

1. Quantum yield for $(Tip)_2SbCl$ (1) in toluene:

$$\boldsymbol{\phi_F} = 0.60 \times \frac{12877}{8659} \times \frac{0.0892}{0.0901} \times \frac{(1.49)^2}{(1.33)^2}$$

$$= 1.1\ \%\ (\text{in Toluene})$$

2. Quantum yield for $(Tip)_2SbCl$ (1) in *n*-hexane:

$$\boldsymbol{\phi_F} = 0.60\ \frac{2742.34}{32763.12}\ \frac{0.0568}{0.0539}\ \frac{(1.375)^2}{(1.333)^2}$$

$$= 5.6\ \%\ (\text{in } n\text{-hexane})$$

S4.7. UV-vis absorption spectrum of $(Tip)_2Sb\text{-}Sb(Tip)_2$ (4)

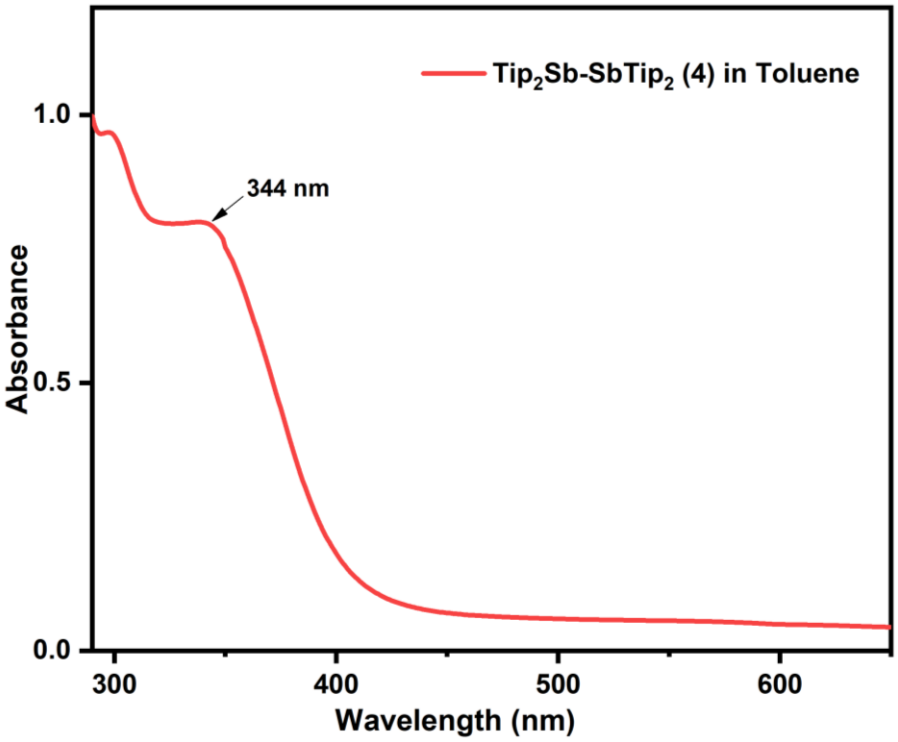

Figure S10. UV-Vis absorption spectrum of $(Tip)_2Sb\text{-}Sb(Tip)_2$ (**4**).

S4.8. Emission spectra of $(Tip)_2Sb\text{-}Sb(Tip)_2$ (4)

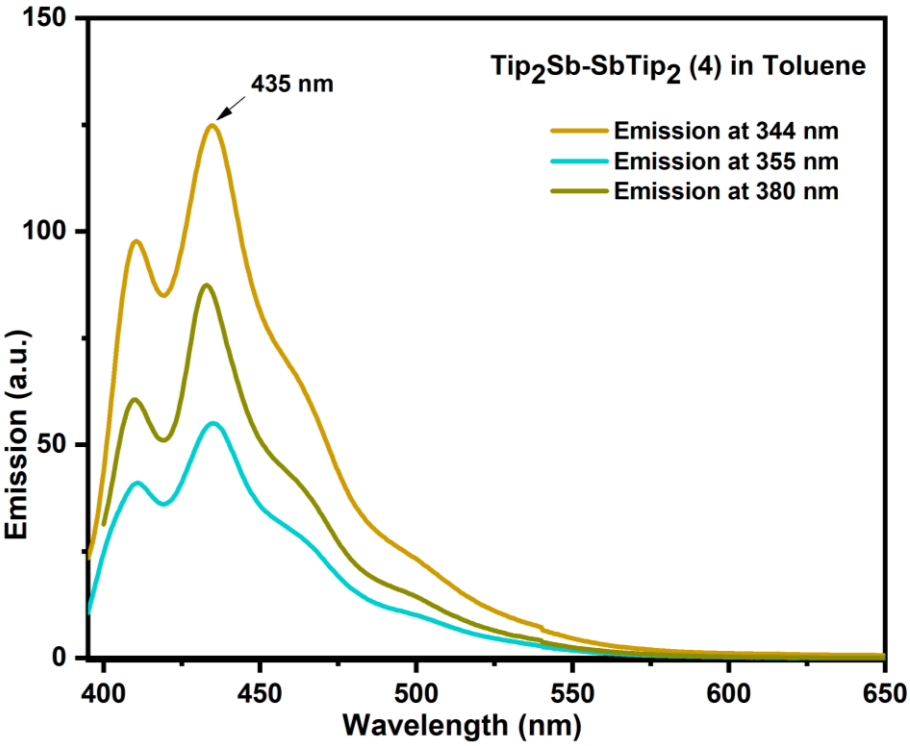

Figure S11: Emission spectra of $(Tip)_2Sb\text{-}Sb(Tip)_2$ (**4**).

S4.9. UV-vis spectra of $[K_3((Tip)_2Sb)_3(THF)_5]$ (6)

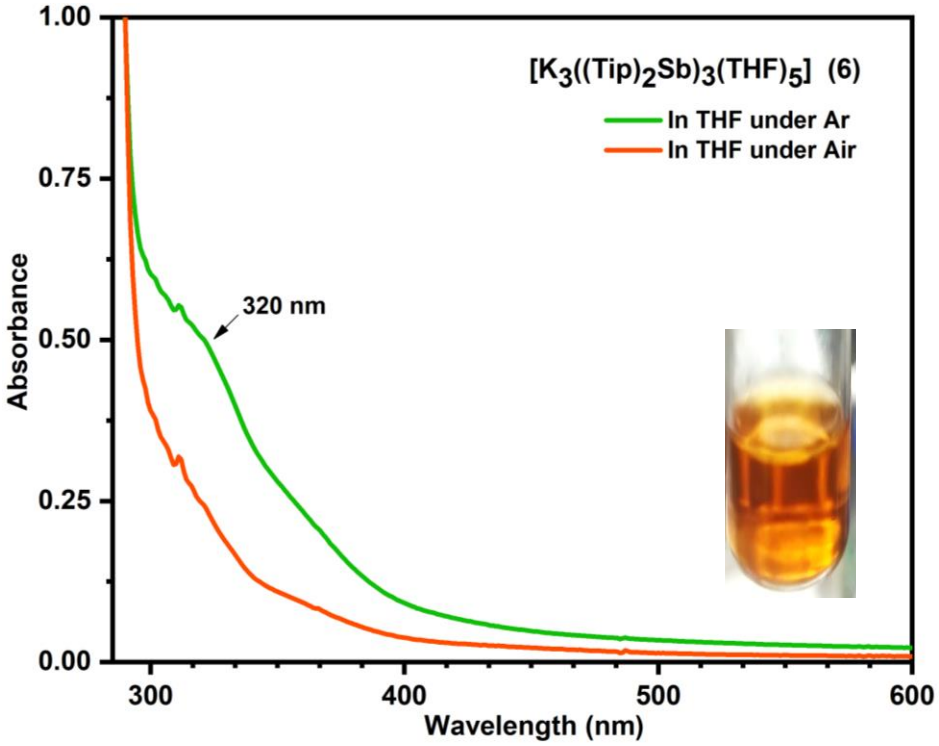

Figure S12. UV-Vis absorption spectra of $[K_3((Tip)_2Sb)_3(THF)_5]$ (**6**).

S4.10. UV-vis spectrum of $[Li_2((Tip)_2Sb)_2(THF)_4]$ (14)

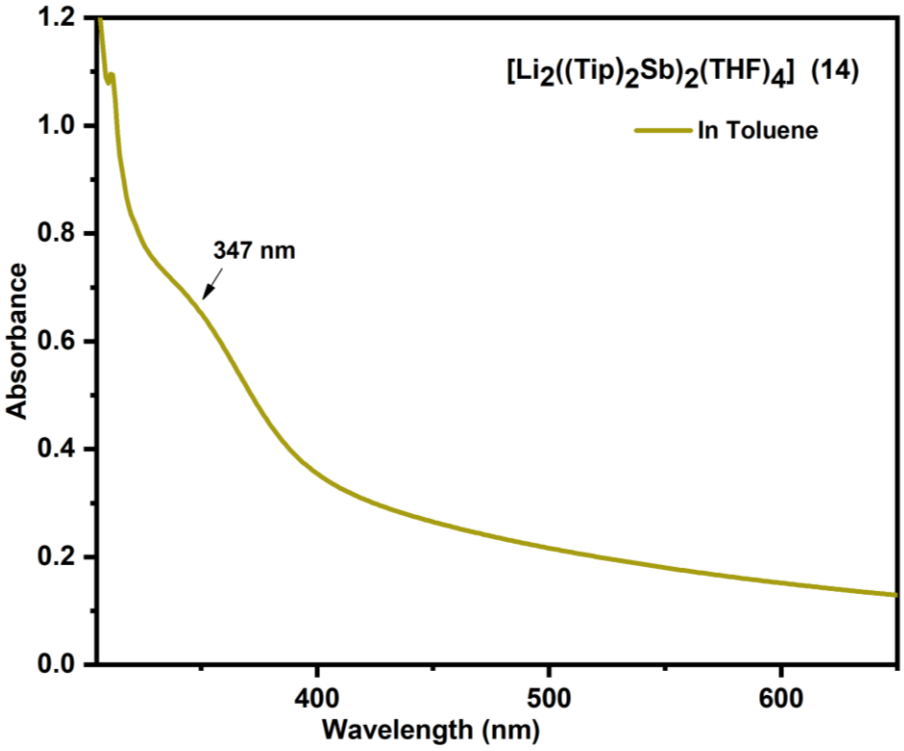

Figure S13. UV-Vis absorption spectrum of $[Li_2((Tip)_2Sb)_2(THF)_4]$ (**14**).

S4.11. UV-vis absorption spectra of $[Na_2((Tip)_2Sb)_2(THF)_2]$·Tol (15)

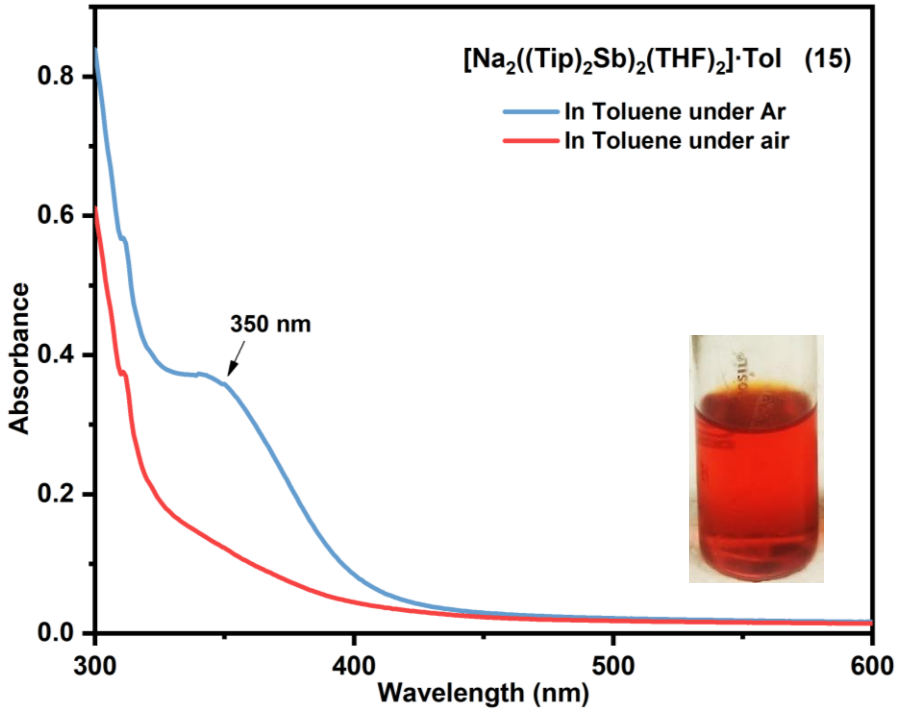

Figure S14. UV-Vis absorption spectra of $[Na_2((Tip)_2Sb)_2(THF)_2]$·Tol (**15**).

S4.12. UV-vis spectra of $[Cs_2((Tip)_2Sb)_2(THF)_2]$ (16)

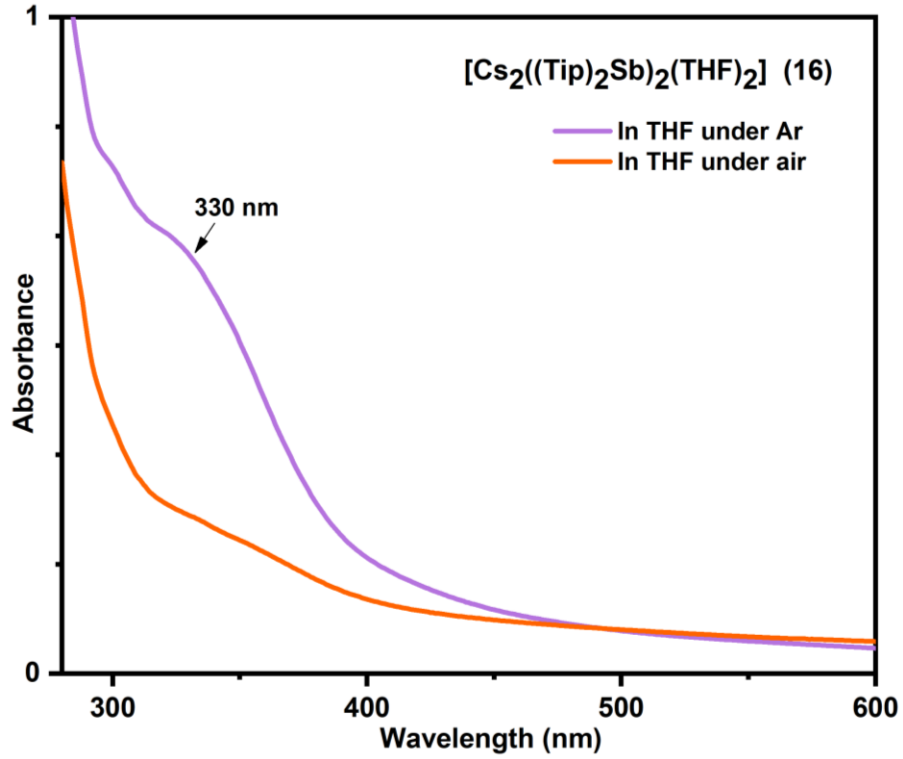

Figure S15. UV-Vis absorption spectra of $[Cs_2((Tip)_2Sb)_2(THF)_4]$ (**16**).

S5. Temperature dependent NMR studies for complexes 14 and 15

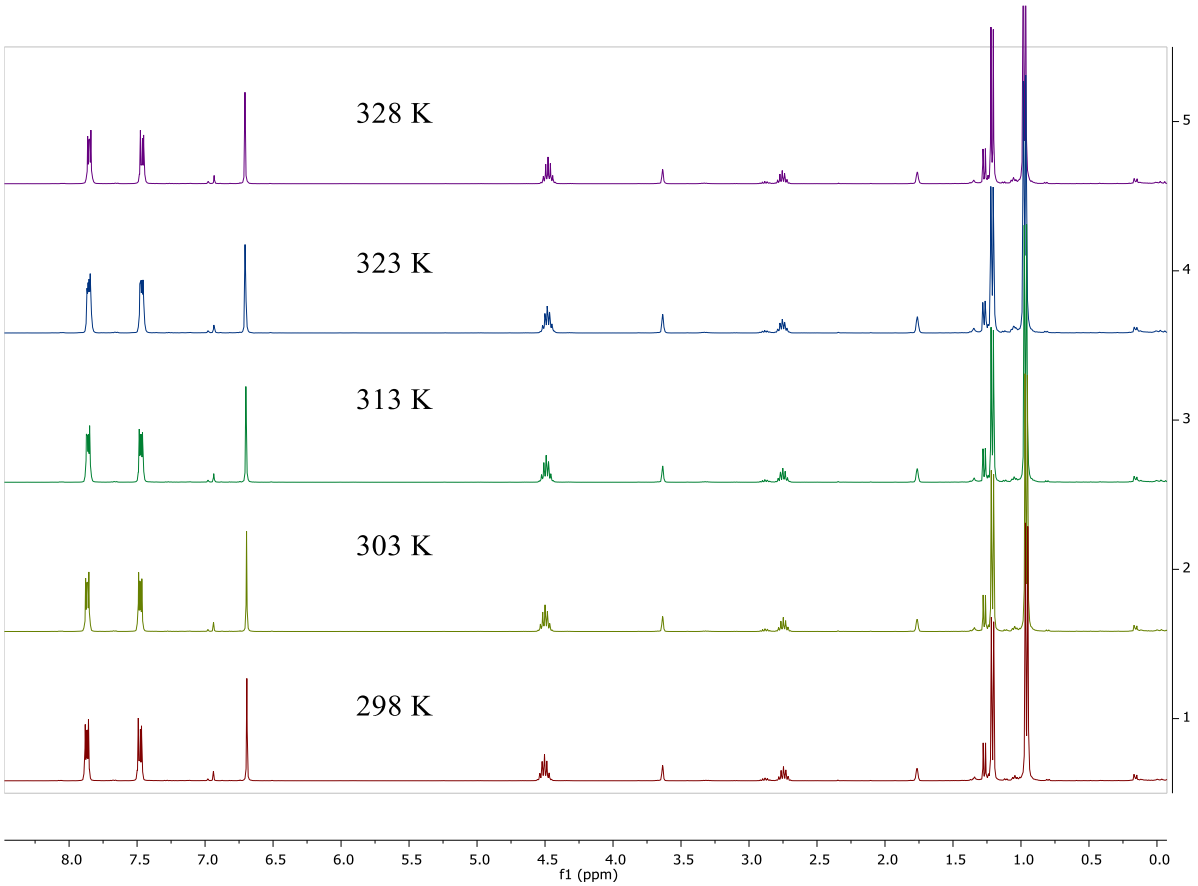

Figure S16. Temperature dependent ^{1}H NMR spectra of complex **14** in THF-D_8.

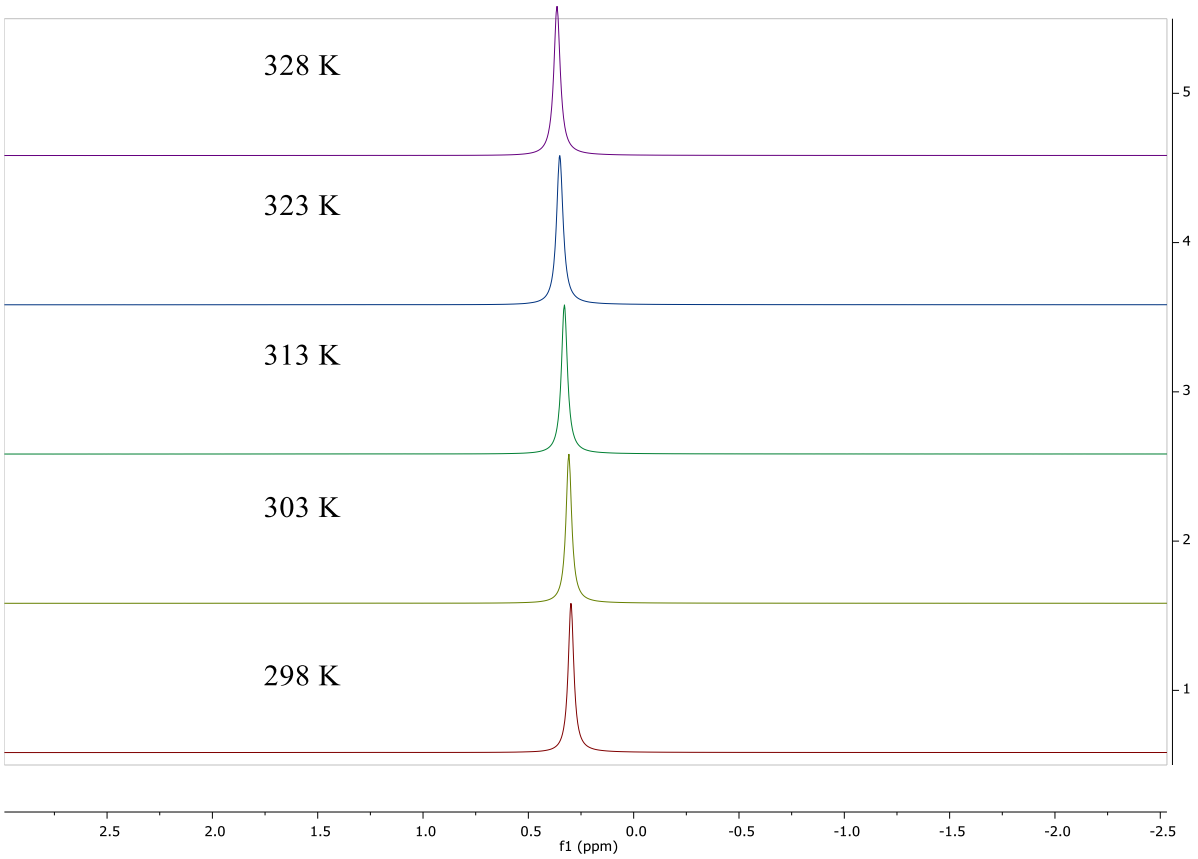

Figure S17. Temperature dependent ^{7}Li NMR spectra of complex **14** in THF-D_8.

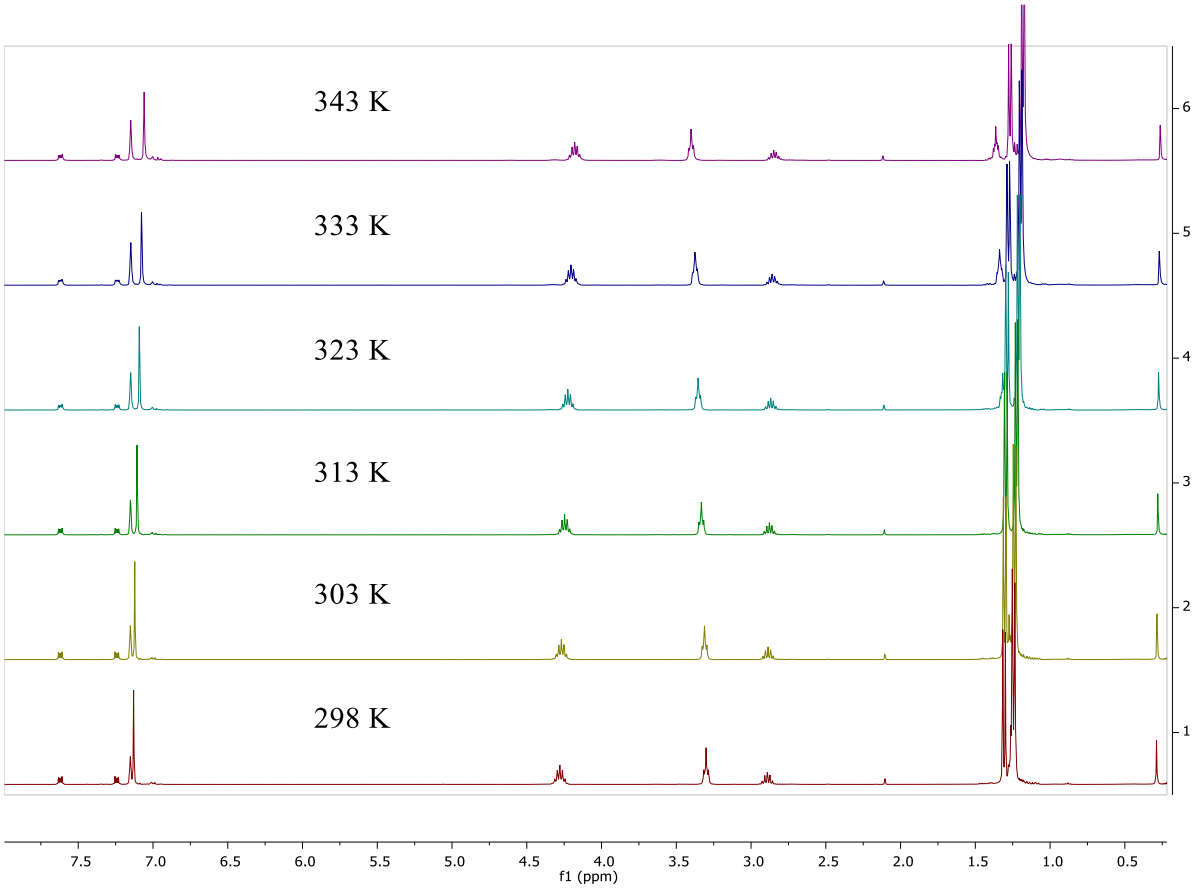

Figure S18. Temperature dependent ^{1}H NMR spectra of complex **15** in C_6D_6.

S6. Cyclic voltammetry (CV) studies of $(Tip)_2SbCl$ (1), $(Tip)_2Sb$-$Sb(Tip_2)$ (4), $[K_3((Tip)_2Sb)_3(THF)_5]$ (6) and $[Na_2((Tip)_2Sb)_2(THF)_2(tol)_2]\cdot Tol$ (15)

The cyclic voltammetry experiments have been performed at a Metrohm-Autolab204 Potentiostat. All experiments have been performed under argon atmosphere in deoxygenated and anhydrous THF solution of 0.1 M [*n*-Bu_4N]PF_6.

The setup consisted of a glassy carbon (GC) working electrode (WE), a Pt wire as the counter electrode (CE) and a Ag wire as the reference electrode (RE). The recorded voltammograms have been referenced to the internal standard $(fc)_2Fe^+/(fc)_2Fe$, which was added after the measurements.

S6.1. CV studies of $(Tip)_2SbCl$ (1)

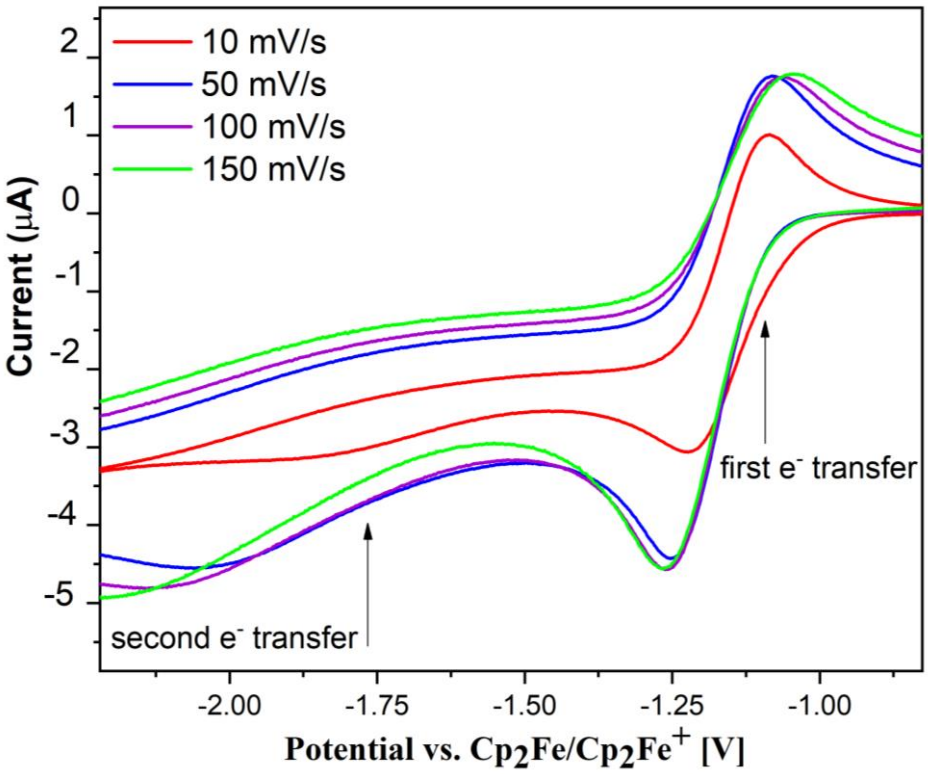

Figure S19. Cyclic voltammogram of $(Tip)_2SbCl$ (**1**) in THF containing 0.1 M [*n*-$Bu_4N]PF_6$ as the electrolyte (CE: Pt, WE: GC, RE: Ag).

S6.2. Electron Spin Resonance (ESR) studies of the reaction mixture containing $(Tip)_2Sb$-Cl (1) and KC_8 in 1:2 molar ratio in THF.

EPR measurements at X-band (8.75-9.65 GHz) were carried out using a **JEOL Model JES FA200** EPR spectrometer at 293 K. The sample preparation was done under argon atmosphere using a glove box technique. The compound $(Tip)_2SbCl$, **1** (5 mg) and KC_8 were taken in 1:1 molar ratio in an oven-dried sample vial and added with cooled (-40 ^oC) THF. The reaction mixture was stirred for 5 minutes and filtered to remove the graphite. The dark red color filtrate was further diluted by the addition of more THF and transferred to a quartz capillary. The capillary with the compound used for measurement was sealed adequately using silicon grease and melted wax to maintain the argon atmosphere.

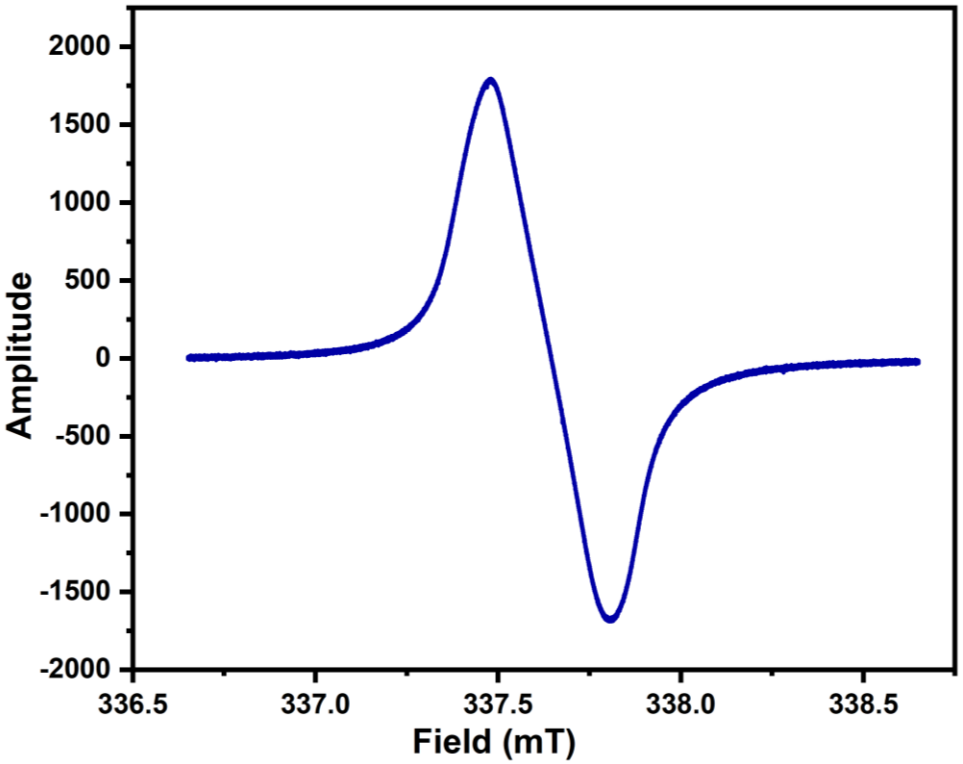

Figure S20. X-band ESR spectrum of the reaction mixture containing $(Tip)_2SbCl$ (**1**) and KC_8 in 1:2 molar ratio in THF at 293 K.

$$\boldsymbol{g} = \frac{\mathrm{h}\nu}{\mu_B H}$$

h = Planck's constant

ν = Operating frequency

μ_B = Bohr magneton

H = Magnetic field

g = Lande factor

$$\boldsymbol{g} = \frac{6.626 \times 10^{-34}\, Js^{-1} \times 9442.750 \times 10^{6}\, s^{-1}}{9.2740 \times 10^{-24}\, JT^{-1} \times 337.5 \times 10^{-3}\, T}$$

$$\boldsymbol{g} = \frac{6.6256 \times 10^{-24}}{3.131 \times 10^{-24}}$$

$$\boldsymbol{g} = 2.1$$

S6.3. CV studies of $(Tip)_2Sb\text{-}Sb(Tip_2)$ (4)

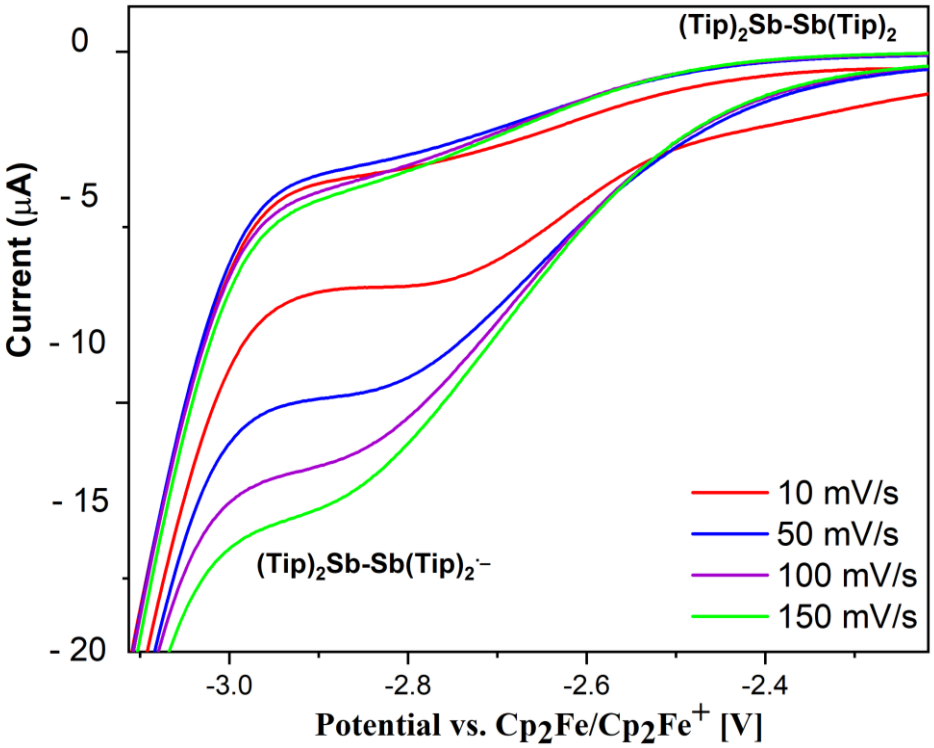

Figure S21. Cyclic voltammogram of $(Tip)_2Sb\text{-}Sb(Tip)_2$ (**4**) in THF containing 0.1 M [*n*-$Bu_4N]PF_6$ as the electrolyte (CE: Pt, WE: GC, RE: Ag). CV suggests the possible reduction of compound **4**.

When $(Tip)_2Sb\text{-}Sb(Tip)_2$ (**4**) was treated with 2 equiv of KC_8 at 0 °C in THF, the reaction mixture turned from bright yellow to a dark brownish-red color, resulting in the formation of $[K_3(THF)_5((Tip)_2Sb)_3]$ (**6**), which was further characterized by NMR spectroscopy.

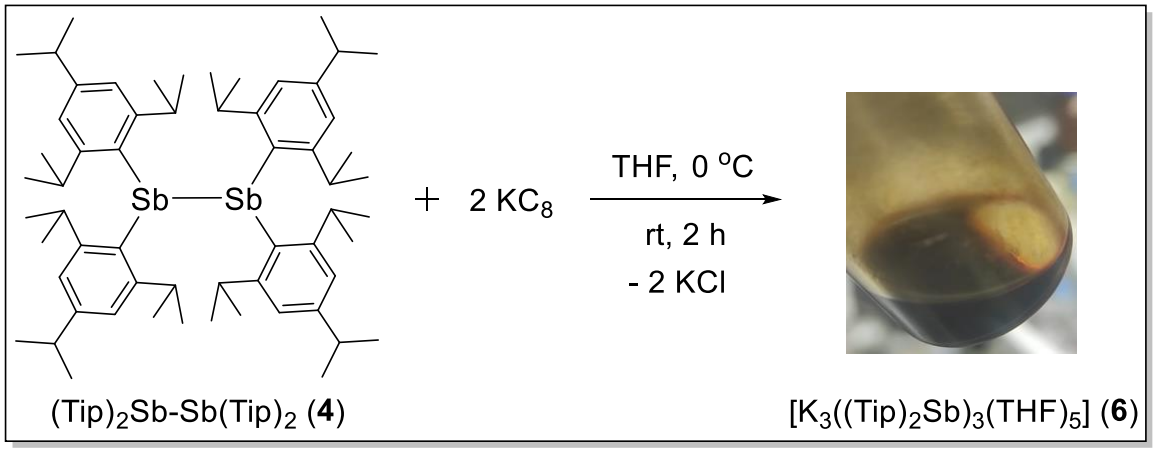

Scheme S11: Synthesis of $[K_3((Tip)_2Sb)_3(THF)_5]$ (**6**) by reduction of $(Tip)_2Sb\text{-}Sb(Tip)_2$ (**4**).

S6.4. CV studies of $[Na_2((Tip)_2Sb)_2(THF)_2(tol)_2]\cdot Tol$ (15)

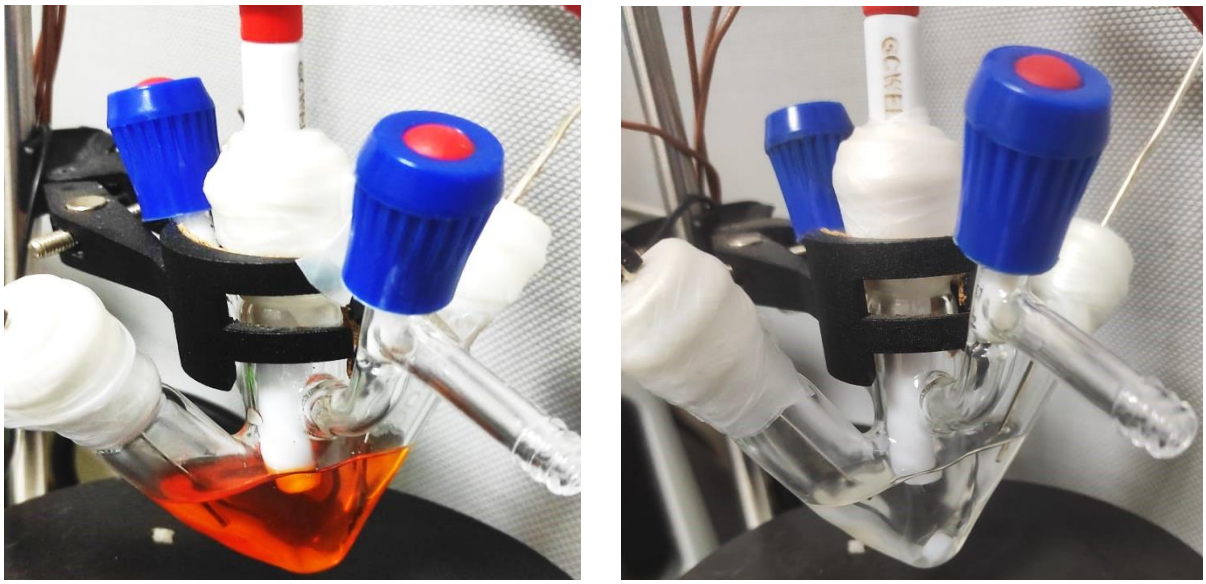

Figure S22. $[Na_2((Tip)_2Sb)_2(THF)_2(tol)_2]$ (**15**) in THF containing 0.1 M [*n*-Bu_4N]PF_6 as the electrolyte. Before scans (left), after 2 min of scans (right). CE: Pt, WE: GC, RE: Ag.

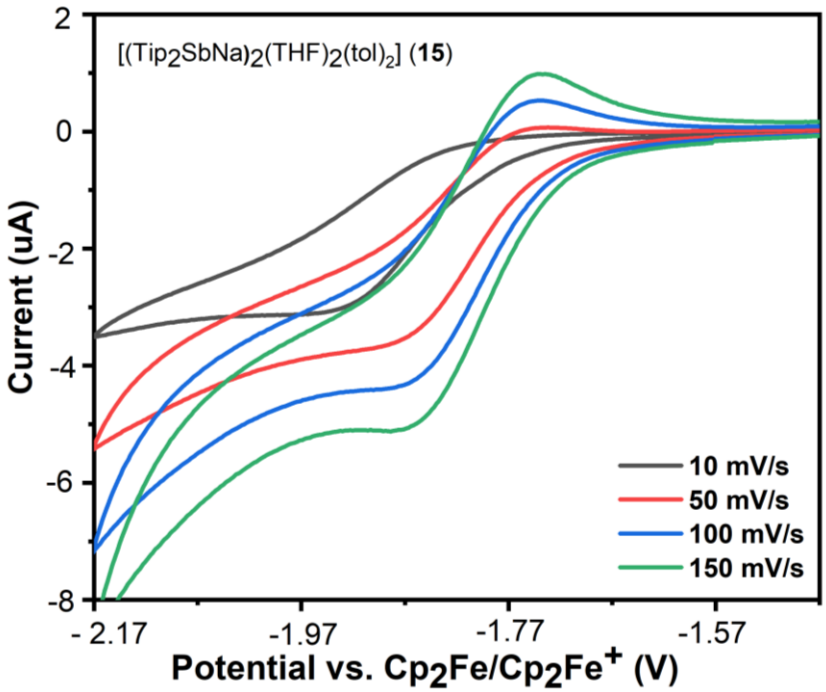

Figure S23. Cyclic voltammogram of $[Na_2((Tip)_2Sb)_2(THF)_2(tol)_2]$ (**15**) in THF containing 0.1 M [*n*-Bu_4N]PF_6 as the electrolyte (CE: Pt, WE: GC, RE: Ag). After giving the scan at 100 mV/s rate (started with 150 mV/s), the color of the solution slowly changed from orange-red to pale yellow.

S7: Application of $[K_3((Tip)_2Sb)_3(THF)_5]$ (6) (monomeric unit: $(Tip)_2Sb^-$) as reducing agents

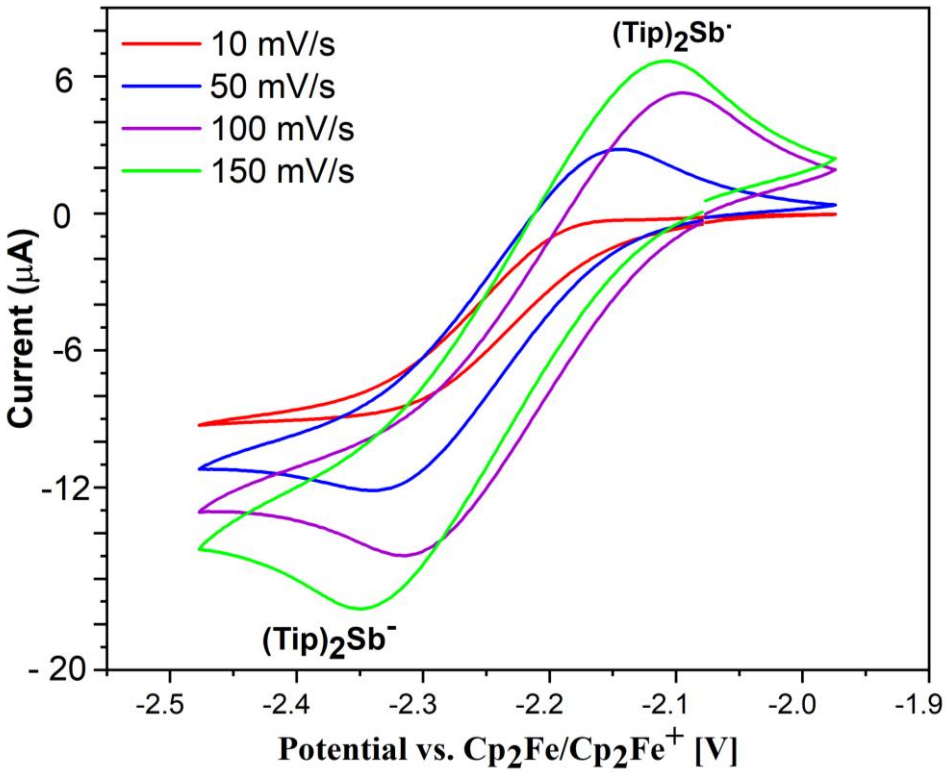

Figure S24. Cyclic voltammogram of $[K_3((Tip)_2Sb)_3(THF)_5]$ **(6)** in THF containing 0.1 M [*n*-Bu_4N]PF_6 as the electrolyte (CE: Pt, WE: GC, RE: Ag).

S7.1. Reduction of $TipPCl_2$ with complex 6 [considering the monomeric $(Tip)_2Sb^-$ fragment as the reducing agent]

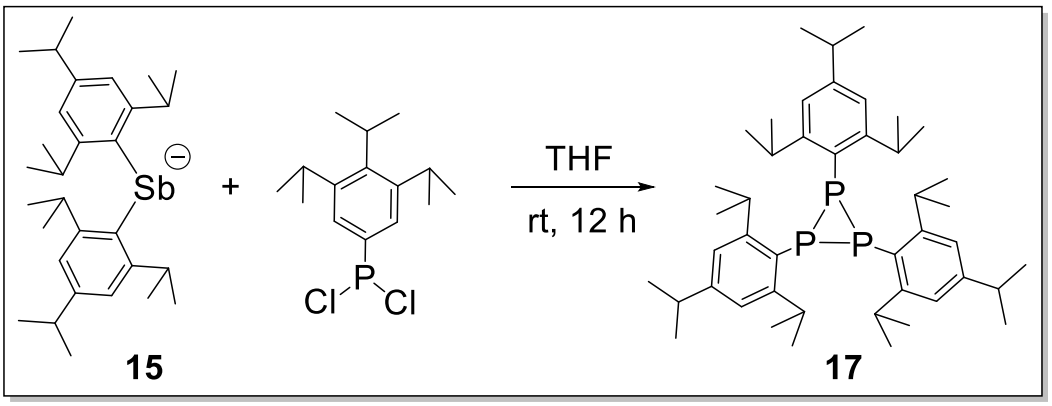

Scheme S12: Synthesis of $(Tip)_3P_3$ (**17**) [1] by the reduction of $TipPCl_2$ using complex **15** as reducing agent.

The pure crystals of complex **6** $[K_3((Tip)_2Sb)_3(THF)_5]$ (198 mg, 0.35 mmol) was taken in an oven-dried 50 ml Schlenk flask and dissolved in dry THF (10 mL). In another Schlenk flask $TipPCl_2$ (106 mg, 0.35 mmol) was taken and dissolved in THF (5 mL), which was then transferred to the solution of complex **6** through a cannula at rt and continued stirring for 12 h. After the addition, color of the reaction mixture turned dark green. THF was removed under vacuum and the solid mass was then characterized as $(Tip)_3P_3$ (**17**) [1] by NMR spectroscopic studies.

^{1}H NMR (400 MHz, C_6D_6, 298 K) *δ*: 6.95 (s, 6H), 3.40 (m, 6H), 2.49 (dt, *J* = 13.9, 6.9 Hz, 3H), 0.95 (d, *J* = 6.9 Hz, 20H), 0.90 (dd, *J* = 6.6, 5.1 Hz, 34H) ppm.

^{31}P NMR (162 MHz, C_6D_6, 298 K) *δ*: -100.73 (d, *J* = 173.2 Hz), -132.80 (t, *J* = 175.8 Hz).

S7.2. Reduction of Cy-cAAC=P-Cl [2] with complex 6 [considering the monomeric $(Tip)_2Sb^-$ fragment as the reducing agent]

The pure crystals of complex **6** $[K_3((Tip)_2Sb)_3(THF)_5]$ (198 mg, 0.35 mmol) was taken in an oven-dried 50 ml Schlenk flask and dissolved in dry THF (10 mL). In another Schlenk flask Cy-cAAC=P-Cl [2] (137 mg, 0.35 mmol) was taken and dissolved in THF (5 mL), which was then transferred to the solution of complex **6** through a cannula at rt and continued stirring for 12 h. After the addition, color of the reaction mixture turned greenish-yellow. THF was removed under vacuum and the solid mass was then characterized as $(Cy\text{-}cAAC)_2P_2$ (**8**) [3] by NMR spectroscopic studies.

^{31}P NMR (162 MHz, THF-D_8, 298 K) *δ*: $(Cy\text{-}cAAC)_2P_2$: 58.47; [3] 48.07 (un-identified), Cy-cAAC=PH: -37.31, -45.52.

The formations of these reaction products suggest that $(Tip)_2Sb^-$ (**5**) [$(Tip)_2Sb^- = (Tip)_2Sb^\bullet + e^-$] being an electron-rich species, transfers an electron to cAAC=PCl (**7**) to form the corresponding radical intermediates; $(cAAC)P^\bullet$ (**7**$^\bullet$), $(Tip)_2Sb^\bullet$ (**3**) and KCl. The two radical intermediates (**7**$^\bullet$, **3**) then undergo energetically more favourable self-dimerization to produce **8** and **4**, respectively (Scheme S13). We believe that the

trinuclear complex **6** acts as three electron donor and hence, reduces the compound **7** to form the dimeric compounds **8** and **4**.

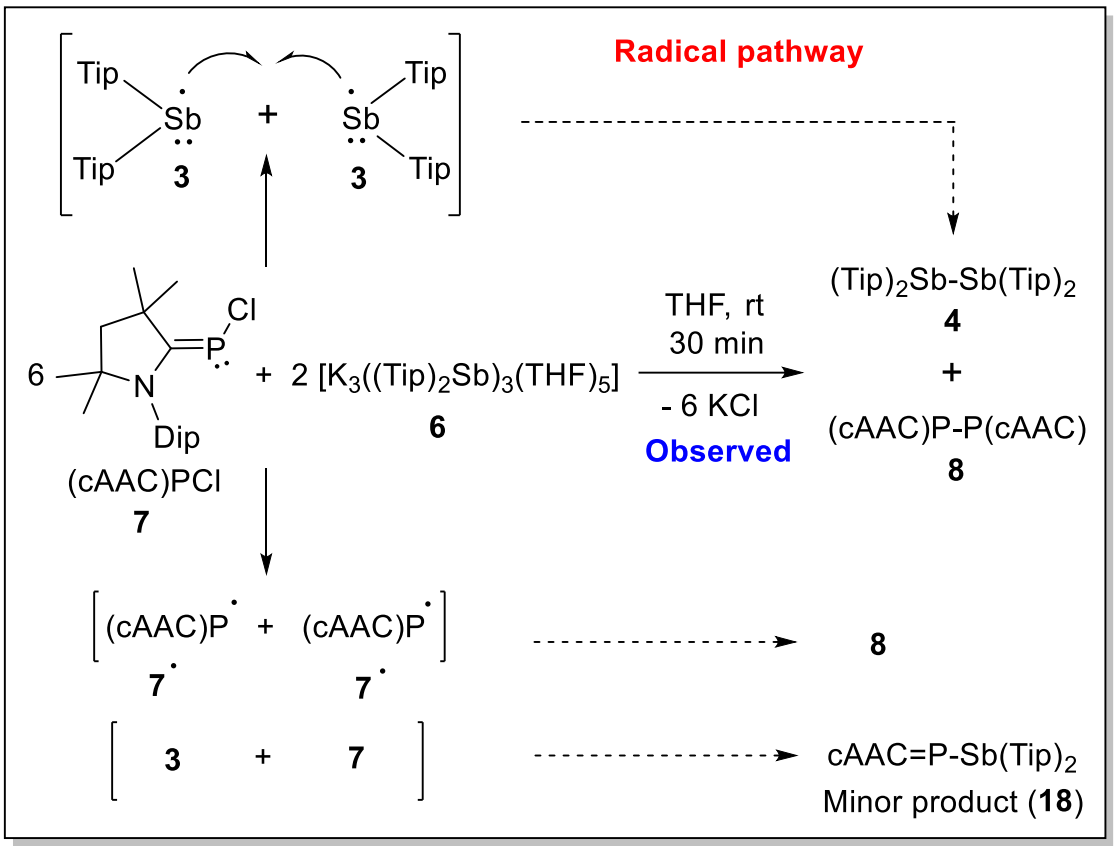

Scheme S13: Reduction of cAAC=PCl (**7**) by compound **6** to generate $cAAC_2P_2$ (**8**).

S8: Computational details

All calculations were performed using Gaussian 09 suite.[4] Geometry optimization was performed at M06-2X [5] /B level of theory, where B was a mixed basis set. B was made up of 6-311G** [6] (for C, H, N & O atoms), def2-TZVPP (for Sb, Cl, P & K atoms) and def2TZVPP effective core potential (for Sb atoms) [7]. Vibrational frequency analysis was also performed at the same level of theory to verify the optimized geometries as true minima (the absence of imaginary frequencies). NBO analysis [8] was performed at M06/def2TZVPP//M06-2X/B level of theory using *NBO version 3.1* program built in Gaussian 09.

Zero-point energy (ZPE) correction was taken from the vibrational frequency calculation output. ZPE corrected free energy values were considered for reaction energetics.

Molecular orbitals (H-atoms are omitted for clarity in all the images of this section):

EDA-NOCV analysis:

The nature of the Sb-Sb bond in $(Tip)_4Sb_2$ (**4**) complex was analysed by energy decomposition analysis (EDA) [9] coupled with natural orbital for chemical valence (NOCV) [10] using ADF 2018.105 program package.[11] EDA-NOCV calculations were carried out at the BP86-D3(BJ)/TZ2P [12] level. EDA-NOCV method involves the decomposition of the intrinsic interaction energy (ΔE_{int}) between two fragments into four energy components as follows:

$$\Delta E_{\text{int}} = \Delta E_{\text{elstat}} + \Delta E_{\text{Pauli}} + \Delta E_{\text{orb}} + \Delta E_{\text{disp}} \quad (1)$$

where the electrostatic ΔE_{elstat} term is originated from the quasi-classical electrostatic interaction between the unperturbed charge distributions of the prepared fragments, the Pauli repulsion ΔE_{Pauli} is the energy change associated with the transformation from the superposition of the unperturbed electron densities of the isolated fragments to the wavefunction, which properly obeys the Pauli principle through explicit anti-symmetrisation and renormalization of the production of the wavefunction. Dispersion interaction, ΔE_{disp} is also obtained as we used D3(BJ). The orbital term ΔE_{orb} comes from the mixing of orbitals, charge transfer and polarization between the isolated fragments. This can be further divided into contributions from each irreducible representation of the point group of the interacting system as follows:

$$\Delta E_{orb} = \sum_{r} \Delta E_{r} \qquad (2)$$

The combined EDA-NOCV method is able to partition the total orbital interactions into pairwise contributions of the orbital interactions which are important in providing a complete picture of the bonding. The charge deformation $\Delta\rho_k(r)$, which comes from the mixing of the orbital pairs $\psi_k(r)$ and $\psi_{-k}(r)$ of the interacting fragments, gives the magnitude and the shape of the charge flow due to the orbital interactions (Equation 3), and the associated orbital energy ΔE_{orb} presents the amount of orbital energy coming from such interaction (Equation 4).

$$\Delta\rho_{orb}(r) = \sum_{k} \Delta\rho_{k}(r) = \sum_{k=1}^{N/2} \nu_k [-\psi_{-k}^2(r) + \psi_k^2(r)] \qquad (3)$$

$$\Delta E_{\text{Orb}} = \sum_{k} \Delta E_{\text{Orb}}^{k} = \sum_{k} \nu_k \left[-F_{-k,-k}^{TS} + F_{k,k}^{TS}\right] \qquad (4)$$

Readers are further referred to the recent reviews articles to know more about the EDA-NOCV method and its application.[13] A very recent report related to equation (1) has been critically discussed by different researchers.[14]

S8.1. Optimization and NBO analysis of $(Tip)_2SbCl$ (1) at M06/def2-TZVPP level of theory.

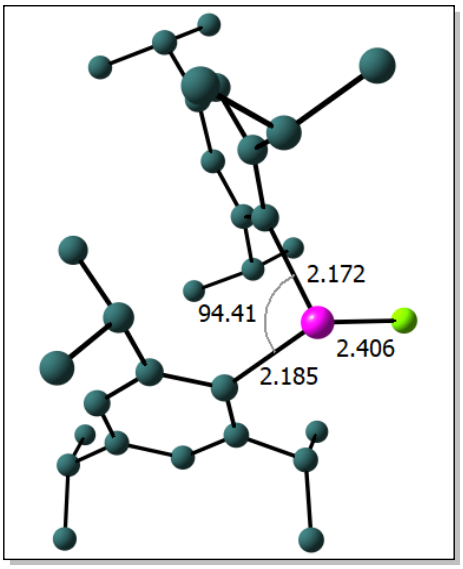

Figure S25: Optimized geometry of $(Tip)_2SbCl$ (**1**) at M06-2X/B level of theory.

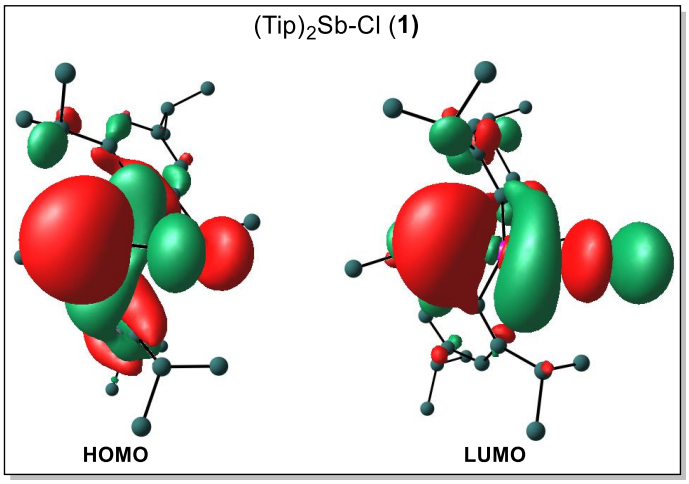

Figure S26: Frontier Molecular orbitals of $(Tip)_2SbCl$ (**1**) calculated at M06-2X/B level of theory.

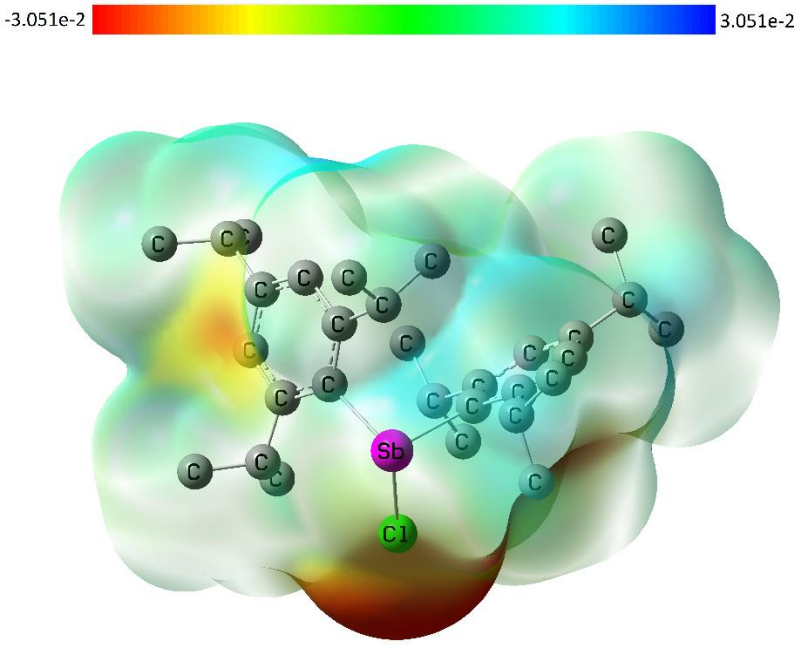

Figure S27: 3D plot of the ***molecular electrostatic potential map*** (in a.u.) of compound **1**.

Table S1: Summary of NBO analysis of $(Tip)_2SbCl$ (**1)** at M06/def2-TZVPP level of theory.

NBO	Occupancy	Atomic contribution	WBI
Sb-Cl	1.981	Sb (94% p) - 22%, Cl (85% p) - 78%	0.732
C2-Sb	1.944	C2 ($sp^{3.16}$) - 68%, Sb (89% p) - 32%	0.819
C10-Sb	1.945	C10 ($sp^{3.19}$) - 68%, Sb (90% p) - 32%,	0.812
Lone Pair on Sb (1)	1.969	$sp^{0.34}$ (s-75%, p-25%)	-

S8.2. Geometry optimization and NBO analysis of the intermediate species, $\mathbf{1}^{\bullet-}$ $[(Tip)_2SbCl]^{\bullet-}$ and 3 $[(Tip)_2SbCl]^{\bullet}$.

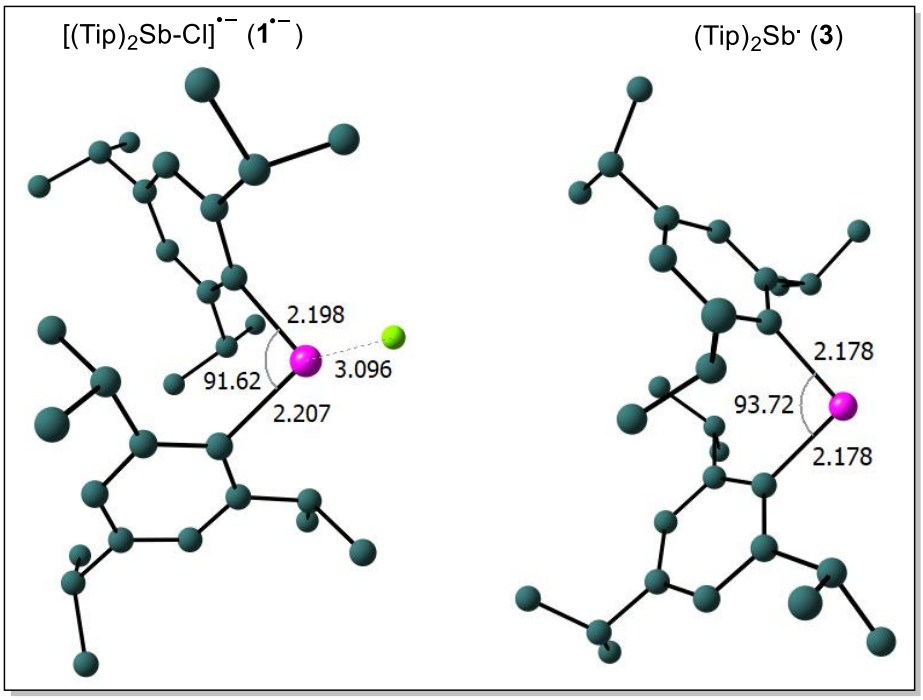

Figure S28: Optimized geometry of $\mathbf{1}^{\bullet-}$ $[(Tip)_2SbCl]^{\bullet-}$ and **3** $[(Tip)_2SbCl]^{\bullet}$ at M06-2X/B level of theory.

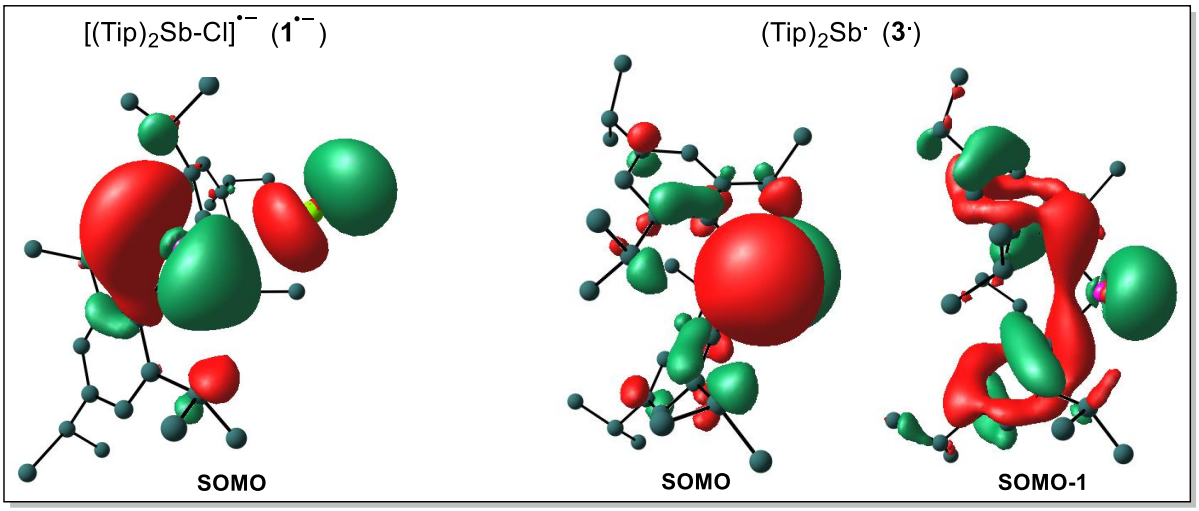

Figure S29: Frontier Molecular orbitals of $\mathbf{1}^{\bullet-}$ $[(Tip)_2SbCl]^{\bullet-}$ and **3** $[(Tip)_2SbCl]^{\bullet}$ at M06-2X/B level of theory.

Table S2: Summary of NBO analysis of $\mathbf{1}^{\bullet-}$ at M06/def2-TZVPP level of theory.

NBO	Occupancy	Atomic contribution	WBI
Sb-Cl	0.991 (β)	Sb (99% p) - 13%, Cl (92% p) - 87%	0.301
Lone pair on Cl (4)	0.960 (α)	84% p	-
C2-Sb	0.968 (α) + 0.966 (β)	C2 ($sp^{2.83}$) - 74%, Sb (93% p) - 26%	0.724
C10-Sb	0.972 (α) + 0.968 (β)	C10 ($sp^{2.84}$) - 72%, Sb (91% p) - 28%,	0.786
Lone Pair on Sb (1)	0.985 (α) + 0.986 (β)	s-85%, p-15%	-
Lone Pair on Sb (2)	0.91633(α)	99.43% p orbital on Sb	-

The presence of additional electron on Cl atom, the highly weakened bonding interaction between Sb-Cl and this bonding interaction carrying only one electron and the presence of an additional electron in the p-orbital of Sb atom is suggestive of [$(Tip)_2SbCl$] radical anion ($\mathbf{1}^{\bullet-}$) being composed of $(Tip)_2Sb^{\bullet}$ (**3**) and the chloride ion.

Table S3: Summary of NBO analysis of **3** [$(Tip)_2Sb^{\bullet}$] at M06-2X/def2-TZVPP level of theory.

NBO	Occupancy	Atomic contribution	WBI
C2-Sb	1.948	C2 ($sp^{2.96}$) - 69%, Sb (89% p) - 31%	0.818
C10-Sb	1.948	C10 ($sp^{2.96}$) - 69%, Sb (89% p) - 31%,	0.819

Lone Pair on Sb (1)	1.978	$sp^{0.34}$ (s-78%, p-22%)	-
Lone Pair on Sb (1)	0.944	p orbital	-

Optimized structure of the intermediate radical anion $1^{\bullet-}$: Evidence for cleaved Sb-Cl bond.

The structure of $\mathbf{1}^{\bullet-}$ is given in the dashed line because even after trying multiple times we were not able to finish the frequency calculation in THF. We have noticed that after optimizing Compound $1^{\cdot-}$, the bond between Sb and Cl has broken and the distance between these two atoms are 3.95 Å. The formation of the radical anion $\mathbf{1}^{\bullet-}$ has also been proved by the solution ESR spectrum of the reaction mixture of compound **1** and KC_8 (see Figure S20).

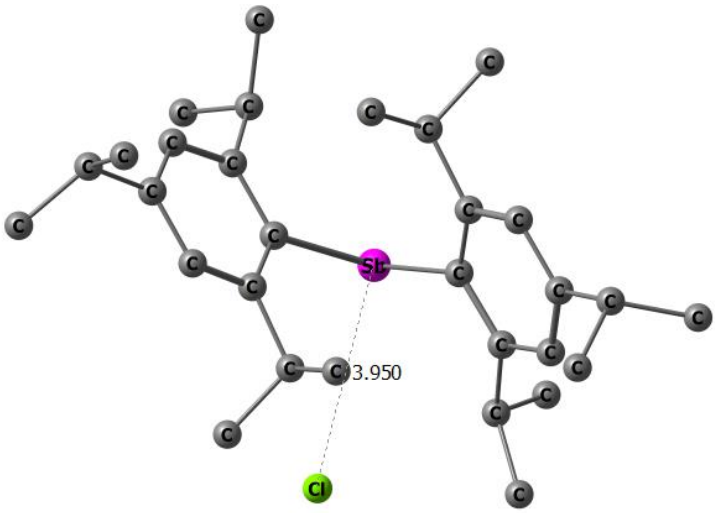

Figure S30: Optimized structure of intermediate $\mathbf{1}^{\bullet-}$ at M06-2X/def2-TZVPP level of theory. Hydrogen atoms are omitted for clarity.

S8.3. Geometry optimization and NBO analysis of $(Tip)_2Sb\text{-}Sb(Tip)_2$ (4).

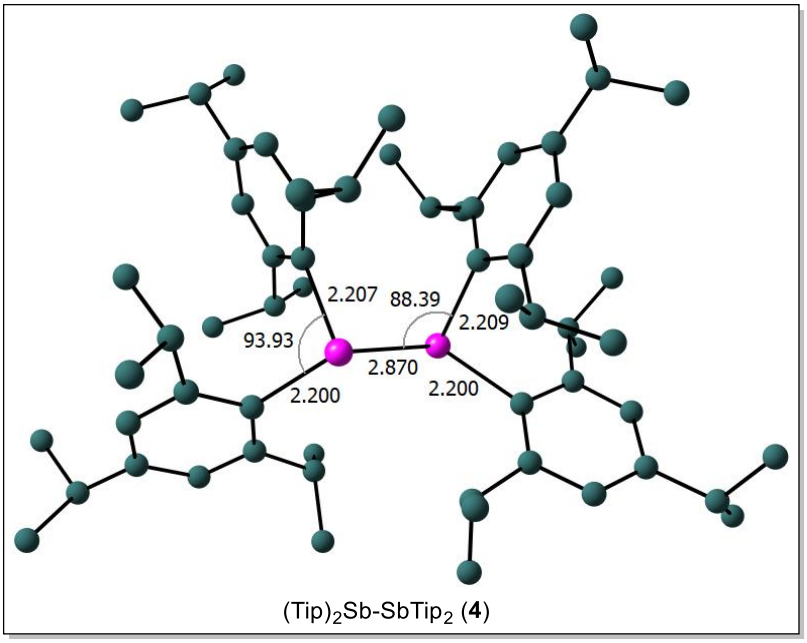

Figure S31: Optimized geometry of $(Tip)_2Sb\text{-}Sb(Tip)_2$ (**4**) at M06-2X/B level of theory.

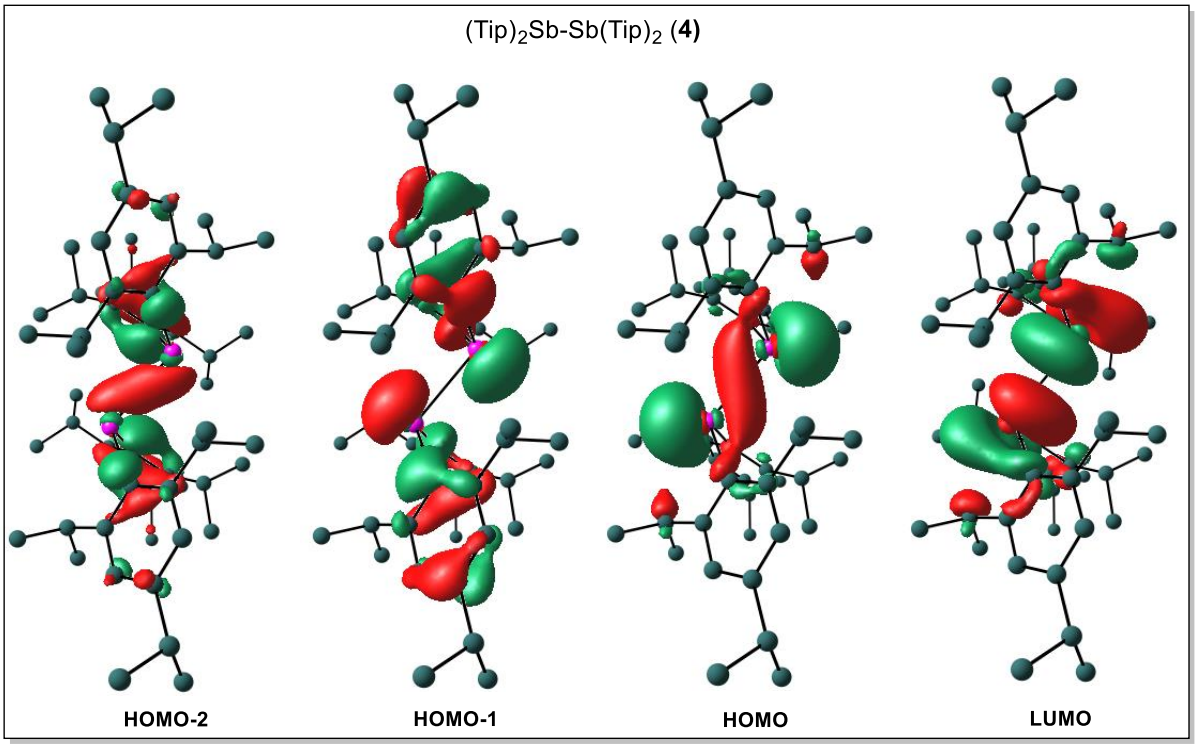

Figure S32: Frontier Molecular orbitals of $(Tip)_2Sb\text{-}Sb(Tip)_2$ (**4**) at M06-2X/B level of theory.

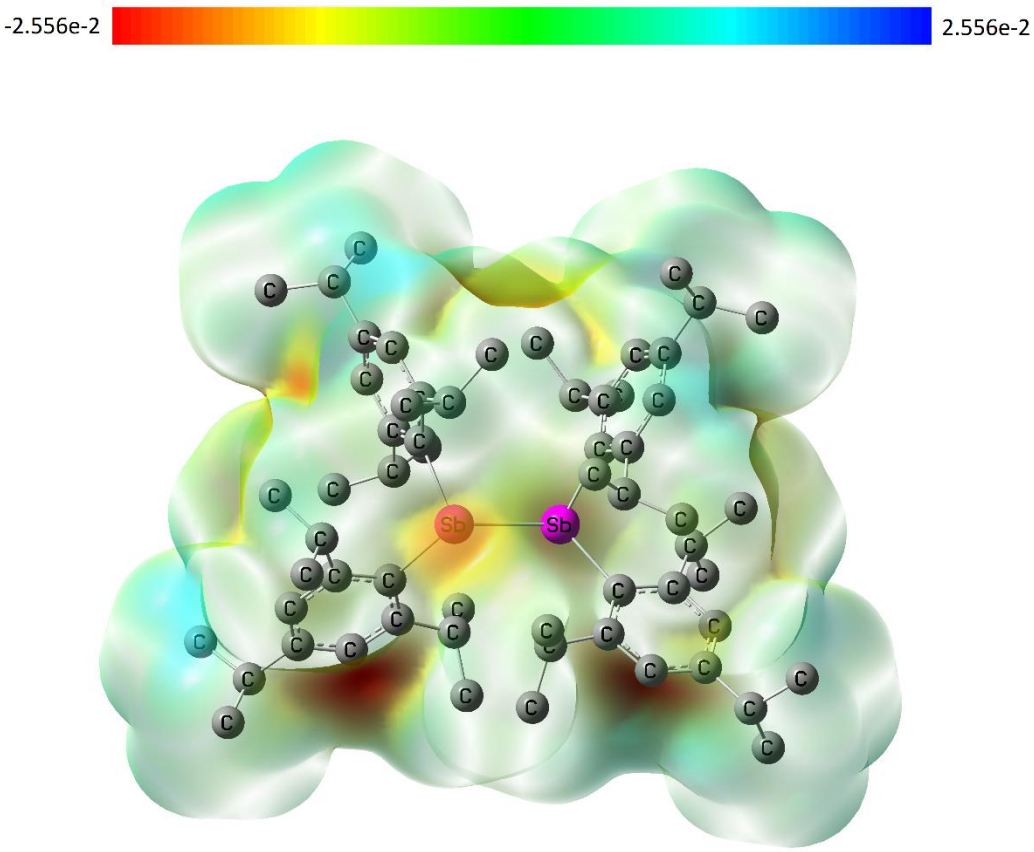

Figure S33: 3D plot of the ***molecular electrostatic potential map*** (in a.u.) of compound **4**.

Table S4: Summary of NBO analysis of $[(Tip)_2Sb\text{-}Sb(Tip)_2]$ **4** at M06/def2-TZVPP level of theory.

NBO	Occupancy	Atomic contribution	WBI
Sb3-Sb78	1.914	Sb (94% p) - 50%, Sb (94% p) - 50%	0.880
C2-Sb3	1.944	C2 (sp^3) - 68%, Sb3 (90% p) - 32%	0.809
C40-Sb3	1.941	C40 (sp^3) - 68%, Sb3 (89% p) - 32%	0.811
C79-Sb78	1.944	C79 (sp^3) - 68%,	0.809

		Sb78 (90% p) - 32%,	
C117-Sb78	1.941	C117 (sp^3) - 68%, Sb78 (90% p) - 32%,	0.811
Lone Pair on Sb3 / Sb78 (1)	1.955	$sp^{0.34}$ (s-74%, p-26%)	-

S8.4. Deformation density plots of compound 4.

$\Delta\rho$, Tip_4Sb_2

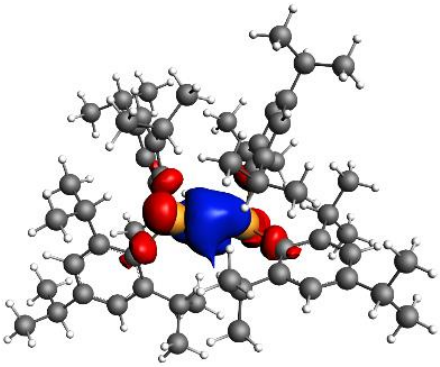

$\Delta\rho_{(2)}$
$\Delta E_{orb(2)}$ = -3.8; $|\nu_{2\alpha}/\nu_{2\beta}|$ = 0.08/0.08

Tip_2Sb (D)

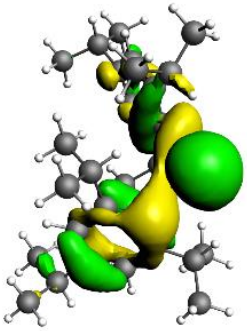

HOMO (ε = -5.74 eV)

Tip_2Sb (D)

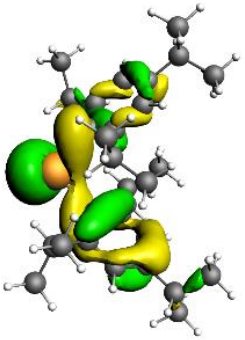

HOMO (ε = -5.76 eV)

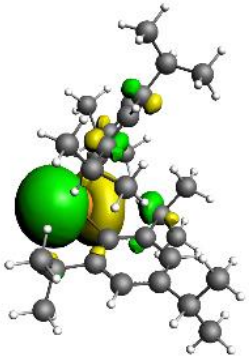

SOMO (ε = -4.12 eV)

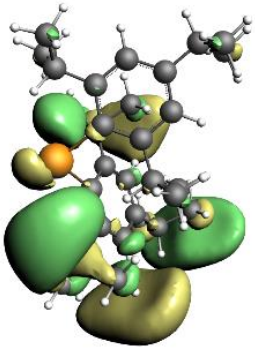

LUMO+15 (ε = 0.84 eV)

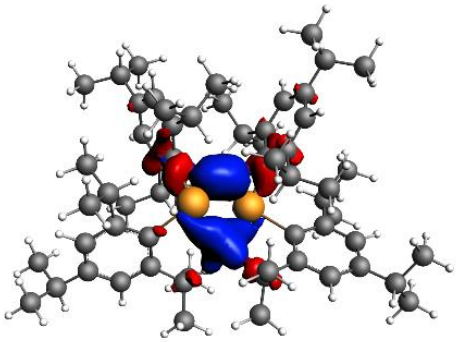

$\Delta\rho_{(3)}$

$\Delta E_{orb(3)}$ = -2.5; $|\nu_{3\alpha}/\nu_{3\beta}|$ = 0.07/0.07

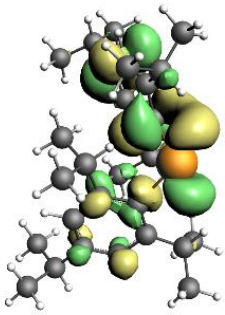

LUMO+2 (ε = -1.24 eV)

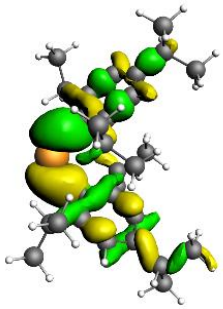

HOMO-5 (ε = -7.04 eV)

Figure 34. The shape of the deformation densities $\Delta\rho_{(2\text{-}3)}$ that correspond to $\Delta E_{orb(2\text{-}3)}$, and the associated MOs of $(Tip)_4Sb_2$ (**4**) and the fragments orbitals of neutral $(Tip)_2Sb$ and $(Tip)_2Sb$ in the doublet state at the BP86-D3(BJ)/TZ2P level. Iso-surface value is 0.0001 for $\Delta\rho_{(2\text{-}3)}$. The eigenvalues $|\nu_n|$ give the size of the charge migration in e. The direction of the charge flow of the deformation densities is red→blue.

Table S5. EDA-NOCV results of Sb-Sb bond of $(Tip)_4Sb_2$ (**4**) compound using two different sets of fragments with different charges and electronic states (S = singlet, D = doublet) and associated bond types at the BP86-D3(BJ)/TZ2P level. Energies are in kcal/mol. The most favorable fragmentation scheme and bond type are given by the smallest ΔE_{orb} value written in red. D = dative and E = electron sharing bond.

Energy	**Interaction**	**$(Tip)_2Sb$ (D) + $(Tip)_2Sb$ (D) (E)**	**$[Tip_2Sb]^+$(S) + $[Tip_2Sb]^-$ (S) (D)**
ΔE_{int}		-65.4	-177.3
ΔE_{Pauli}		156.1	198.9
ΔE_{disp}[a]		-43.0 (19.4%)	-43.0
ΔE_{elstat}[a]		-96.4 (43.5%)	-183.9
ΔE_{orb}[a]		-82.2 (37.1%)	-149.3

$\Delta E_{orb(1)}$[b]	$(Tip)_2Sb–Sb(Tip)_2$ σ e⁻ sharing	-63.1 (76.8%)	-
$\Delta E_{orb(2)}$[b]	$(Tip)_2Sb–Sb(Tip)_2$ polarization	-3.8 (4.6%)	-
$\Delta E_{orb(3)}$[b]	$(Tip)_2Sb←Sb(Tip)_2$ π donation	-2.5 (3.0%)	-
$\Delta E_{orb(rest)}$[b]		-12.8 (15.6%)	-

[a]The values in the parentheses show the contribution to the total attractive interaction $\Delta E_{elstat} + \Delta E_{orb} + \Delta E_{dis}$.

[b]The values in parentheses show the contribution to the total orbital interaction ΔE_{orb}.

S8.5. Comparison between the optimized geometries of Tip_4Sb_2 (4) Mes_4Sb_2 (10) at M06-2X/B level of theory.

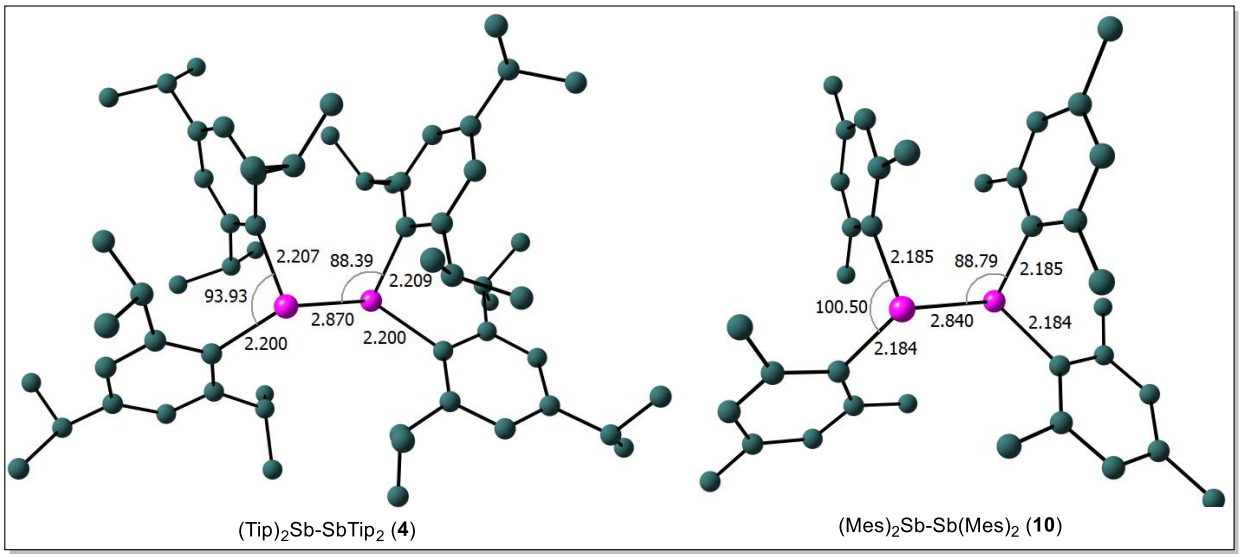

Figure S35: Optimized geometries of **4** and **10** at M06-2X/B level of theory.

S8.4. Geometry optimization and NBO analysis of 5 [(Tip)$_2$Sb]$^-$ at M06/def2-TZVPP level of theory.

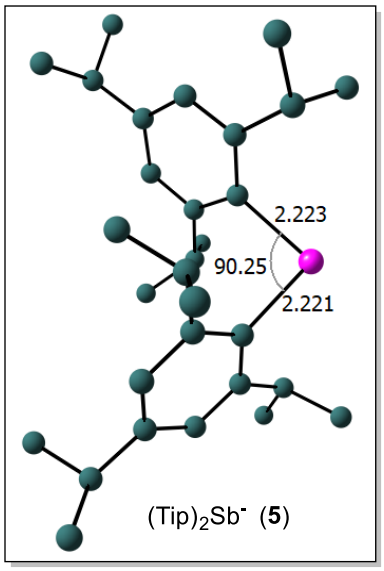

Figure S36: Optimized geometries of **5** [(Tip)$_2$Sb]$^-$ at M06-2X/B level of theory.

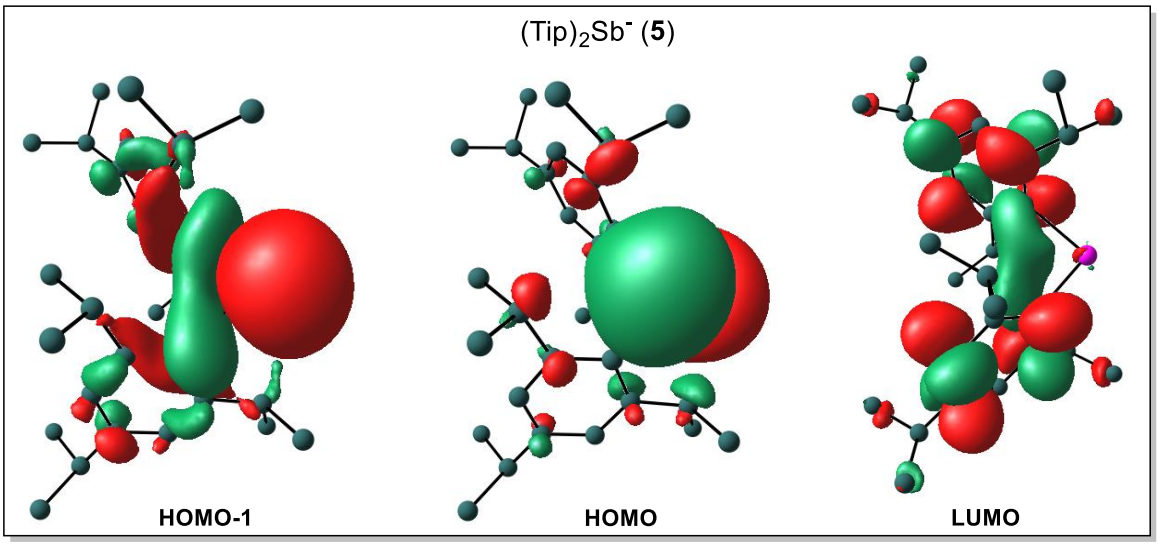

Figure S37: Frontier Molecular orbitals of **5** [(Tip)$_2$Sb]$^-$ at M06-2X/B level of theory.

Table S6: Summary of NBO analysis of **5** $[(Tip)_2Sb]^-$ (singlet) at M06/def2-TZVPP level of theory.

NBO	Occupancy	Atomic contribution	WBI
C2-Sb	1.938	C2 ($sp^{2.58}$) - 71%, Sb (90% p) - 29%	0.835
C10-Sb	1.938	C10 ($sp^{2.58}$) - 71%, Sb (90% p) - 29%,	0.835
Lone Pair on Sb (1)	1.973	s-81%, p-19%	-
Lone Pair on Sb (2)	1.767	p-orbital	-

S8.6. Free energy calculations for Ar_4Sb_2 (10) Ar_4P_2 (19) undergoing oxidation and reduction.

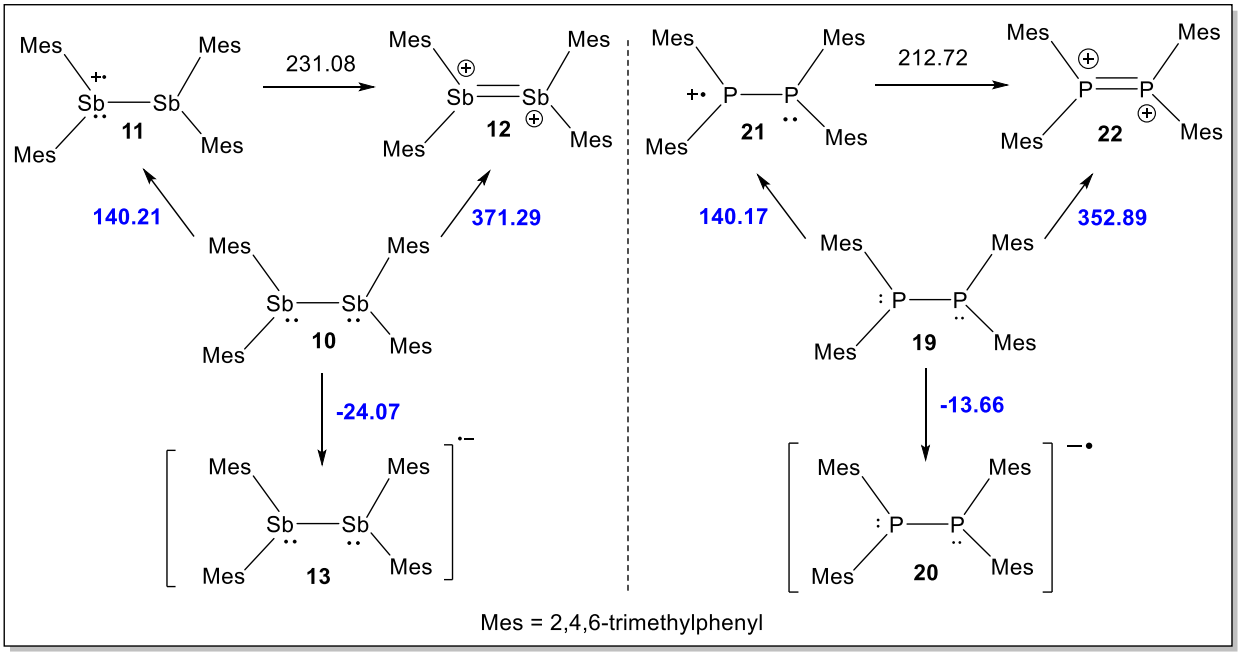

Scheme S14a: Free energy changes for Ar_4Sb_2 (**10**) and Ar_4P_2 (**19**) undergoing oxidation and reduction. Computed at 298 K at M06-2X/B level of theory. Ar = Mes.

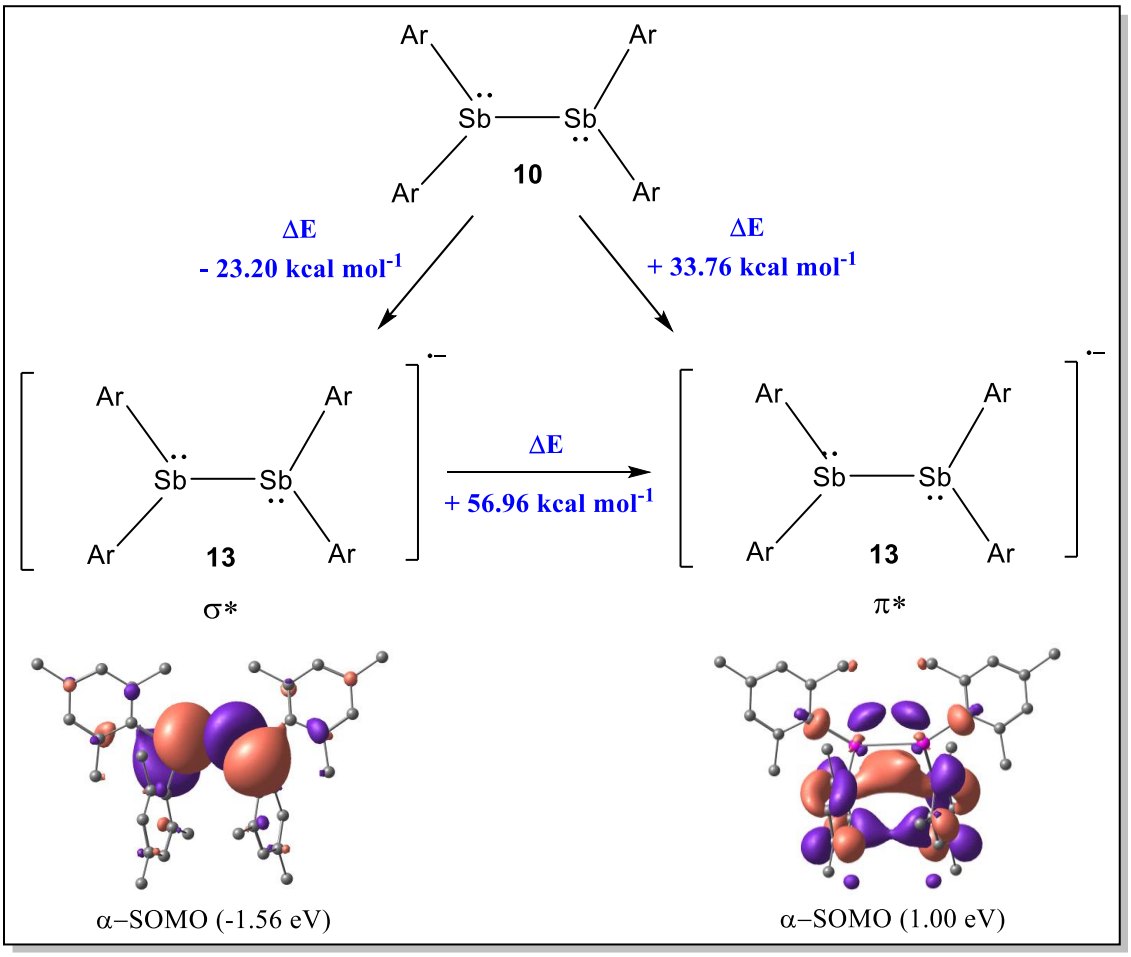

Scheme S14b. The energetics of the electron transfer into the σ* and π* orbitals of **13**.

The stark difference between the oxidation of **11** and the reduction of **4** can be attributed to the very high endothermicity (ΔG = 140.21 kcal/mol) for the formation of the radical-cation $(Mes)_4Sb_2^{\bullet+}$ (**11**) from **10**. The unpaired electron on **11** is shared equally by Sb atoms (spin density = 0.44 each). The unit positive charge is present on Sb (NPA charge = 1.08). The subsequent oxidation of **10** to the dication $(Mes)_4Sb_2^{2+}$ (**12**) is also highly endothermic (ΔG = 231.08 kcal/mol). The Sb atoms in **12** are doubly bonded with the bonds having dominant p character (78 to 85%) and occupancy of 1.72 to 1.80. However, the formation of the corresponding radical-anion $(Mes)_4Sb_2^{\bullet-}$ (**13**) from **10** was found to be highly favourable (ΔG = - 24.07 kcal/mol). The reduction of **4** using KC_8, produced **6**. This reaction proceeds via consecutive one electron reduction. Theoretical calculations showed that the first step of reduction of **10** (Tip-group of **4** has been replaced by the Mes- group, and used for the further calculations

to minimize the computational time) is exothermic (ΔG = -24.07 kcal/mol) and forms a possible intermediate, $(Mes)_4Sb_2^{\bullet-}$ (**13**) in this reaction. The calculated Sb-Sb bond length in **13** was increased by 75 pm relative to the Sb-Sb bond length observed in **10**. The WBI decreased from 0.9 in **10** to 0.24 in **13**. The low energy gap (1.8 eV) between the frontier SOMOs indicate the possibility of further reduction. Attempts at optimizing the product of two-electron reduction of **10**, i.e. dianionic $[(Mes)_4Sb_2]^{2-}$, led to the fragmentation to generate the $(Mes)Sb^-$ anion as expected from the experimental CV data (see Figure 7 in the Main Article for CV of THF solution of Tip_4Sb_2 (**4**)).

A similar theoretical calculation had been carried out for Ar_4P_2, **19** (Ar = Mes) to ascertain their similarities/dissimilarities with that of the corresponding distibine **10** (see SI). It was found that the reduction of Mes_4P_2 to its corresponding radical anion is also exergonic but the magnitude of the free energy is less compared to antimony counterpart. A similar trend was also observed for the oxidation processes.

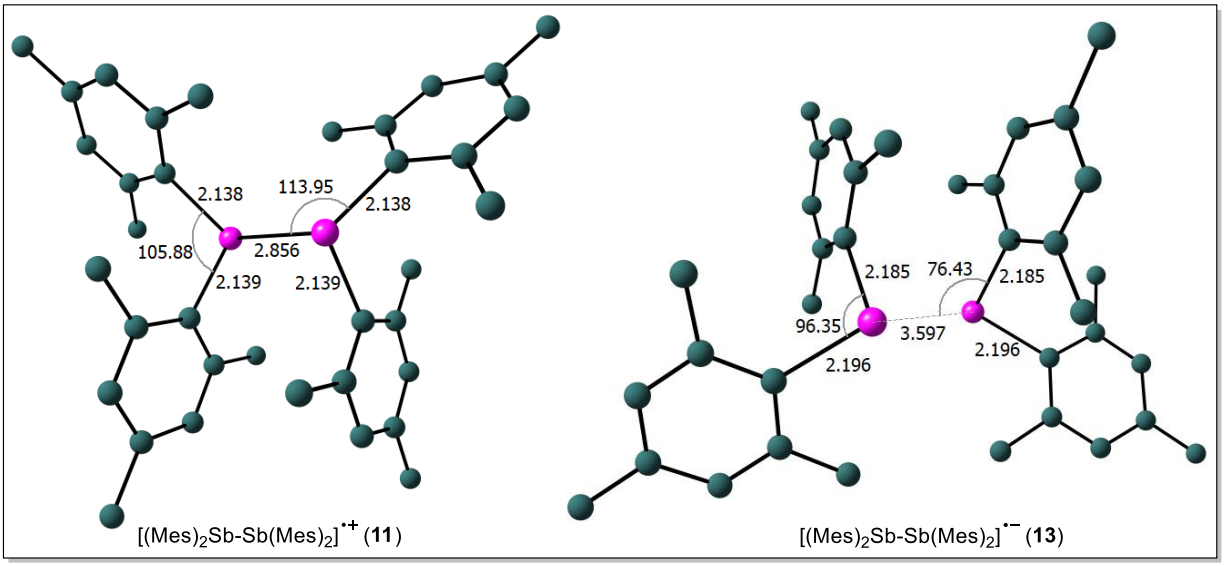

Figure S38: Optimized geometries of **11** and **13** at M06-2X/B level of theory.

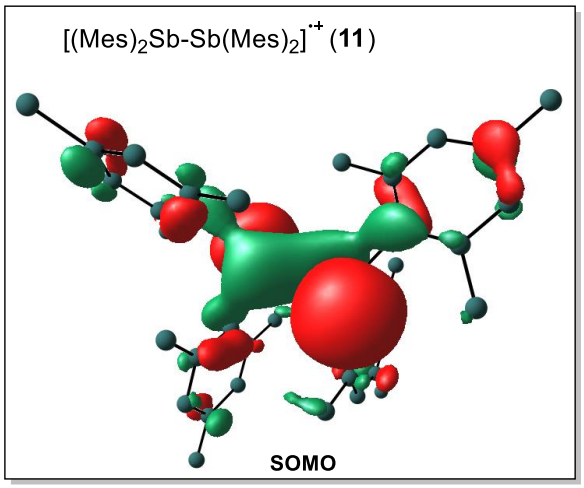

Figure S39: SOMO of the radical cation **11**.

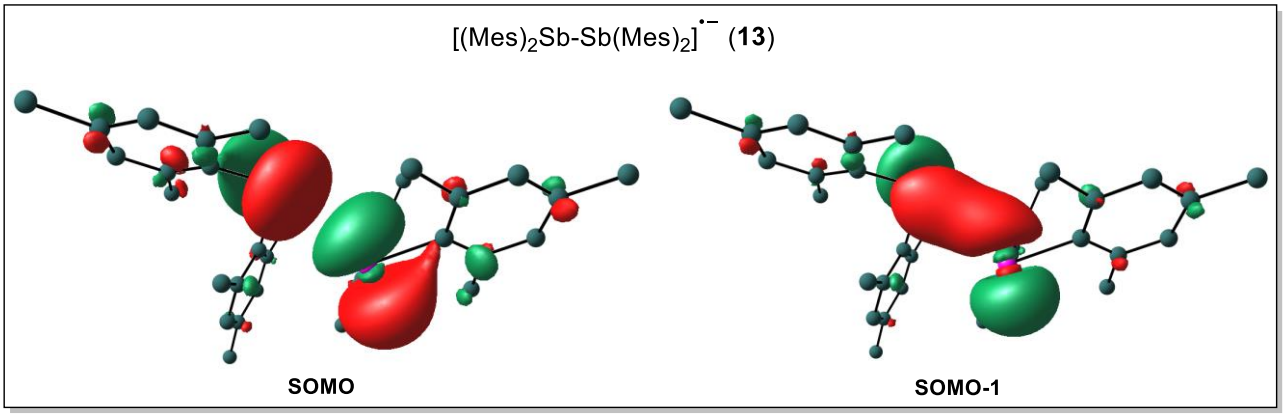

Figure S40: Frontier Molecular Orbitals of the radical anion **13**.

Table S7: HOMO-LUMO energy gaps of compounds **1**, **4**, **10** and various intermediate species in eV.

Compound	***HOMO-LUMO gap (eV)***
1	5.00
1$^{\bullet-}$	2.28 (α-β)
(**1-Cl**)$^{+}$	3.25
3	4.99 (α-β)
4 / **10**	4.05 / 4.32

5 (singlet)	3.04
11	1.71 (α-β)
13	1.81 (α-β)

S8.7. Additional calculations on compound 1 at different levels of theory.

Geometry optimization for compound **1** (in gas phase) was performed at M06-2X/def2-TZVPP level of theory and def2-TZVPP effective core potential (for Sb atoms). Vibrational frequency analysis was also performed at the same level of theory to verify the optimized geometries as true minima (the absence of imaginary frequencies). NBO analysis was performed at M06/def2-TZVPP//M06-2X/def2-TZVPP level of theory using *NBO version 3.1* program built in Gaussian 09.

Zero-point energy (ZPE) correction was taken from the vibrational frequency calculation output. ZPE corrected free energy values were considered for reaction energetics.

HOMO (-7.44) LUMO (-0.37)

Figure 41a: Molecular orbitals of Tip_2SbCl (**1**) in gas phase. The values in the parenthesis indicates the energy of the orbital in eV. H-atoms are omitted for clarity.

Table S8a: Summary of NBO analysis of **1** at M06/def2-TZVPP level of theory (in gas phase).

NBO	Occupancy	Atomic contribution	WBI
Sb1-Cl	1.982	Sb (93% p) - 22%, Cl (83% p) - 78%	0.732
C2-Sb1	1.946	C2 ($sp^{3.08}$) - 68%, Sb (89% p) - 32%	0.808
C10-Sb1	1.949	C10 ($sp^{3.10}$) - 69%, Sb (88% p) - 31%,	0.801
Lone Pair on Sb1 (1)	1.975	$sp^{0.41}$ (s-71%, p-29%)	-

The NBO analysis was performed on the molecules to understand the bonding scenario. On the basis of this, the C2/C10 contribute 68-69% in the C2/C10-Sb1 bond. The Wiberg Bond Index (WBI) indicates that these bonds are single bond. Their bond occupancy is also falling in the same region (~1.95). The Sb1-Cl72 bond is more polarized towards Cl atom (78%). The lone pair located on the Sb1 is majorly of s type. The significant contribution of HOMO is from the Sb lone pair and slightly delocalized over the aryl rings. The major contribution of LUMO is from the Sb1-C2 bond.

The NBO analysis of compound **1** was also conducted in THF using the solvation model, Polarizable Continuum Model (PCM). The observations were very similar to that of the gaseous phase. The relevant findings are summarized in the Table S8b.

Table S8b: Summary of NBO analysis of **1** at M06/def2-TZVPP level of theory in THF.

NBO	Occupancy	Atomic contribution	WBI
Sb1-Cl	1.983	Sb (94% p) - 20%, Cl (82% p) - 80%	0.671
C2-Sb1	1.946	C2 ($sp^{3.08}$) - 69%, Sb (88% p) - 31%	0.808
C10-Sb1	1.949	C10 ($sp^{3.11}$) - 69%, Sb (88% p) - 31%,	0.803
Lone Pair on Sb1 (1)	1.975	$sp^{0.40}$ (s-71%, p-28%)	-

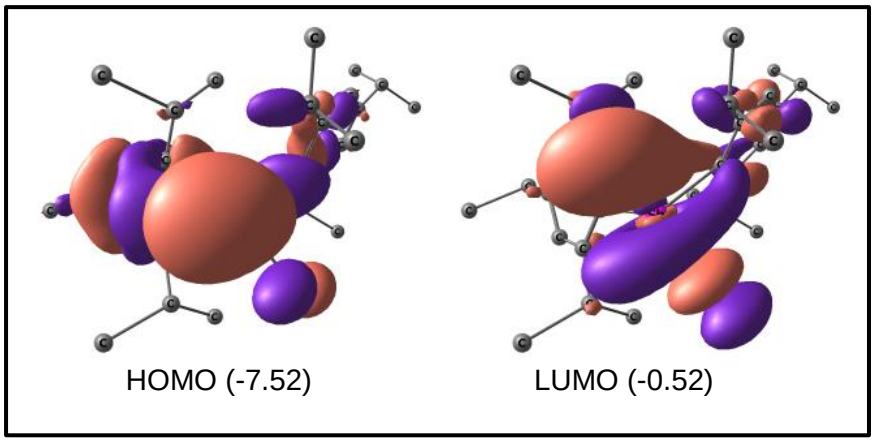

Figure 41b: Molecular orbitals of Tip_2SbCl (**1**) in THF. The values in the parenthesis indicates the energy of the orbital in eV. H-atoms are omitted for clarity.

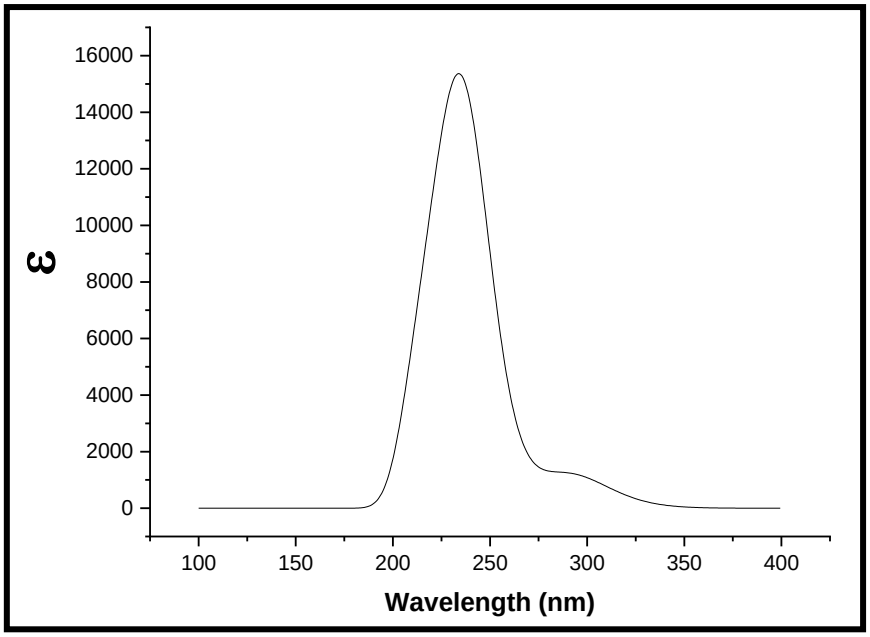

Figure S42: Predicted UV-Vis spectra for **1** at M06-2X/def2-TZVPP level of theory in gas phase.

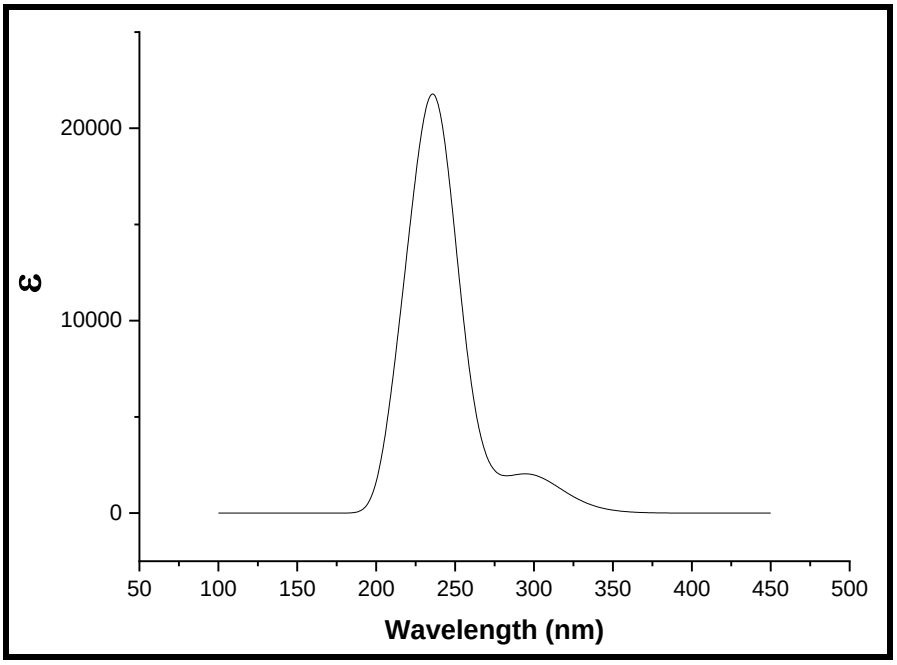

Figure S43: Predicted UV-Vis spectra for **1** at M06-2X/def2-TZVPP level of theory in THF.

The UV-Vis spectrum in THF has been simulated using the solvent model, Polarizable Continuum Model (PCM). A strong absorption is observed at 236 nm. The maximum oscillator strength is observed at 239 nm corresponding to the transition HOMO to LUMO+1. The energy required for this transition is 5.18 eV.

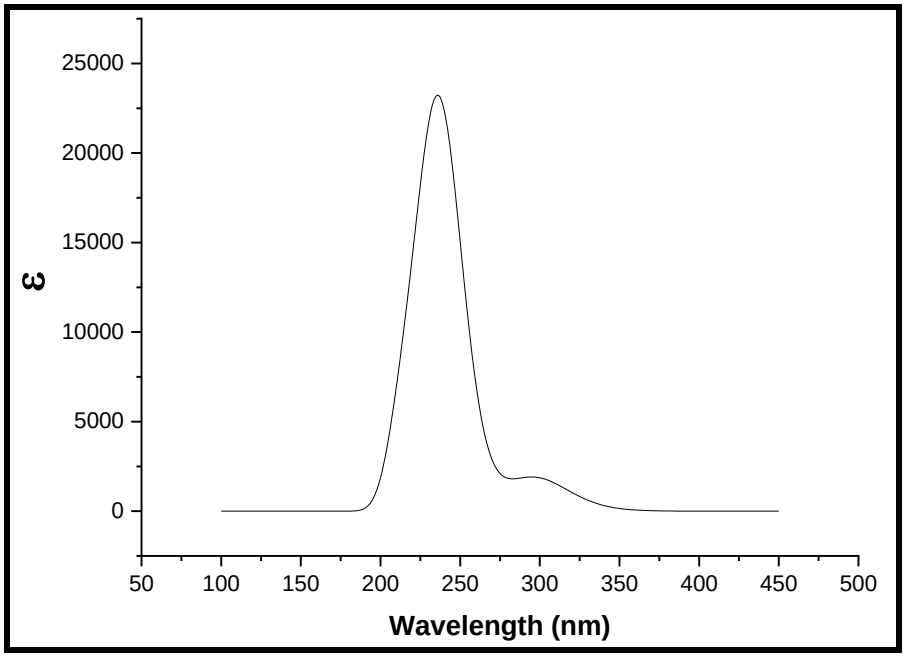

Figure S44: Predicted UV-Vis spectra for **1** at M06-2X/def2-TZVPP level of theory in Toluene.

The simulated UV-Vis spectrum in toluene has been generated using the solvent model, Polarizable Continuum Model (PCM). Strong absorption is observed at 236 nm. The maximum oscillator strength is observed at 239 nm corresponding to the transition HOMO to LUMO+1. The energy required for this transition is 5.19 eV.

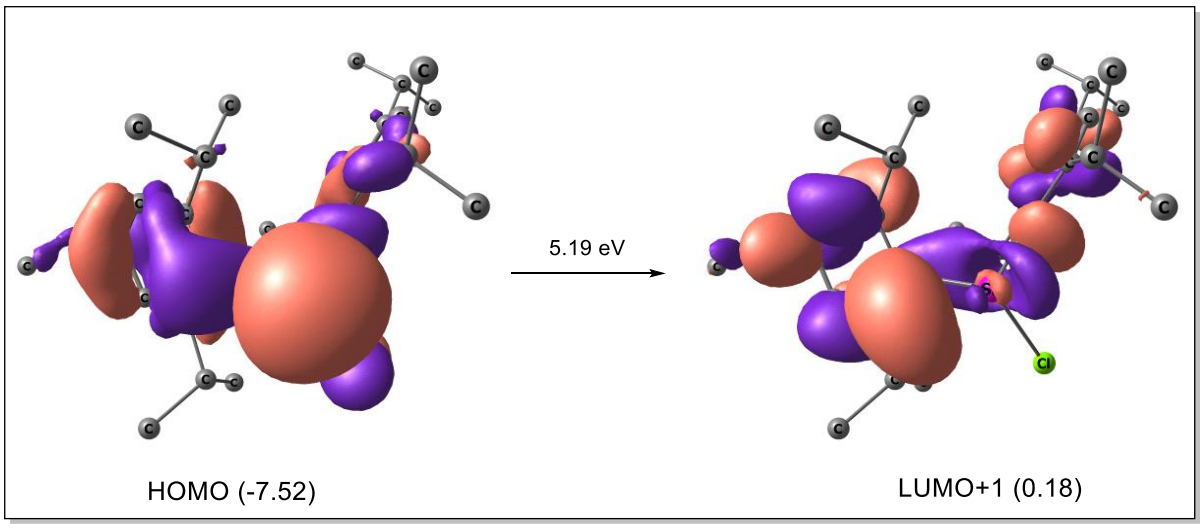

Figure S45: The orbitals involved in the transition. The values in the parenthesis indicates the energy of the orbital in eV. H-atoms are omitted for clarity in all the images of this section

S8.8. Calculation of Bond Dissociation energy (BDE) for Tip_2SbCl (in THF):

The fragments, $Tip_2Sb^{\bullet}$ and $Cl^{\bullet}$, were optimized in M06-2X/def2-TZVPP in THF using the solvent model, PCM. BDE is calculated as the energy difference between products of dissociation and initial system.

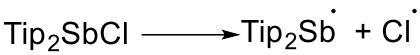

Fragment	Total energy (Hartrees)
$Tip_2Sb^{\bullet}$	-1410.9887742
$Cl^{\bullet}$	-460.1333662
Tip_2SbCl	-1871.2430656

$BDE_{Tip2SbCl}$ = (-1410.9887742+ -460.1333662) – (-1871.2430656)

= -1871.1221404 – (-1871.2430656)

= 0.1209252 Hartrees

= 75.88 kcal/mol (1 Hartree = 627.51 kcal/mol)

S8.9. Calculation of Electron Affinity (EA) for Tip_2SbCl (in THF):

Electron affinity of an atom is defined as the change in the energy of a neutral atom when it gains an electron. The compounds, $Tip_2SbCl^{\bullet-}$ and Tip_2SbCl, were optimized in M06-2X/def2-TZVPP in THF using the solvent model, PCM.

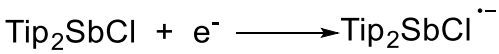

Compound	Total energy (Hartrees)
$Tip_2SbCl^{\bullet-}$	-1871.3516777
Tip_2SbCl	-1871.2430656

$EA_{Tip2SbCl}$ = (-1871.3516777) – (-1871.2430656)

= -0.1086121 Hartrees

= -68.15 kcal/mol (1 Hartree = 627.51 kcal/mol)

The negative sign indicates the release of energy.

S8.10. QTAIM analysis of compound 1:

Quantum theory of atoms in molecules (QTAIM) calculations have been carried out to explore the bonding pattern and electronic interaction of C-Sb. The results are summarized in Table S9. The analysis shows that the electron density ($\boldsymbol{\rho}_r$) at Sb1-C2/C10 bond critical point (BCP) is 0.11 au, and the bond critical point is located almost in the middle of the Sb1-C2/C10 bond which indicates that the bonds are almost equally polarised between the atoms. The Sb1-C2/C10 bonds show positive Laplacian [$\nabla^2\boldsymbol{\rho}$ (r)], which is attributed to the fact that negative Laplacian does not hold good for heavy atoms. The total energy density (**H(r)**) is negative for the electron sharing interactions. The magnitude reflects the covalence of the interaction. The low negative **H(r)** at BCP indicates closed shell interactions. The ellipticity ($\boldsymbol{\varepsilon}_{BCP} = \lambda_1/\lambda_2 - 1$) is a measure of bond order. The ε of selected bonds are given Table S9. They are slightly deviated from zero. So the bond can be considered as a single bond. The ε reaches maximum for a double bond. The ε of formal double bond is of ethylene is 0.45.

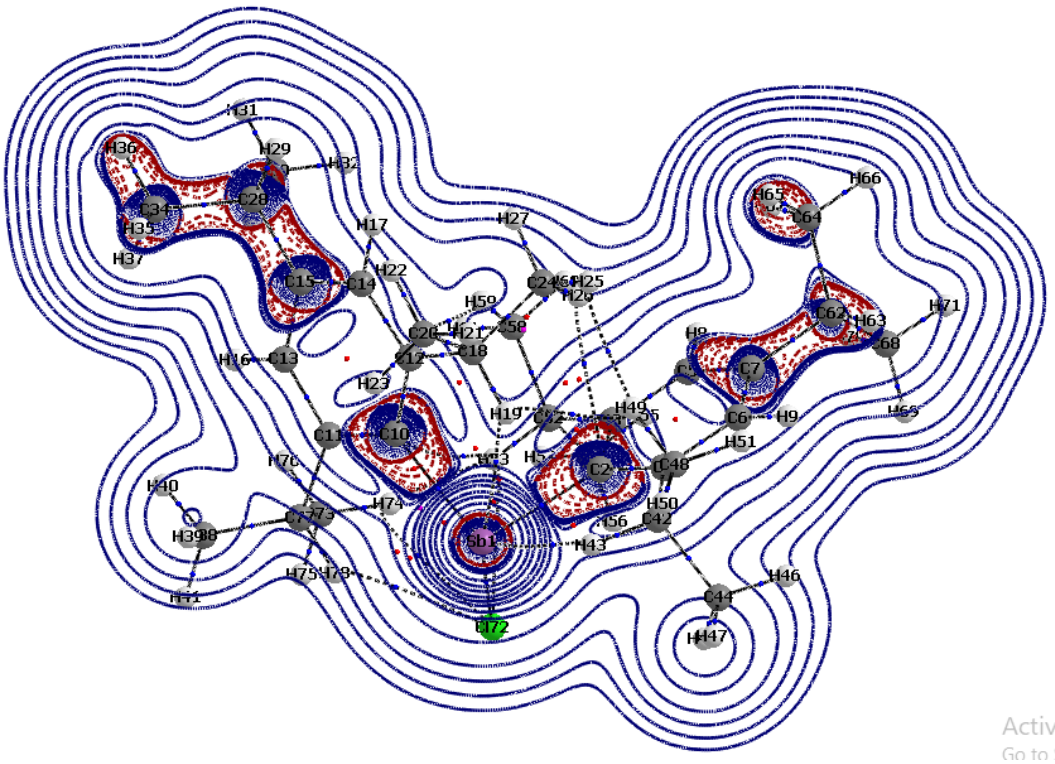

Figure S46: Electron density distribution in contour plot for **1**. Contour plot of Laplacian distribution [$\nabla^2\boldsymbol{\rho}$ (r)] in the C2-Sb1-C10 plane of **1**. Solid blue lines indicate the areas of charge concentration ($\nabla^2\boldsymbol{\rho}$ (r) < 0). Solid lines connecting atomic nuclei (black) are the bond paths. Small blue spheres on the bond path indicates the BCP.

Table S9. AIM results of the C-Sb and Sb-Cl bonds of **1** at the M06-2x/def2-TZVPP level of theory. The values are in au.

	$\boldsymbol{\rho(r)}$	$\nabla^2\boldsymbol{\rho(r)}$	H(r)	V(r)	G(r)	ε_{BCP}
Sb1 - C2	+0.108716	+0.058625	-0.048244	-0.111145	0.062901	+0.040157
Sb1 - C10	+0.106032	+0.058784	-0.046098	-0.106891	0.060793	+0.103252
Sb1 - Cl72	+0.075754	+0.075754	-0.024233	-0.078199	0.053966	+0.049197

S8.11. Optimized geometry and NBO analysis of complex 6 at M06-2x/def2-TZVPP level of theory

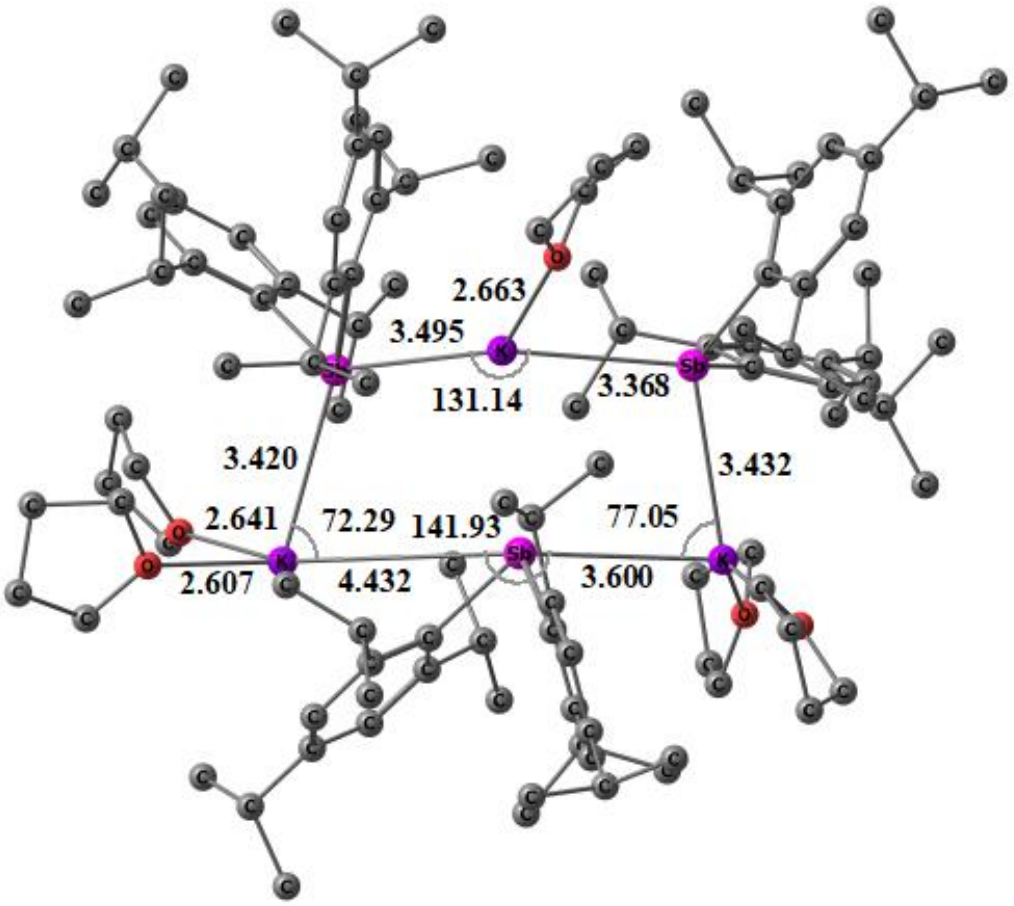

Figure S47. Optimized geometry of complex **6** at M06-2x/def2-TZVPP level of theory. H atoms are omitted for clarity.

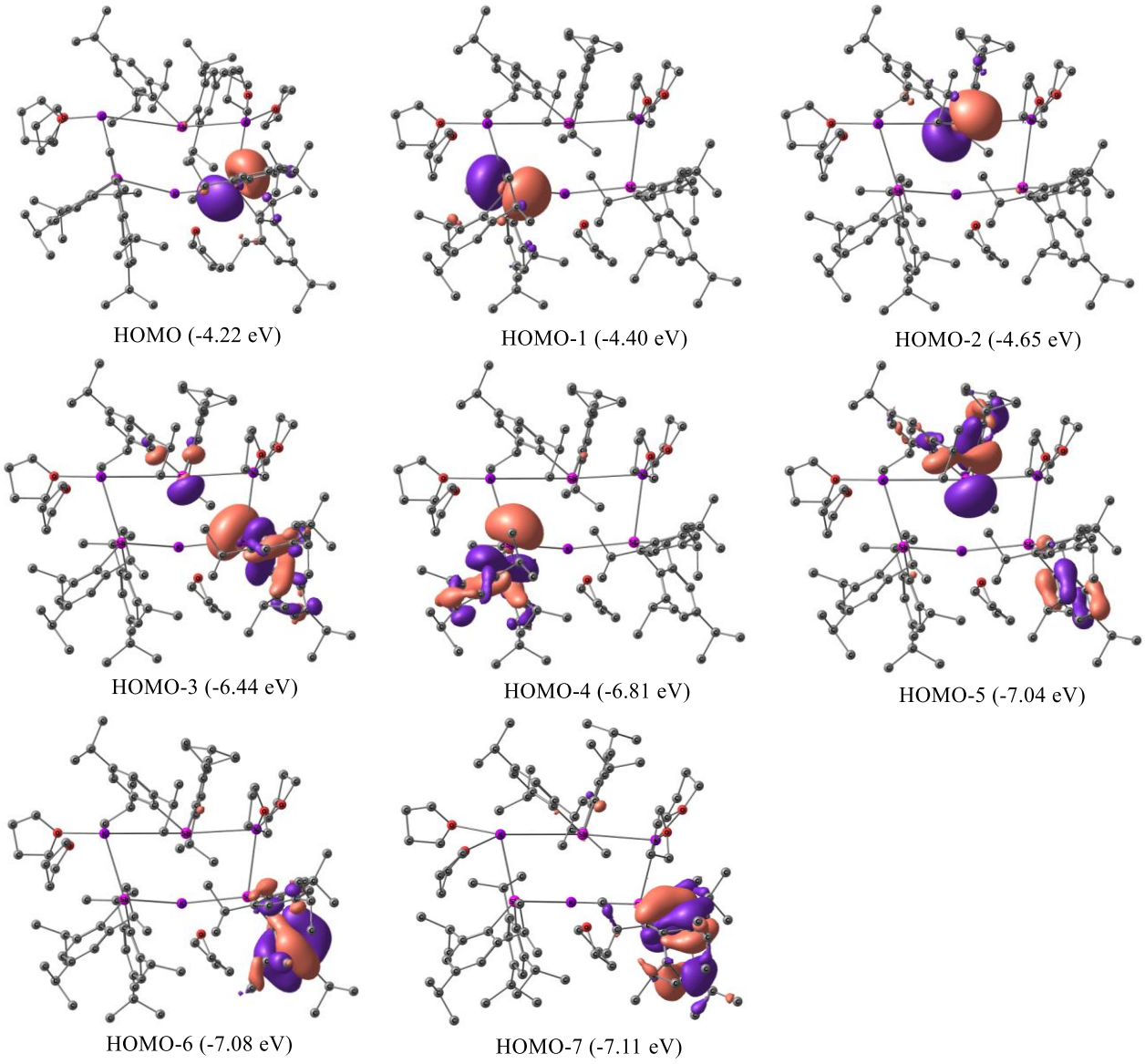

Figure S48: Frontier Molecular Orbitals of **6** at M06-2x/def2-TZVPP level of theory (in gas phase).

The molecular orbitals (MO) from HOMO to HOMO-2 represents the lone pair of electrons in p orbitals, while MO from HOMO-3 to HOMO-5 represents lone pair of electrons in 's' orbitals of the three Sb atoms respectively. The molecular orbitals suggest that the lone pairs of electrons are oriented slightly perpendicular to the Sb-K bond axis. HOMO-6 and HOMO-7 indicate the π electron delocalization on the aromatic ring. The results of NBO calculations show very small Wiberg bond indices 0.05-0.07 for Sb-K bond and correlated well with the positive total energy densities and low electron densities of AIM analysis suggesting Sb-K ionic interactions. No bond occupancies were observed for Sb-K bonds. While the C-Sb bonds show WBI values

of 0.80-0.81 with an occupancy of 1.94 e and spin density majorly concentrated on C atoms (70-71%).

Table S10: NBO analysis of complex **6** at M06-2x/def2-TZVPP level of theory.

NBO	Occupancy	Atomic contribution %	WBI
Sb-K	-	-	0.05
C-Sb	1.95	C: 70.1, s(26.9), p(73.1) Sb: 29.9, s(11.6), p(88.4)	0.81
C-Sb	1.95	C: 71.1, s(27.3), p(72.7) Sb: 28.9, s(10.6), p(89.4)	0.80

S8.12. QTAIM analysis on complex 6

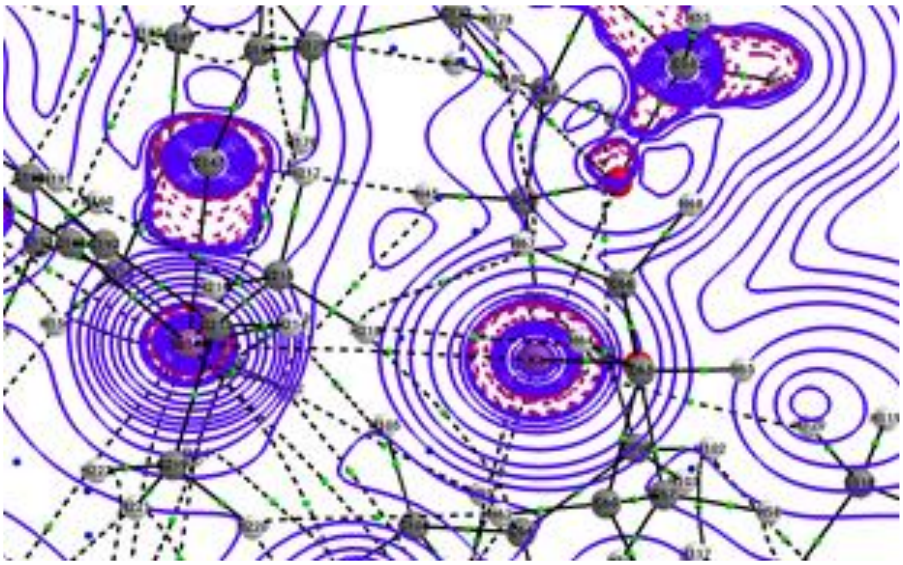

Figure S49a. Electron density distribution in contour plot for **6**. Contour plot of Laplacian distribution [$\nabla^2\boldsymbol{\rho}$ (r)] in the C-Sb-K plane of **6**. Solid blue lines indicate the areas of charge concentration ($\nabla^2\boldsymbol{\rho}$ (r) < 0) while dotted purple lines denotes charge depletion ($\nabla^2\boldsymbol{\rho}$ (r) > 0). Solid lines connecting atomic nuclei (black) are the bond paths and those thick solid blue lines separating the atomic basins indicates the zero-flux surface crossing the molecular plane.

Quantum theory of atoms in molecules (QTAIM) calculations have been carried out to explore the bonding pattern of C-Sb and Sb-K bonds in Sb-trimer complex. The results summarized in Table S11 shows that, the BCPs at Sb-C bonds are characterized with low electron densities (0.088 to 0.0092 au) and the bonds are almost equally polarised between the atoms. The Sb-C bonds show positive Laplacian [$\nabla^2\boldsymbol{\rho}$ (r)] which is attributed to the fact that negative Laplacian does not hold good for heavy atoms.[15] The low negative total energy density **H(r)** (-0.028 to -0.034) at BCP indicates closed shell interactions. The Sb-K bonds of Sb-trimer complex shows very low electron densities (0.01 to 0.014) at BCP's. The positive total energy density **H(r)** and very low Laplacian values at BCP suggests very weak ionic interactions between Sb and K atoms. The ellipticity ($\varepsilon_{BCP} = \lambda_1/\lambda_2 - 1$) is a measure of bond order and the ellipticity values from Table S11 are slightly deviated from the cylindrical contours of electron density expected for a single bond [16] (0.1) but the deviation is very less (0.095-0.167), indicating a C-Sb and Sb-K single bond.

Table S11. AIM results of the C-Sb and Sb-K bonds of complex **6** at the M06-2x/def2TZVPP level of theory. The values are in au.

	$\rho(r)$	$\nabla^2\rho(r)$	H(r)	V(r)	G(r)	ε_{BCP}
Sb1-C1	0.090	+0.134	-0.032	-0.098	+0.066	0.145
Sb1-C2	0.088	+0.136	-0.030	-0.095	+0.065	0.167
Sb1-K1	0.012	+0.035	+0.001	-0.006	+0.007	0.150
Sb2-C3	0.092	+0.137	-0.034	-0.101	+0.067	0.155
Sb2-C4	0.089	+0.140	-0.032	-0.098	+0.066	0.151
Sb2-K2	0.014	+0.040	+0.004	-0.005	+0.009	0.114
Sb3-C5	0.088	+0.134	-0.031	-0.096	+0.065	0.152
Sb3-C6	0.088	+0.144	-0.028	-0.097	+0.069	0.150
Sb3-K3	0.010	+0.030	+0.001	-0.004	+0.005	0.095

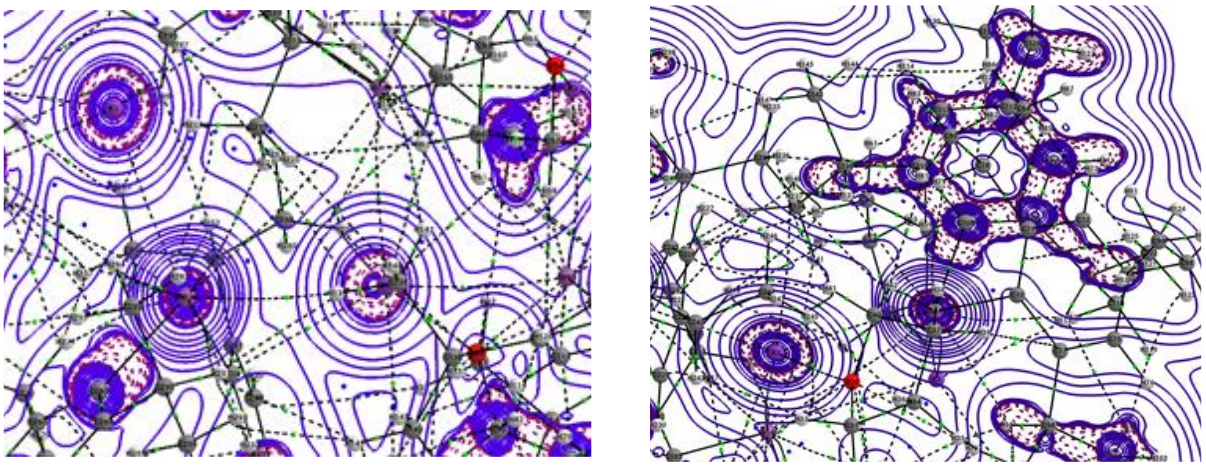

A B

Figure S49b. Electron density distribution in contour plot for **6**. Contour plot of Laplacian distribution [$\nabla^2\boldsymbol{\rho}$ (r)] in the C2-Sb2-K2 (A) and C3-Sb3-K3 plane (B) of **6**.

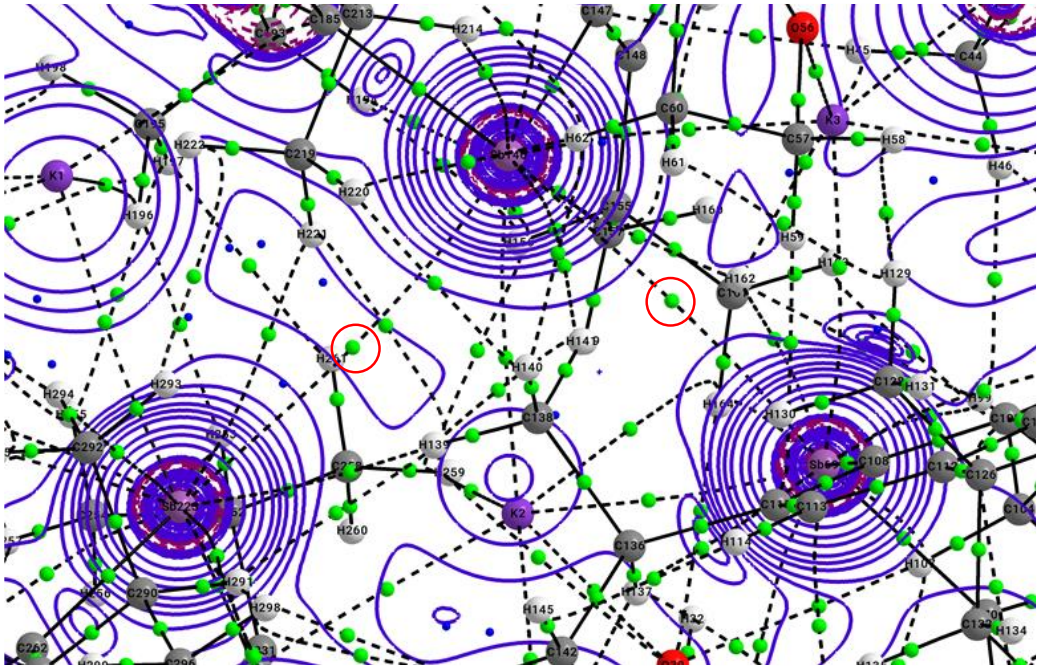

Figure S49c. Electron density distribution in contour plot for **6**. Contour plot of Laplacian distribution [$\nabla^2\boldsymbol{\rho}$ (r)] in the Sb-Sb-Sb plane of **6**. The BCPs showing Sb-Sb transient bond paths are marked by red spheres. Solid blue lines indicate the areas of charge concentration ($\nabla^2\boldsymbol{\rho}$ (r) < 0) while dotted purple lines denotes charge depletion ($\nabla^2\boldsymbol{\rho}$ (r) > 0). Solid lines connecting atomic nuclei (black) are the bond paths and those thick solid blue lines separating the atomic basins indicates the zero-flux surface crossing the molecular plane.

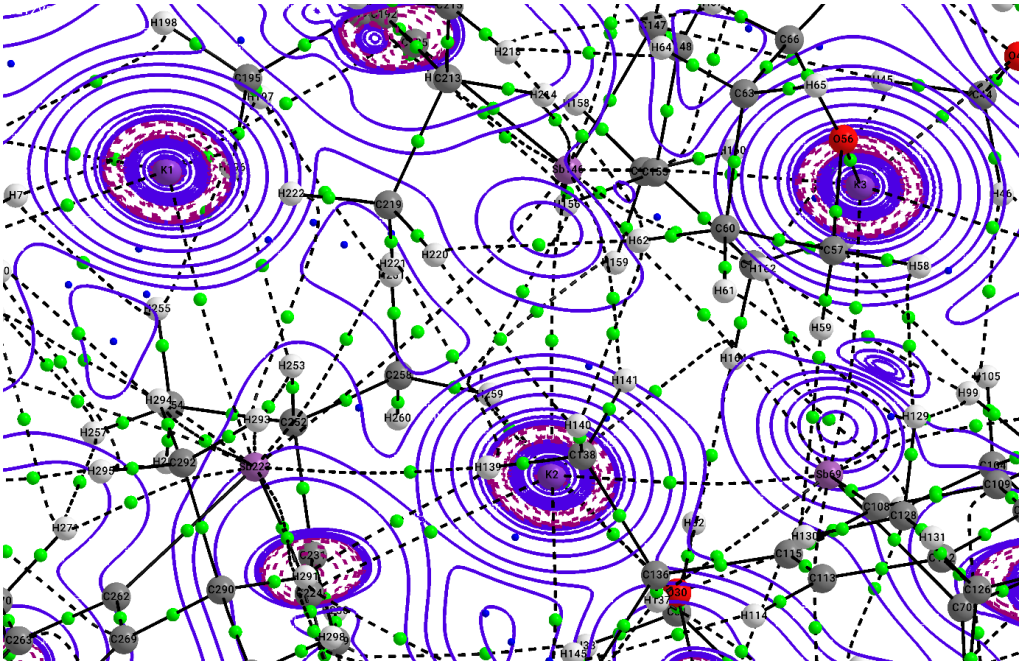

Figure S49d. Electron density distribution in contour plot for **6**. Contour plot of Laplacian distribution [$\nabla^2\boldsymbol{\rho}$ (r)] in the K-K-K plane of **6**. Solid blue lines indicate the areas of charge concentration ($\nabla^2\boldsymbol{\rho}$ (r) < 0) while dotted purple lines denotes charge depletion ($\nabla^2\boldsymbol{\rho}$ (r) > 0). Solid lines connecting atomic nuclei (black) are the bond paths and those thick solid blue lines separating the atomic basins indicates the zero-flux surface crossing the molecular plane.

S8.13. Geometry optimization and NBO analysis of the complex 15 [$Na_2((Tip)_2Sb)_2(THF)_2$] at M06-2X/def2-TZVPP level of theory:

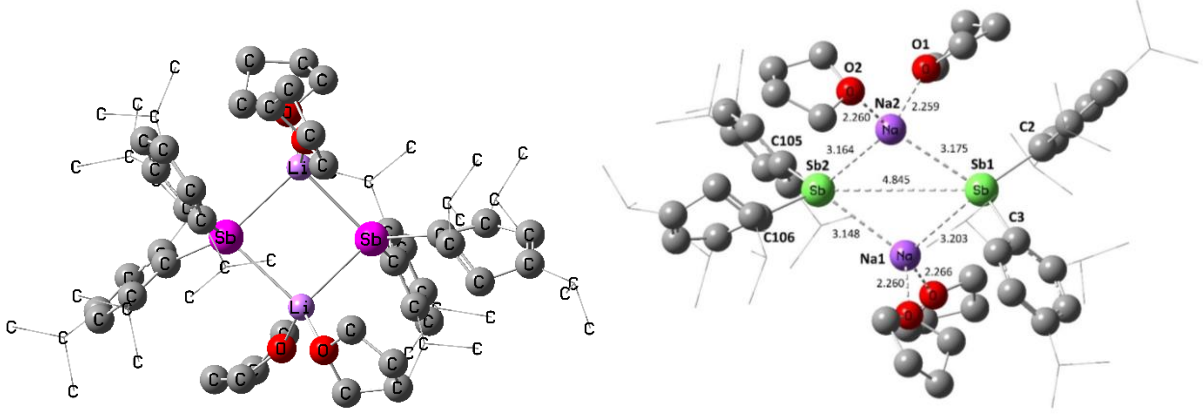

Figure S50: The optimized geometry of the complexes **14** [$Li_2((Tip)_2Sb)_2(THF)_4$] (left) and **15** [$Na_2((Tip)_2Sb)_2(THF)_2$] (right). The ball and stick representations of the above molecule corresponds to the higher ONIOM level (M06-2X/def2-TZVPP) and the wireframe representation is of lower level ONIOM (PM6). Hydrogen atoms are omitted for clarity.

Solvation energy of **14** [$Li_2((Tip)_2Sb)_2(THF)_4$] (left) and **15** [$Na_2((Tip)_2Sb)_2(THF)_2$] (right) were calculated at ONIOM based M06-2x level with Def2TZVPP basis set alongside with PM6. ONIOM method has been employed to calculate the solvation energy difference where all the isopropyl units of each dimer were considered under QM-based PM6 level, and the rest core part of the molecule was deemed with M06-2x/Def2-TZVPP level.

Computational Methods:

The optimization of geometry and vibrational frequencies calculations for complex **15** [$Na_2((Tip)_2Sb)_2(THF)_2$] have been carried out in gas phase in the singlet state at M06-2X/def2-TZVPP level of theory along with the ONIOM method employed.[17] The isopropyl fragments of each of the Tip-groups and hydrogens bonded to the phenyl moieties were calculated with semi-empirical QM-based PM6 level of theory. The zero imaginary frequencies assure the minima on PES. Gaussian 9.0 package has been employed for all the computational calculations. The Partial charges in the molecule, Natural bond orbitals, Wiberg bond indices (WBI) have been estimated from the Natural bond orbital (NBO) analysis using the Gauss view program.

NBO Analysis of complex 15:

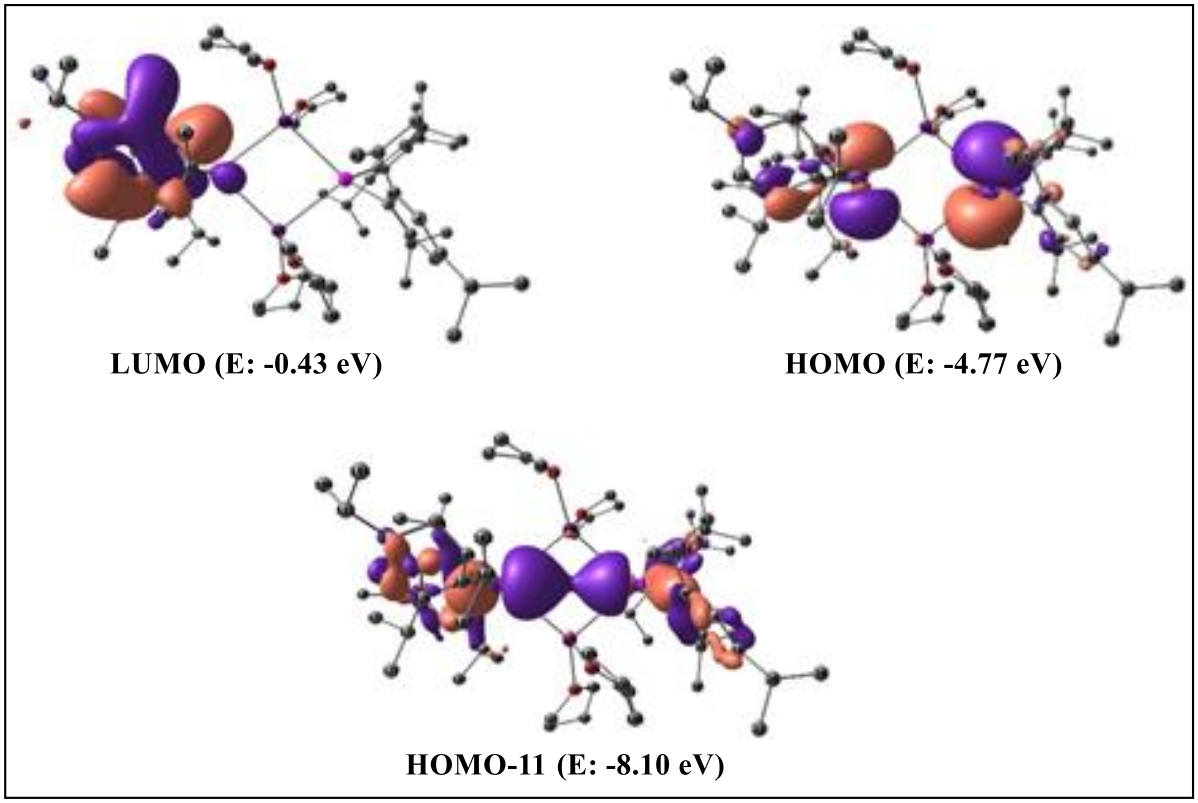

Figure S51: Molecular Orbitals of **15** at M06-2x/def2-TZVPP level of theory (in gas phase).

NBO analysis was carried out to further unravel the bonding nature, electronic structure, charge distribution of complex **15** $[Na_2((Tip)_2Sb)_2(THF)_2]$. The results from Table S12 infer the Sb-C bonds, where the σ bonds are polarized approximately 70% towards the C atom in all the Sb-C bonds. The Sb-C bond order of 0.80-0.86 in these compounds suggests the Sb-C bond is weakly covalent. From the MO analysis, The LUMO is essentially MO containing the π cloud of Tip- group bonded to Sb. HOMO represents the lone pair on the Sb atom which is a π type in nature. The HOMO-11 represents a σ type orbital interaction on Sb1 extending towards Sb2 atom which is a very weak overlap as inferred from 0.014 WBI value. The interaction of Sb atoms with the Na atoms is a very weak interaction in terms of bonding and indicates a electrostatic kind of interaction rather than bonding. The similar kind of interactions were observed from the coordinated THF molecules at Na centre where the bonding seems to be very poor overlap between Na and Oxygen of THF as indicated by 0.001 WBI values.

Table S12: NBO results of the complex **15** at the M06-2X/def2-TZVPP level of theory. Occupation number (ON), and partial charges q.

Bond/Lone pair	**Atomic/Orbital contributions**	**ON**	**WBI**	**q**
Sb1 - C2	Sb1 S (12.52%) P (87.34%) C2 S(27.75%) P (72.17%)	1.94	0.8253	Sb1 = -0.16 C2 = -0.13
Sb1 - C3	Sb1 S (12.11%) P (87.75%) C3 S(28.00%) P(71.91%)	1.94	0.8263	Sb1 = -0.16 C3 = -0.10
Sb2 - C105	Sb2 S (13.78%) P (86.07%) C105 S (30.10%) P (69.79%)	1.94	0.8598	Sb2 = -0.16 C105 = -0.01
Sb2 - C106	Sb2 S (12.69%) P (87.16%) C106 S (27.09%) P (72.84%)	1.94	0.8334	Sb2 = -0.16 C106 = -0.15
Sb1 – LP(1)	S (75.66%) P (24.31%)	1.91191	-	-
Sb1 – LP(2)	P (99.95%)	1.85873	-	-
Sb2 – LP(1)	S (73.82%) P (26.13%)	1.90751	-	-
Sb2 – LP(2)	P (99.85%)	1.80415	-	-

Table S13: Key bonding interactions and their corresponding bond orders.

Bond	**WBI**
Sb1 - Sb2	0.0147
Sb1 - Na1	0.0672
Sb1 - Na2	0.0791

Sb2 - Na1	0.0812
Sb2 - Na2	0.0812
Na1 - O1	0.001
Na2 - O2	0.001

The P type lone pairs shown to have sufficient delocalization from Sb atoms in to pi system of Tip groups as shown from the O.N. The positive partial charge on each of Na atoms whose values ranges from +0.53-0.56 supports the electrostatic attraction between the Na and Sb atoms. The Na atoms are in turn coordinated by THF through oxygen.

S8.14. Calculation of solvation energies of the complexes 14 $[Li_2((Tip)_2Sb)_2(THF)_4]$, and 15 $[Na_2((Tip)_2Sb)_2(THF)_4]$ at M06-2X/def2-TZVPP level of theory:

Solvation energy of $[Li_2((Tip)_2Sb)_2(THF)_4]$ **(14)** and $[Na_2((Tip)_2Sb)_2(THF)_4]$ **(15)** was calculated at ONIOM based M06-2x level with def2-TZVPP basis set alongside with PM6. ONIOM method has been employed to calculate the solvation energy differences where all the isopropyl units of each dimer were considered under QM-based PM6 level, and the rest core part of the molecule was deemed with M06-2x/def2-TZVPP level.

The pictorial representation of the distribution of the ONIOM method for complexes **14** and **15** is given below in Figure S52. The ball and stick model represents the part of the molecule considered under DFT based M06-2x/def2-TZVPP level, and the wireframe model represents the PM6 based calculation.

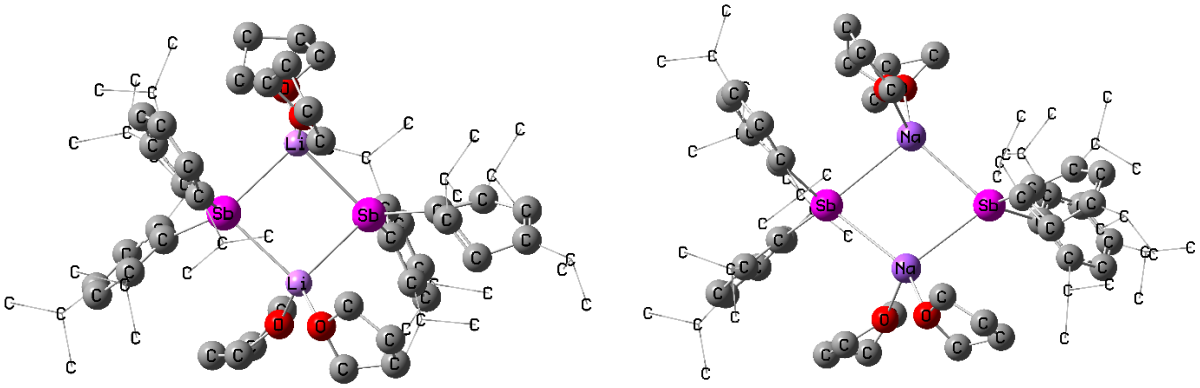

Figure S52: Pictorial representation of the distribution of the ONIOM method for complexes **14** and **15**.

The solvation energies (ONIOM) are given in Table S14 below.

Table S14: Solvation energies of complexes **14** and **15** in Toluene and *n*-Hexane from ONIOM method.

Molecule	**Energy difference $(14)_{Toluene} - (14)_{gas}$ in Kcal/mol**	**Energy difference $(14)_{Hexane} - (14)_{gas}$ in Kcal/mol**
$[Li_2((Tip)_2Sb)_2(THF)_4]$ (14)	-2.875	-4.470
	Energy difference $(15)_{Toluene} - (15)_{gas}$ in Kcal/mol	**Energy difference $(15)_{Hexane} - (15)_{gas}$ in Kcal/mol**
$[Na_2((Tip)_2Sb)_2(THF)_4]$ (15)	-7.846	-5.907

The dimers **14**, **15** were found to be more stable in the solution media compared to the gas phase, as observed from the negative energy difference in toluene and *n*-hexane.

S8.15. Geometry optimization and NBO analysis of the cation Tip_2Sb^+:

The geometry optimization of the cation **Tip_2Sb^+** was carried out in M06-2X/def2-TZVPP level of theory with the inclusion of effective core potential for the Sb atom both in the gas phase and THF. The solvation model used was PCM. The bond length of Sb-Cl bond has slightly elongated when it was optimized in THF. Whereas, the bond angle, C-Sb-C, reduced almost 1.5^o in THF. We have observed almost equal bond length for both the Sb-C bonds. However, latter the bond lengths were slightly different and elongated for Tip_2SbCl (**1**). The C-Sb-C bond angle increased ~ 3^o for Tip_2Sb^+. The cation is more stable in THF than in the gas phase. The energy difference between them is 31.43 kcal/mol.

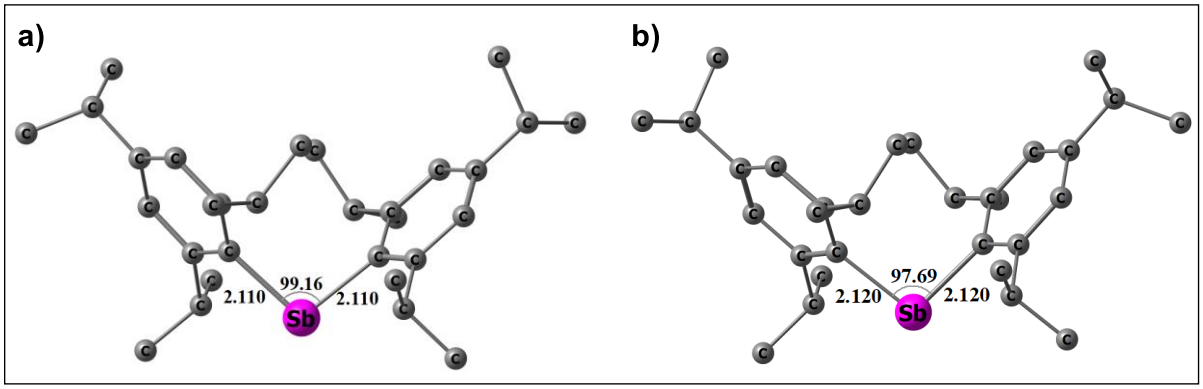

Figure S53: The optimized structures of the cation **Tip$_2$Sb$^+$**: a) in gas phase; b) in THF at M06-2X/def2-TZVPP level of theory.

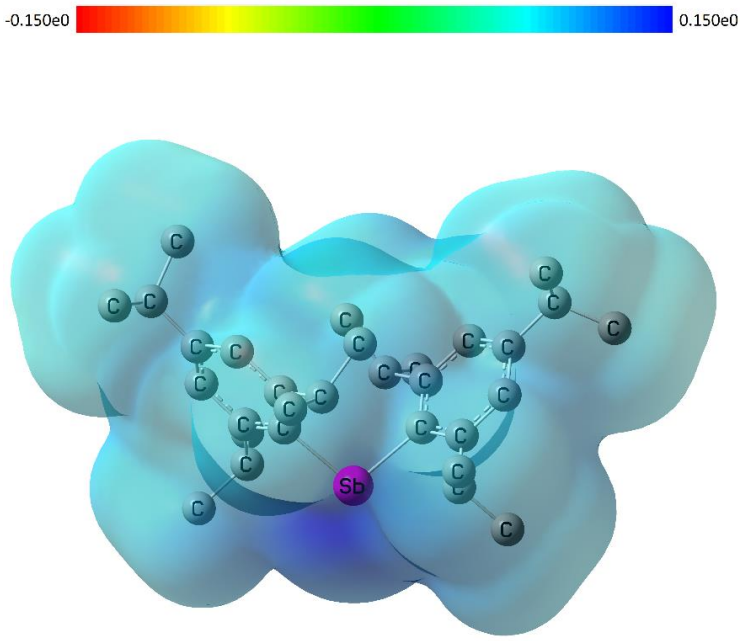

Figure S54: The optimized structures of the cation **Tip$_2$Sb$^+$** a) in gas phase; b) in THF at M06-2X/def2-TZVPP level of theory.

The NBO analysis of **Tip$_2$Sb$^+$** at M06-2X/def2-TZVPP was used to study the nature of bonding, charge distribution and electronic structure. The LUMO of the cation **Tip$_2$Sb$^+$** is the vacant σ^* orbital of Sb. HOMO constitutes the lone pair on the Sb atom. The electron density on the HOMO-1, HOMO-2 and HOMO-3 are located on the Tip-group.

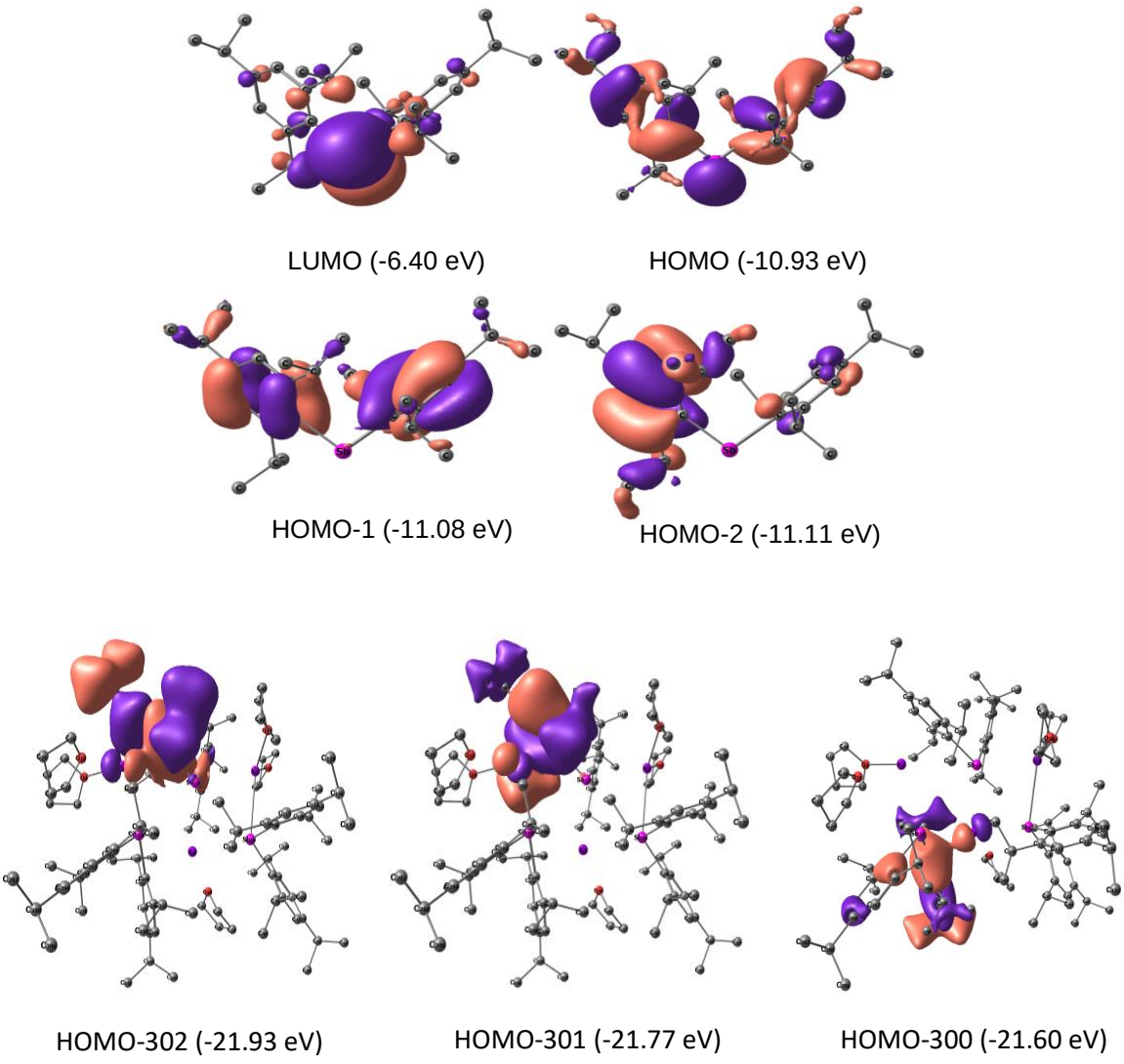

Figure S55: Frontier orbitals of Tip_2Sb^+ in the gas phase (top). Molecular orbitals of Sb_3K_3 of **6** indicating the interaction between the orbitals of K and π cloud of the phenyl rings (bottom). The values in the parentheses indicate the energy of the orbitals.

The C-Sb bonds are having the bond occupancy 1.952. The bond is more polarized towards C. Carbons constitute 69% of the C10/C2-Sb1 bond. The carbons are sp^3 hybridized. The WBI shows that these bonds are single bond.

The NBO analysis of the cation **Tip_2Sb^+** was also conducted in THF using the solvation model, Polarizable Continuum Model (PCM). The observations were very similar to that of the gaseous phase. The relevant findings are summarized in the Tables S15-16.

Table S15: Summary of NBO analysis of Tip_2Sb^+ (**18**) at M06/def2-TZVPP level of theory in gas phase.

NBO	Occupancy	Atomic contribution	WBI
C2-Sb1	1.952	C2 ($sp^{3.32}$) - 69%, Sb (88% p) - 31%	0.848
C10-Sb1	1.952	C10 ($sp^{3.31}$) - 69%, Sb (88% p) - 31%,	0.849
Lone Pair on Sb1 (1)	1.975	(s-76%, p-24%)	-

Table S16: Summary of NBO analysis of Tip_2Sb^+ at M06/def2-TZVPP level of theory in THF.

NBO	Occupancy	Atomic contribution	WBI
C2-Sb1	1.951	C2 ($sp^{3.30}$) - 70%, Sb (88% p) - 30%	0.827
C10-Sb1	1.951	C10 ($sp^{3.30}$) - 70%, Sb (88% p) - 30%,	0.829
Lone Pair on Sb1 (1)	1.976	(s-77%, p-23%)	-

Optimized coordinates:

$(Tip)_2SbCl$ (**1**):

51	0.058091000	-1.986910000	0.372166000
6	1.583300000	-0.528085000	-0.141828000
6	1.407053000	0.428025000	-1.166047000
6	2.754883000	-0.499567000	0.639492000
6	2.399722000	1.385724000	-1.371508000
6	3.721104000	0.477384000	0.390060000
6	3.559993000	1.432832000	-0.604452000
1	2.256543000	2.123109000	-2.156209000
1	4.627560000	0.497272000	0.987404000
6	-1.540520000	-0.506976000	0.538426000
6	-2.748252000	-0.537164000	-0.185375000
6	-1.302686000	0.549611000	1.439041000
6	-3.614130000	0.551926000	-0.104442000
6	-2.220102000	1.600996000	1.514225000
6	-3.360048000	1.641528000	0.723502000
1	-4.523301000	0.542622000	-0.698850000
1	-2.034271000	2.420701000	2.202115000
6	-0.115302000	0.610538000	2.396022000
1	0.535819000	-0.256290000	2.242281000
6	-0.589805000	0.528894000	3.852770000
1	0.268338000	0.506618000	4.529795000
1	-1.201383000	1.395770000	4.113932000
1	-1.188798000	-0.368688000	4.020905000
6	0.746130000	1.857561000	2.164912000
1	1.622200000	1.846614000	2.818816000
1	1.092254000	1.914615000	1.131015000
1	0.176984000	2.763694000	2.388050000
6	-4.301083000	2.828055000	0.762336000
1	-3.909512000	3.529984000	1.506071000
6	-4.325528000	3.540681000	-0.594931000
1	-4.961538000	4.428439000	-0.554989000
1	-3.320851000	3.845677000	-0.895267000
1	-4.720039000	2.877483000	-1.369745000
6	-5.713611000	2.419898000	1.192997000
1	-5.699577000	1.921011000	2.163947000
1	-6.361465000	3.297180000	1.262474000
1	-6.158384000	1.733016000	0.467940000
6	-4.550208000	-2.254735000	-0.569032000
1	-4.540633000	-2.482235000	0.498941000
1	-5.347005000	-1.529621000	-0.751796000
1	-4.799954000	-3.167436000	-1.115277000
6	3.057477000	-1.512386000	1.739467000
1	2.148248000	-2.071109000	1.975800000
6	4.091210000	-2.531588000	1.245887000

1	3.740891000	-3.035180000	0.341980000
1	5.033746000	-2.031634000	1.007170000
1	4.286576000	-3.286159000	2.011949000
6	3.508222000	-0.859895000	3.050666000
1	2.783971000	-0.116674000	3.392963000
1	3.611830000	-1.620443000	3.828247000
1	4.476320000	-0.365507000	2.946066000
6	0.191562000	0.490311000	-2.079962000
1	-0.496302000	-0.301398000	-1.801301000
6	0.586479000	0.235403000	-3.538805000
1	1.246520000	1.021526000	-3.915450000
1	1.099288000	-0.722821000	-3.638715000
1	-0.305811000	0.215901000	-4.170822000
6	-0.573524000	1.810122000	-1.931500000
1	-0.870556000	1.977528000	-0.893445000
1	0.029672000	2.661328000	-2.260057000
1	-1.480986000	1.784566000	-2.542212000
6	4.610177000	2.498135000	-0.845223000
1	5.410002000	2.337093000	-0.114854000
6	4.035515000	3.900606000	-0.616370000
1	3.608141000	3.990953000	0.384539000
1	4.813599000	4.658988000	-0.732439000
1	3.245105000	4.117397000	-1.339987000
6	5.216120000	2.376676000	-2.247648000
1	5.645198000	1.385253000	-2.405184000
1	4.453944000	2.538723000	-3.014611000
1	6.001977000	3.122158000	-2.392130000
17	-0.103265000	-2.900363000	-1.847536000
6	-3.217013000	-1.382635000	-2.525553000
1	-2.241552000	-1.042509000	-2.877853000
1	-3.496680000	-2.262991000	-3.109537000
1	-3.948997000	-0.594476000	-2.725003000
6	-3.187283000	-1.722983000	-1.031679000
1	-2.473393000	-2.534772000	-0.891717000

$(Tip)_2SbCl$ radical anion (**1**$^{\cdot-}$)

51	-0.086614000	1.919411000	0.696680000
6	1.494089000	0.379537000	0.701737000
6	2.635031000	0.564414000	-0.114674000
6	1.377065000	-0.811114000	1.439848000
6	3.604077000	-0.433416000	-0.186022000
6	2.371379000	-1.792750000	1.335899000

6	3.483844000	-1.626985000	0.525312000
1	4.464722000	-0.290290000	-0.831716000
1	2.265667000	-2.721450000	1.892426000
6	-1.579768000	0.473247000	-0.018568000
6	-2.765711000	0.271443000	0.721647000
6	-1.351509000	-0.326572000	-1.156175000
6	-3.645460000	-0.751699000	0.366859000
6	-2.259205000	-1.341003000	-1.476820000
6	-3.398215000	-1.583054000	-0.720897000
1	-4.546188000	-0.918535000	0.948800000
1	-2.057772000	-1.960814000	-2.346753000
17	-0.423671000	3.425758000	-1.987048000
6	0.201275000	-1.110135000	2.361381000
1	-0.471166000	-0.250637000	2.347113000
6	4.519034000	-2.725898000	0.387413000
1	4.220229000	-3.538962000	1.058485000
6	2.831507000	1.852348000	-0.904821000
6	-3.132544000	1.208453000	1.864844000
1	-2.215510000	1.426643000	2.422075000
6	-4.336857000	-2.726006000	-1.053702000
1	-5.179601000	-2.667942000	-0.355574000
6	-0.167759000	-0.150673000	-2.097094000
1	0.428162000	0.691802000	-1.750831000
6	-4.896388000	-2.615859000	-2.475745000
1	-5.389082000	-1.653315000	-2.626235000
1	-4.095305000	-2.699272000	-3.214847000
1	-5.618926000	-3.413952000	-2.671004000
6	-3.643112000	-4.077447000	-0.845329000
1	-3.256452000	-4.161214000	0.172748000
1	-4.333423000	-4.906248000	-1.029584000
1	-2.797278000	-4.179143000	-1.531060000
6	-4.134822000	0.635018000	2.867261000
1	-5.128754000	0.520092000	2.425191000
1	-3.811575000	-0.339783000	3.242210000
1	-4.233102000	1.315078000	3.717308000
6	-3.653190000	2.534212000	1.290163000
1	-2.949131000	2.970646000	0.577065000
1	-4.593080000	2.359869000	0.757105000
1	-3.835435000	3.259741000	2.088672000
6	0.720965000	-1.401096000	-2.133585000
1	1.042272000	-1.694975000	-1.131554000
1	0.191249000	-2.245231000	-2.588312000
1	1.616673000	-1.208208000	-2.732303000
6	-0.643005000	0.230798000	-3.503580000

1	-1.242510000	-0.567594000	-3.954028000
1	-1.224448000	1.152439000	-3.458925000
1	0.222899000	0.412846000	-4.147183000
6	3.657983000	1.688894000	-2.181678000
1	3.279863000	0.865073000	-2.792906000
1	3.588838000	2.605722000	-2.771337000
1	4.716877000	1.506368000	-1.970679000
6	4.542315000	-3.279077000	-1.042302000
1	5.245855000	-4.112677000	-1.128461000
1	3.550083000	-3.624182000	-1.340178000
1	4.848741000	-2.501930000	-1.748183000
6	5.914085000	-2.254062000	0.810388000
1	6.635497000	-3.074770000	0.756028000
1	6.265706000	-1.453442000	0.154119000
1	5.900838000	-1.867753000	1.831600000
6	-0.605611000	-2.323674000	1.885128000
1	-0.953135000	-2.182396000	0.858956000
1	-0.002400000	-3.236498000	1.924794000
1	-1.483221000	-2.469016000	2.522895000
6	0.667001000	-1.289178000	3.810941000
1	1.330766000	-2.152996000	3.910506000
1	1.210394000	-0.404967000	4.152803000
1	-0.191237000	-1.445796000	4.471151000
6	3.449493000	2.931361000	-0.006362000
1	2.842543000	3.094578000	0.887680000
1	4.452670000	2.630970000	0.314971000
1	3.518574000	3.879653000	-0.545704000
1	1.853436000	2.224436000	-1.227000000

$(Tip)_2Sb^+$ **(1-Cl)$^+$**

51	-0.136409000	-1.978477000	-0.129710000
6	1.572494000	-0.760137000	0.183854000
6	2.624850000	-0.556380000	-0.722502000
6	1.552092000	-0.111335000	1.425829000
6	3.609028000	0.365919000	-0.373731000
6	2.571754000	0.782524000	1.742672000
6	3.599644000	1.048588000	0.842854000
1	4.406646000	0.570662000	-1.080842000
1	2.561440000	1.295733000	2.699292000
6	-1.594700000	-0.511746000	-0.551972000
6	-1.319223000	0.772641000	-1.090243000
6	-2.847724000	-0.773907000	0.059453000
6	-2.253935000	1.781035000	-0.907317000

6	-3.733486000	0.288173000	0.236934000
6	-3.450228000	1.571203000	-0.215876000
1	-2.050769000	2.764993000	-1.317671000
1	-4.680573000	0.110803000	0.735228000
6	-3.287676000	-2.148549000	0.552944000
1	-2.606500000	-2.907001000	0.154288000
6	-4.677894000	-2.522798000	0.022978000
1	-4.899949000	-3.561744000	0.273913000
1	-5.457934000	-1.904127000	0.470065000
1	-4.731492000	-2.410211000	-1.061025000
6	-3.251652000	-2.230483000	2.084335000
1	-3.556897000	-3.222646000	2.422244000
1	-2.253849000	-2.027837000	2.486750000
1	-3.934927000	-1.498109000	2.521372000
6	-4.415912000	2.710329000	0.020965000
1	-5.297264000	2.292138000	0.516437000
6	-3.789944000	3.752666000	0.956497000
1	-4.507877000	4.546915000	1.169618000
1	-3.482862000	3.302691000	1.902937000
1	-2.910472000	4.210128000	0.495356000
6	-4.869755000	3.351127000	-1.295427000
1	-5.299360000	2.609634000	-1.971320000
1	-5.624728000	4.114453000	-1.098486000
1	-4.035440000	3.837358000	-1.807517000
6	-0.508592000	1.371535000	-3.382979000
1	-1.083381000	0.544253000	-3.805404000
1	-1.123539000	2.272308000	-3.444166000
1	0.378309000	1.530438000	-4.000953000
6	0.427146000	-0.352417000	2.419961000
1	-0.204565000	-1.198712000	2.051951000
6	0.941405000	-0.828709000	3.781190000
1	1.598579000	-1.693701000	3.679395000
1	1.503870000	-0.030971000	4.271185000
1	0.106204000	-1.093239000	4.432672000
6	-0.503781000	0.854982000	2.552682000
1	-0.903121000	1.169385000	1.586025000
1	-1.338000000	0.624603000	3.219759000
1	0.049106000	1.695453000	2.980349000
6	2.746057000	-1.242798000	-2.081037000
1	2.694801000	-0.455483000	-2.843824000
6	1.650468000	-2.261464000	-2.393204000
1	1.699918000	-3.122516000	-1.715882000
1	0.635398000	-1.818210000	-2.435797000
1	1.777713000	-2.671757000	-3.397470000

6	4.100946000	-1.956825000	-2.217324000
1	4.936290000	-1.270148000	-2.090073000
1	4.192587000	-2.740312000	-1.460831000
1	4.193782000	-2.415249000	-3.203654000
6	4.673296000	2.066160000	1.166412000
1	4.473599000	2.437230000	2.176431000
6	4.599482000	3.255198000	0.200967000
1	3.606439000	3.709822000	0.207877000
1	5.328813000	4.017495000	0.481918000
1	4.823227000	2.941433000	-0.822450000
6	6.069378000	1.434514000	1.161176000
1	6.123175000	0.584733000	1.844030000
1	6.339898000	1.085420000	0.161200000
1	6.816068000	2.169464000	1.467976000
6	0.742152000	2.227074000	-1.353522000
1	1.021637000	2.028511000	-0.316126000
1	1.659316000	2.352715000	-1.934732000
1	0.195146000	3.172357000	-1.388870000
6	-0.095633000	1.083026000	-1.933064000
1	0.538046000	0.198278000	-1.956963000

$(Tip)_2Sb^{\cdot}$ (**3**)

51	-0.035522000	-2.127810000	-0.501932000
6	1.506408000	-0.772311000	0.225388000
6	2.660349000	-0.526914000	-0.548461000
6	1.333567000	-0.082807000	1.439614000
6	3.595998000	0.406683000	-0.108583000
6	2.293842000	0.852236000	1.836238000
6	3.425077000	1.117574000	1.076960000
1	4.480585000	0.592644000	-0.710406000
1	2.151895000	1.394553000	2.766902000
6	-1.591204000	-0.604455000	-0.465569000
6	-1.419569000	0.613345000	-1.156963000
6	-2.750911000	-0.797914000	0.308539000
6	-2.384592000	1.612059000	-1.027608000
6	-3.694423000	0.228161000	0.400931000
6	-3.524493000	1.444400000	-0.247052000
1	-2.238372000	2.553295000	-1.550232000
1	-4.588623000	0.078183000	0.999105000
6	-3.055260000	-2.096558000	1.045243000
1	-2.168513000	-2.736220000	1.010129000
6	-4.189915000	-2.853889000	0.344833000

1	-4.382972000	-3.807315000	0.843123000
1	-5.112025000	-2.266298000	0.363842000
1	-3.941007000	-3.052009000	-0.700038000
6	-3.378613000	-1.880315000	2.528005000
1	-3.505802000	-2.844013000	3.027318000
1	-2.577671000	-1.336025000	3.033553000
1	-4.305221000	-1.316797000	2.658869000
6	-4.543241000	2.557192000	-0.105260000
1	-5.332950000	2.191363000	0.559280000
6	-3.916891000	3.797727000	0.541679000
1	-4.671018000	4.572773000	0.699998000
1	-3.463681000	3.551137000	1.504203000
1	-3.136148000	4.215019000	-0.100071000
6	-5.182923000	2.907371000	-1.453086000
1	-5.642208000	2.028458000	-1.909533000
1	-5.951081000	3.674459000	-1.326789000
1	-4.433538000	3.294444000	-2.148752000
6	-0.664107000	1.185349000	-3.495558000
1	-1.237095000	0.344486000	-3.892414000
1	-1.289395000	2.079620000	-3.559568000
1	0.209030000	1.341975000	-4.134930000
6	0.143056000	-0.285415000	2.367369000
1	-0.501442000	-1.060754000	1.946351000
6	0.589124000	-0.785260000	3.746526000
1	1.178006000	-1.700928000	3.659405000
1	1.199733000	-0.038483000	4.260357000
1	-0.282213000	-0.992685000	4.373833000
6	-0.698105000	0.991455000	2.488320000
1	-1.033119000	1.339146000	1.508392000
1	-1.583024000	0.809826000	3.105048000
1	-0.120925000	1.791949000	2.959820000
6	2.954451000	-1.269748000	-1.845577000
1	2.041758000	-1.778562000	-2.170388000
6	4.016320000	-2.349855000	-1.606726000
1	4.954739000	-1.894664000	-1.277620000
1	3.693407000	-3.048655000	-0.831554000
1	4.210841000	-2.912509000	-2.523361000
6	3.362637000	-0.341059000	-2.993789000
1	2.622080000	0.448348000	-3.144038000
1	4.330442000	0.131363000	-2.809316000
1	3.448708000	-0.910938000	-3.922127000
6	4.430785000	2.165400000	1.508978000
1	4.101660000	2.548834000	2.480391000
6	4.452617000	3.336661000	0.519806000

1	3.456789000	3.769642000	0.403647000
1	5.135110000	4.118855000	0.861596000
1	4.789200000	3.001460000	-0.465150000
6	5.831998000	1.571153000	1.684468000
1	5.819314000	0.737247000	2.388845000
1	6.220606000	1.201212000	0.731761000
1	6.526624000	2.328477000	2.056126000
6	0.601597000	2.087540000	-1.499805000
1	0.924106000	1.893596000	-0.474096000
1	1.493763000	2.252617000	-2.110578000
1	0.016084000	3.011489000	-1.508188000
6	-0.224134000	0.918332000	-2.051353000
1	0.428494000	0.041856000	-2.079269000

$(Tip)_2Sb\text{-}Sb(Tip)_2$ (**4**):

6	2.893413000	-2.765638000	0.427392000
6	2.794970000	-1.701385000	-0.487526000
51	0.996077000	-0.538967000	-0.988564000
6	4.132282000	-3.374623000	0.649041000
1	4.202224000	-4.183728000	1.370761000
6	5.282111000	-2.986912000	-0.022510000
6	5.165979000	-1.960440000	-0.953598000
1	6.047622000	-1.641076000	-1.502057000
6	3.957566000	-1.308879000	-1.193888000
6	1.711536000	-3.345225000	1.188732000
1	0.820536000	-2.776319000	0.918346000
6	1.866801000	-3.254105000	2.711109000
1	1.983277000	-2.222151000	3.046250000
1	2.735936000	-3.823319000	3.051442000
1	0.982678000	-3.669110000	3.201818000
6	1.476742000	-4.799424000	0.765152000
1	0.573190000	-5.198192000	1.231270000
1	2.317552000	-5.429646000	1.065624000
1	1.374905000	-4.875068000	-0.319464000
6	6.617587000	-3.643882000	0.258526000
1	6.446047000	-4.421309000	1.010586000
6	7.610799000	-2.631855000	0.841748000
1	7.823186000	-1.839978000	0.118164000
1	8.555243000	-3.119519000	1.095612000
1	7.207282000	-2.163523000	1.742026000
6	7.190688000	-4.315417000	-0.993693000
1	6.487640000	-5.042279000	-1.405249000

1	8.125672000	-4.830547000	-0.760035000
1	7.401667000	-3.574535000	-1.769524000
6	3.993613000	-0.185609000	-2.223554000
1	3.005394000	0.263417000	-2.298657000
6	4.937089000	0.950199000	-1.811555000
1	4.875038000	1.766558000	-2.536832000
1	5.975980000	0.610604000	-1.772620000
1	4.665223000	1.347989000	-0.830806000
6	4.332760000	-0.722112000	-3.618106000
1	3.625464000	-1.498498000	-3.919316000
1	5.337272000	-1.152536000	-3.643134000
1	4.294625000	0.085914000	-4.353802000
6	1.792176000	1.340309000	-0.149993000
6	1.692613000	2.486005000	-0.969532000
6	2.465625000	3.612577000	-0.680820000
1	2.412868000	4.476000000	-1.337684000
6	3.282197000	3.676539000	0.440990000
6	3.283440000	2.584502000	1.300730000
1	3.878598000	2.630572000	2.208221000
6	2.567387000	1.415866000	1.031427000
6	0.741270000	2.567130000	-2.156731000
1	0.004837000	1.772895000	-2.035333000
6	-0.067882000	3.869214000	-2.164209000
1	-0.872826000	3.790944000	-2.900445000
1	0.547193000	4.731848000	-2.434894000
1	-0.522074000	4.052149000	-1.187817000
6	1.454275000	2.377010000	-3.499939000
1	0.747862000	2.507600000	-4.324557000
1	1.896921000	1.382804000	-3.595757000
1	2.251542000	3.117389000	-3.615410000
6	4.102009000	4.912906000	0.745499000
1	3.962845000	5.609184000	-0.088205000
6	3.603339000	5.599513000	2.022309000
1	2.543091000	5.849949000	1.943275000
1	4.164583000	6.517680000	2.213319000
1	3.728673000	4.942004000	2.887351000
6	5.595424000	4.584751000	0.844059000
1	5.949836000	4.098717000	-0.067434000
1	5.791370000	3.910368000	1.682029000
1	6.179565000	5.494636000	1.002818000
6	2.695854000	0.296775000	2.059085000
1	2.073510000	-0.536623000	1.734084000
6	4.143846000	-0.201488000	2.175514000
1	4.570884000	-0.448459000	1.202930000

1	4.183580000	-1.098061000	2.800953000
1	4.773314000	0.561643000	2.643155000
6	2.201091000	0.720221000	3.450122000
1	1.140345000	0.973130000	3.455649000
1	2.759093000	1.583812000	3.821617000
1	2.351162000	-0.097898000	4.160369000
51	-1.007082000	-0.550210000	1.067260000
6	-2.775838000	-1.755644000	0.557941000
6	-3.966247000	-1.339365000	1.201228000
6	-5.172519000	-1.970318000	0.901468000
1	-6.076351000	-1.631809000	1.399749000
6	-5.257677000	-2.991718000	-0.037214000
6	-4.077645000	-3.416600000	-0.630022000
1	-4.127175000	-4.228979000	-1.349074000
6	-2.836835000	-2.844632000	-0.332297000
6	-4.033684000	-0.220662000	2.235321000
1	-3.038952000	0.201099000	2.372780000
6	-4.461249000	-0.762358000	3.604014000
1	-5.474576000	-1.170630000	3.568245000
1	-4.447786000	0.038213000	4.348703000
1	-3.788679000	-1.556465000	3.936107000
6	-4.932304000	0.938124000	1.787312000
1	-4.616748000	1.331385000	0.818051000
1	-4.880132000	1.752988000	2.515273000
1	-5.976256000	0.620942000	1.710624000
6	-6.591615000	-3.599227000	-0.418414000
1	-6.390213000	-4.406466000	-1.130618000
6	-7.473977000	-2.558712000	-1.118740000
1	-6.966471000	-2.138029000	-1.989581000
1	-7.708850000	-1.735011000	-0.438639000
1	-8.415831000	-3.006098000	-1.446293000
6	-7.312613000	-4.204467000	0.789935000
1	-8.243909000	-4.684228000	0.478990000
1	-7.564281000	-3.432437000	1.521896000
1	-6.688211000	-4.949128000	1.287241000
6	-1.622480000	-3.485294000	-0.995530000
1	-0.718674000	-3.048469000	-0.560046000
6	-1.578850000	-3.252341000	-2.511983000
1	-2.479182000	-3.654317000	-2.985624000
1	-0.713926000	-3.761223000	-2.946031000
1	-1.504460000	-2.194700000	-2.768714000
6	-1.587598000	-4.993328000	-0.707793000
1	-2.423885000	-5.502789000	-1.191183000
1	-1.648166000	-5.193071000	0.363777000

1	-0.667796000	-5.435443000	-1.094198000
6	-1.825389000	1.305806000	0.193274000
6	-2.554927000	1.362177000	-1.019490000
6	-3.247764000	2.529785000	-1.344124000
1	-3.807415000	2.557262000	-2.274878000
6	-3.272119000	3.642382000	-0.509716000
6	-2.506219000	3.594428000	0.646495000
1	-2.477423000	4.468419000	1.291468000
6	-1.756448000	2.466985000	0.992631000
6	-2.662155000	0.215820000	-2.018558000
1	-2.082238000	-0.619334000	-1.633178000
6	-2.095659000	0.570898000	-3.401683000
1	-2.310145000	-0.239468000	-4.104284000
1	-1.014152000	0.711653000	-3.385100000
1	-2.554889000	1.480650000	-3.798379000
6	-4.112627000	-0.260519000	-2.177780000
1	-4.710804000	0.492686000	-2.699523000
1	-4.580161000	-0.462765000	-1.213761000
1	-4.138944000	-1.180654000	-2.768913000
6	-4.078076000	4.873693000	-0.868941000
1	-3.950587000	5.594482000	-0.054379000
6	-5.570748000	4.546343000	-0.982848000
1	-6.148940000	5.450742000	-1.187974000
1	-5.943829000	4.096815000	-0.060128000
1	-5.751886000	3.840034000	-1.797541000
6	-3.557331000	5.520326000	-2.157391000
1	-3.665803000	4.836249000	-3.003896000
1	-2.499767000	5.777764000	-2.067883000
1	-4.118280000	6.429758000	-2.386972000
6	-0.875630000	2.573238000	2.229106000
1	-0.222826000	1.701803000	2.239552000
6	0.053110000	3.790543000	2.165289000
1	0.592969000	3.816807000	1.217111000
1	0.790185000	3.736491000	2.972143000
1	-0.499544000	4.727330000	2.279782000
6	-1.688232000	2.580505000	3.527939000
1	-2.376283000	3.430788000	3.543662000
1	-1.022832000	2.667537000	4.391328000
1	-2.276610000	1.667838000	3.646910000

$(Tip)_2Sb^-$ (**5**) [singlet]:

51	0.000014000	1.634018000	-0.000025000
6	-1.675246000	0.230990000	-0.132988000

6	-2.883987000	0.552134000	0.529622000
6	-1.669732000	-0.938789000	-0.927960000
6	-3.996345000	-0.281569000	0.437473000
6	-2.801515000	-1.757459000	-0.991534000
6	-3.973460000	-1.456884000	-0.308731000
1	-4.907199000	-0.006803000	0.966096000
1	-2.765826000	-2.653069000	-1.609195000
6	1.675233000	0.230969000	0.133008000
6	2.883994000	0.552160000	-0.529533000
6	1.669709000	-0.938860000	0.927924000
6	3.996362000	-0.281540000	-0.437392000
6	2.801480000	-1.757533000	0.991459000
6	3.973453000	-1.456910000	0.308710000
1	4.907237000	-0.006718000	-0.965948000
1	2.765783000	-2.653177000	1.609072000
6	-0.471327000	-1.337546000	-1.751772000
1	-0.032333000	-0.457859000	-2.231486000
1	0.321552000	-1.778983000	-1.140627000
1	-0.757747000	-2.065035000	-2.515742000
6	-5.171267000	-2.372199000	-0.359302000
1	-5.150839000	-2.998030000	-1.254731000
1	-5.199502000	-3.039218000	0.508913000
1	-6.104449000	-1.802950000	-0.364778000
6	-3.007952000	1.812261000	1.350968000
1	-2.257982000	1.830363000	2.147003000
1	-2.823463000	2.700655000	0.739035000
1	-4.006555000	1.898718000	1.786786000
6	3.007978000	1.812342000	-1.350788000
1	2.258062000	1.830471000	-2.146876000
1	2.823418000	2.700687000	-0.738802000
1	4.006606000	1.898860000	-1.786536000
6	5.171219000	-2.372279000	0.359251000
1	5.198706000	-3.040194000	-0.508298000
1	6.104445000	-1.803097000	0.363404000
1	5.151454000	-2.997205000	1.255330000
6	0.471308000	-1.337643000	1.751736000
1	0.032215000	-0.457952000	2.231346000
1	-0.321507000	-1.779249000	1.140627000
1	0.757787000	-2.065009000	2.515802000

$(Tip)_2Sb^-$ (**5**) [triplet]:

51	-0.000001000	0.000044000	-1.095016000
6	-2.216116000	-0.026544000	-0.244995000

6	-2.921056000	1.168159000	-0.008216000
6	-2.819130000	-1.224781000	0.182505000
6	-4.169796000	1.154596000	0.617509000
6	-4.067822000	-1.219509000	0.806012000
6	-4.761600000	-0.033729000	1.036052000
1	-4.697507000	2.093868000	0.778373000
1	-4.515037000	-2.162862000	1.117340000
6	2.216124000	0.026562000	-0.245019000
6	2.921038000	-1.168162000	-0.008283000
6	2.819158000	1.224770000	0.182543000
6	4.169769000	-1.154653000	0.617464000
6	4.067838000	1.219445000	0.806068000
6	4.761589000	0.033640000	1.036071000
1	4.697461000	-2.093942000	0.778291000
1	4.515069000	2.162778000	1.117437000
6	-2.115824000	-2.547250000	-0.023613000
1	-1.834794000	-2.683597000	-1.071882000
1	-1.187550000	-2.580723000	0.556174000
1	-2.746087000	-3.386774000	0.281161000
6	-6.094116000	-0.036705000	1.743950000
1	-6.673998000	-0.928344000	1.491400000
1	-5.968318000	-0.024907000	2.831831000
1	-6.686168000	0.840812000	1.472309000
6	-2.335599000	2.497492000	-0.428789000
1	-1.423633000	2.716039000	0.136625000
1	-2.052056000	2.484578000	-1.485169000
1	-3.045146000	3.313312000	-0.267449000
6	2.335554000	-2.497465000	-0.428916000
1	1.423578000	-2.716010000	0.136484000
1	2.052018000	-2.484503000	-1.485296000
1	3.045079000	-3.313309000	-0.267603000
6	6.094096000	0.036569000	1.743985000
1	5.968284000	0.024979000	2.831866000
1	6.686039000	-0.841069000	1.472500000
1	6.674097000	0.928090000	1.491288000
6	2.115899000	2.547265000	-0.023565000
1	1.834960000	2.683669000	-1.071852000
1	1.187580000	2.580736000	0.556149000
1	2.746161000	3.386757000	0.281298000

$(Mes)_2Sb\text{-}Sb(Mes)_2$ (**10**):

6	-2.396641000	-2.751660000	-0.530638000
6	-2.516121000	-1.714759000	0.416353000

51	-1.005945000	-0.250149000	1.002473000
6	-3.463447000	-3.633954000	-0.717075000
1	-3.360802000	-4.426932000	-1.452308000
6	-4.653590000	-3.525800000	-0.009357000
6	-4.765547000	-2.491526000	0.911629000
1	-5.690110000	-2.376685000	1.470219000
6	-3.722371000	-1.595576000	1.140522000
6	-1.836957000	1.560068000	0.103337000
6	-1.541642000	2.774005000	0.760628000
6	-1.967179000	3.980774000	0.207411000
1	-1.712639000	4.907259000	0.714345000
6	-2.707216000	4.030994000	-0.969016000
6	-3.010908000	2.829362000	-1.596070000
1	-3.582402000	2.844499000	-2.519651000
6	-2.583180000	1.598548000	-1.092063000
51	1.006069000	-0.249940000	-1.002476000
6	2.516517000	-1.714238000	-0.416272000
6	3.722685000	-1.594897000	-1.140551000
6	4.766019000	-2.490682000	-0.911729000
1	5.690521000	-2.375706000	-1.470390000
6	4.654312000	-3.524940000	0.009306000
6	3.464266000	-3.633229000	0.717160000
1	3.361804000	-4.426185000	1.452442000
6	2.397306000	-2.751105000	0.530791000
6	1.836565000	1.560475000	-0.103303000
6	2.582727000	1.599159000	1.092126000
6	3.010123000	2.830091000	1.596122000
1	3.581580000	2.845393000	2.519723000
6	2.706194000	4.031630000	0.969015000
6	1.966242000	3.981207000	-0.207464000
1	1.711564000	4.907613000	-0.714473000
6	1.541030000	2.774325000	-0.760664000
6	3.181179000	5.347700000	1.526955000
1	3.409205000	5.266928000	2.590626000
1	4.089193000	5.677362000	1.014256000
1	2.426721000	6.125470000	1.394132000
6	0.761808000	2.832588000	-2.054284000
1	1.219910000	2.205785000	-2.824147000
1	-0.268493000	2.494020000	-1.917916000
1	0.724503000	3.856492000	-2.427844000
6	2.929235000	0.369462000	1.895043000
1	2.057195000	-0.274254000	2.021259000
1	3.707408000	-0.226453000	1.412223000
1	3.283157000	0.655772000	2.885998000

6	3.952254000	-0.494066000	-2.153383000
1	3.229019000	-0.545194000	-2.972457000
1	3.865295000	0.497210000	-1.697215000
1	4.949884000	-0.576262000	-2.585205000
6	1.207390000	-2.945450000	1.443884000
1	1.170620000	-2.171153000	2.215235000
1	0.248158000	-2.935220000	0.926628000
1	1.281058000	-3.906390000	1.954167000
6	5.775254000	-4.510410000	0.211861000
1	5.742985000	-4.944050000	1.212458000
1	5.700784000	-5.329541000	-0.508940000
1	6.747805000	-4.035012000	0.073549000
6	-1.206565000	-2.945892000	-1.443552000
1	-1.169901000	-2.171727000	-2.215038000
1	-0.247400000	-2.935374000	-0.926177000
1	-1.279969000	-3.906930000	-1.953692000
6	-5.774381000	-4.511432000	-0.211986000
1	-5.741959000	-4.945100000	-1.212566000
1	-5.699868000	-5.330523000	0.508854000
1	-6.747004000	-4.036147000	-0.073782000
6	-3.952200000	-0.494732000	2.153271000
1	-3.228851000	-0.545509000	2.972268000
1	-3.865603000	0.496515000	1.696972000
1	-4.949749000	-0.577215000	2.585224000
6	-2.929370000	0.368756000	-1.894980000
1	-2.057165000	-0.274756000	-2.021150000
1	-3.707441000	-0.227330000	-1.412216000
1	-3.283289000	0.654983000	-2.885962000
6	-0.762240000	2.832502000	2.054126000
1	-1.220283000	2.205914000	2.824201000
1	0.268012000	2.493822000	1.917684000
1	-0.724793000	3.856492000	2.427436000
6	-3.182499000	5.346931000	-1.527029000
1	-3.409747000	5.266226000	-2.590873000
1	-4.091034000	5.676052000	-1.014910000
1	-2.428507000	6.125038000	-1.393564000

$[(Mes)_2Sb\text{-}Sb(Mes)_2]^{+1}$ (**11**):

6	2.441550000	-2.752816000	0.600873000
6	2.592500000	-1.745315000	-0.368447000

51	1.142403000	-0.250771000	-0.853812000
6	3.485366000	-3.660863000	0.777503000
1	3.378912000	-4.436296000	1.529470000
6	4.656215000	-3.606046000	0.027890000
6	4.777846000	-2.600274000	-0.927733000
1	5.684700000	-2.539210000	-1.521429000
6	3.765603000	-1.670806000	-1.144661000
6	1.925464000	1.591008000	-0.099478000
6	1.527089000	2.757570000	-0.783882000
6	1.900968000	3.997145000	-0.271991000
1	1.584911000	4.895889000	-0.792638000
6	2.675270000	4.114475000	0.879056000
6	3.075297000	2.947863000	1.525587000
1	3.678902000	3.022433000	2.424684000
6	2.713761000	1.683055000	1.065598000
51	-1.144112000	-0.248849000	0.858268000
6	-2.595888000	-1.740783000	0.369339000
6	-3.770822000	-1.663086000	1.142431000
6	-4.784996000	-2.589897000	0.923041000
1	-5.693242000	-2.526261000	1.514325000
6	-4.663527000	-3.596199000	-0.032000000
6	-3.490767000	-3.654372000	-0.778363000
1	-3.384312000	-4.430369000	-1.529756000
6	-2.445035000	-2.749058000	-0.599203000
6	-1.921862000	1.593598000	0.099675000
6	-2.709119000	1.685951000	-1.066146000
6	-3.067847000	2.950925000	-1.527794000
1	-3.670633000	3.025681000	-2.427433000
6	-2.665960000	4.117530000	-0.882362000
6	-1.892509000	3.999984000	0.269179000
1	-1.574763000	4.898685000	0.788863000
6	-1.521453000	2.760227000	0.782770000
6	-3.085464000	5.468588000	-1.393297000
1	-3.299522000	5.440091000	-2.461879000
1	-3.992593000	5.799136000	-0.880118000
1	-2.312869000	6.217141000	-1.212255000
6	-0.717758000	2.723417000	2.061745000
1	-1.241804000	2.167357000	2.845274000
1	0.265928000	2.267905000	1.915289000
1	-0.550838000	3.733558000	2.435060000
6	-3.162825000	0.485331000	-1.858290000
1	-2.327361000	-0.181420000	-2.087106000
1	-3.908128000	-0.100629000	-1.315428000
1	-3.602841000	0.801888000	-2.803323000

6	-3.974433000	-0.588109000	2.186352000
1	-3.203183000	-0.627191000	2.964103000
1	-3.965018000	0.413519000	1.742744000
1	-4.934330000	-0.713255000	2.685881000
6	-1.243472000	-2.881892000	-1.503883000
1	-1.165099000	-2.034537000	-2.191501000
1	-0.301279000	-2.956961000	-0.955459000
1	-1.325606000	-3.783667000	-2.109717000
6	-5.758897000	-4.608731000	-0.226067000
1	-5.710165000	-5.059609000	-1.217338000
1	-5.666252000	-5.410110000	0.511869000
1	-6.742085000	-4.153767000	-0.099096000
6	1.241968000	-2.882075000	1.508719000
1	1.165739000	-2.032674000	2.193987000
1	0.298457000	-2.958089000	0.962630000
1	1.324810000	-3.782134000	2.117000000
6	5.749563000	-4.621281000	0.219213000
1	5.700321000	-5.074355000	1.209447000
1	5.655068000	-5.420714000	-0.520593000
1	6.733609000	-4.167957000	0.092916000
6	3.969325000	-0.596404000	-2.189131000
1	3.195821000	-0.633189000	-2.964749000
1	3.963957000	0.405177000	-1.745354000
1	4.927493000	-0.724214000	-2.691290000
6	3.165627000	0.482263000	1.858506000
1	2.328374000	-0.180991000	2.091073000
1	3.907140000	-0.107286000	1.314401000
1	3.609568000	0.798815000	2.801694000
6	0.723159000	2.720569000	-2.062672000
1	1.247105000	2.164054000	-2.845956000
1	-0.260624000	2.265328000	-1.916123000
1	0.556407000	3.730607000	-2.436346000
6	3.097590000	5.465412000	1.388001000
1	3.317575000	5.436758000	2.455369000
1	4.001772000	5.796105000	0.869745000
1	2.323957000	6.213969000	1.211358000

$[(Mes)_2Sb\text{-}Sb(Mes)_2]^{+2}$ (**12**) [singlet]:

6	2.651895000	-2.554915000	0.733093000
6	2.750943000	-1.590401000	-0.285827000

51	1.276101000	-0.156711000	-0.717983000
6	3.735147000	-3.411266000	0.911477000
1	3.688205000	-4.152222000	1.702518000
6	4.872246000	-3.354137000	0.106142000
6	4.924072000	-2.393344000	-0.907222000
1	5.801327000	-2.341559000	-1.544270000
6	3.880685000	-1.504040000	-1.122283000
6	1.904250000	1.765735000	-0.178016000
6	1.264680000	2.845023000	-0.834579000
6	1.524509000	4.134029000	-0.384308000
1	1.043338000	4.969630000	-0.881855000
6	2.399963000	4.383695000	0.672228000
6	3.031692000	3.298174000	1.287771000
1	3.716732000	3.487006000	2.107935000
6	2.816203000	1.987489000	0.886983000
51	-1.201221000	-0.332766000	0.644941000
6	-2.486260000	-1.947741000	0.294495000
6	-3.661573000	-1.937679000	1.074766000
6	-4.566682000	-2.972872000	0.900509000
1	-5.473379000	-2.985554000	1.497175000
6	-4.339487000	-4.004505000	-0.017449000
6	-3.162220000	-3.985031000	-0.764072000
1	-2.977511000	-4.781575000	-1.476740000
6	-2.208379000	-2.981079000	-0.619137000
6	-2.127086000	1.471157000	0.138041000
6	-3.043473000	1.558163000	-0.939640000
6	-3.502261000	2.819755000	-1.293317000
1	-4.196369000	2.908919000	-2.122712000
6	-3.100837000	3.977564000	-0.619816000
6	-2.199889000	3.855960000	0.439095000
1	-1.891378000	4.746964000	0.976114000
6	-1.703952000	2.622387000	0.842284000
6	-3.659656000	5.314075000	-1.008808000
1	-3.794120000	5.387706000	-2.088615000
1	-4.642253000	5.449942000	-0.547045000
1	-3.019923000	6.129999000	-0.673894000
6	-0.784707000	2.561555000	2.038419000
1	-1.275625000	2.080256000	2.889527000
1	0.147787000	2.028503000	1.823979000
1	-0.502542000	3.566047000	2.352920000
6	-3.517931000	0.366272000	-1.735322000
1	-2.685314000	-0.241194000	-2.103485000
1	-4.163573000	-0.286070000	-1.142337000
1	-4.086060000	0.698279000	-2.602643000

6	-3.967364000	-0.831874000	2.057824000
1	-3.107643000	-0.588385000	2.697610000
1	-4.285266000	0.083199000	1.548216000
1	-4.767765000	-1.128030000	2.734924000
6	-0.969718000	-3.017917000	-1.477669000
1	-0.943672000	-2.175894000	-2.178221000
1	-0.050464000	-2.999894000	-0.883043000
1	-0.942276000	-3.931429000	-2.069883000
6	-5.336564000	-5.115931000	-0.165750000
1	-5.108295000	-5.747667000	-1.022885000
1	-5.336181000	-5.742274000	0.730345000
1	-6.345418000	-4.716270000	-0.284077000
6	1.471785000	-2.672788000	1.664311000
1	1.305358000	-1.745620000	2.223242000
1	0.547873000	-2.925641000	1.134520000
1	1.640579000	-3.462867000	2.394482000
6	6.004264000	-4.321495000	0.295874000
1	5.991414000	-4.760261000	1.292869000
1	5.923361000	-5.134333000	-0.431335000
1	6.967493000	-3.834646000	0.138989000
6	3.993564000	-0.454031000	-2.203033000
1	3.107961000	-0.428502000	-2.853896000
1	4.144678000	0.544634000	-1.778826000
1	4.838137000	-0.659722000	-2.859643000
6	3.542342000	0.884451000	1.617362000
1	2.856670000	0.135789000	2.024193000
1	4.248743000	0.364464000	0.966217000
1	4.103380000	1.299585000	2.452926000
6	0.367949000	2.672004000	-2.036514000
1	0.953530000	2.414557000	-2.923871000
1	-0.397167000	1.903507000	-1.892797000
1	-0.162501000	3.599925000	-2.249835000
6	2.693994000	5.783844000	1.122263000
1	2.727221000	5.847664000	2.211045000
1	3.674313000	6.093639000	0.748697000
1	1.954845000	6.490945000	0.747543000

$[(Mes)_2Sb\text{-}Sb(Mes)_2]^{+2}$ (**12**) [triplet]:

6	3.484513000	-0.872541000	0.817617000
6	3.181103000	-0.038294000	-0.275512000

51	1.227995000	0.570193000	-0.767373000
6	4.822397000	-1.171051000	1.040932000
1	5.084184000	-1.795195000	1.889205000
6	5.842759000	-0.687836000	0.216741000
6	5.498074000	0.125650000	-0.863372000
1	6.280271000	0.506175000	-1.511686000
6	4.177172000	0.459102000	-1.139269000
6	0.673304000	2.526563000	-0.214525000
6	-0.477720000	3.056476000	-0.825857000
6	-0.981869000	4.256611000	-0.327371000
1	-1.873192000	4.676471000	-0.782945000
6	-0.363039000	4.937231000	0.717758000
6	0.797903000	4.391739000	1.276658000
1	1.289954000	4.918879000	2.087718000
6	1.346134000	3.195905000	0.833147000
51	-0.887373000	-0.810696000	0.605239000
6	-1.030501000	-2.885670000	0.313675000
6	-1.984946000	-3.527472000	1.129774000
6	-2.166476000	-4.894352000	0.956746000
1	-2.901485000	-5.405876000	1.569156000
6	-1.422881000	-5.626322000	0.029982000
6	-0.472489000	-4.954281000	-0.744226000
1	0.106964000	-5.516650000	-1.468988000
6	-0.245896000	-3.589968000	-0.620748000
6	-2.606658000	0.292208000	0.082089000
6	-3.366647000	-0.091057000	-1.038679000
6	-4.472543000	0.691190000	-1.354272000
1	-5.074671000	0.418372000	-2.215161000
6	-4.826401000	1.816207000	-0.604777000
6	-4.034477000	2.165562000	0.489639000
1	-4.299606000	3.036853000	1.079787000
6	-2.920078000	1.417394000	0.861479000
6	-6.052094000	2.610458000	-0.955624000
1	-6.212210000	2.636927000	-2.033762000
1	-6.933616000	2.148058000	-0.502828000
1	-5.986011000	3.632582000	-0.583778000
6	-2.119103000	1.816981000	2.076228000
1	-2.171101000	1.048508000	2.854376000
1	-1.066601000	2.000597000	1.828986000
1	-2.507486000	2.739317000	2.507114000
6	-3.027956000	-1.282390000	-1.899869000
1	-1.980689000	-1.268172000	-2.224889000
1	-3.196456000	-2.224395000	-1.371251000
1	-3.642786000	-1.289574000	-2.798656000

6	-2.809415000	-2.787063000	2.155504000
1	-2.177742000	-2.294050000	2.902255000
1	-3.455536000	-2.034368000	1.690163000
1	-3.457626000	-3.475352000	2.695509000
6	0.787433000	-2.937804000	-1.505941000
1	0.340735000	-2.176258000	-2.153971000
1	1.599521000	-2.482772000	-0.928427000
1	1.246461000	-3.678047000	-2.159848000
6	-1.652203000	-7.097968000	-0.148043000
1	-2.401903000	-7.263048000	-0.927743000
1	-0.738659000	-7.608055000	-0.453494000
1	-2.021763000	-7.555337000	0.769459000
6	2.444936000	-1.418122000	1.765077000
1	1.837053000	-0.619949000	2.204762000
1	1.783618000	-2.143027000	1.276383000
1	2.923124000	-1.941534000	2.592124000
6	7.277937000	-1.015110000	0.506385000
1	7.690166000	-0.283348000	1.207572000
1	7.375359000	-2.000600000	0.962155000
1	7.882822000	-0.985047000	-0.399502000
6	3.859180000	1.339413000	-2.324305000
1	3.271663000	0.805323000	-3.077919000
1	3.313425000	2.243827000	-2.028910000
1	4.773992000	1.673014000	-2.812012000
6	2.599890000	2.674418000	1.490544000
1	2.444717000	1.697185000	1.957707000
1	3.419401000	2.570956000	0.775442000
1	2.926082000	3.359192000	2.271488000
6	-1.156679000	2.442342000	-2.023079000
1	-0.764875000	2.882911000	-2.943975000
1	-1.022842000	1.357246000	-2.098294000
1	-2.232274000	2.623650000	-1.988916000
6	-0.897327000	6.251128000	1.209787000
1	-0.745832000	6.363055000	2.283861000
1	-0.369389000	7.072020000	0.716024000
1	-1.958895000	6.359545000	0.988749000

$[(Mes)_2Sb\text{-}Sb(Mes)_2]^{-1}$ (**13**):

6	-3.112716000	-2.841597000	0.367796000

6	-3.207673000	-1.467997000	0.675124000
51	-1.386163000	-0.335804000	1.145681000
6	-4.258791000	-3.590359000	0.105774000
1	-4.157768000	-4.646124000	-0.135426000
6	-5.527642000	-3.020032000	0.137949000
6	-5.620844000	-1.668163000	0.444009000
1	-6.601979000	-1.199842000	0.477806000
6	-4.492337000	-0.889179000	0.716030000
6	-1.807807000	1.357731000	-0.168973000
6	-1.625319000	2.668056000	0.326042000
6	-1.874538000	3.768798000	-0.490448000
1	-1.719816000	4.768041000	-0.089121000
6	-2.306857000	3.623000000	-1.806118000
6	-2.485365000	2.334093000	-2.290124000
1	-2.814001000	2.194618000	-3.317252000
6	-2.239388000	1.203258000	-1.502652000
51	1.386274000	-0.335710000	-1.145494000
6	3.207855000	-1.467740000	-0.674779000
6	4.492510000	-0.888908000	-0.715989000
6	5.621104000	-1.667874000	-0.444311000
1	6.602221000	-1.199537000	-0.478381000
6	5.528009000	-3.019762000	-0.138285000
6	4.259176000	-3.590096000	-0.105767000
1	4.158235000	-4.645865000	0.135446000
6	3.113005000	-2.841348000	-0.367443000
6	1.807556000	1.358042000	0.168968000
6	2.239272000	1.203763000	1.502621000
6	2.485144000	2.334702000	2.289976000
1	2.814011000	2.195374000	3.317050000
6	2.306341000	3.623532000	1.805881000
6	1.873830000	3.769139000	0.490248000
1	1.718862000	4.768323000	0.088865000
6	1.624758000	2.668289000	-0.326141000
6	2.516314000	4.828706000	2.686574000
1	3.134868000	4.581903000	3.551811000
1	3.001831000	5.639860000	2.138324000
1	1.559417000	5.208789000	3.058879000
6	1.176145000	2.918330000	-1.745215000
1	1.928824000	2.562970000	-2.456144000
1	0.248029000	2.387446000	-1.968912000
1	1.002375000	3.983794000	-1.913023000
6	2.480447000	-0.147249000	2.132832000
1	1.713066000	-0.864911000	1.833008000
1	3.445322000	-0.561513000	1.824369000

1	2.473329000	-0.063301000	3.221553000
6	4.708241000	0.572748000	-1.026079000
1	4.077330000	0.894413000	-1.859042000
1	4.442907000	1.201916000	-0.171525000
1	5.753707000	0.760555000	-1.280799000
6	1.772550000	-3.530707000	-0.285860000
1	1.134126000	-3.048084000	0.460105000
1	1.235741000	-3.473329000	-1.237361000
1	1.888090000	-4.584833000	-0.024372000
6	6.758897000	-3.853318000	0.114957000
1	6.584229000	-4.584148000	0.908229000
1	7.050071000	-4.407391000	-0.783064000
1	7.604918000	-3.228288000	0.407777000
6	-1.772193000	-3.530856000	0.286619000
1	-1.133580000	-3.048220000	-0.459177000
1	-1.235688000	-3.473353000	1.238287000
1	-1.887533000	-4.585016000	0.025178000
6	-6.758444000	-3.853596000	-0.115701000
1	-6.583570000	-4.584279000	-0.909063000
1	-7.049791000	-4.407835000	0.782160000
1	-7.604422000	-3.228548000	-0.408602000
6	-4.708197000	0.572479000	1.026033000
1	-4.077288000	0.894259000	1.858947000
1	-4.442988000	1.201628000	0.171423000
1	-5.753674000	0.760184000	1.280797000
6	-2.480226000	-0.147834000	-2.132829000
1	-1.712757000	-0.865335000	-1.832859000
1	-3.445070000	-0.562260000	-1.824502000
1	-2.472945000	-0.063934000	-3.221553000
6	-1.176817000	2.918290000	1.745113000
1	-1.929430000	2.562815000	2.456056000
1	-0.248598000	2.387607000	1.968845000
1	-1.003276000	3.983801000	1.912859000
6	-2.516863000	4.828052000	-2.686968000
1	-3.135382000	4.581121000	-3.552193000
1	-3.002430000	5.639254000	-2.138832000
1	-1.559969000	5.208128000	-3.059291000

[$(Mes)_2P$-$P(Mes)_2$] (**19**):

6	2.089007000	-2.608537000	0.678900000
6	2.152249000	-1.571371000	-0.278583000

15	0.829021000	-0.356797000	-0.759689000
6	3.197551000	-3.435558000	0.863727000
1	3.134172000	-4.222752000	1.609212000
6	4.375941000	-3.286606000	0.144548000
6	4.417843000	-2.281330000	-0.810918000
1	5.318292000	-2.150043000	-1.404059000
6	3.334047000	-1.437727000	-1.048008000
6	1.587770000	1.257052000	-0.251004000
6	1.442696000	2.323742000	-1.169181000
6	2.024262000	3.556409000	-0.887138000
1	1.893982000	4.370039000	-1.594311000
6	2.771322000	3.773188000	0.265829000
6	2.922297000	2.713201000	1.149311000
1	3.495067000	2.861719000	2.060260000
6	2.345356000	1.462223000	0.919595000
15	-0.829075000	-0.356802000	0.759898000
6	-2.152242000	-1.571406000	0.278679000
6	-3.334069000	-1.437742000	1.048020000
6	-4.417913000	-2.281269000	0.810802000
1	-5.318395000	-2.149951000	1.403882000
6	-4.376003000	-3.286479000	-0.144719000
6	-3.197541000	-3.435491000	-0.863794000
1	-3.134151000	-4.222665000	-1.609302000
6	-2.088966000	-2.608566000	-0.678832000
6	-1.587860000	1.257038000	0.251141000
6	-2.345418000	1.462162000	-0.919501000
6	-2.922265000	2.713152000	-1.149331000
1	-3.495014000	2.861630000	-2.060301000
6	-2.771183000	3.773230000	-0.265961000
6	-2.024161000	3.556503000	0.887029000
1	-1.893779000	4.370205000	1.594096000
6	-1.442732000	2.323794000	1.169218000
6	-3.418331000	5.107613000	-0.527929000
1	-3.630432000	5.242230000	-1.589426000
1	-4.364270000	5.188712000	0.014883000
1	-2.776826000	5.926657000	-0.198006000
6	-0.704548000	2.183760000	2.479531000
1	-1.140291000	1.393532000	3.095473000
1	0.345444000	1.935333000	2.326874000
1	-0.752449000	3.120404000	3.035891000
6	-2.566731000	0.405054000	-1.974412000
1	-1.666435000	-0.184322000	-2.148104000
1	-3.365394000	-0.283276000	-1.685956000
1	-2.850583000	0.878435000	-2.915747000

6	-3.498098000	-0.403342000	2.137841000
1	-2.619469000	-0.368658000	2.786582000
1	-3.639898000	0.599379000	1.726192000
1	-4.365873000	-0.645928000	2.751702000
6	-0.905791000	-2.885855000	-1.577754000
1	-0.791548000	-2.118311000	-2.345813000
1	0.041139000	-2.949610000	-1.041933000
1	-1.049819000	-3.840961000	-2.083927000
6	-5.545036000	-4.211228000	-0.359181000
1	-5.569500000	-4.584227000	-1.384252000
1	-5.480408000	-5.075699000	0.307705000
1	-6.489880000	-3.705069000	-0.154905000
6	0.905967000	-2.885751000	1.578019000
1	0.792134000	-2.118388000	2.346327000
1	-0.041165000	-2.949058000	1.042507000
1	1.049848000	-3.841041000	2.083887000
6	5.544933000	-4.211461000	0.358786000
1	5.568846000	-4.585456000	1.383503000
1	5.480755000	-5.075272000	-0.308997000
1	6.489854000	-3.705026000	0.155537000
6	3.498056000	-0.403296000	-2.137798000
1	2.619516000	-0.368798000	-2.786675000
1	3.639601000	0.599460000	-1.726160000
1	4.365972000	-0.645721000	-2.751522000
6	2.566659000	0.405179000	1.974569000
1	1.666405000	-0.184258000	2.148235000
1	3.365396000	-0.283100000	1.686187000
1	2.850422000	0.878620000	2.915902000
6	0.704414000	2.183647000	-2.479431000
1	1.139897000	1.393194000	-3.095260000
1	-0.345629000	1.935506000	-2.326632000
1	0.752493000	3.120181000	-3.035960000
6	3.418589000	5.107553000	0.527592000
1	3.632498000	5.241503000	1.588806000
1	4.363546000	5.189249000	-0.016836000
1	2.776317000	5.926671000	0.199333000

$[(Mes)_2P\text{-}P(Mes)_2]^{\cdot -}$ (**20**):

6	3.022675000	-2.570245000	0.693416000
6	3.037414000	-1.565276000	-0.297881000

15	1.448945000	-0.839752000	-0.879119000
6	4.206000000	-3.207875000	1.061024000
1	4.174066000	-3.965772000	1.840226000
6	5.424822000	-2.894891000	0.467406000
6	5.430804000	-1.921164000	-0.526068000
1	6.369509000	-1.667710000	-1.013802000
6	4.267850000	-1.262543000	-0.923645000
6	1.648631000	0.960723000	-0.708451000
6	0.788995000	1.732106000	-1.539917000
6	0.813867000	3.120018000	-1.497840000
1	0.127657000	3.673909000	-2.134078000
6	1.663253000	3.814086000	-0.644104000
6	2.474878000	3.063830000	0.199875000
1	3.116275000	3.582969000	0.909408000
6	2.478903000	1.669019000	0.202239000
15	-1.448758000	-0.839643000	0.878893000
6	-3.037128000	-1.565497000	0.297800000
6	-4.267578000	-1.262852000	0.923612000
6	-5.430491000	-1.921592000	0.526110000
1	-6.369199000	-1.668180000	1.013864000
6	-5.424469000	-2.895407000	-0.467274000
6	-4.205633000	-3.208353000	-1.060879000
1	-4.173632000	-3.966362000	-1.839968000
6	-3.022352000	-2.570573000	-0.693380000
6	-1.648860000	0.960781000	0.708394000
6	-2.479215000	1.669053000	-0.202237000
6	-2.475265000	3.063864000	-0.199859000
1	-3.116708000	3.582975000	-0.909370000
6	-1.663673000	3.814163000	0.644124000
6	-0.814269000	3.120128000	1.497867000
1	-0.128152000	3.674048000	2.134181000
6	-0.789298000	1.732220000	1.539892000
6	-1.695455000	5.320473000	0.616363000
1	-1.776678000	5.693854000	-0.408482000
1	-2.551231000	5.712513000	1.176294000
1	-0.787958000	5.738946000	1.056502000
6	0.164922000	1.058053000	2.489393000
1	-0.375348000	0.540628000	3.288865000
1	0.754965000	0.301100000	1.965094000
1	0.851783000	1.787093000	2.925576000
6	-3.368059000	0.996651000	-1.221920000
1	-2.895445000	0.115572000	-1.656628000
1	-4.315296000	0.659161000	-0.790638000
1	-3.595397000	1.699197000	-2.027174000

6	-4.360923000	-0.229203000	2.016533000
1	-3.562666000	-0.374409000	2.749847000
1	-4.234127000	0.784330000	1.624025000
1	-5.329001000	-0.288573000	2.518639000
6	-1.739429000	-2.945613000	-1.391117000
1	-1.277670000	-2.079640000	-1.874247000
1	-0.994157000	-3.311191000	-0.679449000
1	-1.915971000	-3.720972000	-2.139702000
6	-6.690905000	-3.615776000	-0.856788000
1	-6.614896000	-4.024849000	-1.866461000
1	-6.896120000	-4.448680000	-0.176643000
1	-7.552920000	-2.945358000	-0.824867000
6	1.739745000	-2.945255000	1.391157000
1	1.277849000	-2.079231000	1.874064000
1	0.994573000	-3.311055000	0.679487000
1	1.916308000	-3.720456000	2.139900000
6	6.691314000	-3.615103000	0.857036000
1	6.615110000	-4.024529000	1.866550000
1	6.896895000	-4.447733000	0.176667000
1	7.553194000	-2.944490000	0.825575000
6	4.361107000	-0.228897000	-2.016570000
1	3.562911000	-0.374224000	-2.749926000
1	4.234135000	0.784609000	-1.624053000
1	5.329222000	-0.288105000	-2.518624000
6	3.367699000	0.996645000	1.221976000
1	2.895141000	0.115479000	1.656566000
1	4.315018000	0.659265000	0.790783000
1	3.594866000	1.699162000	2.027304000
6	-0.165164000	1.057918000	-2.489456000
1	0.375181000	0.540691000	-3.289010000
1	-0.755102000	0.300826000	-1.965253000
1	-0.852090000	1.786935000	-2.925575000
6	1.694956000	5.320408000	-0.616413000
1	1.776617000	5.693841000	0.408364000
1	2.550448000	5.712452000	-1.176776000
1	0.787234000	5.738765000	-1.056196000

$[(Mes)_2P\text{-}P(Mes)_2]^{\cdot+}$ (**21**):

6	2.002761000	-2.569627000	0.803925000
6	2.117141000	-1.579936000	-0.198676000

15	0.911360000	-0.279005000	-0.575054000
6	3.066475000	-3.449496000	0.987698000
1	2.984972000	-4.202223000	1.764781000
6	4.222368000	-3.401283000	0.215424000
6	4.295689000	-2.441403000	-0.790060000
1	5.178125000	-2.401951000	-1.420853000
6	3.267313000	-1.536651000	-1.025706000
6	1.673034000	1.329988000	-0.231622000
6	1.484959000	2.342433000	-1.199829000
6	2.119586000	3.564959000	-1.015512000
1	1.973230000	4.346840000	-1.753554000
6	2.945612000	3.810100000	0.079120000
6	3.121852000	2.793514000	1.013960000
1	3.753996000	2.974097000	1.877593000
6	2.504818000	1.551603000	0.886740000
15	-0.911379000	-0.278966000	0.575023000
6	-2.117196000	-1.579859000	0.198604000
6	-3.267323000	-1.536620000	1.025717000
6	-4.295683000	-2.441394000	0.790136000
1	-5.178073000	-2.401984000	1.420998000
6	-4.222412000	-3.401254000	-0.215383000
6	-3.066587000	-3.449408000	-0.987745000
1	-2.985118000	-4.202110000	-1.764853000
6	-2.002869000	-2.569518000	-0.804020000
6	-1.672985000	1.330058000	0.231586000
6	-2.504784000	1.551707000	-0.886754000
6	-3.121824000	2.793623000	-1.013927000
1	-3.753981000	2.974231000	-1.877545000
6	-2.945564000	3.810182000	-0.079064000
6	-2.119505000	3.565012000	1.015540000
1	-1.973125000	4.346878000	1.753594000
6	-1.484874000	2.342483000	1.199809000
6	-3.648823000	5.130561000	-0.228366000
1	-3.920983000	5.320582000	-1.266635000
1	-4.567151000	5.136512000	0.365129000
1	-3.022767000	5.951238000	0.123967000
6	-0.654501000	2.138964000	2.441935000
1	-1.047519000	1.322030000	3.053492000
1	0.383544000	1.907535000	2.198782000
1	-0.658953000	3.042489000	3.050684000
6	-2.743898000	0.526313000	-1.966632000
1	-1.833588000	-0.024309000	-2.213330000
1	-3.498507000	-0.203629000	-1.661621000
1	-3.096308000	1.017710000	-2.873437000

6	-3.433385000	-0.553882000	2.160751000
1	-2.538042000	-0.508631000	2.787596000
1	-3.641560000	0.456105000	1.797891000
1	-4.263260000	-0.859052000	2.796894000
6	-0.807108000	-2.737147000	-1.703898000
1	-0.592916000	-1.832410000	-2.278737000
1	0.096077000	-2.996726000	-1.146203000
1	-0.988549000	-3.542124000	-2.414608000
6	-5.340293000	-4.384361000	-0.423800000
1	-5.307737000	-4.815411000	-1.424315000
1	-5.260767000	-5.202292000	0.297429000
1	-6.312133000	-3.910366000	-0.279855000
6	0.806946000	-2.737260000	1.703730000
1	0.592797000	-1.832554000	2.278639000
1	-0.096235000	-2.996731000	1.145982000
1	0.988306000	-3.542306000	2.414382000
6	5.340226000	-4.384398000	0.423924000
1	5.308340000	-4.814492000	1.424874000
1	5.259990000	-5.203010000	-0.296452000
1	6.312046000	-3.910731000	0.278806000
6	3.433465000	-0.553875000	-2.160692000
1	2.538072000	-0.508359000	-2.787442000
1	3.641911000	0.456035000	-1.797770000
1	4.263200000	-0.859193000	-2.796946000
6	2.743932000	0.526171000	1.966582000
1	1.833610000	-0.024421000	2.213307000
1	3.498492000	-0.203800000	1.661515000
1	3.096406000	1.017524000	2.873386000
6	0.654596000	2.138965000	-2.441971000
1	1.047426000	1.321862000	-3.053421000
1	-0.383514000	1.907821000	-2.198823000
1	0.659285000	3.042419000	-3.050825000
6	3.648874000	5.130472000	0.228481000
1	3.920830000	5.320547000	1.266794000
1	4.567321000	5.136364000	-0.364828000
1	3.022908000	5.951143000	-0.124024000

$[(Mes)_2P\text{-}P(Mes)_2]^{+2}$ (**22**):

6	2.456796000	1.639110000	1.149521000
6	1.530263000	1.863674000	0.101407000
15	0.002471000	0.997923000	-0.002162000

6	3.593575000	2.436233000	1.173659000
1	4.310502000	2.293905000	1.975294000
6	3.840321000	3.419435000	0.213334000
6	2.906946000	3.605388000	-0.811235000
1	3.093225000	4.362240000	-1.565829000
6	1.747923000	2.852621000	-0.896411000
6	-1.525886000	1.862621000	-0.105222000
6	-2.459276000	1.626736000	-1.145680000
6	-3.604940000	2.409902000	-1.159842000
1	-4.330777000	2.254445000	-1.951297000
6	-3.852369000	3.395144000	-0.200727000
6	-2.913054000	3.592408000	0.815245000
1	-3.102625000	4.345187000	1.572824000
6	-1.744793000	2.851640000	0.891661000
15	0.002666000	-0.997916000	0.002237000
6	1.530545000	-1.863503000	-0.101434000
6	1.748306000	-2.852505000	0.896324000
6	2.907426000	-3.605121000	0.811126000
1	3.093774000	-4.362021000	1.565653000
6	3.840839000	-3.418945000	-0.213371000
6	3.594010000	-2.435684000	-1.173614000
1	4.310955000	-2.293176000	-1.975202000
6	2.457113000	-1.638736000	-1.149474000
6	-1.525553000	-1.862869000	0.105291000
6	-1.744414000	-2.851726000	-0.891738000
6	-2.912615000	-3.592612000	-0.815381000
1	-3.102151000	-4.345291000	-1.573067000
6	-3.851885000	-3.395610000	0.200667000
6	-3.604501000	-2.410498000	1.159941000
1	-4.330324000	-2.255234000	1.951448000
6	-2.458919000	-1.627224000	1.145831000
6	-5.090073000	-4.237011000	0.279240000
1	-5.307156000	-4.720306000	-0.672341000
1	-4.955186000	-5.019791000	1.031615000
1	-5.952565000	-3.640356000	0.578833000
6	-2.282637000	-0.590240000	2.224373000
1	-1.242114000	-0.479834000	2.538877000
1	-2.640815000	0.385820000	1.883119000
1	-2.864633000	-0.865975000	3.102818000
6	-0.782744000	-3.107318000	-2.025391000
1	-0.448140000	-2.177671000	-2.496600000
1	0.103010000	-3.651468000	-1.686415000
1	-1.266127000	-3.705150000	-2.796534000
6	0.790329000	-3.099481000	2.035017000

1	0.458509000	-2.166379000	2.501384000
1	-0.097347000	-3.644406000	1.702373000
1	1.275582000	-3.692974000	2.808380000
6	2.281016000	-0.602430000	-2.228502000
1	1.240355000	-0.491232000	-2.542344000
1	2.639437000	0.373566000	-1.887253000
1	2.862536000	-0.878428000	-3.107133000
6	5.093453000	-4.240971000	-0.263671000
1	5.439962000	-4.374295000	-1.288319000
1	5.888522000	-3.734371000	0.292006000
1	4.944112000	-5.220477000	0.190137000
6	2.280770000	0.602852000	2.228615000
1	1.240148000	0.491770000	2.542637000
1	2.639069000	-0.373190000	1.887361000
1	2.862435000	0.878851000	3.107151000
6	5.092810000	4.241653000	0.263604000
1	5.439704000	4.374507000	1.288179000
1	5.887745000	3.735505000	-0.292676000
1	4.943110000	5.221370000	-0.189642000
6	0.789895000	3.099405000	-2.035098000
1	0.457993000	2.166229000	-2.501253000
1	-0.097739000	3.644435000	-1.702497000
1	1.275108000	3.692738000	-2.808613000
6	-0.783078000	3.107499000	2.025218000
1	-0.448495000	2.177963000	2.496662000
1	0.102671000	3.651547000	1.686074000
1	-1.266415000	3.705557000	2.796215000
6	-2.282969000	0.589612000	-2.224084000
1	-1.242445000	0.479186000	-2.538577000
1	-2.641107000	-0.386416000	-1.882692000
1	-2.864991000	0.865216000	-3.102551000
6	-5.090610000	4.236461000	-0.279351000
1	-5.308193000	4.719088000	0.672460000
1	-4.955401000	5.019795000	-1.031093000
1	-5.952902000	3.639952000	-0.579783000

Coordinates for complex 6:

19	-4.190882000	1.934758000	0.567169000
19	0.262656000	-1.004903000	-1.381743000

19	3.321693000	2.251706000	1.656767000
8	-6.141510000	2.222909000	-1.138568000
6	-6.308941000	1.328279000	-2.238822000
1	-5.908694000	0.342106000	-1.953240000
1	-5.725175000	1.699002000	-3.098557000
6	-7.802727000	1.337854000	-2.541978000
1	-8.333131000	0.626120000	-1.891042000
1	-8.022689000	1.073292000	-3.584222000
6	-8.176333000	2.777100000	-2.181603000
1	-7.888857000	3.458009000	-2.996708000
1	-9.245094000	2.919086000	-1.976537000
6	-7.301881000	3.025394000	-0.953570000
1	-6.996243000	4.077435000	-0.844147000
1	-7.807370000	2.712681000	-0.022119000
8	-6.319632000	0.982380000	1.806907000
6	-6.845642000	0.841906000	3.126524000
1	-7.272011000	1.803806000	3.448981000
1	-6.020569000	0.581496000	3.809384000
6	-7.885191000	-0.278467000	3.052220000
1	-8.879028000	0.136224000	2.824534000
1	-7.958720000	-0.843329000	3.990752000
6	-7.374077000	-1.113965000	1.876750000
1	-6.551428000	-1.776433000	2.185699000
1	-8.146011000	-1.736074000	1.404572000
6	-6.845810000	-0.032193000	0.947011000
1	-6.039882000	-0.386232000	0.283137000
1	-7.654213000	0.399148000	0.326892000
8	1.754380000	-2.112089000	-3.289768000
6	1.803423000	-2.265433000	-4.697911000
1	1.935547000	-1.268181000	-5.142994000
1	0.843985000	-2.686009000	-5.051885000
6	2.972343000	-3.231885000	-4.978905000
1	3.851679000	-2.695654000	-5.358311000
1	2.690030000	-3.977836000	-5.734251000

6	3.265080000	-3.870022000	-3.601054000
1	3.307580000	-4.967091000	-3.637948000
1	4.219637000	-3.507849000	-3.189756000
6	2.109595000	-3.374064000	-2.731356000
1	1.236272000	-4.052637000	-2.781291000
1	2.390033000	-3.210289000	-1.679967000
8	4.977354000	3.826409000	0.348629000
6	4.645784000	3.429885000	-0.991977000
1	3.555338000	3.522357000	-1.128762000
1	4.934089000	2.376349000	-1.133637000
6	5.384702000	4.398765000	-1.909626000
1	4.845648000	4.558364000	-2.853308000
1	6.396191000	4.028030000	-2.136896000
6	5.460679000	5.650839000	-1.034162000
1	6.239835000	6.361463000	-1.340659000
1	4.485977000	6.164630000	-1.037556000
6	5.720802000	5.038969000	0.337285000
1	6.793120000	4.817905000	0.480820000
1	5.379575000	5.668538000	1.171906000
8	3.039504000	2.631644000	4.225766000
6	2.998004000	1.386865000	4.927657000
1	3.925566000	1.256076000	5.513264000
1	2.939773000	0.564520000	4.199334000
6	1.781977000	1.505069000	5.832265000
1	1.799984000	0.794829000	6.668816000
1	0.864813000	1.332627000	5.245603000
6	1.879872000	2.971388000	6.257363000
1	0.935362000	3.394036000	6.624756000
1	2.632496000	3.081543000	7.052221000
6	2.360899000	3.643303000	4.967782000
1	1.513846000	4.012503000	4.364992000
1	3.045135000	4.484788000	5.153674000
51	3.228628000	-0.858176000	0.206935000
6	4.794931000	-2.170044000	-0.622329000

6	4.938174000	-3.517185000	-0.192814000
6	5.979995000	-4.300865000	-0.700550000
1	6.084229000	-5.330209000	-0.343487000
6	6.887162000	-3.820089000	-1.646129000
6	6.704702000	-2.518129000	-2.102283000
1	7.384521000	-2.133262000	-2.869108000
6	5.676611000	-1.695417000	-1.620440000
6	4.002562000	-4.198290000	0.802565000
1	3.183925000	-3.500516000	1.023117000
6	3.368206000	-5.462809000	0.210856000
1	2.861660000	-5.251785000	-0.742785000
1	4.119731000	-6.245872000	0.025411000
1	2.622393000	-5.876639000	0.907099000
6	4.711343000	-4.525760000	2.121723000
1	5.145975000	-3.625344000	2.578834000
1	4.002304000	-4.961806000	2.843408000
1	5.520859000	-5.256171000	1.959063000
6	8.007869000	-4.694096000	-2.175140000
1	8.583273000	-4.083493000	-2.890444000
6	7.458268000	-5.908193000	-2.930103000
1	6.877975000	-6.555849000	-2.254808000
1	8.275167000	-6.510675000	-3.355463000
1	6.793340000	-5.595573000	-3.748147000
6	8.958473000	-5.126437000	-1.055242000
1	9.363880000	-4.253886000	-0.523582000
1	9.798710000	-5.712322000	-1.457567000
1	8.433137000	-5.753498000	-0.318538000
6	5.536928000	-0.325045000	-2.271652000
1	4.731171000	0.211090000	-1.746915000
6	6.804465000	0.521620000	-2.137293000
1	6.662672000	1.508507000	-2.606043000
1	7.060207000	0.676026000	-1.077334000
1	7.667577000	0.045312000	-2.626804000
6	5.104825000	-0.476842000	-3.733324000

1	4.985447000	0.504718000	-4.217919000
1	5.845550000	-1.052676000	-4.311614000
1	4.141521000	-1.007097000	-3.782209000
6	3.719580000	-1.263506000	2.330911000
6	4.999501000	-0.949449000	2.850976000
6	5.310107000	-1.264553000	4.183774000
1	6.309762000	-1.036675000	4.566676000
6	4.397521000	-1.879552000	5.034178000
6	3.128237000	-2.167599000	4.523547000
1	2.396394000	-2.651083000	5.175306000
6	2.775705000	-1.874077000	3.203115000
6	6.110327000	-0.303583000	2.029272000
1	5.675224000	-0.010497000	1.062150000
6	6.656487000	0.964554000	2.696457000
1	7.335031000	1.497062000	2.012774000
1	5.852159000	1.660024000	2.987383000
1	7.223824000	0.731029000	3.610533000
6	7.245261000	-1.292213000	1.738861000
1	8.015240000	-0.821393000	1.107406000
1	7.727891000	-1.620697000	2.673849000
1	6.871832000	-2.181348000	1.210674000
6	4.773125000	-2.255073000	6.455226000
1	5.811186000	-1.919761000	6.614186000
6	3.889567000	-1.546891000	7.485896000
1	3.951042000	-0.454046000	7.375185000
1	2.835248000	-1.841842000	7.366371000
1	4.195920000	-1.805881000	8.510569000
6	4.735249000	-3.773925000	6.650358000
1	5.382223000	-4.279366000	5.919490000
1	5.068276000	-4.049392000	7.662415000
1	3.712524000	-4.158208000	6.514471000
6	1.358673000	-2.182508000	2.743716000
1	1.420960000	-2.415091000	1.668476000
6	0.471354000	-0.941808000	2.881243000

1	-0.534646000	-1.126505000	2.467654000
1	0.371832000	-0.665563000	3.945539000
1	0.890992000	-0.074911000	2.340587000
6	0.706520000	-3.378157000	3.434387000
1	-0.248236000	-3.611825000	2.938379000
1	1.348469000	-4.271338000	3.386205000
1	0.478821000	-3.176661000	4.493228000
51	0.178212000	2.273447000	-0.097333000
6	1.026888000	3.949004000	-1.291351000
6	1.355402000	3.792086000	-2.666890000
6	1.842856000	4.876517000	-3.401407000
1	2.078552000	4.744324000	-4.459510000
6	2.016841000	6.141302000	-2.830812000
6	1.707787000	6.284588000	-1.482985000
1	1.841706000	7.267109000	-1.018617000
6	1.228463000	5.219084000	-0.702976000
6	1.207598000	2.442365000	-3.356217000
1	0.261746000	2.011091000	-2.985857000
6	1.124910000	2.506481000	-4.879777000
1	0.344922000	3.206448000	-5.215912000
1	0.887422000	1.510607000	-5.282813000
1	2.080711000	2.817109000	-5.329402000
6	2.334252000	1.495695000	-2.929491000
1	2.409159000	1.408600000	-1.833935000
1	3.305778000	1.870631000	-3.293182000
1	2.194073000	0.479391000	-3.338712000
6	2.484638000	7.320596000	-3.663035000
1	2.560450000	8.185004000	-2.982662000
6	3.868089000	7.083487000	-4.274059000
1	4.618341000	6.888568000	-3.494123000
1	4.194800000	7.959430000	-4.854274000
1	3.854097000	6.218115000	-4.955041000
6	1.457245000	7.665245000	-4.746055000
1	0.468088000	7.852218000	-4.304238000

1	1.353635000	6.834425000	-5.461111000
1	1.763596000	8.559607000	-5.309295000
6	0.987379000	5.527672000	0.771697000
1	0.632258000	4.607434000	1.252980000
6	2.300826000	5.917930000	1.460084000
1	2.156665000	6.035568000	2.545563000
1	2.689994000	6.873325000	1.072403000
1	3.078931000	5.156773000	1.285701000
6	-0.087044000	6.599598000	0.977879000
1	-0.285578000	6.744512000	2.051844000
1	-1.031751000	6.309264000	0.494193000
1	0.228770000	7.570121000	0.562988000
6	-1.594019000	3.512016000	0.416393000
6	-2.375745000	4.110113000	-0.604837000
6	-3.483121000	4.907730000	-0.267536000
1	-4.078370000	5.356218000	-1.069042000
6	-3.862263000	5.138873000	1.052866000
6	-3.091701000	4.544539000	2.057917000
1	-3.371450000	4.712320000	3.100329000
6	-1.982184000	3.741593000	1.766306000
6	-2.134127000	3.894628000	-2.095375000
1	-1.250373000	3.256867000	-2.199781000
6	-3.302945000	3.130862000	-2.727884000
1	-3.417781000	2.132656000	-2.268720000
1	-3.127287000	2.982483000	-3.805302000
1	-4.259791000	3.665098000	-2.610723000
6	-1.845161000	5.206083000	-2.830784000
1	-2.716324000	5.880914000	-2.819809000
1	-1.591379000	5.003721000	-3.883110000
1	-0.991473000	5.729889000	-2.374107000
6	-5.064611000	5.997993000	1.393790000
1	-5.534076000	6.287794000	0.438912000
6	-4.639483000	7.279551000	2.116881000
1	-5.507613000	7.925775000	2.314910000

1	-3.911693000	7.845752000	1.518845000
1	-4.167723000	7.041096000	3.082655000
6	-6.101044000	5.221423000	2.212491000
1	-5.692068000	4.936929000	3.194403000
1	-6.411875000	4.298664000	1.698325000
1	-6.997726000	5.833471000	2.391018000
6	-1.272119000	3.046933000	2.919068000
1	-0.210722000	2.953537000	2.630603000
6	-1.341383000	3.792961000	4.250706000
1	-2.356876000	3.791118000	4.675859000
1	-1.015376000	4.839235000	4.147440000
1	-0.690403000	3.297872000	4.986846000
6	-1.824881000	1.625720000	3.079440000
1	-1.304894000	1.082995000	3.883723000
1	-1.711975000	1.025058000	2.160099000
1	-2.896396000	1.662625000	3.347129000
51	-3.001105000	-1.191752000	-0.145386000
6	-2.276091000	-2.457142000	-1.826732000
6	-1.850061000	-3.791831000	-1.581876000
6	-1.518574000	-4.625328000	-2.657552000
1	-1.221178000	-5.656523000	-2.444671000
6	-1.554134000	-4.191212000	-3.982806000
6	-1.891839000	-2.858406000	-4.207238000
1	-1.895160000	-2.485516000	-5.236592000
6	-2.233151000	-1.988657000	-3.162864000
6	-1.680916000	-4.395975000	-0.190002000
1	-1.962931000	-3.633474000	0.546284000
6	-0.210385000	-4.747460000	0.067566000
1	-0.082662000	-5.163732000	1.078474000
1	0.160687000	-5.496358000	-0.650266000
1	0.442088000	-3.859707000	-0.009659000
6	-2.586255000	-5.611717000	0.031934000
1	-2.496305000	-5.969608000	1.069525000
1	-3.641919000	-5.358828000	-0.147310000

1	-2.309923000	-6.445311000	-0.633903000
6	-1.269027000	-5.135344000	-5.135452000
1	-1.196613000	-4.518700000	-6.047367000
6	0.053990000	-5.887124000	-4.971576000
1	0.898641000	-5.192457000	-4.855604000
1	0.033487000	-6.541033000	-4.086298000
1	0.249980000	-6.522947000	-5.847697000
6	-2.434590000	-6.113481000	-5.320568000
1	-3.381126000	-5.574178000	-5.467612000
1	-2.266115000	-6.769983000	-6.187568000
1	-2.546406000	-6.747755000	-4.427477000
6	-2.529517000	-0.541539000	-3.539963000
1	-2.616352000	0.034199000	-2.605794000
6	-3.863562000	-0.417903000	-4.281267000
1	-4.072170000	0.633128000	-4.536294000
1	-3.840768000	-0.996797000	-5.218109000
1	-4.692382000	-0.800126000	-3.667533000
6	-1.401213000	0.084253000	-4.367340000
1	-0.410463000	-0.072601000	-3.909286000
1	-1.355845000	-0.340667000	-5.382601000
1	-1.552167000	1.170347000	-4.466580000
6	-4.428496000	-2.735275000	0.555890000
6	-5.434681000	-3.248564000	-0.296051000
6	-6.297524000	-4.253962000	0.168583000
1	-7.062530000	-4.652308000	-0.505394000
6	-6.208082000	-4.776002000	1.454135000
6	-5.225604000	-4.251399000	2.298594000
1	-5.142644000	-4.644691000	3.314169000
6	-4.349434000	-3.247054000	1.879515000
6	-5.649983000	-2.777283000	-1.729571000
1	-4.970891000	-1.928847000	-1.891310000
6	-7.079726000	-2.273768000	-1.959450000
1	-7.365414000	-1.516175000	-1.213869000
1	-7.171380000	-1.820385000	-2.960174000

1	-7.813819000	-3.092326000	-1.901292000
6	-5.298213000	-3.861441000	-2.753987000
1	-4.265674000	-4.215214000	-2.624699000
1	-5.974263000	-4.726671000	-2.657282000
1	-5.396688000	-3.468812000	-3.778999000
6	-7.138514000	-5.876370000	1.926730000
1	-7.813144000	-6.111374000	1.087101000
6	-7.999907000	-5.414966000	3.105999000
1	-8.570983000	-4.511130000	2.848185000
1	-8.709555000	-6.200645000	3.406107000
1	-7.371503000	-5.178810000	3.978650000
6	-6.362052000	-7.149200000	2.276546000
1	-5.756938000	-7.487974000	1.423643000
1	-5.679397000	-6.969057000	3.121330000
1	-7.046805000	-7.961310000	2.563921000
6	-3.355470000	-2.675499000	2.880197000
1	-2.435234000	-2.447077000	2.316557000
6	-3.880334000	-1.346928000	3.437228000
1	-3.121589000	-0.852154000	4.063710000
1	-4.166836000	-0.653825000	2.627907000
1	-4.776937000	-1.526196000	4.055052000
6	-2.985200000	-3.613581000	4.026930000
1	-2.657283000	-4.595375000	3.653747000
1	-2.161566000	-3.179320000	4.612190000
1	-3.827226000	-3.774024000	4.718020000

Coordinates of Tip_2Sb^+ (Gas phase)

51	0.019539000	-1.894044000	-0.635875000
6	-1.531666000	-0.718824000	0.180414000
6	-2.649605000	-0.458691000	-0.625601000
6	-1.404929000	-0.163533000	1.457462000
6	-3.623632000	0.399751000	-0.141100000
6	-2.404004000	0.696940000	1.898955000

6	-3.511129000	0.998879000	1.113766000
1	-4.489830000	0.620721000	-0.753687000
1	-2.322854000	1.146309000	2.882090000
6	1.602024000	-0.505648000	-0.496258000
6	2.721150000	-0.868920000	0.262386000
6	1.499666000	0.757796000	-1.094037000
6	3.727648000	0.072024000	0.440023000
6	2.524555000	1.667737000	-0.880418000
6	3.642115000	1.346841000	-0.111013000
1	4.601507000	-0.183084000	1.028198000
1	2.455228000	2.653418000	-1.325561000
6	-0.233552000	-0.478802000	2.365549000
1	0.387099000	-1.248373000	1.875933000
6	-4.567082000	1.963181000	1.600344000
1	-4.281359000	2.275975000	2.606880000
6	-2.815525000	-1.097236000	-1.993453000
6	2.863155000	-2.250168000	0.876360000
1	1.903753000	-2.791404000	0.767482000
6	4.727152000	2.368578000	0.135257000
1	5.530197000	1.864467000	0.677261000
6	0.323822000	1.145438000	-1.968611000
1	-0.320345000	0.259537000	-2.097077000
6	5.304570000	2.912416000	-1.172318000
1	5.668898000	2.109242000	-1.812134000
1	4.554115000	3.476520000	-1.728029000
1	6.134103000	3.586887000	-0.962447000
6	4.197552000	3.504626000	1.013943000
1	3.809986000	3.126885000	1.960359000
1	4.991462000	4.220038000	1.227168000
1	3.392056000	4.038830000	0.506580000
6	3.148721000	-2.207694000	2.377208000
1	4.115675000	-1.741977000	2.567723000
1	2.390867000	-1.640062000	2.917151000
1	3.181955000	-3.217887000	2.783768000

6	3.918296000	-3.069014000	0.132912000
1	3.691054000	-3.139807000	-0.930814000
1	4.895359000	-2.595168000	0.235612000
1	3.985815000	-4.075501000	0.544860000
6	-0.522432000	2.237708000	-1.315591000
1	-0.877932000	1.934231000	-0.330037000
1	0.070324000	3.146682000	-1.199399000
1	-1.386737000	2.481730000	-1.934578000
6	0.769903000	1.549923000	-3.374655000
1	1.372907000	2.457342000	-3.340557000
1	1.364689000	0.767876000	-3.845818000
1	-0.098229000	1.753801000	-4.002087000
6	-3.086828000	-0.077988000	-3.099118000
1	-2.321672000	0.697681000	-3.130863000
1	-3.120926000	-0.573408000	-4.068861000
1	-4.050241000	0.407266000	-2.942916000
6	-4.612691000	3.207161000	0.709329000
1	-5.333309000	3.924923000	1.100261000
1	-3.638166000	3.692733000	0.654178000
1	-4.919084000	2.945511000	-0.305094000
6	-5.942122000	1.298108000	1.679634000
1	-6.673406000	1.998102000	2.082809000
1	-6.286720000	0.993832000	0.690039000
1	-5.922590000	0.415419000	2.318077000
6	0.647466000	0.749371000	2.591659000
1	1.017450000	1.158773000	1.650503000
1	0.076277000	1.527607000	3.100205000
1	1.503071000	0.500529000	3.220595000
6	-0.691804000	-1.089437000	3.691245000
1	-1.266566000	-0.365669000	4.268946000
1	-1.318010000	-1.966783000	3.531168000
1	0.170761000	-1.381450000	4.290674000
6	-3.894665000	-2.179353000	-1.958959000
1	-3.676276000	-2.938108000	-1.207360000

1	-4.858072000	-1.731727000	-1.710973000
1	-3.986708000	-2.664513000	-2.930338000
1	-1.868812000	-1.598717000	-2.272146000

Coordinates of Tip_2Sb^+ (THF)

51	0.020429000	-1.944355000	-0.592764000
6	-1.518760000	-0.720385000	0.198839000
6	-2.641173000	-0.476311000	-0.604911000
6	-1.382391000	-0.127479000	1.457763000
6	-3.610725000	0.399263000	-0.139183000
6	-2.375273000	0.750098000	1.882130000
6	-3.486300000	1.032724000	1.096644000
1	-4.479735000	0.604658000	-0.753596000
1	-2.284087000	1.228573000	2.850626000
6	1.591198000	-0.524626000	-0.493647000
6	2.716446000	-0.855304000	0.270477000
6	1.476756000	0.725167000	-1.118035000
6	3.716498000	0.098595000	0.422264000
6	2.493514000	1.651187000	-0.928563000
6	3.616604000	1.358433000	-0.157673000
1	4.594277000	-0.135289000	1.013256000
1	2.408321000	2.627196000	-1.392485000
6	-0.206575000	-0.414991000	2.369602000
1	0.408543000	-1.202174000	1.906789000
6	-4.534179000	2.015702000	1.565099000
1	-4.234687000	2.359166000	2.557342000
6	-2.819388000	-1.151247000	-1.953031000
6	2.876268000	-2.216241000	0.923854000
1	1.924897000	-2.770941000	0.841262000
6	4.691761000	2.396793000	0.065077000
1	5.505244000	1.909613000	0.606814000
6	0.296325000	1.090715000	-1.995610000
1	-0.346203000	0.204322000	-2.101120000
6	5.251090000	2.932066000	-1.253530000

1	5.629085000	2.124756000	-1.880588000
1	4.484301000	3.468416000	-1.814536000
1	6.067023000	3.628118000	-1.058791000
6	4.156234000	3.538231000	0.932689000
1	3.778515000	3.165364000	1.885164000
1	4.944401000	4.264665000	1.132193000
1	3.341045000	4.055864000	0.423438000
6	3.178217000	-2.123503000	2.419167000
1	4.140934000	-1.639961000	2.585113000
1	2.417562000	-1.551073000	2.949651000
1	3.226227000	-3.121713000	2.852938000
6	3.935712000	-3.044341000	0.196782000
1	3.695535000	-3.154500000	-0.860615000
1	4.907082000	-2.553800000	0.274892000
1	4.018124000	-4.035091000	0.642992000
6	-0.544732000	2.201069000	-1.365802000
1	-0.891537000	1.924368000	-0.369266000
1	0.048493000	3.113317000	-1.281288000
1	-1.414633000	2.424688000	-1.985002000
6	0.737078000	1.465231000	-3.411384000
1	1.343640000	2.371035000	-3.397439000
1	1.324006000	0.668654000	-3.867775000
1	-0.135333000	1.657647000	-4.036671000
6	-3.114478000	-0.164157000	-3.081568000
1	-2.357322000	0.617335000	-3.144051000
1	-3.150451000	-0.688510000	-4.035942000
1	-4.081805000	0.314462000	-2.928378000
6	-4.589384000	3.230943000	0.636504000
1	-5.303446000	3.962605000	1.014977000
1	-3.613220000	3.709716000	0.554773000
1	-4.907849000	2.937081000	-0.365292000
6	-5.909419000	1.357226000	1.682320000
1	-6.636066000	2.072262000	2.068528000
1	-6.261879000	1.016552000	0.707399000

1	-5.881187000	0.498052000	2.352237000
6	0.675878000	0.819783000	2.553109000
1	1.038645000	1.201476000	1.597683000
1	0.108198000	1.611778000	3.044337000
1	1.536736000	0.586774000	3.181336000
6	-0.661215000	-0.976386000	3.717991000
1	-1.228938000	-0.228884000	4.272378000
1	-1.290639000	-1.856227000	3.588508000
1	0.204477000	-1.252451000	4.320553000
6	-3.892406000	-2.237257000	-1.874594000
1	-3.655106000	-2.974640000	-1.107677000
1	-4.854564000	-1.787138000	-1.625521000
1	-3.991677000	-2.746576000	-2.832829000
1	-1.875922000	-1.653461000	-2.232008000

S9. X-Ray Crystallographic details for 1-2, 4, 6, 14-15

The data were either collected from shock-cooled crystals at 100(2) on a BRUKER D8 three circle diffractometer equipped with an INCOATEC Mo Microsource (compounds **4, 6**) or INCOATEC Ag Microsource (compound **2**) or Bruker Mo Rotating Anode (compound **1**) with mirror optics or from shock-cooled crystals at 200(2) on a BRUKER D8 VENTURE four circle diffractometer equipped with an INCOATEC Mo Microsource and graphite monochromator (compounds **14**, **15**). The data were integrated with SAINT.[18] A multi-scan absorption correction was applied using SADABS.[19] The structures were solved by SHELXT [20] and refined on F^2 using SHELXL [21] in the graphical user interface ShelXle.[22]

Table S17: Crystal data and structure refinement.

Compound	**1**	**2**	**4**	**6**	**14**	**15**
Empirical formula	$C_{30}H_{46}Br_{0.17}Cl_{0.83}Sb$	$C_{48}H_{96}Br_{3.42}Cl_{10.58}Mg_4O_{12}Sb_2$	$C_{66}H_{106}Sb_2$	$C_{119}H_{199}K_3O_5Sb_3$	$C_{38}H_{62}LiO_2Sb$	$C_{48}H_{70}NaOSb$
CCDC number	2078143	2078144	2078145	2078146	2078147	2078148
Formula weight	571.52	1854.25	1143.0	2192.32	679.56	807.78
Temperature [K]	100(2)	100(2)	100(2)	100(2)	200(2)	200(2)
Wavelength [Å]	0.71073	0.56086	0.71073	0.71073	0.71073	0.71073
Crystal system	Monoclinic	Triclinic	Triclinic	Monoclinic	Triclinic	Triclinic
Space group	$P2_1/n$	$P\bar{1}$	$P\bar{1}$	$P2_1/c$	$P\bar{1}$	$P\bar{1}$
a [Å]	13.211(2)	11.492(2)	13.255(2)	14.898(2)	11.723(2)	14.024(3)
b [Å]	9.615(2)	12.810(2)	19.142(3)	36.172(3)	12.824(2)	14.249(3)
c [Å]	23.311(3)	13.501(2)	25.810(4)	23.327(3)	13.869(3)	14.446(2)
α [°]	90	97.01(2)	108.36(3)	90	81.53(2)	66.86(2)
β [°]	95.76(2)	107.72(2)	92.72(2)	101.37(2)	89.90(2)	61.49(2)
γ [°]	90	98.91(2)	90.10(2)	90	69.05(2)	78.69(2)

V [Å^3]	2946.1(9)	1839.9(6)	6207(2)	12324(3)	1923.0(7)	2332.4(9)
Z	4	1	4	4	2	2
ρ [Mgm^{-3}]	1.289	1.673	1.223	1.182	1.174	1.150
μ [mm^{-1}]	1.259	1.623	0.906	0.801	0.745	0.631
F (000)	1188	930	2416	4652	720	856
Crystal size [mm^3]	0.207 x 0.131 x 0.112	0.261 x 0.172 x 0.123	0.213 x 0.186 x 0.157	0.302 x 0.248 x 0.122	0.250 x 0.230 x 0.200	0.200 x 0.180 x 0.150
θ-area [°]	1.856 to 26.643	1.291 to 20.589	0.832 to 25.357	1.053 to 26.384	2.447 to 26.407	2.966 to 26.363
Index ranges	-16 ≤ h ≤ 16, -12 ≤ k ≤ 12, -29 ≤ l ≤ 29	-14 ≤ h ≤ 14, -15 ≤ k ≤ 16, -16 ≤ l ≤ 16	-15 ≤ h ≤ 15, -23 ≤ k ≤ 23, -31 ≤ l ≤ 31	-18 ≤ h ≤ 18, -45 ≤ k ≤ 45, -29 ≤ l ≤ 29	-14 ≤ h ≤ 14, -16 ≤ k ≤ 16, -17 ≤ l ≤ 17	-17 ≤ h ≤ 17, -17 ≤ k ≤ 17, -18 ≤ l ≤ 18
Total number of reflections	85505	68068	238565	357097	80094	109940
Unique reflections	6120	7593	22677	25205	7840	9515
R_{int}	0.0429	0.0506	0.0466	0.0648	0.0270	0.0534
Max. and min. transmission	0.7454 and 0.7073	0.7445 and 0.6772	0.7452 and 0.7001	0.7454 and 0.6491	0.4296 and 0.3616	0.4296 and 0.3715

Data / restraints / parameters	6120 / 523 / 351	7593 / 1741 / 561	22677 / 267 / 1334	25205 / 10755 / 2162	7840 / 3761 / 790	9515 / 2338 / 711
Goodness-of-fit on F^2	1.051	1.018	1.169	1.061	1.139	1.153
$R1$ [$I>2\sigma(I)$]	0.0194	0.0261	0.0363	0.0312	0.0210	0.0337
$wR2$ [$I>2\sigma(I)$]	0.0447	0.0573	0.0777	0.0657	0.0534	0.0719
$R1$ [all data]	0.0229	0.0408	0.0426	0.0467	0.0236	0.0431
$wR2$ [all data]	0.0461	0.0633	0.0803	0.0731	0.0562	0.0816
Largest diff. peak and hole max. / min. [e·Å	0.520 and -0.268	0.834 and -0.699	0.966 and -0.997	0.556 and -0.482	0.804 and -0.376	2.258 and -0.606

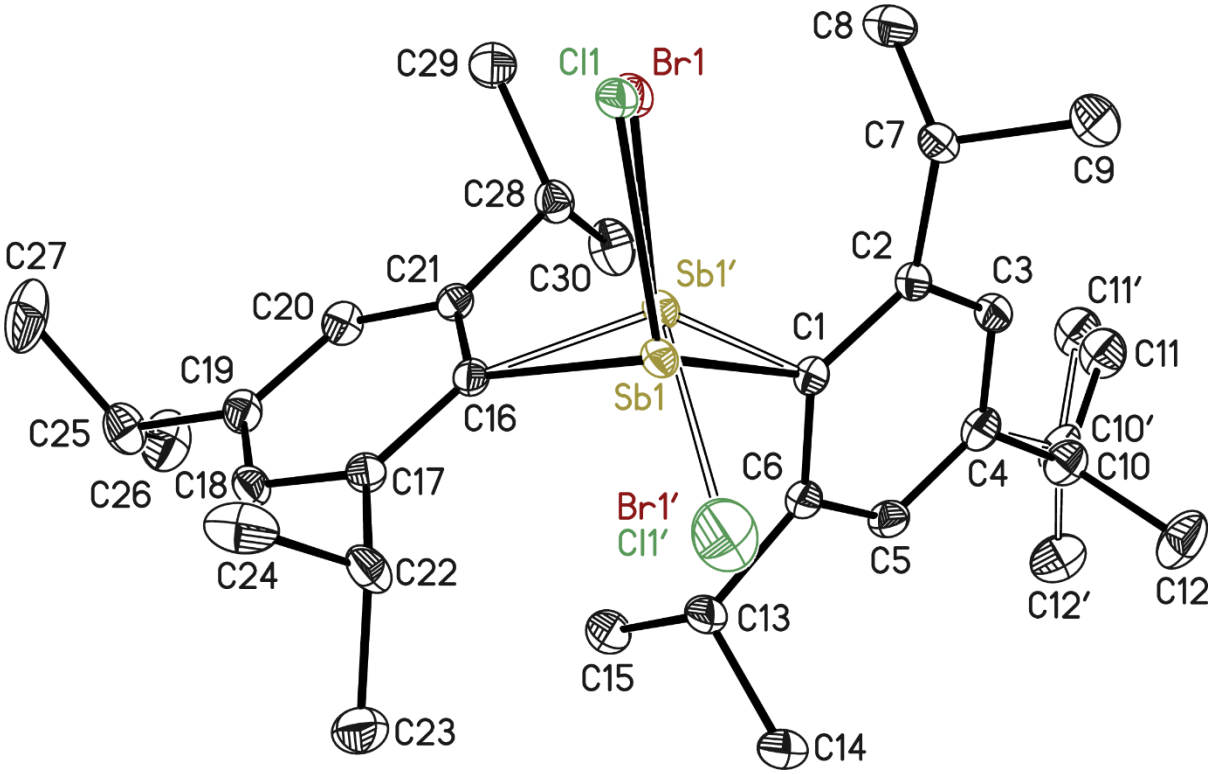

Figure S56: Asymmetric unit of **1**. The anisotropic displacement parameters are depicted at the 50% probability level. The hydrogen atoms are omitted for clarity.

The antimony and halogen atoms are disordered about two positions. They were refined with distance restraints and constraints for the anisotropic displacement parameters.

The occupancy of the minor position of antimony refined to 0.0574(10), the occupancies of chlorine refined to 0.802(2) and 0.026(2) and those of bromine to 0.1409(14) and 0.0312(15).

A further disorder was found at one ^{i}Pr-group. The group was refined with distance restraints and restraints for the anisotropic displacement parameters. The occupancy of the minor position refined to 0.070(4).

Table S18: Bond lengths [Å] and angles [°] for **1**.

Cl(1)-Sb(1)	2.436(4)	C(1)-C(6)	1.411(2)
Br(1)-Sb(1)	2.441(11)	C(2)-C(3)	1.396(2)
Sb(1)-C(16)	2.1725(15)	C(2)-C(7)	1.527(2)
Sb(1)-C(1)	2.1918(16)	C(6)-C(5)	1.391(2)
Br(1')-Sb(1')	2.504(6)	C(6)-C(13)	1.526(2)
Sb(1')-C(1)	2.114(3)	C(7)-C(8)	1.523(2)
Sb(1')-C(16)	2.163(3)	C(7)-C(9)	1.531(2)
C(1)-C(2)	1.409(2)	C(3)-C(4)	1.389(2)

C(4)-C(5)	1.386(2)	C(6)-C(1)-Sb(1)	113.73(11)
C(4)-C(10)	1.521(3)	C(3)-C(2)-C(1)	119.07(14)
C(4)-C(10')	1.529(16)	C(3)-C(2)-C(7)	118.17(14)
C(10)-C(11)	1.517(3)	C(1)-C(2)-C(7)	122.75(14)
C(10)-C(12)	1.519(4)	C(5)-C(6)-C(1)	119.13(14)
C(10')-C(12')	1.40(4)	C(5)-C(6)-C(13)	117.30(14)
C(10')-C(11')	1.522(18)	C(1)-C(6)-C(13)	123.54(14)
C(13)-C(15)	1.528(2)	C(8)-C(7)-C(2)	112.07(14)
C(13)-C(14)	1.533(2)	C(8)-C(7)-C(9)	110.58(14)
C(16)-C(17)	1.406(2)	C(2)-C(7)-C(9)	112.40(13)
C(16)-C(21)	1.413(2)	C(4)-C(3)-C(2)	122.23(15)
C(17)-C(18)	1.397(2)	C(5)-C(4)-C(3)	117.75(15)
C(17)-C(22)	1.529(2)	C(5)-C(4)-C(10)	118.85(18)
C(18)-C(19)	1.387(2)	C(3)-C(4)-C(10)	123.26(19)
C(19)-C(20)	1.389(2)	C(5)-C(4)-C(10')	122.5(15)
C(19)-C(25)	1.524(2)	C(3)-C(4)-C(10')	119.7(14)
C(20)-C(21)	1.396(2)	C(4)-C(5)-C(6)	122.44(15)
C(21)-C(28)	1.523(2)	C(11)-C(10)-C(12)	111.8(3)
C(22)-C(24)	1.526(2)	C(11)-C(10)-C(4)	113.9(2)
C(22)-C(23)	1.527(2)	C(12)-C(10)-C(4)	110.0(2)
C(25)-C(26)	1.523(2)	C(12')-C(10')-C(11')	117(3)
C(25)-C(27)	1.529(3)	C(12')-C(10')-C(4)	122(2)
C(28)-C(29)	1.528(2)	C(11')-C(10')-C(4)	114(2)
C(28)-C(30)	1.530(2)	C(6)-C(13)-C(15)	112.01(14)
		C(6)-C(13)-C(14)	111.13(13)
C(16)-Sb(1)-C(1)	99.13(6)	C(15)-C(13)-C(14)	111.21(14)
C(16)-Sb(1)-Cl(1)	92.43(13)	C(17)-C(16)-C(21)	119.94(13)
C(1)-Sb(1)-Cl(1)	108.15(13)	C(17)-C(16)-Sb(1')	128.92(15)
C(16)-Sb(1)-Br(1)	94.7(3)	C(21)-C(16)-Sb(1')	110.79(15)
C(1)-Sb(1)-Br(1)	105.1(3)	C(17)-C(16)-Sb(1)	116.94(11)
Cl(1)-Sb(1)-Br(1)	3.5(4)	C(21)-C(16)-Sb(1)	123.12(11)
C(1)-Sb(1')-C(16)	101.93(12)	C(18)-C(17)-C(16)	118.96(14)
C(1)-Sb(1')-Br(1')	87.54(19)	C(18)-C(17)-C(22)	117.07(13)
C(16)-Sb(1')-Br(1')	101.14(19)	C(16)-C(17)-C(22)	123.98(13)
C(2)-C(1)-C(6)	119.28(14)	C(19)-C(18)-C(17)	122.09(14)
C(2)-C(1)-Sb(1')	116.80(15)	C(18)-C(19)-C(20)	118.13(14)
C(6)-C(1)-Sb(1')	123.75(15)	C(18)-C(19)-C(25)	120.00(14)
C(2)-C(1)-Sb(1)	126.75(11)	C(20)-C(19)-C(25)	121.84(14)

C(19)-C(20)-C(21)	122.22(14)	C(26)-C(25)-C(19)	112.84(14)
C(20)-C(21)-C(16)	118.64(14)	C(26)-C(25)-C(27)	110.21(15)
C(20)-C(21)-C(28)	117.79(13)	C(19)-C(25)-C(27)	110.61(14)
C(16)-C(21)-C(28)	123.56(13)	C(21)-C(28)-C(29)	111.36(13)
C(24)-C(22)-C(23)	110.35(14)	C(21)-C(28)-C(30)	112.00(13)
C(24)-C(22)-C(17)	110.97(13)	C(29)-C(28)-C(30)	111.20(14)
C(23)-C(22)-C(17)	112.50(13)		

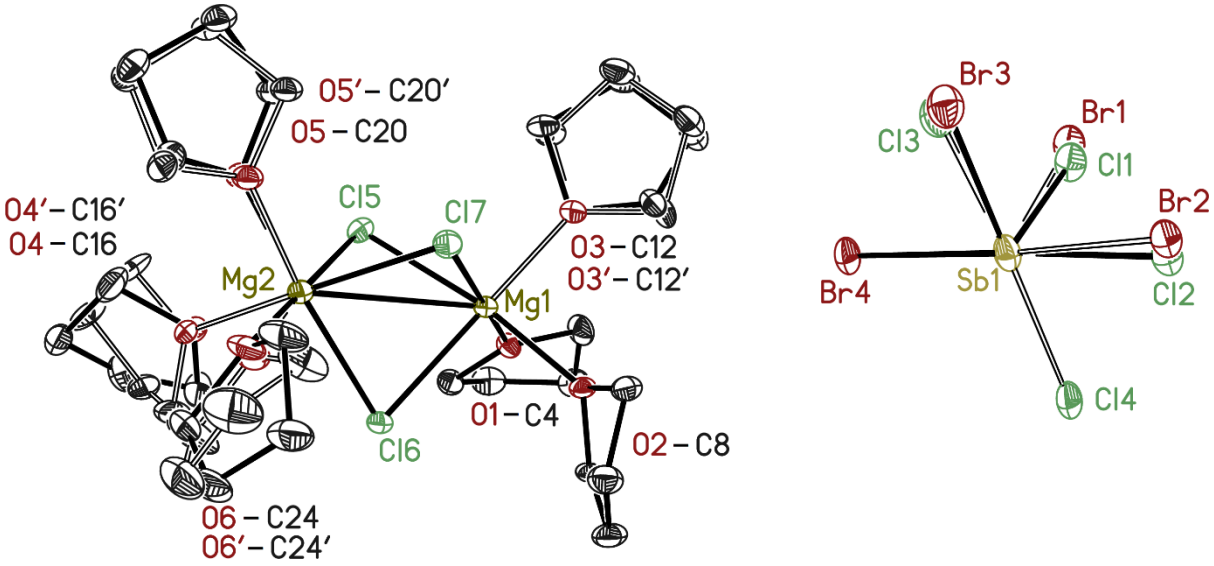

Figure S57: Asymmetric unit of **2**. The anisotropic displacement parameters are depicted at the 50% probability level. The hydrogen atoms are omitted for clarity.

Four of the THF molecules are disordered about two positions. The occupancies of the minor positions refined to 0.204(12) (O3′-C12′), 0.336(10) (O4′-C16′), 0.150(11) (O5′-C20′), 0.314(13) (O6-C24).

The occupancy of the bromine atoms refined to 0.672(2) (Br3), 0.769(2) (Br4), 0.109(2) (Br1) and 0.158(2) (Br2).

All disordered groups were refined with distance restraints and restraints for the anisotropic displacement parameters.

Table S19: Bond lengths [Å] and angles [°] for **2**.

Sb(1)-Cl(1)	2.361(3)	Sb(1)-Br(3)	2.601(2)
Sb(1)-Cl(3)	2.468(12)	Sb(1)-Cl(4)#1	2.845(12)
Sb(1)-Cl(2)	2.516(4)	Sb(1)-Br(4)	2.8763(18)
Sb(1)-Br(1)	2.565(10)	Mg(1)-O(1)	2.0551(19)
Sb(1)-Br(2)	2.595(9)	Mg(1)-O(2)	2.0774(18)

Mg(1)-O(3)	2.082(4)	C(14)-C(15)	1.490(8)
Mg(1)-O(3')	2.091(12)	C(15)-C(16)	1.512(7)
Mg(1)-Cl(7)	2.4786(13)	O(4')-C(16')	1.451(12)
Mg(1)-Cl(5)	2.5127(11)	O(4')-C(13')	1.455(12)
Mg(1)-Cl(6)	2.5224(11)	C(13')-C(14')	1.496(12)
Mg(1)-Mg(2)	3.1514(14)	C(14')-C(15')	1.513(11)
Mg(2)-O(5)	2.063(3)	C(15')-C(16')	1.515(11)
Mg(2)-O(5')	2.070(13)	O(5)-C(20)	1.459(5)
Mg(2)-O(6)	2.077(13)	O(5)-C(17)	1.470(4)
Mg(2)-O(4')	2.080(11)	C(17)-C(18)	1.515(5)
Mg(2)-O(6')	2.082(6)	C(18)-C(19)	1.522(5)
Mg(2)-O(4)	2.113(6)	C(19)-C(20)	1.508(5)
Mg(2)-Cl(6)	2.4791(12)	O(5')-C(20')	1.454(14)
Mg(2)-Cl(5)	2.5042(12)	O(5')-C(17')	1.458(13)
Mg(2)-Cl(7)	2.5427(11)	C(17')-C(18')	1.510(14)
O(1)-C(4)	1.451(3)	C(18')-C(19')	1.507(14)
O(1)-C(1)	1.461(3)	C(19')-C(20')	1.509(14)
C(1)-C(2)	1.513(4)	O(6)-C(24)	1.450(12)
C(2)-C(3)	1.517(4)	O(6)-C(21)	1.451(13)
C(3)-C(4)	1.510(4)	C(21)-C(22)	1.506(12)
O(2)-C(8)	1.446(3)	C(22)-C(23)	1.515(13)
O(2)-C(5)	1.461(3)	C(23)-C(24)	1.508(13)
C(5)-C(6)	1.528(4)	O(6')-C(24')	1.447(7)
C(6)-C(7)	1.525(4)	O(6')-C(21')	1.455(8)
C(7)-C(8)	1.511(4)	C(21')-C(22')	1.503(9)
O(3)-C(12)	1.452(6)	C(22')-C(23')	1.498(8)
O(3)-C(9)	1.456(7)	C(23')-C(24')	1.501(9)
C(9)-C(10)	1.519(5)		
C(10)-C(11)	1.516(5)	Cl(1)-Sb(1)-Cl(2)	90.47(15)
C(11)-C(12)	1.537(6)	Cl(3)-Sb(1)-Br(1)	88.4(5)
O(3')-C(12')	1.460(14)	Cl(3)-Sb(1)-Br(2)	90.6(3)
O(3')-C(9')	1.463(14)	Br(1)-Sb(1)-Br(2)	91.1(4)
C(9')-C(10')	1.509(13)	Cl(1)-Sb(1)-Br(3)	92.63(11)
C(10')-C(11')	1.483(13)	Cl(2)-Sb(1)-Br(3)	93.13(8)
C(11')-C(12')	1.528(13)	Cl(1)-Sb(1)-Cl(4)#1	86.0(4)
O(4)-C(16)	1.458(8)	Cl(3)-Sb(1)-Cl(4)#1	174.8(4)
O(4)-C(13)	1.465(7)	Cl(2)-Sb(1)-Cl(4)#1	87.9(3)
C(13)-C(14)	1.512(7)	Br(1)-Sb(1)-Cl(4)#1	90.3(5)

Br(2)-Sb(1)-Cl(4)#1	94.6(4)	O(5)-Mg(2)-Cl(6)	176.48(13)
Br(3)-Sb(1)-Cl(4)#1	178.4(4)	O(5')-Mg(2)-Cl(6)	169.7(8)
Cl(1)-Sb(1)-Br(4)	87.11(11)	O(6)-Mg(2)-Cl(6)	95.0(12)
Cl(2)-Sb(1)-Br(4)	175.11(8)	O(4')-Mg(2)-Cl(6)	94.1(4)
Br(3)-Sb(1)-Br(4)	91.23(5)	O(6')-Mg(2)-Cl(6)	90.9(6)
O(1)-Mg(1)-O(2)	87.50(7)	O(4)-Mg(2)-Cl(6)	91.2(2)
O(1)-Mg(1)-O(3)	87.5(5)	O(5)-Mg(2)-Cl(5)	93.13(12)
O(2)-Mg(1)-O(3)	91.33(18)	O(5')-Mg(2)-Cl(5)	98.9(7)
O(1)-Mg(1)-O(3')	88(2)	O(6)-Mg(2)-Cl(5)	179.7(10)
O(2)-Mg(1)-O(3')	89.7(7)	O(4')-Mg(2)-Cl(5)	95.7(7)
O(1)-Mg(1)-Cl(7)	174.78(6)	O(6')-Mg(2)-Cl(5)	175.9(6)
O(2)-Mg(1)-Cl(7)	97.55(6)	O(4)-Mg(2)-Cl(5)	88.5(3)
O(3)-Mg(1)-Cl(7)	91.0(5)	Cl(6)-Mg(2)-Cl(5)	85.11(4)
O(3')-Mg(1)-Cl(7)	90(2)	O(5)-Mg(2)-Cl(7)	92.03(13)
O(1)-Mg(1)-Cl(5)	90.09(6)	O(5')-Mg(2)-Cl(7)	86.2(8)
O(2)-Mg(1)-Cl(5)	171.95(6)	O(6)-Mg(2)-Cl(7)	95.8(8)
O(3)-Mg(1)-Cl(5)	96.24(17)	O(4')-Mg(2)-Cl(7)	178.8(5)
O(3')-Mg(1)-Cl(5)	97.9(7)	O(6')-Mg(2)-Cl(7)	94.7(4)
Cl(7)-Mg(1)-Cl(5)	85.09(4)	O(4)-Mg(2)-Cl(7)	171.7(3)
O(1)-Mg(1)-Cl(6)	96.32(6)	Cl(6)-Mg(2)-Cl(7)	84.75(4)
O(2)-Mg(1)-Cl(6)	88.60(6)	Cl(5)-Mg(2)-Cl(7)	83.93(4)
O(3)-Mg(1)-Cl(6)	176.2(5)	O(5)-Mg(2)-Mg(1)	125.08(13)
O(3')-Mg(1)-Cl(6)	175.0(18)	O(5')-Mg(2)-Mg(1)	124.4(7)
Cl(7)-Mg(1)-Cl(6)	85.19(4)	O(6)-Mg(2)-Mg(1)	128.7(11)
Cl(5)-Mg(1)-Cl(6)	84.03(4)	O(4')-Mg(2)-Mg(1)	128.7(6)
O(1)-Mg(1)-Mg(2)	125.64(6)	O(6')-Mg(2)-Mg(1)	125.2(5)
O(2)-Mg(1)-Mg(2)	125.40(6)	O(4)-Mg(2)-Mg(1)	121.9(3)
O(3)-Mg(1)-Mg(2)	127.2(4)	Cl(6)-Mg(2)-Mg(1)	51.56(3)
O(3')-Mg(1)-Mg(2)	127.9(15)	Cl(5)-Mg(2)-Mg(1)	51.20(3)
Cl(7)-Mg(1)-Mg(2)	52.04(3)	Cl(7)-Mg(2)-Mg(1)	50.23(3)
Cl(5)-Mg(1)-Mg(2)	50.97(3)	Mg(2)-Cl(5)-Mg(1)	77.83(4)
Cl(6)-Mg(1)-Mg(2)	50.33(3)	Mg(2)-Cl(6)-Mg(1)	78.11(4)
O(5)-Mg(2)-O(6)	86.7(12)	Mg(1)-Cl(7)-Mg(2)	77.74(4)
O(5')-Mg(2)-O(4')	94.9(9)	C(4)-O(1)-C(1)	109.57(18)
O(5')-Mg(2)-O(6')	84.9(9)	C(4)-O(1)-Mg(1)	124.92(15)
O(4')-Mg(2)-O(6')	85.6(7)	C(1)-O(1)-Mg(1)	125.14(14)
O(5)-Mg(2)-O(4)	91.8(2)	O(1)-C(1)-C(2)	105.5(2)
O(6)-Mg(2)-O(4)	91.7(8)	C(1)-C(2)-C(3)	102.7(2)

C(4)-C(3)-C(2)	102.3(2)	C(13')-C(14')-C(15')	102.0(9)
O(1)-C(4)-C(3)	104.3(2)	C(14')-C(15')-C(16')	102.6(9)
C(8)-O(2)-C(5)	107.11(17)	O(4')-C(16')-C(15')	106.0(9)
C(8)-O(2)-Mg(1)	125.46(14)	C(20)-O(5)-C(17)	108.2(3)
C(5)-O(2)-Mg(1)	121.75(14)	C(20)-O(5)-Mg(2)	128.8(3)
O(2)-C(5)-C(6)	106.26(19)	C(17)-O(5)-Mg(2)	121.9(3)
C(7)-C(6)-C(5)	104.8(2)	O(5)-C(17)-C(18)	106.0(3)
C(8)-C(7)-C(6)	102.4(2)	C(17)-C(18)-C(19)	103.2(4)
O(2)-C(8)-C(7)	103.91(19)	C(20)-C(19)-C(18)	101.5(3)
C(12)-O(3)-C(9)	105.4(5)	O(5)-C(20)-C(19)	103.9(4)
C(12)-O(3)-Mg(1)	121.9(5)	C(20')-O(5')-C(17')	106.7(16)
C(9)-O(3)-Mg(1)	123.5(5)	C(20')-O(5')-Mg(2)	127(2)
O(3)-C(9)-C(10)	104.0(5)	C(17')-O(5')-Mg(2)	125.9(16)
C(11)-C(10)-C(9)	104.6(3)	O(5')-C(17')-C(18')	104.6(13)
C(10)-C(11)-C(12)	105.4(3)	C(19')-C(18')-C(17')	105.5(13)
O(3)-C(12)-C(11)	104.6(4)	C(18')-C(19')-C(20')	106.3(13)
C(12')-O(3')-C(9')	107.5(13)	O(5')-C(20')-C(19')	104.1(16)
C(12')-O(3')-Mg(1)	122.5(14)	C(24)-O(6)-C(21)	108.5(11)
C(9')-O(3')-Mg(1)	129.8(14)	C(24)-O(6)-Mg(2)	124.3(19)
O(3')-C(9')-C(10')	105.4(14)	C(21)-O(6)-Mg(2)	124.7(15)
C(11')-C(10')-C(9')	106.6(10)	O(6)-C(21)-C(22)	105.7(14)
C(10')-C(11')-C(12')	106.8(11)	C(21)-C(22)-C(23)	102.7(10)
O(3')-C(12')-C(11')	104.8(15)	C(24)-C(23)-C(22)	108.0(10)
C(16)-O(4)-C(13)	108.3(5)	O(6)-C(24)-C(23)	105.2(12)
C(16)-O(4)-Mg(2)	125.2(5)	C(24')-O(6')-C(21')	107.1(6)
C(13)-O(4)-Mg(2)	124.9(5)	C(24')-O(6')-Mg(2)	122.6(9)
O(4)-C(13)-C(14)	106.1(5)	C(21')-O(6')-Mg(2)	124.2(7)
C(15)-C(14)-C(13)	103.2(5)	O(6')-C(21')-C(22')	103.7(6)
C(14)-C(15)-C(16)	102.7(5)	C(23')-C(22')-C(21')	104.1(6)
O(4)-C(16)-C(15)	105.0(5)	C(22')-C(23')-C(24')	104.7(6)
C(16')-O(4')-C(13')	108.7(9)	O(6')-C(24')-C(23')	107.7(6)
C(16')-O(4')-Mg(2)	118.9(11)		
C(13')-O(4')-Mg(2)	126.2(9)		
O(4')-C(13')-C(14')	103.9(10)		

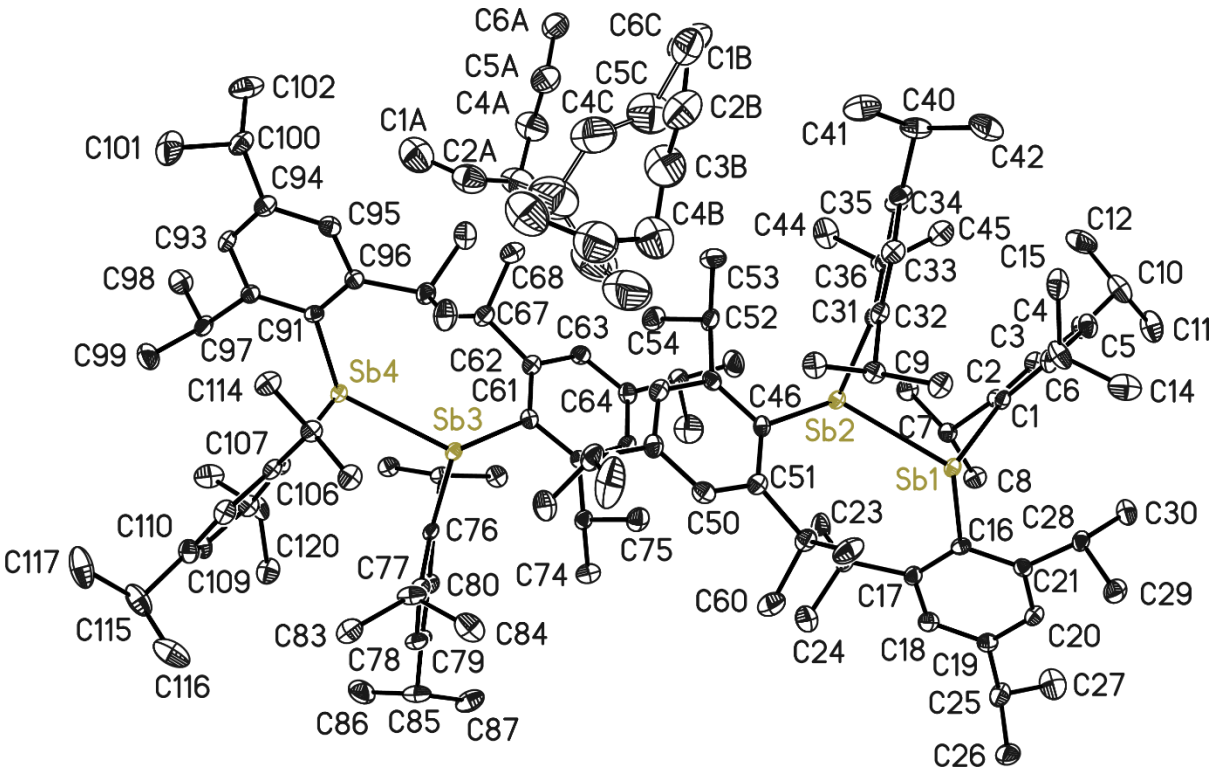

Figure S58: Asymmetric unit of **4**. The anisotropic displacement parameters are depicted at the 50% probability level. The hydrogen atoms are omitted for clarity.

A solvent hexane molecule is disordered about two positions. It was refined with distance restraints and restraints for the anisotropic displacement parameters. The occupancy of the minor position (C1B-C6B) refined to 0.475(7).

The structure can also be solved in a smaller unit cell (a = 13.255(2), b = 13.428(2), c = 18.330(3), α = 72.28(2), β = 88.14(2), γ = 87.32(2)). Then the asymmetric unit contains only one molecule of $(Tip)_4Sb_2$, which suffers from severe disorder.

Table S20: Bond lengths [Å] and angles [°] for **4**.

Sb(1)-C(16)	2.207(3)	C(1)-C(6)	1.415(5)
Sb(1)-C(1)	2.213(3)	C(2)-C(3)	1.390(5)
Sb(1)-Sb(2)	2.8587(6)	C(2)-C(7)	1.524(5)
Sb(2)-C(46)	2.203(3)	C(3)-C(4)	1.389(5)
Sb(2)-C(31)	2.209(3)	C(4)-C(5)	1.387(5)
Sb(3)-C(76)	2.209(3)	C(4)-C(10)	1.520(5)
Sb(3)-C(61)	2.212(3)	C(5)-C(6)	1.392(5)
Sb(3)-Sb(4)	2.8669(6)	C(6)-C(13)	1.528(5)
Sb(4)-C(91)	2.210(3)	C(7)-C(8)	1.532(5)
Sb(4)-C(106)	2.212(3)	C(7)-C(9)	1.539(5)
C(1)-C(2)	1.414(5)	C(10)-C(11)	1.531(6)

C(10)-C(12)	1.535(6)	C(49)-C(50)	1.391(5)
C(13)-C(15)	1.526(6)	C(49)-C(55)	1.514(5)
C(13)-C(14)	1.535(6)	C(50)-C(51)	1.396(5)
C(16)-C(17)	1.413(5)	C(51)-C(58)	1.521(5)
C(16)-C(21)	1.414(5)	C(52)-C(53)	1.527(5)
C(17)-C(18)	1.398(5)	C(52)-C(54)	1.537(5)
C(17)-C(22)	1.532(5)	C(55)-C(56)	1.520(6)
C(18)-C(19)	1.384(5)	C(55)-C(57)	1.529(6)
C(19)-C(20)	1.392(5)	C(58)-C(60)	1.531(6)
C(19)-C(25)	1.524(5)	C(58)-C(59)	1.540(5)
C(20)-C(21)	1.397(5)	C(61)-C(62)	1.413(5)
C(21)-C(28)	1.532(5)	C(61)-C(66)	1.414(5)
C(22)-C(23)	1.526(5)	C(62)-C(63)	1.396(5)
C(22)-C(24)	1.528(6)	C(62)-C(67)	1.528(5)
C(25)-C(27)	1.516(6)	C(63)-C(64)	1.383(5)
C(25)-C(26)	1.527(6)	C(64)-C(65)	1.397(5)
C(28)-C(29)	1.531(5)	C(64)-C(70)	1.521(5)
C(28)-C(30)	1.532(5)	C(65)-C(66)	1.397(5)
C(31)-C(36)	1.406(5)	C(66)-C(73)	1.527(5)
C(31)-C(32)	1.422(5)	C(67)-C(69)	1.527(5)
C(32)-C(33)	1.393(5)	C(67)-C(68)	1.546(5)
C(32)-C(37)	1.521(5)	C(70)-C(72)	1.522(6)
C(33)-C(34)	1.390(5)	C(70)-C(71)	1.523(6)
C(34)-C(35)	1.389(5)	C(73)-C(74)	1.524(5)
C(34)-C(40)	1.517(5)	C(73)-C(75)	1.538(5)
C(35)-C(36)	1.403(5)	C(76)-C(77)	1.409(5)
C(36)-C(43)	1.524(5)	C(76)-C(81)	1.420(5)
C(37)-C(39)	1.534(5)	C(77)-C(78)	1.389(5)
C(37)-C(38)	1.534(5)	C(77)-C(82)	1.537(5)
C(40)-C(42)	1.527(6)	C(78)-C(79)	1.386(5)
C(40)-C(41)	1.531(6)	C(79)-C(80)	1.385(5)
C(43)-C(44)	1.528(5)	C(79)-C(85)	1.517(5)
C(43)-C(45)	1.529(5)	C(80)-C(81)	1.397(5)
C(46)-C(47)	1.414(5)	C(81)-C(88)	1.527(5)
C(46)-C(51)	1.422(5)	C(82)-C(84)	1.529(6)
C(47)-C(48)	1.397(5)	C(82)-C(83)	1.533(5)
C(47)-C(52)	1.526(5)	C(85)-C(87)	1.525(5)
C(48)-C(49)	1.386(5)	C(85)-C(86)	1.537(6)

C(88)-C(90)	1.530(5)	C(2B)-C(3B)	1.503(12)
C(88)-C(89)	1.537(5)	C(3B)-C(4B)	1.537(13)
C(91)-C(96)	1.411(5)	C(4B)-C(5B)	1.474(12)
C(91)-C(92)	1.418(5)	C(5B)-C(6B)	1.528(13)
C(92)-C(93)	1.398(5)	C(1C)-C(2C)	1.521(13)
C(92)-C(97)	1.529(5)	C(2C)-C(3C)	1.460(13)
C(93)-C(94)	1.389(5)	C(3C)-C(4C)	1.526(13)
C(94)-C(95)	1.392(5)	C(4C)-C(5C)	1.506(12)
C(94)-C(100)	1.519(5)	C(5C)-C(6C)	1.532(13)
C(95)-C(96)	1.395(5)		
C(96)-C(103)	1.531(5)	C(16)-Sb(1)-C(1)	95.89(13)
C(97)-C(99)	1.523(5)	C(16)-Sb(1)-Sb(2)	112.52(9)
C(97)-C(98)	1.534(5)	C(1)-Sb(1)-Sb(2)	91.27(9)
C(100)-C(101)	1.528(6)	C(46)-Sb(2)-C(31)	95.87(13)
C(100)-C(102)	1.529(6)	C(46)-Sb(2)-Sb(1)	111.83(9)
C(103)-C(105)	1.521(6)	C(31)-Sb(2)-Sb(1)	90.84(9)
C(103)-C(104)	1.529(6)	C(76)-Sb(3)-C(61)	96.18(12)
C(106)-C(111)	1.414(5)	C(76)-Sb(3)-Sb(4)	91.72(9)
C(106)-C(107)	1.421(5)	C(61)-Sb(3)-Sb(4)	112.66(9)
C(107)-C(108)	1.392(5)	C(91)-Sb(4)-C(106)	96.57(12)
C(107)-C(112)	1.519(5)	C(91)-Sb(4)-Sb(3)	112.29(9)
C(108)-C(109)	1.382(5)	C(106)-Sb(4)-Sb(3)	92.09(9)
C(109)-C(110)	1.389(5)	C(2)-C(1)-C(6)	118.4(3)
C(109)-C(115)	1.520(5)	C(2)-C(1)-Sb(1)	124.1(2)
C(110)-C(111)	1.398(5)	C(6)-C(1)-Sb(1)	117.2(2)
C(111)-C(118)	1.517(5)	C(3)-C(2)-C(1)	119.5(3)
C(112)-C(113)	1.535(5)	C(3)-C(2)-C(7)	116.4(3)
C(112)-C(114)	1.538(5)	C(1)-C(2)-C(7)	124.1(3)
C(115)-C(117)	1.525(6)	C(4)-C(3)-C(2)	122.4(3)
C(115)-C(116)	1.535(6)	C(5)-C(4)-C(3)	117.7(3)
C(118)-C(119)	1.526(5)	C(5)-C(4)-C(10)	121.7(3)
C(118)-C(120)	1.529(5)	C(3)-C(4)-C(10)	120.6(3)
C(1A)-C(2A)	1.547(7)	C(4)-C(5)-C(6)	122.2(3)
C(2A)-C(3A)	1.488(7)	C(5)-C(6)-C(1)	119.7(3)
C(3A)-C(4A)	1.548(7)	C(5)-C(6)-C(13)	117.6(3)
C(4A)-C(5A)	1.509(6)	C(1)-C(6)-C(13)	122.7(3)
C(5A)-C(6A)	1.507(6)	C(2)-C(7)-C(8)	112.0(3)
C(1B)-C(2B)	1.533(14)	C(2)-C(7)-C(9)	111.1(3)

C(8)-C(7)-C(9)	109.7(3)	C(35)-C(34)-C(40)	122.1(3)
C(4)-C(10)-C(11)	112.0(3)	C(33)-C(34)-C(40)	120.5(3)
C(4)-C(10)-C(12)	110.9(3)	C(34)-C(35)-C(36)	122.0(3)
C(11)-C(10)-C(12)	109.8(3)	C(35)-C(36)-C(31)	120.1(3)
C(15)-C(13)-C(6)	112.2(3)	C(35)-C(36)-C(43)	117.1(3)
C(15)-C(13)-C(14)	110.2(3)	C(31)-C(36)-C(43)	122.7(3)
C(6)-C(13)-C(14)	111.9(3)	C(32)-C(37)-C(39)	111.8(3)
C(17)-C(16)-C(21)	119.0(3)	C(32)-C(37)-C(38)	111.8(3)
C(17)-C(16)-Sb(1)	128.0(3)	C(39)-C(37)-C(38)	109.7(3)
C(21)-C(16)-Sb(1)	113.0(2)	C(34)-C(40)-C(42)	110.8(3)
C(18)-C(17)-C(16)	118.9(3)	C(34)-C(40)-C(41)	111.4(3)
C(18)-C(17)-C(22)	116.0(3)	C(42)-C(40)-C(41)	110.1(4)
C(16)-C(17)-C(22)	125.1(3)	C(36)-C(43)-C(44)	112.2(3)
C(19)-C(18)-C(17)	122.9(3)	C(36)-C(43)-C(45)	112.8(3)
C(18)-C(19)-C(20)	117.6(3)	C(44)-C(43)-C(45)	110.3(3)
C(18)-C(19)-C(25)	120.7(3)	C(47)-C(46)-C(51)	118.7(3)
C(20)-C(19)-C(25)	121.6(3)	C(47)-C(46)-Sb(2)	113.7(2)
C(19)-C(20)-C(21)	122.0(3)	C(51)-C(46)-Sb(2)	127.6(2)
C(20)-C(21)-C(16)	119.6(3)	C(48)-C(47)-C(46)	119.7(3)
C(20)-C(21)-C(28)	116.1(3)	C(48)-C(47)-C(52)	116.0(3)
C(16)-C(21)-C(28)	124.3(3)	C(46)-C(47)-C(52)	124.3(3)
C(23)-C(22)-C(24)	107.6(3)	C(49)-C(48)-C(47)	122.4(3)
C(23)-C(22)-C(17)	113.5(3)	C(48)-C(49)-C(50)	117.3(3)
C(24)-C(22)-C(17)	111.1(3)	C(48)-C(49)-C(55)	121.0(3)
C(27)-C(25)-C(19)	113.4(3)	C(50)-C(49)-C(55)	121.6(3)
C(27)-C(25)-C(26)	111.2(3)	C(49)-C(50)-C(51)	123.0(3)
C(19)-C(25)-C(26)	109.6(3)	C(50)-C(51)-C(46)	118.8(3)
C(29)-C(28)-C(21)	111.7(3)	C(50)-C(51)-C(58)	116.6(3)
C(29)-C(28)-C(30)	111.0(3)	C(46)-C(51)-C(58)	124.6(3)
C(21)-C(28)-C(30)	112.1(3)	C(47)-C(52)-C(53)	112.3(3)
C(36)-C(31)-C(32)	118.2(3)	C(47)-C(52)-C(54)	111.9(3)
C(36)-C(31)-Sb(2)	117.3(2)	C(53)-C(52)-C(54)	110.8(3)
C(32)-C(31)-Sb(2)	124.0(2)	C(49)-C(55)-C(56)	112.1(3)
C(33)-C(32)-C(31)	119.4(3)	C(49)-C(55)-C(57)	110.8(3)
C(33)-C(32)-C(37)	116.1(3)	C(56)-C(55)-C(57)	110.6(4)
C(31)-C(32)-C(37)	124.5(3)	C(51)-C(58)-C(60)	111.4(3)
C(34)-C(33)-C(32)	122.8(3)	C(51)-C(58)-C(59)	113.3(3)
C(35)-C(34)-C(33)	117.4(3)	C(60)-C(58)-C(59)	107.7(3)

C(62)-C(61)-C(66)	119.1(3)	C(84)-C(82)-C(77)	112.0(3)
C(62)-C(61)-Sb(3)	127.6(3)	C(83)-C(82)-C(77)	112.0(3)
C(66)-C(61)-Sb(3)	113.3(2)	C(79)-C(85)-C(87)	112.0(3)
C(63)-C(62)-C(61)	118.9(3)	C(79)-C(85)-C(86)	111.0(3)
C(63)-C(62)-C(67)	116.6(3)	C(87)-C(85)-C(86)	109.4(3)
C(61)-C(62)-C(67)	124.6(3)	C(81)-C(88)-C(90)	112.4(3)
C(64)-C(63)-C(62)	123.0(3)	C(81)-C(88)-C(89)	111.4(3)
C(63)-C(64)-C(65)	117.5(3)	C(90)-C(88)-C(89)	109.7(3)
C(63)-C(64)-C(70)	121.2(3)	C(96)-C(91)-C(92)	118.6(3)
C(65)-C(64)-C(70)	121.4(3)	C(96)-C(91)-Sb(4)	127.8(3)
C(66)-C(65)-C(64)	122.0(3)	C(92)-C(91)-Sb(4)	113.6(2)
C(65)-C(66)-C(61)	119.4(3)	C(93)-C(92)-C(91)	119.4(3)
C(65)-C(66)-C(73)	116.3(3)	C(93)-C(92)-C(97)	116.4(3)
C(61)-C(66)-C(73)	124.3(3)	C(91)-C(92)-C(97)	124.2(3)
C(69)-C(67)-C(62)	113.3(3)	C(94)-C(93)-C(92)	122.5(3)
C(69)-C(67)-C(68)	107.3(3)	C(93)-C(94)-C(95)	117.3(3)
C(62)-C(67)-C(68)	111.6(3)	C(93)-C(94)-C(100)	122.7(3)
C(64)-C(70)-C(72)	111.2(3)	C(95)-C(94)-C(100)	119.9(3)
C(64)-C(70)-C(71)	111.8(3)	C(94)-C(95)-C(96)	122.6(3)
C(72)-C(70)-C(71)	111.2(4)	C(95)-C(96)-C(91)	119.6(3)
C(74)-C(73)-C(66)	112.9(3)	C(95)-C(96)-C(103)	116.0(3)
C(74)-C(73)-C(75)	110.8(3)	C(91)-C(96)-C(103)	124.4(3)
C(66)-C(73)-C(75)	111.3(3)	C(99)-C(97)-C(92)	112.2(3)
C(77)-C(76)-C(81)	118.0(3)	C(99)-C(97)-C(98)	111.1(3)
C(77)-C(76)-Sb(3)	117.2(2)	C(92)-C(97)-C(98)	112.1(3)
C(81)-C(76)-Sb(3)	124.4(2)	C(94)-C(100)-C(101)	113.0(3)
C(78)-C(77)-C(76)	120.3(3)	C(94)-C(100)-C(102)	109.6(3)
C(78)-C(77)-C(82)	117.6(3)	C(101)-C(100)-C(102)	110.9(4)
C(76)-C(77)-C(82)	122.0(3)	C(105)-C(103)-C(104)	108.2(3)
C(79)-C(78)-C(77)	122.2(3)	C(105)-C(103)-C(96)	110.7(3)
C(80)-C(79)-C(78)	117.4(3)	C(104)-C(103)-C(96)	113.5(3)
C(80)-C(79)-C(85)	120.7(3)	C(111)-C(106)-C(107)	118.9(3)
C(78)-C(79)-C(85)	121.8(3)	C(111)-C(106)-Sb(4)	116.6(2)
C(79)-C(80)-C(81)	122.7(3)	C(107)-C(106)-Sb(4)	124.2(2)
C(80)-C(81)-C(76)	119.2(3)	C(108)-C(107)-C(106)	118.8(3)
C(80)-C(81)-C(88)	116.3(3)	C(108)-C(107)-C(112)	116.8(3)
C(76)-C(81)-C(88)	124.4(3)	C(106)-C(107)-C(112)	124.4(3)
C(84)-C(82)-C(83)	111.0(3)	C(109)-C(108)-C(107)	123.2(3)

C(108)-C(109)-C(110)	117.3(3)	C(111)-C(118)-C(120)	113.0(3)
C(108)-C(109)-C(115)	120.6(3)	C(119)-C(118)-C(120)	110.3(3)
C(110)-C(109)-C(115)	122.0(3)	C(3A)-C(2A)-C(1A)	113.3(5)
C(109)-C(110)-C(111)	122.6(3)	C(2A)-C(3A)-C(4A)	114.0(5)
C(110)-C(111)-C(106)	119.1(3)	C(5A)-C(4A)-C(3A)	113.5(4)
C(110)-C(111)-C(118)	117.6(3)	C(6A)-C(5A)-C(4A)	112.1(4)
C(106)-C(111)-C(118)	123.2(3)	C(3B)-C(2B)-C(1B)	109.4(13)
C(107)-C(112)-C(113)	111.3(3)	C(2B)-C(3B)-C(4B)	114.7(10)
C(107)-C(112)-C(114)	112.2(3)	C(5B)-C(4B)-C(3B)	113.9(10)
C(113)-C(112)-C(114)	109.6(3)	C(4B)-C(5B)-C(6B)	115.1(11)
C(109)-C(115)-C(117)	112.2(4)	C(3C)-C(2C)-C(1C)	116.1(11)
C(109)-C(115)-C(116)	110.8(3)	C(2C)-C(3C)-C(4C)	114.1(11)
C(117)-C(115)-C(116)	109.9(4)	C(5C)-C(4C)-C(3C)	113.6(10)
C(111)-C(118)-C(119)	112.6(3)	C(4C)-C(5C)-C(6C)	114.0(13)

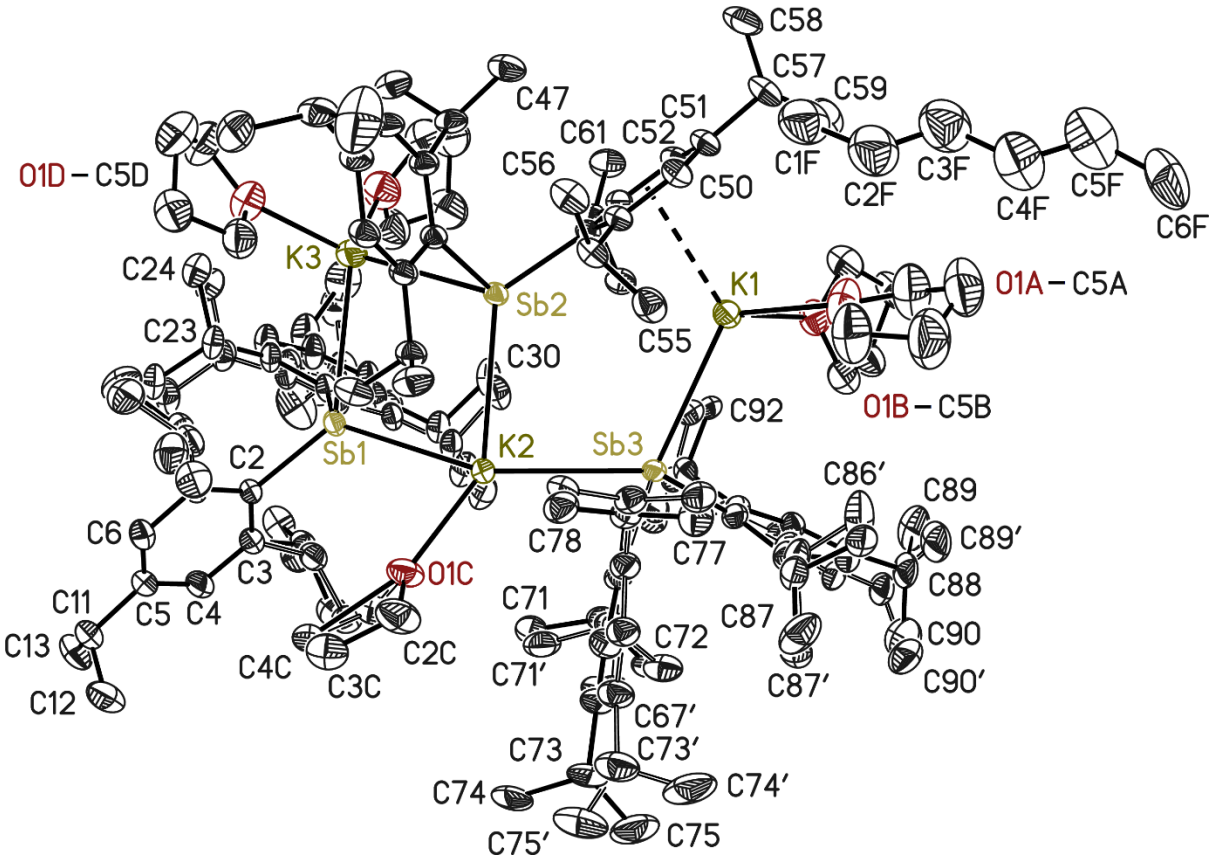

Figure S59: Asymmetric unit of **6**. The anisotropic displacement parameters are depicted at the 50% probability level. The hydrogen atoms as well as disordered positions in all of the coordinating THF and hexane molecules are omitted for clarity.

Each of the THF molecules is disordered about two positions. The occupancies of the minor positions refined to 0.312(5) (O1A′ – C5A′), 0.242(7) (O1B′ – C5B′), 0.446(4) (O1C′ – C5C′), 0.189(4) (O1D′ – C5D′), 0.284(8) (O1E′ – C5E′).

The hexane molecule is disordered about 7 positions. The sum of occupancies was fixed to 1.5. The occupancies for the individual positions were initially refined and then fixed to 0.4 (C1F – C6F), 0.3 (C1G – C6G), 0.2 (C1H – C6H), 0.1 (C1I – C6I), 0.2 (C1J – C6J), 0.2 (C1K – C6K), 0.1 (C1L – C6L).

Three of the Tip substituents were disordered about two positions, in one substituent the disorder was only treated on the isopropyl groups. The occupancies of the minor positions refined to 0.435(8) (C8′ – 10′), 0.45(2) (C14 – C16), 0.477(4) (C17′ – C31′), 0.364(5) (C64′ – C78′), 0.208(7) (C79 – C93).

All disordered groups were refined with distance restraints and restraints for the anisotropic displacement parameters.

Complex **6** crystallizes in monoclinic space group $P2_1/c$. Each Sb atom shows a distorted tetrahedral environment. As expected for a $(Tip)_2Sb^-$ fragment bearing two lone pairs, it adopts a bent structure with C_{Tip}-Sb-C_{Tip} angles (~ 95°) smaller than 109.5°. The coordination environments of each K ion of trimeric $((Tip)_2Sb\text{-}K)_3(THF)_5$ are different. This unprecedented trinuclear cluster (6) has adopted a near-U-shaped structure (angle between two K_2Sb_2 planes is 150°). K2 and K3 ions have adopted a distorted tetrahedral geometry with small interactions with the nearest aromatic rings. The K1 centre is bonded to Sb3 centre (3.5421(8) Å) and the two THF molecules with an additional π-interaction (η^6) with the nearest aromatic ring of the Tip- group bonded to Sb2 atom. The K1-C_{Tip} distances are in the range of 3.173(2) to 3.387(3) Å. The average distance from the centre of the nearest Ar_{Tip} ring is 2.938 Å. In comparison, the K3 centre is relatively far from the nearest Ar_{Tip} rings (K3-Tip_{center} 4.49-4.58 Å). The distance from K3 to nearest aromatic C-atoms are in the range of 3.31/3.70-3.51/3.76 Å. The K2 ion is coordinated by three Sb-atoms and one THF molecule.

Table S21: Bond lengths [Å] and angles [°] for **6**.

K(1)-O(1B')	2.617(19)	K(1)-C(48)	3.173(2)
K(1)-O(1A)	2.674(7)	K(1)-C(49)	3.184(3)
K(1)-O(1B)	2.702(6)	K(1)-C(53)	3.202(2)
K(1)-O(1A')	2.745(16)	K(1)-C(50)	3.290(3)

K(1)-C(52)	3.296(3)	C(2B')-C(3B')	1.490(13)
K(1)-C(51)	3.387(3)	C(3B')-C(4B')	1.527(13)
K(1)-C(5B')	3.505(16)	C(4B')-C(5B')	1.507(13)
K(1)-Sb(3)	3.5421(8)	O(1C)-C(2C)	1.417(7)
K(2)-O(1C)	2.633(6)	O(1C)-C(5C)	1.438(7)
K(2)-O(1C')	2.649(7)	C(2C)-C(3C)	1.512(8)
K(2)-C(64')	3.41(5)	C(3C)-C(4C)	1.524(7)
K(2)-Sb(3)	3.4217(6)	C(4C)-C(5C)	1.507(7)
K(2)-C(64)	3.43(3)	O(1C')-C(5C')	1.418(9)
K(2)-Sb(1)	3.4966(6)	O(1C')-C(2C')	1.423(9)
K(2)-C(5C')	3.511(7)	C(2C')-C(3C')	1.567(9)
K(2)-C(5C)	3.522(5)	C(3C')-C(4C')	1.512(10)
K(2)-Sb(2)	3.5583(8)	C(4C')-C(5C')	1.473(9)
K(3)-O(1D)	2.606(4)	O(1D)-C(5D)	1.422(5)
K(3)-O(1E')	2.638(2)	O(1D)-C(2D)	1.438(5)
K(3)-O(1E)	2.638(2)	C(2D)-C(3D)	1.496(5)
K(3)-O(1D')	2.826(18)	C(3D)-C(4D)	1.534(7)
K(3)-C(2D)	3.310(4)	C(4D)-C(5D)	1.515(7)
K(3)-Sb(1)	3.4597(9)	O(1D')-C(2D')	1.428(13)
K(3)-C(2E)	3.514(7)	O(1D')-C(5D')	1.435(13)
K(3)-Sb(2)	3.5234(7)	C(2D')-C(3D')	1.504(13)
O(1A)-C(5A)	1.433(10)	C(3D')-C(4D')	1.523(14)
O(1A)-C(2A)	1.440(12)	C(4D')-C(5D')	1.503(13)
C(2A)-C(3A)	1.445(7)	O(1E)-C(5E)	1.425(7)
C(3A)-C(4A)	1.588(9)	O(1E)-C(2E)	1.433(7)
C(4A)-C(5A)	1.427(8)	C(2E)-C(3E)	1.445(7)
O(1A')-C(5A')	1.434(13)	C(3E)-C(4E)	1.571(8)
O(1A')-C(2A')	1.441(14)	C(4E)-C(5E)	1.512(8)
C(2A')-C(3A')	1.485(12)	O(1E')-C(2E')	1.429(12)
C(3A')-C(4A')	1.619(13)	O(1E')-C(5E')	1.435(13)
C(4A')-C(5A')	1.469(12)	C(2E')-C(3E')	1.483(12)
O(1B)-C(5B)	1.443(6)	C(3E')-C(4E')	1.541(13)
O(1B)-C(2B)	1.445(7)	C(4E')-C(5E')	1.499(14)
C(2B)-C(3B)	1.500(6)	Sb(1)-C(17')	2.188(8)
C(3B)-C(4B)	1.523(6)	Sb(1)-C(2)	2.197(2)
C(4B)-C(5B)	1.495(6)	Sb(1)-C(17)	2.208(7)
O(1B')-C(2B')	1.418(13)	C(2)-C(3)	1.412(4)
O(1B')-C(5B')	1.426(13)	C(2)-C(7)	1.413(3)

C(3)-C(4)	1.398(4)	C(19')-C(20')	1.383(8)
C(3)-C(8')	1.522(8)	C(20')-C(21')	1.388(8)
C(3)-C(8)	1.553(7)	C(20')-C(26')	1.524(8)
C(4)-C(5)	1.381(4)	C(21')-C(22')	1.400(8)
C(5)-C(6)	1.385(4)	C(22')-C(29')	1.512(7)
C(5)-C(11)	1.526(4)	C(23')-C(24')	1.523(8)
C(6)-C(7)	1.391(3)	C(23')-C(25')	1.535(9)
C(7)-C(14')	1.521(8)	C(26')-C(28')	1.503(9)
C(7)-C(14)	1.528(10)	C(26')-C(27')	1.525(10)
C(8)-C(9)	1.525(8)	C(29')-C(30')	1.529(9)
C(8)-C(10)	1.552(7)	C(29')-C(31')	1.531(8)
C(11)-C(13)	1.523(5)	Sb(2)-C(48)	2.196(2)
C(11)-C(12)	1.525(4)	Sb(2)-C(33)	2.210(2)
C(14)-C(15)	1.533(10)	C(33)-C(38)	1.412(3)
C(14)-C(16)	1.534(10)	C(33)-C(34)	1.418(3)
C(8')-C(10')	1.522(9)	C(34)-C(35)	1.388(3)
C(8')-C(9')	1.531(9)	C(34)-C(39)	1.529(3)
C(14')-C(16')	1.517(9)	C(35)-C(36)	1.393(4)
C(14')-C(15')	1.528(9)	C(36)-C(37)	1.383(3)
C(17)-C(18)	1.420(7)	C(36)-C(42)	1.519(3)
C(17)-C(22)	1.424(8)	C(37)-C(38)	1.401(3)
C(18)-C(19)	1.402(7)	C(38)-C(45)	1.528(3)
C(18)-C(23)	1.518(7)	C(39)-C(41)	1.521(4)
C(19)-C(20)	1.381(7)	C(39)-C(40)	1.524(4)
C(20)-C(21)	1.388(7)	C(42)-C(44)	1.501(5)
C(20)-C(26)	1.526(7)	C(42)-C(43)	1.505(4)
C(21)-C(22)	1.406(7)	C(45)-C(46)	1.533(4)
C(22)-C(29)	1.517(7)	C(45)-C(47)	1.536(4)
C(23)-C(24)	1.533(8)	C(48)-C(49)	1.416(3)
C(23)-C(25)	1.538(8)	C(48)-C(53)	1.421(3)
C(26)-C(28)	1.490(9)	C(49)-C(50)	1.404(3)
C(26)-C(27)	1.527(9)	C(49)-C(54)	1.528(3)
C(29)-C(31)	1.526(8)	C(50)-C(51)	1.388(3)
C(29)-C(30)	1.538(9)	C(51)-C(52)	1.392(4)
C(17')-C(22')	1.405(8)	C(51)-C(57)	1.521(3)
C(17')-C(18')	1.413(8)	C(52)-C(53)	1.398(3)
C(18')-C(19')	1.399(8)	C(53)-C(60)	1.519(3)
C(18')-C(23')	1.522(8)	C(54)-C(55)	1.532(4)

C(54)-C(56)	1.534(4)	C(76')-C(78')	1.530(12)
C(57)-C(59)	1.514(4)	C(79)-C(80)	1.408(13)
C(57)-C(58)	1.515(4)	C(79)-C(84)	1.420(12)
C(60)-C(62)	1.528(3)	C(80)-C(81)	1.416(13)
C(60)-C(61)	1.535(3)	C(80)-C(85)	1.531(13)
Sb(3)-C(79')	2.195(4)	C(81)-C(82)	1.381(12)
Sb(3)-C(79)	2.203(13)	C(82)-C(83)	1.387(12)
Sb(3)-C(64')	2.203(11)	C(82)-C(88)	1.521(12)
Sb(3)-C(64)	2.217(7)	C(83)-C(84)	1.403(12)
C(64)-C(69)	1.414(7)	C(84)-C(91)	1.525(12)
C(64)-C(65)	1.418(8)	C(85)-C(87)	1.533(13)
C(65)-C(66)	1.409(7)	C(85)-C(86)	1.534(14)
C(65)-C(70)	1.522(7)	C(88)-C(90)	1.496(13)
C(66)-C(67)	1.381(7)	C(88)-C(89)	1.500(13)
C(67)-C(68)	1.384(7)	C(91)-C(92)	1.522(13)
C(67)-C(73)	1.526(6)	C(91)-C(93)	1.523(13)
C(68)-C(69)	1.404(7)	C(79')-C(84')	1.411(5)
C(69)-C(76)	1.520(7)	C(79')-C(80')	1.416(5)
C(70)-C(72)	1.535(8)	C(80')-C(81')	1.419(6)
C(70)-C(71)	1.536(8)	C(80')-C(85')	1.524(6)
C(73)-C(74)	1.490(7)	C(81')-C(82')	1.385(5)
C(73)-C(75)	1.518(8)	C(82')-C(83')	1.386(5)
C(76)-C(77)	1.525(8)	C(82')-C(88')	1.530(5)
C(76)-C(78)	1.533(8)	C(83')-C(84')	1.397(5)
C(64')-C(69')	1.413(11)	C(84')-C(91')	1.520(5)
C(64')-C(65')	1.418(11)	C(85')-C(86')	1.528(6)
C(65')-C(66')	1.405(11)	C(85')-C(87')	1.532(6)
C(65')-C(70')	1.524(11)	C(88')-C(89')	1.525(6)
C(66')-C(67')	1.383(10)	C(88')-C(90')	1.538(6)
C(67')-C(68')	1.391(10)	C(91')-C(92')	1.528(5)
C(67')-C(73')	1.531(10)	C(91')-C(93')	1.538(6)
C(68')-C(69')	1.391(11)	C(1F)-C(2F)	1.450(13)
C(69')-C(76')	1.519(11)	C(2F)-C(3F)	1.461(11)
C(70')-C(72')	1.528(12)	C(3F)-C(4F)	1.511(12)
C(70')-C(71')	1.536(12)	C(4F)-C(5F)	1.500(12)
C(73')-C(74')	1.472(11)	C(5F)-C(6F)	1.529(12)
C(73')-C(75')	1.505(11)	C(1G)-C(2G)	1.478(13)
C(76')-C(77')	1.524(12)	C(2G)-C(3G)	1.507(12)

C(3G)-C(4G)	1.486(11)	O(1A')-K(1)-C(49)	102.1(4)
C(4G)-C(5G)	1.480(11)	C(48)-K(1)-C(49)	25.74(6)
C(5G)-C(6G)	1.472(12)	O(1B')-K(1)-C(53)	105.5(6)
C(1H)-C(2H)	1.492(15)	O(1A)-K(1)-C(53)	130.1(3)
C(2H)-C(3H)	1.480(14)	O(1B)-K(1)-C(53)	105.64(17)
C(3H)-C(4H)	1.461(12)	O(1A')-K(1)-C(53)	129.8(6)
C(4H)-C(5H)	1.484(12)	C(48)-K(1)-C(53)	25.75(6)
C(5H)-C(6H)	1.510(14)	C(49)-K(1)-C(53)	44.74(6)
C(1I)-C(2I)	1.479(15)	O(1B')-K(1)-C(50)	122.0(5)
C(2I)-C(3I)	1.479(15)	O(1A)-K(1)-C(50)	84.3(2)
C(3I)-C(4I)	1.486(15)	O(1B)-K(1)-C(50)	126.44(15)
C(4I)-C(5I)	1.494(15)	O(1A')-K(1)-C(50)	83.8(5)
C(5I)-C(6I)	1.490(15)	C(48)-K(1)-C(50)	44.30(6)
C(1J)-C(2J)	1.506(14)	C(49)-K(1)-C(50)	24.98(6)
C(2J)-C(3J)	1.486(14)	C(53)-K(1)-C(50)	50.66(6)
C(3J)-C(4J)	1.505(13)	O(1B')-K(1)-C(52)	92.1(5)
C(4J)-C(5J)	1.485(13)	O(1A)-K(1)-C(52)	107.7(3)
C(5J)-C(6J)	1.470(13)	O(1B)-K(1)-C(52)	94.27(15)
C(1K)-C(2K)	1.449(14)	O(1A')-K(1)-C(52)	107.6(7)
C(2K)-C(3K)	1.457(14)	C(48)-K(1)-C(52)	44.31(6)
C(3K)-C(4K)	1.529(14)	C(49)-K(1)-C(52)	50.86(6)
C(4K)-C(5K)	1.458(14)	C(53)-K(1)-C(52)	24.79(6)
C(5K)-C(6K)	1.459(14)	C(50)-K(1)-C(52)	42.29(6)
C(1L)-C(2L)	1.477(15)	O(1B')-K(1)-C(51)	99.5(5)
C(2L)-C(3L)	1.498(15)	O(1A)-K(1)-C(51)	86.7(3)
C(3L)-C(4L)	1.517(15)	O(1B)-K(1)-C(51)	103.45(14)
C(4L)-C(5L)	1.486(15)	O(1A')-K(1)-C(51)	86.4(6)
C(5L)-C(6L)	1.487(15)	C(48)-K(1)-C(51)	51.44(6)
		C(49)-K(1)-C(51)	43.60(6)
O(1A)-K(1)-O(1B)	82.9(3)	C(53)-K(1)-C(51)	43.42(6)
O(1B')-K(1)-O(1A')	79.4(9)	C(50)-K(1)-C(51)	23.93(6)
O(1B')-K(1)-C(48)	131.2(6)	C(52)-K(1)-C(51)	24.00(6)
O(1A)-K(1)-C(48)	127.65(19)	O(1B')-K(1)-C(5B')	21.2(4)
O(1B)-K(1)-C(48)	130.99(18)	O(1A')-K(1)-C(5B')	75.6(5)
O(1A')-K(1)-C(48)	127.1(4)	C(48)-K(1)-C(5B')	148.6(3)
O(1B')-K(1)-C(49)	142.0(5)	C(49)-K(1)-C(5B')	163.0(3)
O(1A)-K(1)-C(49)	102.73(18)	C(53)-K(1)-C(5B')	124.2(3)
O(1B)-K(1)-C(49)	144.94(15)	C(50)-K(1)-C(5B')	140.2(3)

C(52)-K(1)-C(5B')	113.2(3)	C(5C')-K(2)-Sb(2)	134.35(13)
C(51)-K(1)-C(5B')	119.6(3)	C(5C)-K(2)-Sb(2)	144.76(9)
O(1B')-K(1)-Sb(3)	99.0(6)	O(1D)-K(3)-O(1E)	113.41(10)
O(1A)-K(1)-Sb(3)	122.3(3)	O(1E')-K(3)-O(1D')	106.0(4)
O(1B)-K(1)-Sb(3)	93.77(16)	O(1D)-K(3)-C(2D)	24.66(10)
O(1A')-K(1)-Sb(3)	122.4(7)	O(1E)-K(3)-C(2D)	137.85(10)
C(48)-K(1)-Sb(3)	97.18(4)	O(1D)-K(3)-Sb(1)	109.64(12)
C(49)-K(1)-Sb(3)	110.94(5)	O(1E')-K(3)-Sb(1)	118.31(6)
C(53)-K(1)-Sb(3)	106.34(5)	O(1E)-K(3)-Sb(1)	118.31(6)
C(50)-K(1)-Sb(3)	135.83(5)	O(1D')-K(3)-Sb(1)	113.8(5)
C(52)-K(1)-Sb(3)	129.93(5)	C(2D)-K(3)-Sb(1)	93.63(8)
C(51)-K(1)-Sb(3)	148.15(5)	O(1D)-K(3)-C(2E)	125.97(16)
C(5B')-K(1)-Sb(3)	83.6(3)	O(1E)-K(3)-C(2E)	21.46(13)
O(1C)-K(2)-C(64')	89.2(4)	C(2D)-K(3)-C(2E)	149.56(16)
O(1C)-K(2)-Sb(3)	126.54(16)	Sb(1)-K(3)-C(2E)	96.85(12)
O(1C')-K(2)-Sb(3)	125.54(18)	O(1D)-K(3)-Sb(2)	116.08(10)
C(64')-K(2)-Sb(3)	37.7(4)	O(1E')-K(3)-Sb(2)	112.42(6)
O(1C')-K(2)-C(64)	88.1(3)	O(1E)-K(3)-Sb(2)	112.42(6)
Sb(3)-K(2)-C(64)	37.7(2)	O(1D')-K(3)-Sb(2)	121.8(4)
O(1C)-K(2)-Sb(1)	81.12(15)	C(2D)-K(3)-Sb(2)	96.68(7)
O(1C')-K(2)-Sb(1)	85.43(17)	Sb(1)-K(3)-Sb(2)	83.973(16)
C(64')-K(2)-Sb(1)	162.2(3)	C(2E)-K(3)-Sb(2)	112.76(13)
Sb(3)-K(2)-Sb(1)	146.67(2)	C(5A)-O(1A)-C(2A)	109.1(6)
C(64)-K(2)-Sb(1)	160.20(19)	C(5A)-O(1A)-K(1)	125.2(6)
O(1C')-K(2)-C(5C')	21.3(2)	C(2A)-O(1A)-K(1)	122.8(7)
Sb(3)-K(2)-C(5C')	104.36(13)	O(1A)-C(2A)-C(3A)	106.8(6)
C(64)-K(2)-C(5C')	66.9(2)	C(2A)-C(3A)-C(4A)	105.0(6)
Sb(1)-K(2)-C(5C')	105.54(13)	C(5A)-C(4A)-C(3A)	100.9(6)
O(1C)-K(2)-C(5C)	21.39(13)	C(4A)-C(5A)-O(1A)	108.5(6)
C(64')-K(2)-C(5C)	95.8(4)	C(5A')-O(1A')-C(2A')	106.0(12)
Sb(3)-K(2)-C(5C)	128.17(10)	C(5A')-O(1A')-K(1)	121.0(10)
Sb(1)-K(2)-C(5C)	70.12(9)	C(2A')-O(1A')-K(1)	132.4(11)
O(1C)-K(2)-Sb(2)	135.16(15)	O(1A')-C(2A')-C(3A')	106.6(10)
O(1C')-K(2)-Sb(2)	126.00(17)	C(2A')-C(3A')-C(4A')	102.3(10)
C(64')-K(2)-Sb(2)	114.1(4)	C(5A')-C(4A')-C(3A')	94.2(10)
Sb(3)-K(2)-Sb(2)	86.662(14)	O(1A')-C(5A')-C(4A')	106.9(12)
C(64)-K(2)-Sb(2)	115.7(2)	C(5B)-O(1B)-C(2B)	108.6(4)
Sb(1)-K(2)-Sb(2)	82.928(13)	C(5B)-O(1B)-K(1)	123.3(4)

C(2B)-O(1B)-K(1)	127.5(4)	C(2D)-C(3D)-C(4D)	100.2(4)
O(1B)-C(2B)-C(3B)	106.8(5)	C(5D)-C(4D)-C(3D)	101.8(4)
C(2B)-C(3B)-C(4B)	102.7(4)	O(1D)-C(5D)-C(4D)	105.1(4)
C(5B)-C(4B)-C(3B)	101.7(4)	C(2D')-O(1D')-C(5D')	109.6(12)
O(1B)-C(5B)-C(4B)	104.5(4)	C(2D')-O(1D')-K(3)	128.1(11)
C(2B')-O(1B')-C(5B')	109.9(13)	C(5D')-O(1D')-K(3)	119.6(11)
C(2B')-O(1B')-K(1)	132.0(14)	O(1D')-C(2D')-C(3D')	106.7(12)
C(5B')-O(1B')-K(1)	117.1(12)	C(2D')-C(3D')-C(4D')	103.8(12)
O(1B')-C(2B')-C(3B')	107.7(12)	C(5D')-C(4D')-C(3D')	101.6(12)
C(2B')-C(3B')-C(4B')	103.6(11)	O(1D')-C(5D')-C(4D')	104.8(12)
C(5B')-C(4B')-C(3B')	102.5(10)	C(5E)-O(1E)-C(2E)	109.7(5)
O(1B')-C(5B')-C(4B')	107.2(11)	C(5E)-O(1E)-K(3)	124.1(6)
O(1B')-C(5B')-K(1)	41.6(9)	C(2E)-O(1E)-K(3)	116.2(3)
C(4B')-C(5B')-K(1)	148.8(10)	O(1E)-C(2E)-C(3E)	105.4(5)
C(2C)-O(1C)-C(5C)	104.6(5)	O(1E)-C(2E)-K(3)	42.4(2)
C(2C)-O(1C)-K(2)	136.4(4)	C(3E)-C(2E)-K(3)	128.3(5)
C(5C)-O(1C)-K(2)	116.7(4)	C(2E)-C(3E)-C(4E)	103.5(5)
O(1C)-C(2C)-C(3C)	106.9(5)	C(5E)-C(4E)-C(3E)	98.2(7)
C(2C)-C(3C)-C(4C)	103.8(5)	O(1E)-C(5E)-C(4E)	107.2(5)
C(5C)-C(4C)-C(3C)	103.8(4)	C(2E')-O(1E')-C(5E')	106.1(11)
O(1C)-C(5C)-C(4C)	103.9(5)	C(2E')-O(1E')-K(3)	126.5(7)
O(1C)-C(5C)-K(2)	41.9(3)	C(5E')-O(1E')-K(3)	124.4(16)
C(4C)-C(5C)-K(2)	138.8(3)	O(1E')-C(2E')-C(3E')	111.7(10)
C(5C')-O(1C')-C(2C')	106.8(6)	C(2E')-C(3E')-C(4E')	100.6(10)
C(5C')-O(1C')-K(2)	116.1(5)	C(5E')-C(4E')-C(3E')	102.9(14)
C(2C')-O(1C')-K(2)	135.3(5)	O(1E')-C(5E')-C(4E')	106.3(13)
O(1C')-C(2C')-C(3C')	103.7(6)	C(17')-Sb(1)-C(2)	95.7(3)
C(4C')-C(3C')-C(2C')	105.0(6)	C(2)-Sb(1)-C(17)	95.2(3)
C(5C')-C(4C')-C(3C')	103.8(6)	C(17')-Sb(1)-K(3)	84.5(3)
O(1C')-C(5C')-C(4C')	106.8(6)	C(2)-Sb(1)-K(3)	135.20(7)
O(1C')-C(5C')-K(2)	42.7(4)	C(17)-Sb(1)-K(3)	77.9(3)
C(4C')-C(5C')-K(2)	127.4(5)	C(17')-Sb(1)-K(2)	118.7(2)
C(5D)-O(1D)-C(2D)	109.7(4)	C(2)-Sb(1)-K(2)	120.47(7)
C(5D)-O(1D)-K(3)	142.7(3)	C(17)-Sb(1)-K(2)	126.4(2)
C(2D)-O(1D)-K(3)	106.2(2)	K(3)-Sb(1)-K(2)	97.464(16)
O(1D)-C(2D)-C(3D)	106.4(4)	C(3)-C(2)-C(7)	117.7(2)
O(1D)-C(2D)-K(3)	49.1(2)	C(3)-C(2)-Sb(1)	120.87(17)
C(3D)-C(2D)-K(3)	155.4(3)	C(7)-C(2)-Sb(1)	121.38(18)

C(4)-C(3)-C(2)	119.9(2)	C(19)-C(20)-C(26)	120.5(5)
C(4)-C(3)-C(8')	117.4(5)	C(21)-C(20)-C(26)	121.4(5)
C(2)-C(3)-C(8')	121.4(5)	C(20)-C(21)-C(22)	121.7(5)
C(4)-C(3)-C(8)	115.8(4)	C(21)-C(22)-C(17)	120.0(5)
C(2)-C(3)-C(8)	123.8(4)	C(21)-C(22)-C(29)	118.6(5)
C(5)-C(4)-C(3)	122.6(3)	C(17)-C(22)-C(29)	121.4(5)
C(4)-C(5)-C(6)	117.2(2)	C(18)-C(23)-C(24)	111.8(5)
C(4)-C(5)-C(11)	122.0(3)	C(18)-C(23)-C(25)	111.2(5)
C(6)-C(5)-C(11)	120.7(3)	C(24)-C(23)-C(25)	110.3(6)
C(5)-C(6)-C(7)	122.6(3)	C(28)-C(26)-C(20)	112.2(6)
C(6)-C(7)-C(2)	120.1(2)	C(28)-C(26)-C(27)	110.7(7)
C(6)-C(7)-C(14')	117.2(5)	C(20)-C(26)-C(27)	110.5(6)
C(2)-C(7)-C(14')	122.3(5)	C(22)-C(29)-C(31)	114.3(5)
C(6)-C(7)-C(14)	116.5(6)	C(22)-C(29)-C(30)	111.8(6)
C(2)-C(7)-C(14)	122.9(6)	C(31)-C(29)-C(30)	109.0(7)
C(9)-C(8)-C(10)	110.0(6)	C(22')-C(17')-C(18')	118.8(6)
C(9)-C(8)-C(3)	111.3(5)	C(22')-C(17')-Sb(1)	120.8(5)
C(10)-C(8)-C(3)	114.2(5)	C(18')-C(17')-Sb(1)	120.4(5)
C(13)-C(11)-C(12)	111.5(3)	C(19')-C(18')-C(17')	119.7(6)
C(13)-C(11)-C(5)	113.1(3)	C(19')-C(18')-C(23')	116.8(6)
C(12)-C(11)-C(5)	109.4(3)	C(17')-C(18')-C(23')	123.5(6)
C(7)-C(14)-C(15)	113.9(9)	C(20')-C(19')-C(18')	122.1(6)
C(7)-C(14)-C(16)	113.0(8)	C(19')-C(20')-C(21')	117.6(5)
C(15)-C(14)-C(16)	109.7(8)	C(19')-C(20')-C(26')	121.9(6)
C(3)-C(8')-C(10')	107.6(6)	C(21')-C(20')-C(26')	120.5(6)
C(3)-C(8')-C(9')	115.7(6)	C(20')-C(21')-C(22')	122.6(6)
C(10')-C(8')-C(9')	111.5(7)	C(21')-C(22')-C(17')	119.2(6)
C(16')-C(14')-C(7)	111.9(6)	C(21')-C(22')-C(29')	118.5(6)
C(16')-C(14')-C(15')	111.6(7)	C(17')-C(22')-C(29')	122.3(6)
C(7)-C(14')-C(15')	110.2(7)	C(18')-C(23')-C(24')	112.5(6)
C(18)-C(17)-C(22)	117.8(6)	C(18')-C(23')-C(25')	112.1(6)
C(18)-C(17)-Sb(1)	120.3(5)	C(24')-C(23')-C(25')	111.1(7)
C(22)-C(17)-Sb(1)	121.8(5)	C(28')-C(26')-C(20')	111.7(7)
C(19)-C(18)-C(17)	119.6(6)	C(28')-C(26')-C(27')	110.2(8)
C(19)-C(18)-C(23)	117.3(5)	C(20')-C(26')-C(27')	111.2(8)
C(17)-C(18)-C(23)	123.1(6)	C(22')-C(29')-C(30')	110.4(6)
C(20)-C(19)-C(18)	122.7(5)	C(22')-C(29')-C(31')	115.1(6)
C(19)-C(20)-C(21)	118.1(5)	C(30')-C(29')-C(31')	111.4(7)

C(48)-Sb(2)-C(33)	94.27(9)	C(50)-C(49)-K(1)	81.72(15)
C(48)-Sb(2)-K(3)	128.18(6)	C(48)-C(49)-K(1)	76.67(14)
C(33)-Sb(2)-K(3)	78.47(7)	C(54)-C(49)-K(1)	110.76(15)
C(48)-Sb(2)-K(2)	128.81(6)	C(51)-C(50)-C(49)	122.5(2)
C(33)-Sb(2)-K(2)	123.32(6)	C(51)-C(50)-K(1)	81.94(16)
K(3)-Sb(2)-K(2)	95.177(16)	C(49)-C(50)-K(1)	73.30(14)
C(38)-C(33)-C(34)	118.0(2)	C(50)-C(51)-C(52)	117.4(2)
C(38)-C(33)-Sb(2)	121.33(17)	C(50)-C(51)-C(57)	121.1(2)
C(34)-C(33)-Sb(2)	120.59(17)	C(52)-C(51)-C(57)	121.4(2)
C(35)-C(34)-C(33)	120.1(2)	C(50)-C(51)-K(1)	74.12(15)
C(35)-C(34)-C(39)	118.2(2)	C(52)-C(51)-K(1)	74.35(15)
C(33)-C(34)-C(39)	121.7(2)	C(57)-C(51)-K(1)	123.28(18)
C(34)-C(35)-C(36)	122.4(2)	C(51)-C(52)-C(53)	122.3(2)
C(37)-C(36)-C(35)	117.2(2)	C(51)-C(52)-K(1)	81.65(16)
C(37)-C(36)-C(42)	121.8(2)	C(53)-C(52)-K(1)	73.85(14)
C(35)-C(36)-C(42)	120.9(2)	C(52)-C(53)-C(48)	120.1(2)
C(36)-C(37)-C(38)	122.7(2)	C(52)-C(53)-C(60)	119.0(2)
C(37)-C(38)-C(33)	119.5(2)	C(48)-C(53)-C(60)	121.0(2)
C(37)-C(38)-C(45)	116.6(2)	C(52)-C(53)-K(1)	81.36(15)
C(33)-C(38)-C(45)	123.9(2)	C(48)-C(53)-K(1)	75.96(14)
C(41)-C(39)-C(40)	110.6(2)	C(60)-C(53)-K(1)	111.61(15)
C(41)-C(39)-C(34)	110.7(2)	C(49)-C(54)-C(55)	110.7(2)
C(40)-C(39)-C(34)	114.3(2)	C(49)-C(54)-C(56)	112.9(2)
C(44)-C(42)-C(43)	111.0(3)	C(55)-C(54)-C(56)	110.4(2)
C(44)-C(42)-C(36)	110.5(3)	C(59)-C(57)-C(58)	110.7(3)
C(43)-C(42)-C(36)	112.9(2)	C(59)-C(57)-C(51)	112.1(2)
C(38)-C(45)-C(46)	111.7(2)	C(58)-C(57)-C(51)	110.5(3)
C(38)-C(45)-C(47)	112.4(2)	C(53)-C(60)-C(62)	110.7(2)
C(46)-C(45)-C(47)	109.8(2)	C(53)-C(60)-C(61)	114.6(2)
C(49)-C(48)-C(53)	117.9(2)	C(62)-C(60)-C(61)	109.3(2)
C(49)-C(48)-Sb(2)	121.07(16)	C(79')-Sb(3)-C(64')	96.7(12)
C(53)-C(48)-Sb(2)	121.03(17)	C(79)-Sb(3)-C(64)	94.1(17)
C(49)-C(48)-K(1)	77.58(14)	C(79')-Sb(3)-K(2)	140.8(4)
C(53)-C(48)-K(1)	78.28(14)	C(79)-Sb(3)-K(2)	143.2(17)
Sb(2)-C(48)-K(1)	114.76(9)	C(64')-Sb(3)-K(2)	70.8(15)
C(50)-C(49)-C(48)	119.8(2)	C(64)-Sb(3)-K(2)	71.5(8)
C(50)-C(49)-C(54)	116.8(2)	C(79')-Sb(3)-K(1)	104.3(5)
C(48)-C(49)-C(54)	123.5(2)	C(79)-Sb(3)-K(1)	102.5(19)

C(64')-Sb(3)-K(1)	132.3(6)	C(67')-C(66')-C(65')	123.1(10)
C(64)-Sb(3)-K(1)	135.5(3)	C(66')-C(67')-C(68')	117.0(9)
K(2)-Sb(3)-K(1)	111.479(15)	C(66')-C(67')-C(73')	123.5(9)
C(69)-C(64)-C(65)	117.2(6)	C(68')-C(67')-C(73')	119.4(9)
C(69)-C(64)-Sb(3)	122.3(5)	C(67')-C(68')-C(69')	123.1(10)
C(65)-C(64)-Sb(3)	120.5(5)	C(68')-C(69')-C(64')	119.0(11)
C(69)-C(64)-K(2)	99.2(13)	C(68')-C(69')-C(76')	117.7(10)
C(65)-C(64)-K(2)	99.4(14)	C(64')-C(69')-C(76')	123.3(11)
Sb(3)-C(64)-K(2)	70.8(6)	C(65')-C(70')-C(72')	113.3(12)
C(66)-C(65)-C(64)	119.8(6)	C(65')-C(70')-C(71')	111.6(12)
C(66)-C(65)-C(70)	116.7(6)	C(72')-C(70')-C(71')	111.3(12)
C(64)-C(65)-C(70)	123.4(6)	C(74')-C(73')-C(75')	112.5(9)
C(67)-C(66)-C(65)	122.4(6)	C(74')-C(73')-C(67')	112.6(8)
C(66)-C(67)-C(68)	117.4(5)	C(75')-C(73')-C(67')	112.3(8)
C(66)-C(67)-C(73)	123.3(6)	C(69')-C(76')-C(77')	113.6(12)
C(68)-C(67)-C(73)	119.3(6)	C(69')-C(76')-C(78')	111.6(12)
C(67)-C(68)-C(69)	122.3(6)	C(77')-C(76')-C(78')	110.6(14)
C(68)-C(69)-C(64)	120.2(6)	C(80)-C(79)-C(84)	115.1(12)
C(68)-C(69)-C(76)	117.9(6)	C(80)-C(79)-Sb(3)	123.5(11)
C(64)-C(69)-C(76)	121.8(6)	C(84)-C(79)-Sb(3)	121.4(11)
C(65)-C(70)-C(72)	112.5(7)	C(79)-C(80)-C(81)	119.3(18)
C(65)-C(70)-C(71)	110.9(7)	C(79)-C(80)-C(85)	123.9(15)
C(72)-C(70)-C(71)	110.3(7)	C(81)-C(80)-C(85)	111.3(14)
C(74)-C(73)-C(75)	111.1(6)	C(82)-C(81)-C(80)	119.4(13)
C(74)-C(73)-C(67)	111.8(5)	C(81)-C(82)-C(83)	116.3(11)
C(75)-C(73)-C(67)	112.6(5)	C(81)-C(82)-C(88)	120.6(11)
C(69)-C(76)-C(77)	111.7(7)	C(83)-C(82)-C(88)	123.2(12)
C(69)-C(76)-C(78)	111.7(7)	C(82)-C(83)-C(84)	123.4(13)
C(77)-C(76)-C(78)	109.9(9)	C(83)-C(84)-C(79)	119.5(13)
C(69')-C(64')-C(65')	119.4(11)	C(83)-C(84)-C(91)	119.5(13)
C(69')-C(64')-Sb(3)	119.4(10)	C(79)-C(84)-C(91)	120.5(13)
C(65')-C(64')-Sb(3)	119.8(10)	C(80)-C(85)-C(87)	109.8(17)
C(69')-C(64')-K(2)	103(2)	C(80)-C(85)-C(86)	107.9(15)
C(65')-C(64')-K(2)	106(2)	C(87)-C(85)-C(86)	111.2(16)
Sb(3)-C(64')-K(2)	71.6(11)	C(90)-C(88)-C(89)	110.2(16)
C(66')-C(65')-C(64')	118.4(10)	C(90)-C(88)-C(82)	112.8(15)
C(66')-C(65')-C(70')	118.1(10)	C(89)-C(88)-C(82)	112.2(11)
C(64')-C(65')-C(70')	123.4(11)	C(92)-C(91)-C(93)	112.3(17)

C(92)-C(91)-C(84)	111.5(15)	C(2I)-C(3I)-C(4I)	119(2)
C(93)-C(91)-C(84)	113.6(16)	C(3I)-C(4I)-C(5I)	121(2)
C(84')-C(79')-C(80')	119.1(4)	C(6I)-C(5I)-C(4I)	117(2)
C(84')-C(79')-Sb(3)	120.7(3)	C(3J)-C(2J)-C(1J)	102.4(15)
C(80')-C(79')-Sb(3)	120.0(4)	C(2J)-C(3J)-C(4J)	114.0(15)
C(79')-C(80')-C(81')	118.1(5)	C(5J)-C(4J)-C(3J)	116.8(14)
C(79')-C(80')-C(85')	122.8(4)	C(6J)-C(5J)-C(4J)	115.4(13)
C(81')-C(80')-C(85')	118.8(4)	C(1K)-C(2K)-C(3K)	136(2)
C(82')-C(81')-C(80')	122.6(4)	C(2K)-C(3K)-C(4K)	101.1(16)
C(81')-C(82')-C(83')	117.7(3)	C(5K)-C(4K)-C(3K)	126(2)
C(81')-C(82')-C(88')	122.6(4)	C(4K)-C(5K)-C(6K)	131(2)
C(83')-C(82')-C(88')	119.6(4)	C(1L)-C(2L)-C(3L)	116(2)
C(82')-C(83')-C(84')	122.1(4)	C(2L)-C(3L)-C(4L)	111(2)
C(83')-C(84')-C(79')	119.9(4)	C(5L)-C(4L)-C(3L)	117(2)
C(83')-C(84')-C(91')	117.1(4)	C(4L)-C(5L)-C(6L)	125(3)
C(79')-C(84')-C(91')	123.1(4)		
C(80')-C(85')-C(86')	111.8(5)		
C(80')-C(85')-C(87')	113.0(5)		
C(86')-C(85')-C(87')	111.6(5)		
C(89')-C(88')-C(82')	110.3(4)		
C(89')-C(88')-C(90')	111.6(5)		
C(82')-C(88')-C(90')	111.3(4)		
C(84')-C(91')-C(92')	110.6(4)		
C(84')-C(91')-C(93')	113.0(5)		
C(92')-C(91')-C(93')	110.6(5)		
C(1F)-C(2F)-C(3F)	116.5(13)		
C(2F)-C(3F)-C(4F)	118.6(11)		
C(5F)-C(4F)-C(3F)	119.5(12)		
C(4F)-C(5F)-C(6F)	119.5(11)		
C(1G)-C(2G)-C(3G)	109.3(14)		
C(4G)-C(3G)-C(2G)	118.5(12)		
C(5G)-C(4G)-C(3G)	120.1(11)		
C(6G)-C(5G)-C(4G)	119.0(12)		
C(3H)-C(2H)-C(1H)	119.8(19)		
C(4H)-C(3H)-C(2H)	122.0(18)		
C(3H)-C(4H)-C(5H)	168(2)		
C(4H)-C(5H)-C(6H)	136(2)		
C(3I)-C(2I)-C(1I)	117(2)		

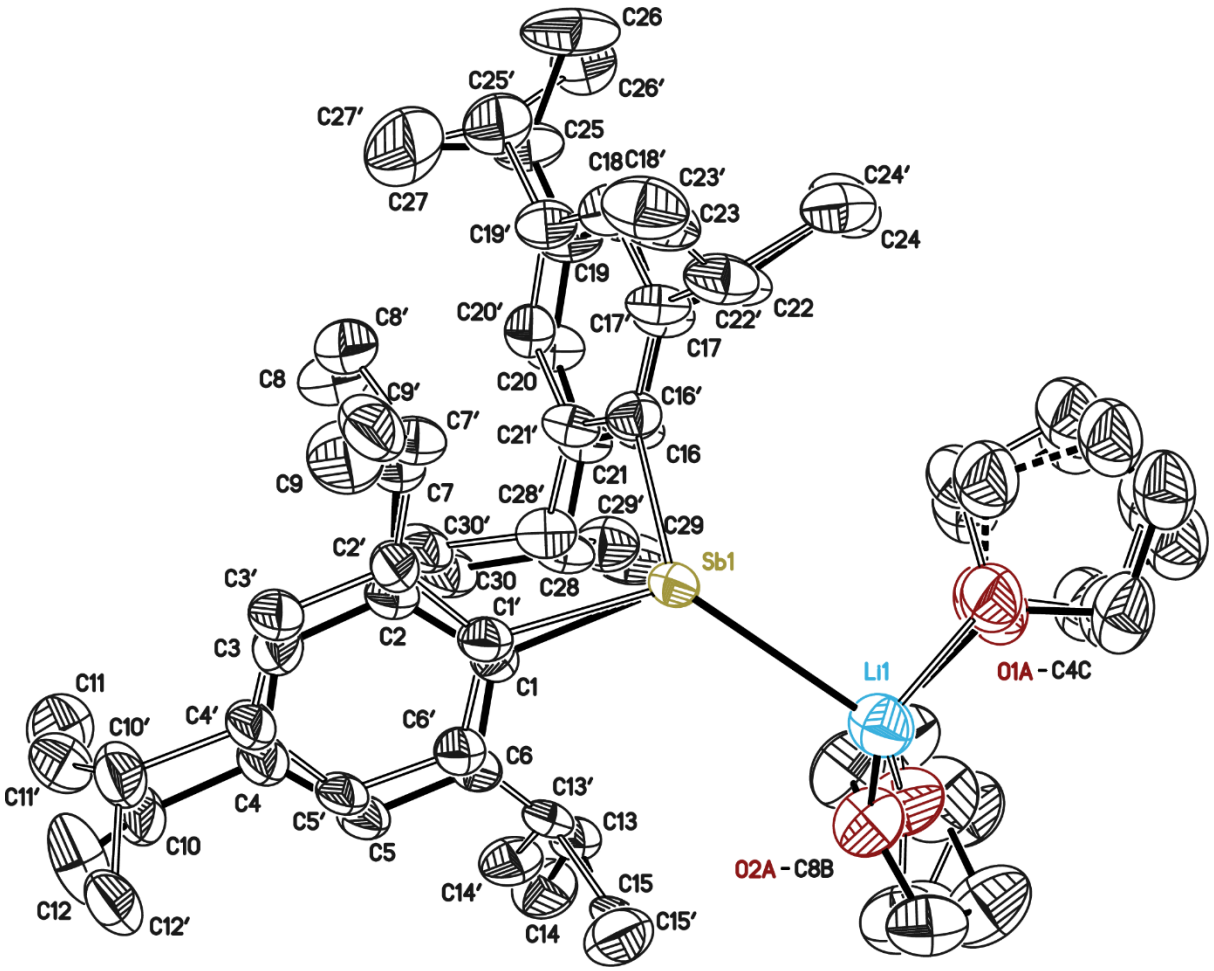

Figure S60: Asymmetric unit of **14**. The anisotropic displacement parameters are depicted at the 50% probability level. The hydrogen atoms are omitted for clarity.

Both tri(isopropyl)phenyl substituents and one THF molecule are disordered about two positions. They were refined with distance restraints and constraints for the anisotropic displacement parameters. The occupancies of the minor positions of the substituents refined to 0.085(4) (C1′-15′) and 0.188(7) (C16′-C30′), the occupancy of the minor position (O2B-C8B) of the THF molecule refined to 0.280(8).

The second THF molecule is disordered about 3 positions It was refined with distance restraints and restraints for the anisotropic displacement parameters. The sum of the occupancies of all three positions was restrained to be one. The occupancies refined to 0.532(3) (O1A-C4A), 0.346(3) (O1B-C4B) and 0.122(3) (O1C-C4C).

Table S22. Bond lengths [Å] and angles [°] for **14**.

Li(1)-O(2B)	1.893(10)	Li(1)-O(1C)	1.978(13)
Li(1)-O(1A)	1.955(7)	Li(1)-Sb(1)	2.916(4)
Li(1)-O(1B)	1.966(10)	Li(1)-Sb(1)#1	3.014(4)
Li(1)-O(2A)	1.967(5)	Sb(1)-C(1)	2.193(2)

Sb(1)-C(1')	2.207(14)	C(19)-C(25)	1.527(3)
Sb(1)-C(16)	2.209(3)	C(20)-C(21)	1.395(4)
Sb(1)-C(16')	2.215(13)	C(21)-C(28)	1.524(4)
C(1)-C(2)	1.411(3)	C(22)-C(23)	1.526(5)
C(1)-C(6)	1.419(3)	C(22)-C(24)	1.534(5)
C(2)-C(3)	1.397(3)	C(25)-C(26)	1.521(4)
C(2)-C(7)	1.528(3)	C(25)-C(27)	1.523(7)
C(3)-C(4)	1.389(3)	C(28)-C(29)	1.529(4)
C(4)-C(5)	1.384(3)	C(28)-C(30)	1.531(5)
C(4)-C(10)	1.519(3)	C(16')-C(17')	1.394(12)
C(5)-C(6)	1.395(3)	C(16')-C(21')	1.408(12)
C(6)-C(13)	1.524(3)	C(17')-C(18')	1.406(12)
C(7)-C(8)	1.525(4)	C(17')-C(22')	1.514(12)
C(7)-C(9)	1.527(4)	C(18')-C(19')	1.382(12)
C(10)-C(12)	1.510(4)	C(19')-C(20')	1.382(11)
C(10)-C(11)	1.529(4)	C(19')-C(25')	1.536(11)
C(13)-C(14)	1.525(3)	C(20')-C(21')	1.402(12)
C(13)-C(15)	1.534(3)	C(21')-C(28')	1.508(12)
C(1')-C(2')	1.396(12)	C(22')-C(23')	1.524(13)
C(1')-C(6')	1.400(12)	C(22')-C(24')	1.530(14)
C(2')-C(3')	1.402(13)	C(25')-C(26')	1.492(12)
C(2')-C(7')	1.512(13)	C(25')-C(27')	1.504(13)
C(3')-C(4')	1.379(12)	C(28')-C(29')	1.512(13)
C(4')-C(5')	1.375(12)	C(28')-C(30')	1.525(13)
C(4')-C(10')	1.531(13)	O(1A)-C(4A)	1.434(9)
C(5')-C(6')	1.408(13)	O(1A)-C(1A)	1.440(9)
C(6')-C(13')	1.501(13)	C(1A)-C(2A)	1.483(7)
C(7')-C(9')	1.529(14)	C(2A)-C(3A)	1.525(7)
C(7')-C(8')	1.538(14)	C(3A)-C(4A)	1.474(8)
C(10')-C(11')	1.497(14)	O(1B)-C(4B)	1.428(12)
C(10')-C(12')	1.522(14)	O(1B)-C(1B)	1.447(10)
C(13')-C(15')	1.513(14)	C(1B)-C(2B)	1.499(9)
C(13')-C(14')	1.527(14)	C(2B)-C(3B)	1.500(10)
C(16)-C(17)	1.409(4)	C(3B)-C(4B)	1.510(11)
C(16)-C(21)	1.419(4)	O(1C)-C(1C)	1.429(14)
C(17)-C(18)	1.397(4)	O(1C)-C(4C)	1.454(13)
C(17)-C(22)	1.529(4)	C(1C)-C(2C)	1.504(14)
C(18)-C(19)	1.378(4)	C(2C)-C(3C)	1.486(15)
C(19)-C(20)	1.387(4)	C(3C)-C(4C)	1.520(14)

O(2A)-C(5A)	1.419(5)	C(4)-C(3)-C(2)	122.24(19)
O(2A)-C(8A)	1.431(6)	C(5)-C(4)-C(3)	117.49(17)
C(5A)-C(6A)	1.460(6)	C(5)-C(4)-C(10)	121.14(18)
C(6A)-C(7A)	1.553(8)	C(3)-C(4)-C(10)	121.37(19)
C(7A)-C(8A)	1.476(7)	C(4)-C(5)-C(6)	122.32(18)
O(2B)-C(8B)	1.426(13)	C(5)-C(6)-C(1)	120.08(18)
O(2B)-C(5B)	1.450(11)	C(5)-C(6)-C(13)	117.69(18)
C(5B)-C(6B)	1.499(12)	C(1)-C(6)-C(13)	122.23(18)
C(6B)-C(7B)	1.513(14)	C(8)-C(7)-C(9)	111.0(2)
C(7B)-C(8B)	1.493(13)	C(8)-C(7)-C(2)	111.8(2)
		C(9)-C(7)-C(2)	111.8(2)
O(2B)-Li(1)-O(1B)	96.6(8)	C(12)-C(10)-C(4)	111.8(2)
O(1A)-Li(1)-O(2A)	104.8(5)	C(12)-C(10)-C(11)	110.7(3)
O(2B)-Li(1)-Sb(1)	127.7(5)	C(4)-C(10)-C(11)	110.9(2)
O(1A)-Li(1)-Sb(1)	103.6(3)	C(6)-C(13)-C(14)	113.6(2)
O(1B)-Li(1)-Sb(1)	98.1(4)	C(6)-C(13)-C(15)	110.4(2)
O(2A)-Li(1)-Sb(1)	118.8(2)	C(14)-C(13)-C(15)	110.3(3)
O(1C)-Li(1)-Sb(1)	101.3(7)	C(2')-C(1')-C(6')	121.6(12)
O(2B)-Li(1)-Sb(1)#1	130.2(4)	C(2')-C(1')-Sb(1)	120.3(10)
O(1A)-Li(1)-Sb(1)#1	107.8(5)	C(6')-C(1')-Sb(1)	117.8(11)
O(1B)-Li(1)-Sb(1)#1	105.6(7)	C(1')-C(2')-C(3')	117.7(13)
O(2A)-Li(1)-Sb(1)#1	126.5(2)	C(1')-C(2')-C(7')	124.7(14)
O(1C)-Li(1)-Sb(1)#1	116.9(8)	C(3')-C(2')-C(7')	117.3(13)
Sb(1)-Li(1)-Sb(1)#1	92.97(10)	C(4')-C(3')-C(2')	121.2(13)
C(1)-Sb(1)-C(16)	95.1(2)	C(5')-C(4')-C(3')	120.3(12)
C(1')-Sb(1)-C(16')	91.9(16)	C(5')-C(4')-C(10')	120.1(14)
C(1)-Sb(1)-Li(1)	121.20(10)	C(3')-C(4')-C(10')	119.1(14)
C(1')-Sb(1)-Li(1)	128.5(6)	C(4')-C(5')-C(6')	120.3(13)
C(16)-Sb(1)-Li(1)	119.3(2)	C(1')-C(6')-C(5')	118.5(12)
C(16')-Sb(1)-Li(1)	123.9(11)	C(1')-C(6')-C(13')	122.4(14)
C(1)-Sb(1)-Li(1)#1	95.47(13)	C(5')-C(6')-C(13')	118.7(14)
C(16)-Sb(1)-Li(1)#1	139.88(13)	C(2')-C(7')-C(9')	113.0(16)
Li(1)-Sb(1)-Li(1)#1	87.03(10)	C(2')-C(7')-C(8')	110.1(16)
C(2)-C(1)-C(6)	117.63(17)	C(9')-C(7')-C(8')	108.4(18)
C(2)-C(1)-Sb(1)	120.41(15)	C(11')-C(10')-C(12')	116.5(19)
C(6)-C(1)-Sb(1)	121.88(15)	C(11')-C(10')-C(4')	114.0(19)
C(3)-C(2)-C(1)	120.17(19)	C(12')-C(10')-C(4')	110.5(15)
C(3)-C(2)-C(7)	116.73(19)	C(6')-C(13')-C(15')	115.7(19)
C(1)-C(2)-C(7)	123.10(18)	C(6')-C(13')-C(14')	117.8(16)

C(15')-C(13')-C(14')	110.4(18)	C(17')-C(22')-C(24')	109.9(15)
C(17)-C(16)-C(21)	117.6(3)	C(23')-C(22')-C(24')	108.4(16)
C(17)-C(16)-Sb(1)	121.3(2)	C(26')-C(25')-C(27')	114.7(14)
C(21)-C(16)-Sb(1)	121.0(2)	C(26')-C(25')-C(19')	111.9(11)
C(18)-C(17)-C(16)	120.6(3)	C(27')-C(25')-C(19')	115.6(13)
C(18)-C(17)-C(22)	116.7(3)	C(21')-C(28')-C(29')	113.6(15)
C(16)-C(17)-C(22)	122.7(3)	C(21')-C(28')-C(30')	111.5(12)
C(19)-C(18)-C(17)	122.1(3)	C(29')-C(28')-C(30')	111.0(14)
C(18)-C(19)-C(20)	117.0(2)	C(4A)-O(1A)-C(1A)	107.5(5)
C(18)-C(19)-C(25)	123.2(3)	C(4A)-O(1A)-Li(1)	129.7(7)
C(20)-C(19)-C(25)	119.8(2)	C(1A)-O(1A)-Li(1)	122.9(6)
C(19)-C(20)-C(21)	123.3(3)	O(1A)-C(1A)-C(2A)	107.4(5)
C(20)-C(21)-C(16)	119.1(3)	C(1A)-C(2A)-C(3A)	104.9(4)
C(20)-C(21)-C(28)	117.0(3)	C(4A)-C(3A)-C(2A)	101.4(4)
C(16)-C(21)-C(28)	123.8(3)	O(1A)-C(4A)-C(3A)	107.2(6)
C(23)-C(22)-C(17)	110.6(4)	C(4B)-O(1B)-C(1B)	108.9(8)
C(23)-C(22)-C(24)	110.4(4)	C(4B)-O(1B)-Li(1)	124.0(8)
C(17)-C(22)-C(24)	112.2(3)	C(1B)-O(1B)-Li(1)	126.7(8)
C(26)-C(25)-C(27)	110.0(5)	O(1B)-C(1B)-C(2B)	106.8(7)
C(26)-C(25)-C(19)	113.9(3)	C(1B)-C(2B)-C(3B)	102.8(6)
C(27)-C(25)-C(19)	109.6(4)	C(2B)-C(3B)-C(4B)	104.2(7)
C(21)-C(28)-C(29)	110.3(3)	O(1B)-C(4B)-C(3B)	107.1(8)
C(21)-C(28)-C(30)	112.7(3)	C(1C)-O(1C)-C(4C)	106.6(11)
C(29)-C(28)-C(30)	110.9(4)	C(1C)-O(1C)-Li(1)	112.1(13)
C(17')-C(16')-C(21')	117.6(11)	C(4C)-O(1C)-Li(1)	135.7(16)
C(17')-C(16')-Sb(1)	122.9(10)	O(1C)-C(1C)-C(2C)	108.6(12)
C(21')-C(16')-Sb(1)	119.2(10)	C(3C)-C(2C)-C(1C)	101.9(12)
C(16')-C(17')-C(18')	119.6(12)	C(2C)-C(3C)-C(4C)	101.6(12)
C(16')-C(17')-C(22')	123.4(13)	O(1C)-C(4C)-C(3C)	102.6(13)
C(18')-C(17')-C(22')	116.3(12)	C(5A)-O(2A)-C(8A)	106.9(4)
C(19')-C(18')-C(17')	122.6(12)	C(5A)-O(2A)-Li(1)	119.4(4)
C(20')-C(19')-C(18')	118.0(10)	C(8A)-O(2A)-Li(1)	127.3(4)
C(20')-C(19')-C(25')	121.1(10)	O(2A)-C(5A)-C(6A)	107.0(4)
C(18')-C(19')-C(25')	120.9(10)	C(5A)-C(6A)-C(7A)	105.2(5)
C(19')-C(20')-C(21')	120.5(11)	C(8A)-C(7A)-C(6A)	103.8(4)
C(20')-C(21')-C(16')	121.5(11)	O(2A)-C(8A)-C(7A)	107.6(4)
C(20')-C(21')-C(28')	114.9(11)	C(8B)-O(2B)-C(5B)	105.3(9)
C(16')-C(21')-C(28')	123.5(12)	C(8B)-O(2B)-Li(1)	130.9(9)
C(17')-C(22')-C(23')	115.6(16)	C(5B)-O(2B)-Li(1)	122.1(9)

O(2B)-C(5B)-C(6B)	102.3(10)	C(8B)-C(7B)-C(6B)	102.2(11)
C(5B)-C(6B)-C(7B)	98.3(10)	O(2B)-C(8B)-C(7B)	107.6(10)

Symmetry transformations used to generate equivalent atoms:
#1 -x+1,-y+1,-z+1

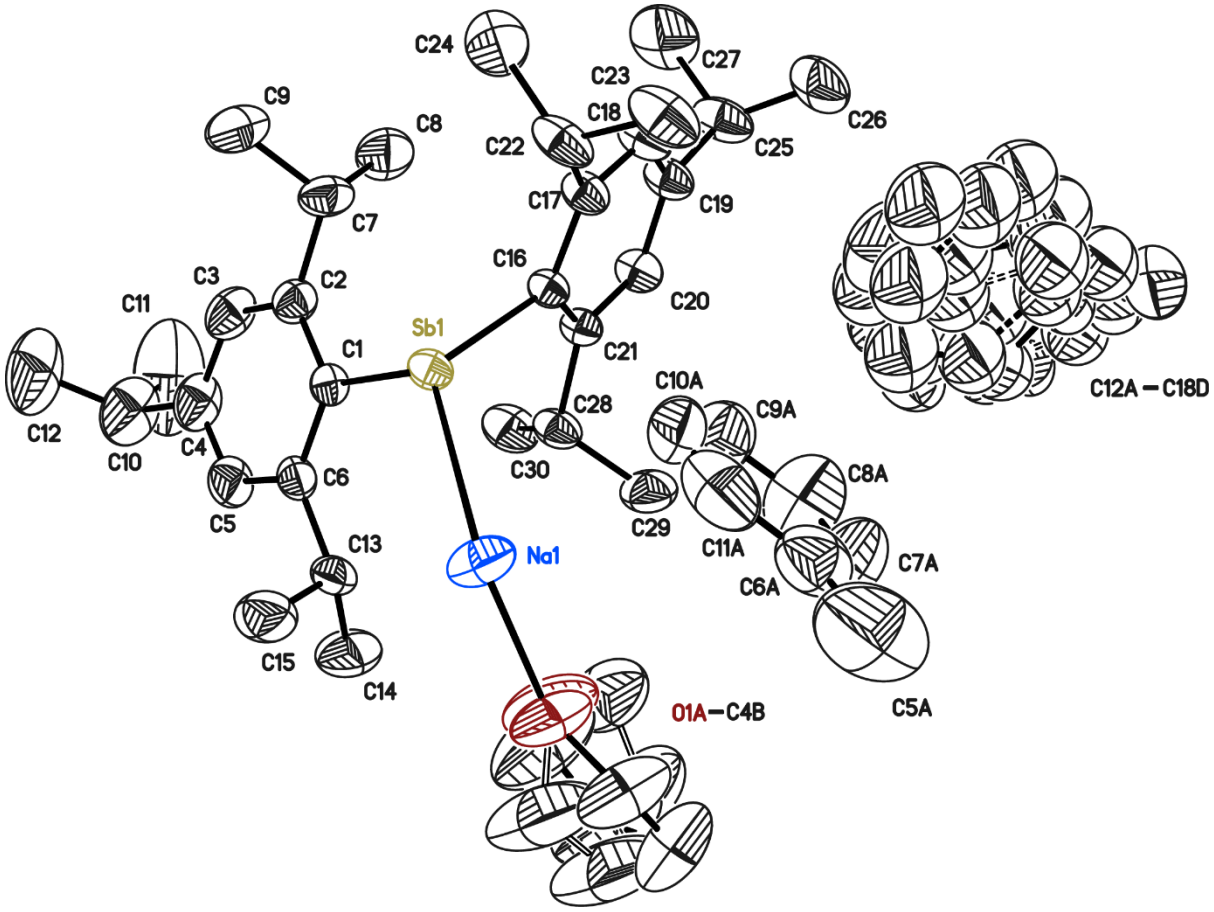

Figure S61: Asymmetric unit of **15**. The anisotropic displacement parameters are depicted at the 50% probability level. The hydrogen atoms are omitted for clarity.

The THF molecule is disordered about two positions. It was refined with distance restraints and constraints for the anisotropic displacement parameters. The occupancy of the minor position (O1B-C4B) refined to 0.408(12).

One toluene molecule is disordered about 4 positions It was refined with distance restraints and restraints for the anisotropic displacement parameters. The sum of the occupancies of all four positions was restrained to be one. The occupancies refined to 0.367(3) (C12A-C18A), 0.234(3) (C12D-C18D), 0.220(3) (C12C-C18C) and 0.179(3) (C12B-C18B).

Table S23. Bond lengths [Å] and bond angles [°] of complex **15**

Sb(1)-C(1)	2.195(2)	O(1A)-C(1A)	1.413(11)
Sb(1)-C(16)	2.197(2)	O(1A)-C(4A)	1.419(11)
Sb(1)-Na(1)	3.1564(16)	C(1A)-C(2A)	1.413(10)
Sb(1)-Na(1)#1	3.1579(15)	C(2A)-C(3A)	1.535(15)
Na(1)-O(1B)	2.215(15)	C(3A)-C(4A)	1.371(11)
Na(1)-O(1A)	2.281(9)	O(1B)-C(1B)	1.417(13)
Na(1)-C(10A)	3.014(5)	O(1B)-C(4B)	1.422(13)
C(1)-C(2)	1.409(4)	C(1B)-C(2B)	1.401(13)
C(1)-C(6)	1.419(3)	C(2B)-C(3B)	1.540(18)
C(2)-C(3)	1.393(4)	C(3B)-C(4B)	1.365(13)
C(2)-C(7)	1.524(4)	C(5A)-C(6A)	1.496(6)
C(3)-C(4)	1.389(5)	C(6A)-C(7A)	1.363(6)
C(4)-C(5)	1.371(5)	C(6A)-C(11A)	1.404(6)
C(4)-C(10)	1.521(4)	C(7A)-C(8A)	1.359(6)
C(5)-C(6)	1.394(4)	C(8A)-C(9A)	1.333(6)
C(6)-C(13)	1.515(4)	C(9A)-C(10A)	1.353(6)
C(7)-C(9)	1.526(4)	C(10A)-C(11A)	1.391(6)
C(7)-C(8)	1.531(5)	C(12A)-C(13A)	1.451(13)
C(10)-C(11)	1.467(7)	C(13A)-C(14A)	1.374(12)
C(10)-C(12)	1.487(6)	C(13A)-C(18A)	1.379(12)
C(13)-C(15)	1.528(4)	C(14A)-C(15A)	1.349(12)
C(13)-C(14)	1.531(4)	C(15A)-C(16A)	1.398(12)
C(16)-C(17)	1.409(3)	C(16A)-C(17A)	1.385(12)
C(16)-C(21)	1.411(3)	C(17A)-C(18A)	1.351(12)
C(17)-C(18)	1.395(4)	C(12B)-C(13B)	1.467(16)
C(17)-C(22)	1.525(3)	C(13B)-C(14B)	1.375(13)
C(18)-C(19)	1.384(4)	C(13B)-C(18B)	1.385(13)
C(19)-C(20)	1.377(4)	C(14B)-C(15B)	1.363(14)
C(19)-C(25)	1.524(4)	C(15B)-C(16B)	1.391(14)
C(20)-C(21)	1.395(3)	C(16B)-C(17B)	1.376(14)
C(21)-C(28)	1.524(3)	C(17B)-C(18B)	1.386(14)
C(22)-C(24)	1.517(5)	C(12C)-C(13C)	1.463(15)
C(22)-C(23)	1.519(5)	C(13C)-C(14C)	1.377(13)
C(25)-C(26)	1.515(5)	C(13C)-C(18C)	1.390(13)
C(25)-C(27)	1.518(5)	C(14C)-C(15C)	1.388(13)
C(28)-C(30)	1.517(4)	C(15C)-C(16C)	1.385(14)
C(28)-C(29)	1.535(4)	C(16C)-C(17C)	1.371(13)

C(17C)-C(18C)	1.381(13)	C(9)-C(7)-C(8)	110.6(3)
C(12D)-C(13D)	1.480(16)	C(11)-C(10)-C(12)	113.2(5)
C(13D)-C(14D)	1.376(13)	C(11)-C(10)-C(4)	112.7(4)
C(13D)-C(18D)	1.382(13)	C(12)-C(10)-C(4)	112.3(3)
C(14D)-C(15D)	1.359(13)	C(6)-C(13)-C(15)	112.1(2)
C(15D)-C(16D)	1.374(13)	C(6)-C(13)-C(14)	113.9(3)
C(16D)-C(17D)	1.372(13)	C(15)-C(13)-C(14)	110.2(3)
C(17D)-C(18D)	1.371(13)	C(17)-C(16)-C(21)	117.9(2)
		C(17)-C(16)-Sb(1)	121.45(17)
C(1)-Sb(1)-C(16)	95.98(9)	C(21)-C(16)-Sb(1)	120.42(17)
C(1)-Sb(1)-Na(1)	122.65(7)	C(18)-C(17)-C(16)	119.9(2)
C(16)-Sb(1)-Na(1)	122.39(7)	C(18)-C(17)-C(22)	117.3(2)
C(1)-Sb(1)-Na(1)#1	100.48(7)	C(16)-C(17)-C(22)	122.7(2)
C(16)-Sb(1)-Na(1)#1	124.28(7)	C(19)-C(18)-C(17)	122.2(2)
Na(1)-Sb(1)-Na(1)#1	91.38(4)	C(20)-C(19)-C(18)	117.4(2)
O(1B)-Na(1)-C(10A)	104.4(7)	C(20)-C(19)-C(25)	121.2(2)
O(1A)-Na(1)-C(10A)	104.6(4)	C(18)-C(19)-C(25)	121.4(2)
O(1B)-Na(1)-Sb(1)	120.5(4)	C(19)-C(20)-C(21)	122.7(2)
O(1A)-Na(1)-Sb(1)	125.5(3)	C(20)-C(21)-C(16)	119.6(2)
C(10A)-Na(1)-Sb(1)	85.52(11)	C(20)-C(21)-C(28)	117.3(2)
O(1A)-Na(1)-Sb(1)#1	141.8(3)	C(16)-C(21)-C(28)	123.0(2)
C(10A)-Na(1)-Sb(1)#1	93.57(10)	C(24)-C(22)-C(23)	110.5(3)
Sb(1)-Na(1)-Sb(1)#1	88.62(4)	C(24)-C(22)-C(17)	112.5(3)
C(2)-C(1)-C(6)	117.9(2)	C(23)-C(22)-C(17)	111.7(3)
C(2)-C(1)-Sb(1)	120.80(18)	C(26)-C(25)-C(27)	109.7(3)
C(6)-C(1)-Sb(1)	121.21(18)	C(26)-C(25)-C(19)	113.0(3)
C(3)-C(2)-C(1)	119.9(3)	C(27)-C(25)-C(19)	111.0(3)
C(3)-C(2)-C(7)	117.2(3)	C(30)-C(28)-C(21)	113.5(2)
C(1)-C(2)-C(7)	123.0(2)	C(30)-C(28)-C(29)	111.1(2)
C(4)-C(3)-C(2)	122.3(3)	C(21)-C(28)-C(29)	110.1(2)
C(5)-C(4)-C(3)	117.5(3)	C(1A)-O(1A)-C(4A)	107.0(7)
C(5)-C(4)-C(10)	120.8(3)	C(1A)-O(1A)-Na(1)	130.5(8)
C(3)-C(4)-C(10)	121.7(3)	C(4A)-O(1A)-Na(1)	121.2(8)
C(4)-C(5)-C(6)	122.8(3)	O(1A)-C(1A)-C(2A)	109.4(7)
C(5)-C(6)-C(1)	119.6(3)	C(1A)-C(2A)-C(3A)	105.1(7)
C(5)-C(6)-C(13)	118.3(2)	C(4A)-C(3A)-C(2A)	105.1(9)
C(1)-C(6)-C(13)	122.2(2)	C(3A)-C(4A)-O(1A)	111.8(9)
C(2)-C(7)-C(9)	111.8(3)	C(1B)-O(1B)-C(4B)	109.3(11)
C(2)-C(7)-C(8)	112.0(3)	C(1B)-O(1B)-Na(1)	130.9(10)

C(4B)-O(1B)-Na(1)	119.7(10)	C(14B)-C(13B)-C(12B)	120.9(17)
C(2B)-C(1B)-O(1B)	108.2(11)	C(18B)-C(13B)-C(12B)	121.1(18)
C(1B)-C(2B)-C(3B)	105.8(10)	C(15B)-C(14B)-C(13B)	119.6(17)
C(4B)-C(3B)-C(2B)	106.7(10)	C(14B)-C(15B)-C(16B)	122.5(18)
C(3B)-C(4B)-O(1B)	109.3(11)	C(17B)-C(16B)-C(15B)	118.1(17)
C(7A)-C(6A)-C(11A)	115.9(4)	C(16B)-C(17B)-C(18B)	118.8(17)
C(7A)-C(6A)-C(5A)	122.0(5)	C(13B)-C(18B)-C(17B)	122.5(17)
C(11A)-C(6A)-C(5A)	122.1(5)	C(14C)-C(13C)-C(18C)	120.5(15)
C(8A)-C(7A)-C(6A)	123.5(5)	C(14C)-C(13C)-C(12C)	122.3(17)
C(9A)-C(8A)-C(7A)	120.4(5)	C(18C)-C(13C)-C(12C)	117.2(17)
C(8A)-C(9A)-C(10A)	119.5(5)	C(13C)-C(14C)-C(15C)	122.2(16)
C(9A)-C(10A)-C(11A)	121.1(4)	C(16C)-C(15C)-C(14C)	115.7(16)
C(9A)-C(10A)-Na(1)	93.8(3)	C(17C)-C(16C)-C(15C)	122.9(17)
C(11A)-C(10A)-Na(1)	101.6(3)	C(16C)-C(17C)-C(18C)	120.2(17)
C(10A)-C(11A)-C(6A)	119.6(4)	C(17C)-C(18C)-C(13C)	118.1(16)
C(14A)-C(13A)-C(18A)	120.8(12)	C(14D)-C(13D)-C(18D)	119.2(15)
C(14A)-C(13A)-C(12A)	122.1(13)	C(14D)-C(13D)-C(12D)	124.9(18)
C(18A)-C(13A)-C(12A)	117.0(13)	C(18D)-C(13D)-C(12D)	114.8(17)
C(15A)-C(14A)-C(13A)	120.5(13)	C(15D)-C(14D)-C(13D)	120.7(16)
C(14A)-C(15A)-C(16A)	120.3(13)	C(14D)-C(15D)-C(16D)	118.8(16)
C(17A)-C(16A)-C(15A)	117.1(13)	C(17D)-C(16D)-C(15D)	120.2(16)
C(18A)-C(17A)-C(16A)	123.0(14)	C(18D)-C(17D)-C(16D)	117.9(17)
C(17A)-C(18A)-C(13A)	117.6(13)	C(17D)-C(18D)-C(13D)	118.0(16)
C(14B)-C(13B)-C(18B)	118.0(15)		

Symmetry transformations used to generate equivalent atoms:
#1 -x+1,-y+1,-z+1

S10. NMR and Mass spectra of compounds 1, 4, 6, 14-21

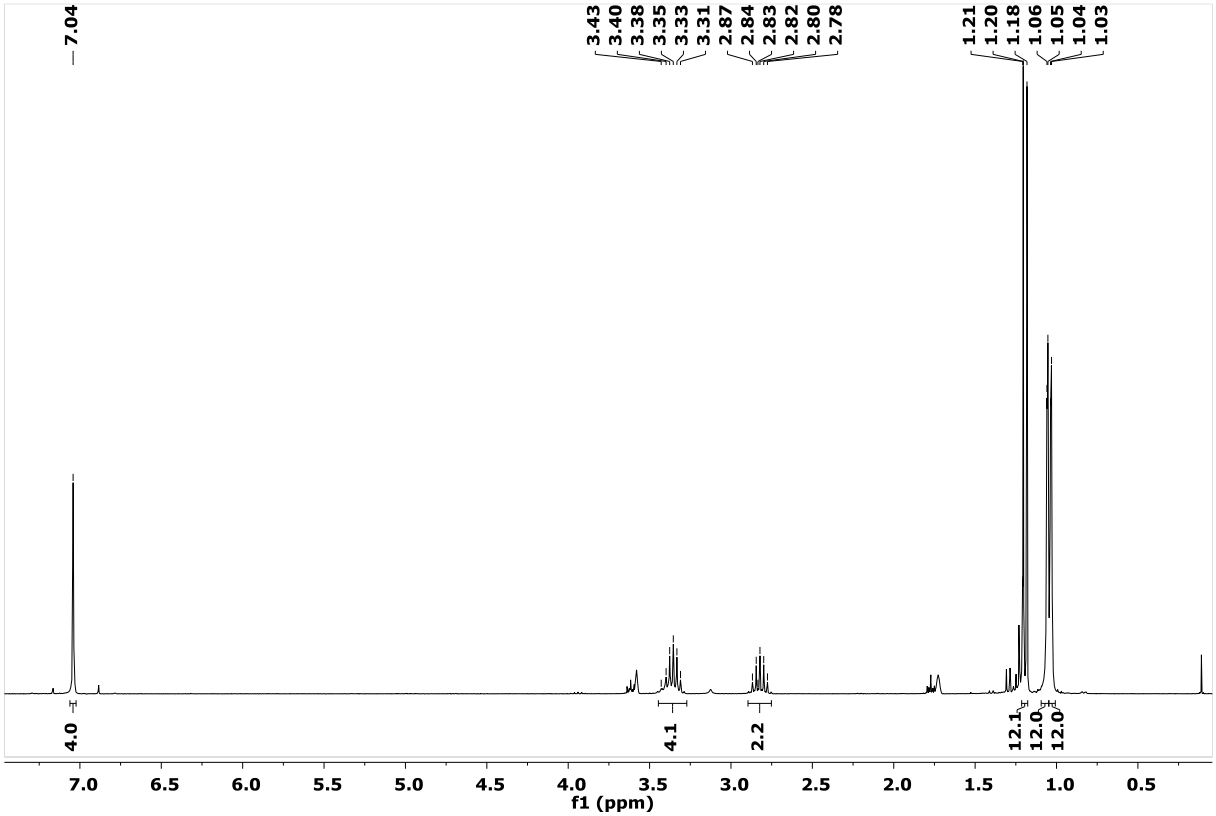

Figure S62: ^{1}H NMR spectrum of compound **1** (298 K, 300 MHz, THF-D_8).

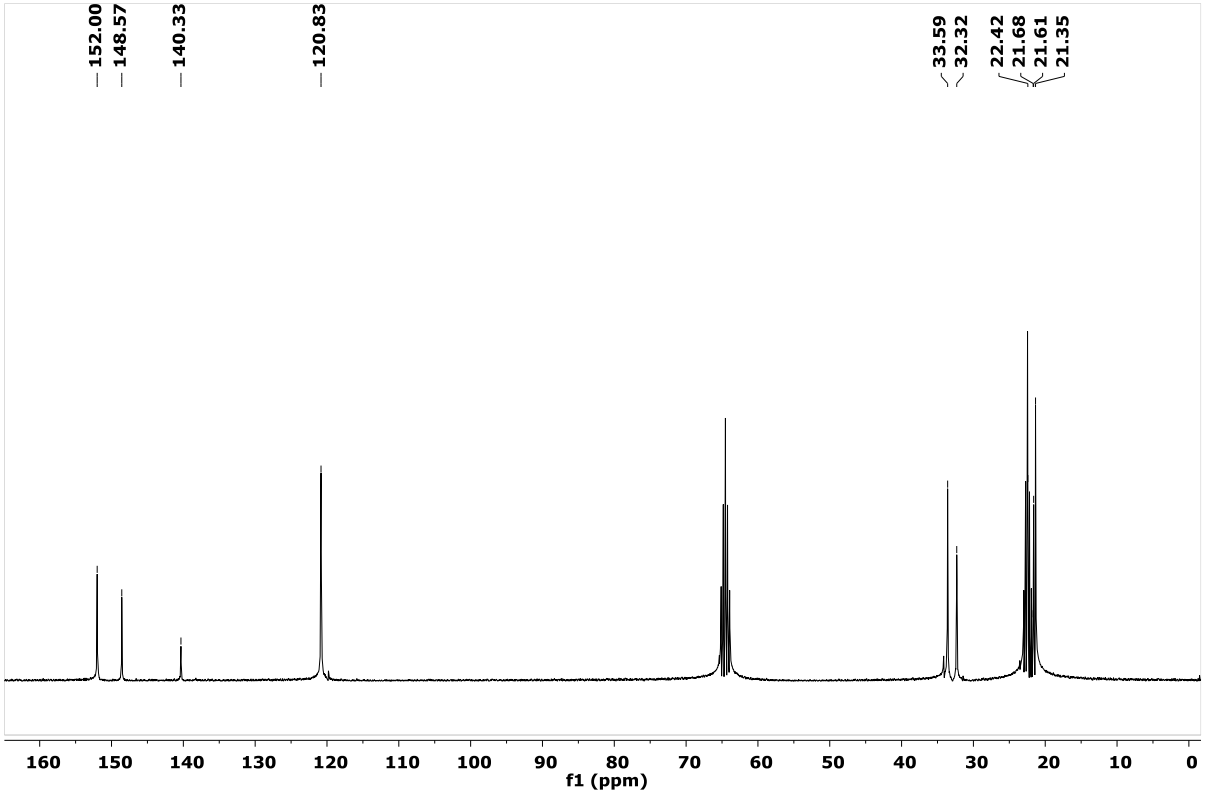

Figure S63: ^{13}C NMR Spectrum of compound **1** (298 K, 75 MHz, THF-D_8).

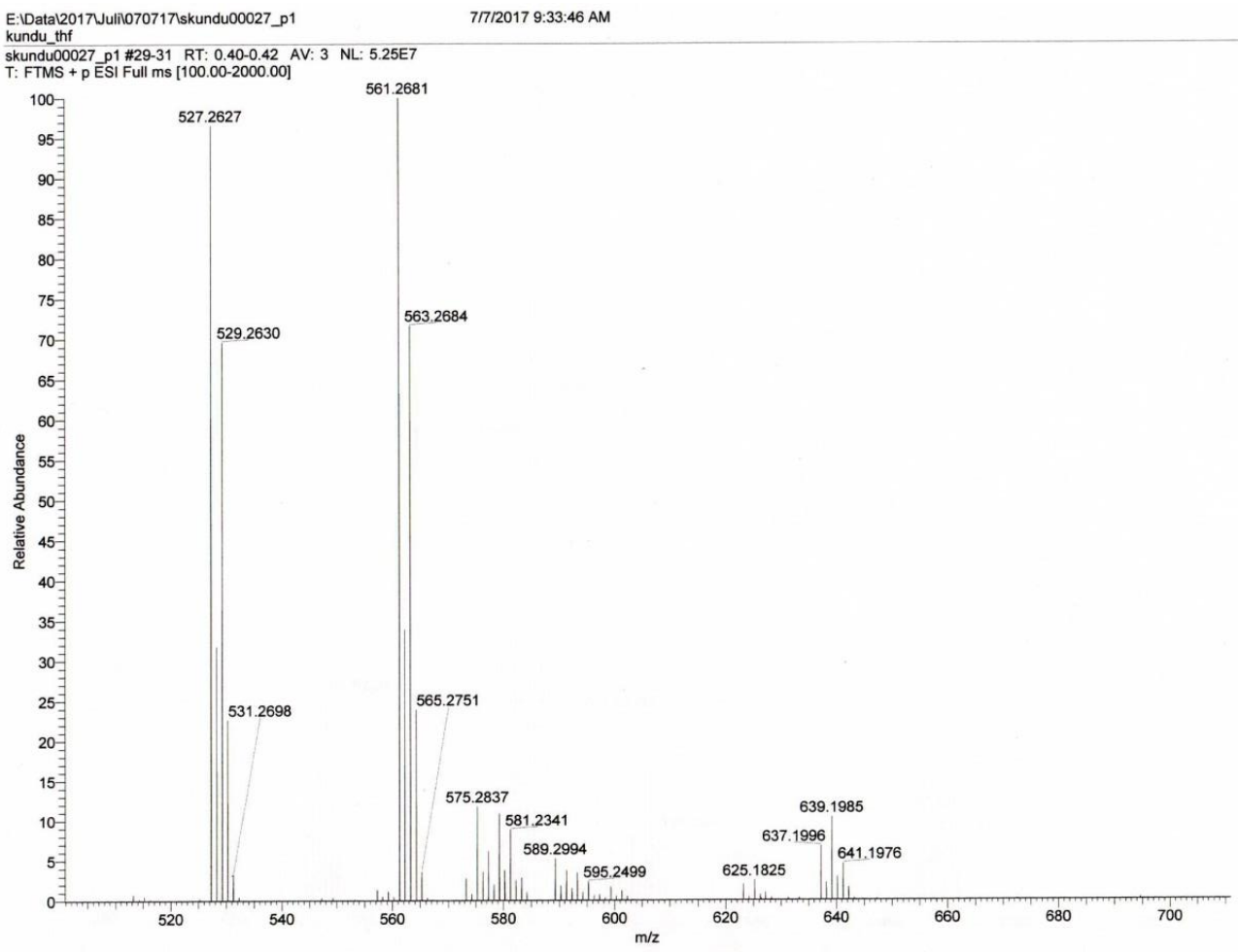

Figure S64: Experimental EI-MS spectrum of compound **1**.

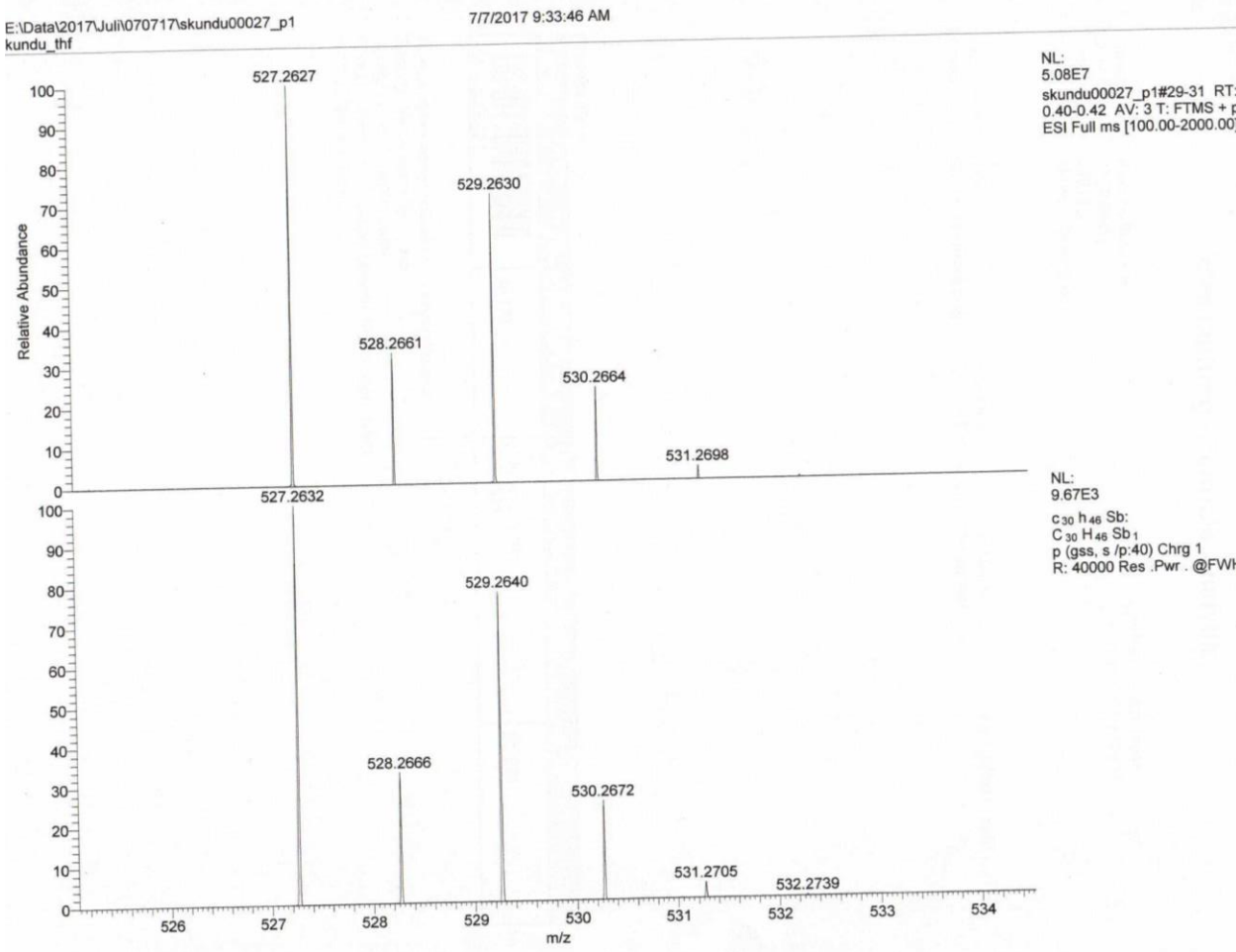

Figure S65: Experimental (top) and Simulated (bottom) Mass spectra of compound **1**.

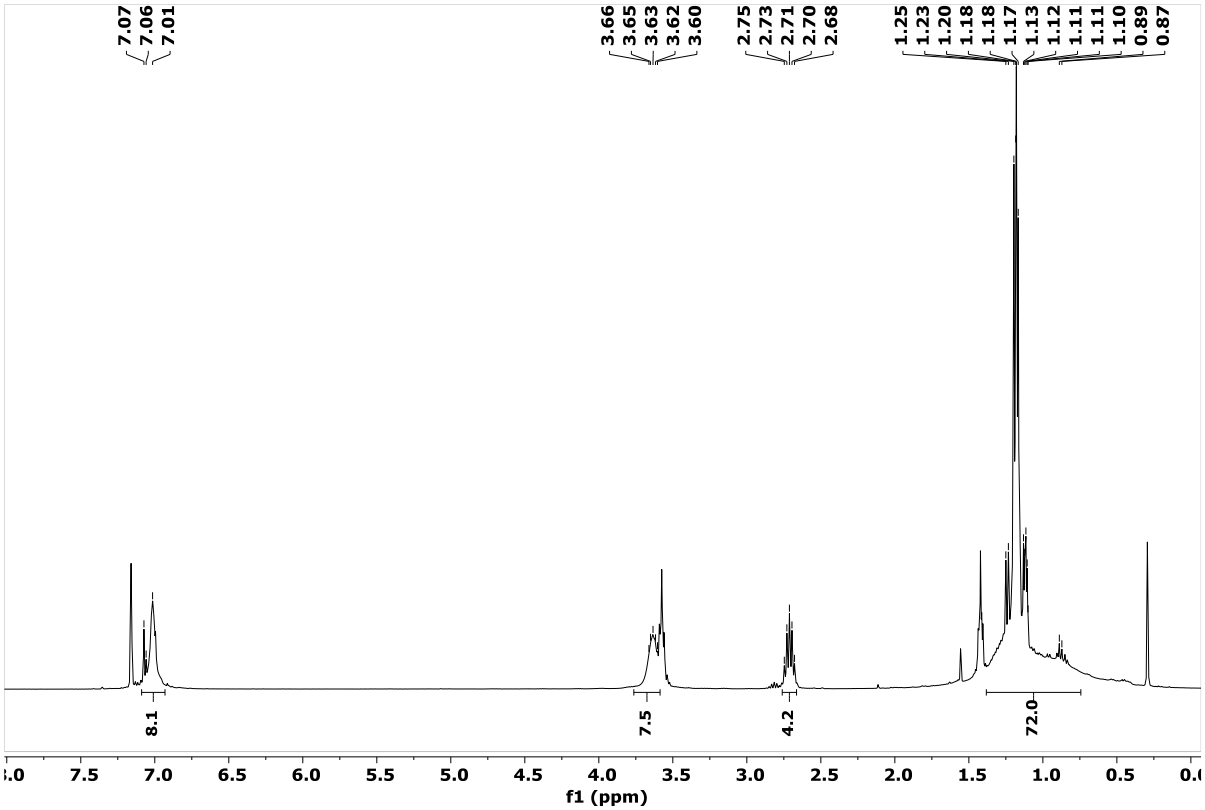

Figure S66: ^{1}H NMR spectrum of compound **4** (298 K, 400 MHz, C_6D_6).

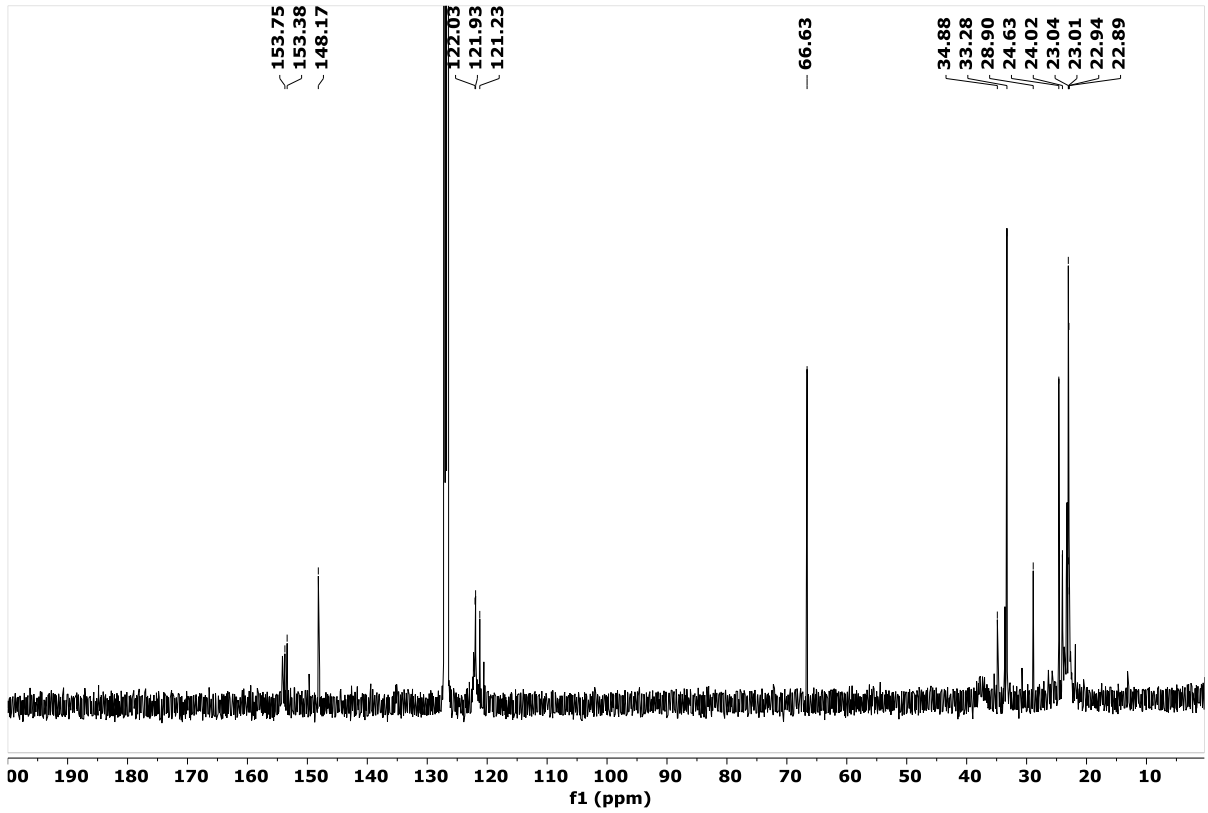

Figure S67: ^{13}C NMR spectrum of compound **4** (298 K, 101 MHz, C_6D_6).

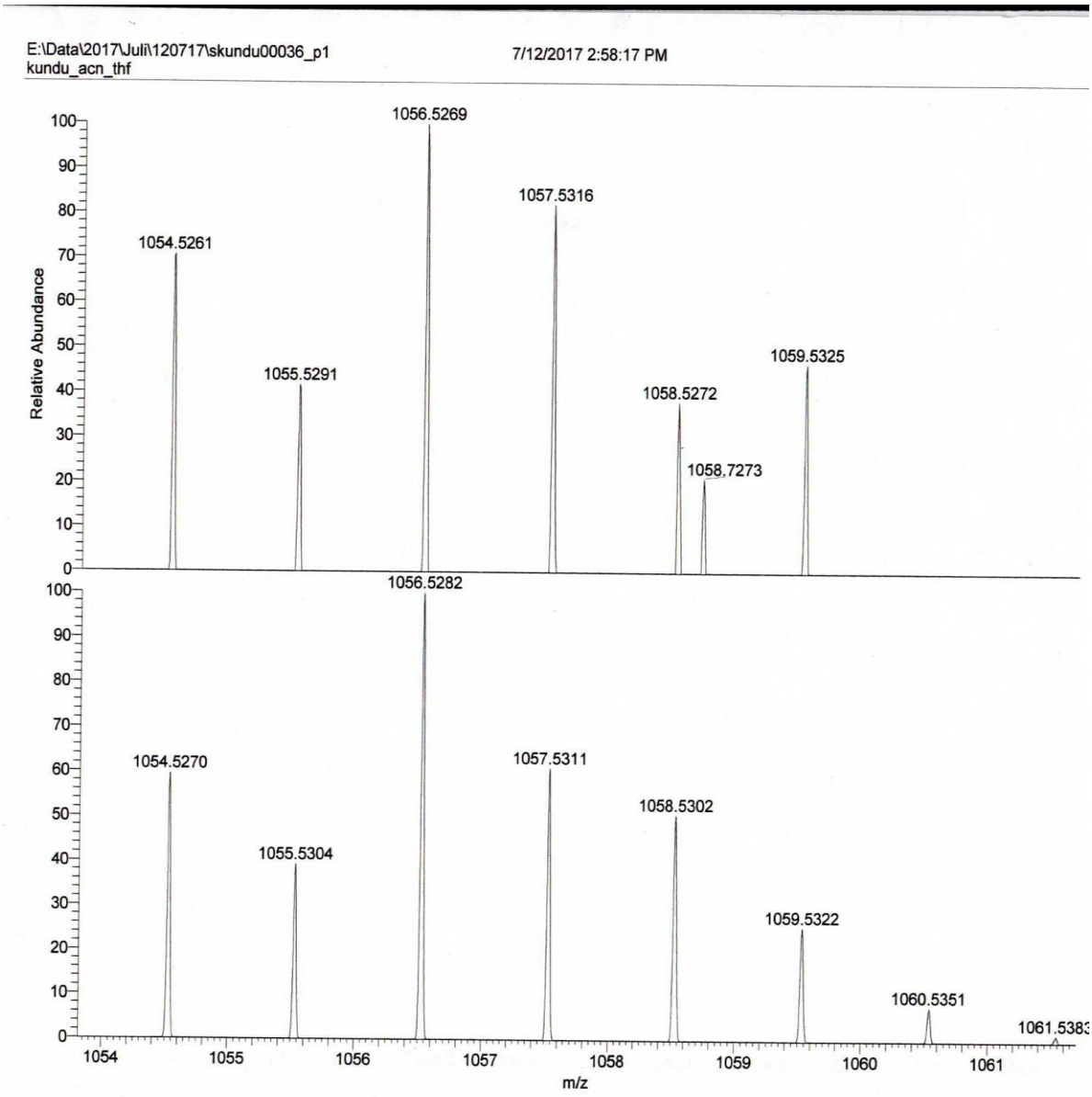

Figure S68: Experimental (top) and Simulated (bottom) mass spectra for [**4**]$^{+1}$.

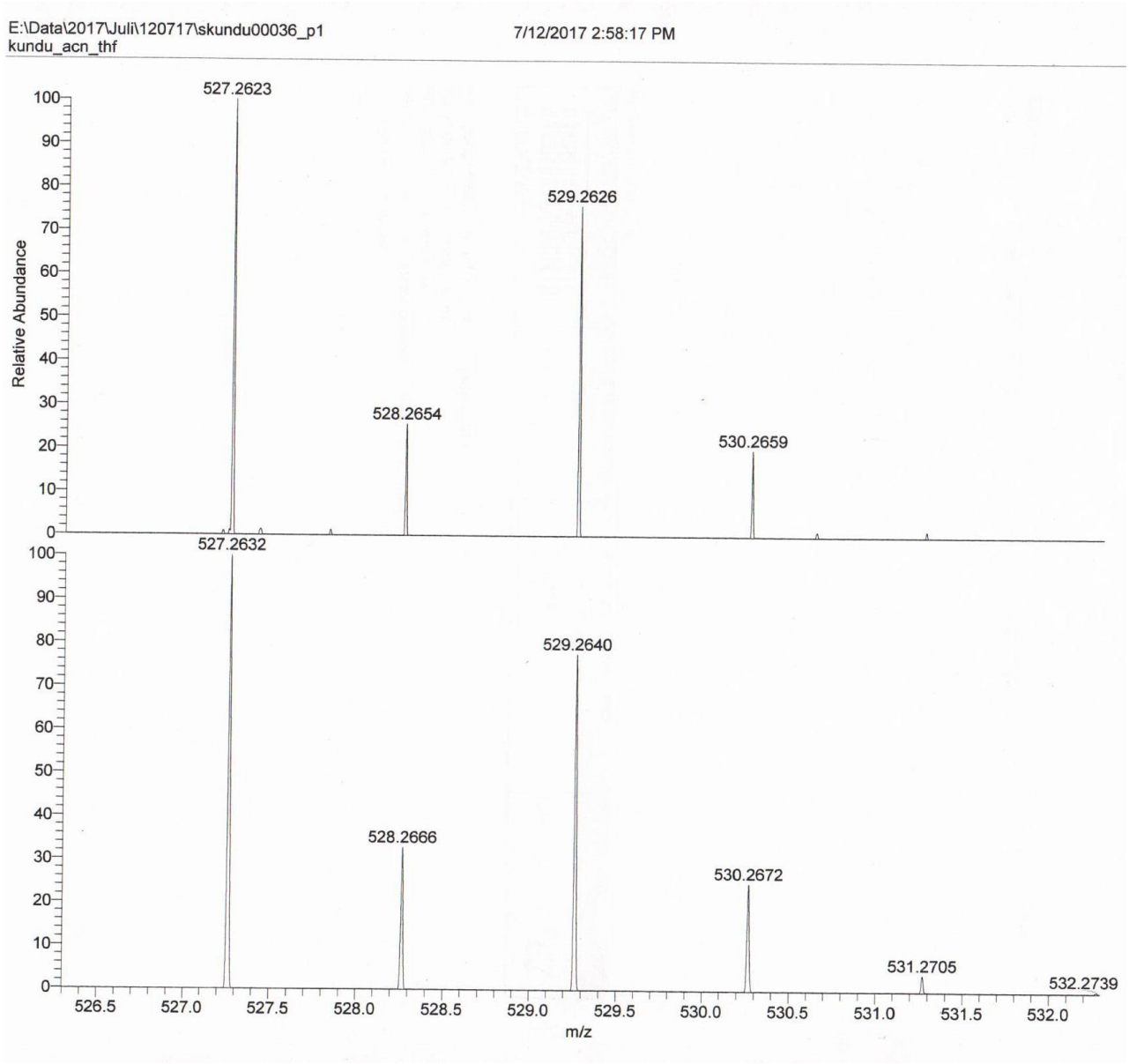

Figure S69: Experimental (top) and Simulated (bottom) mass spectra for [**4**]$^{+2}$.

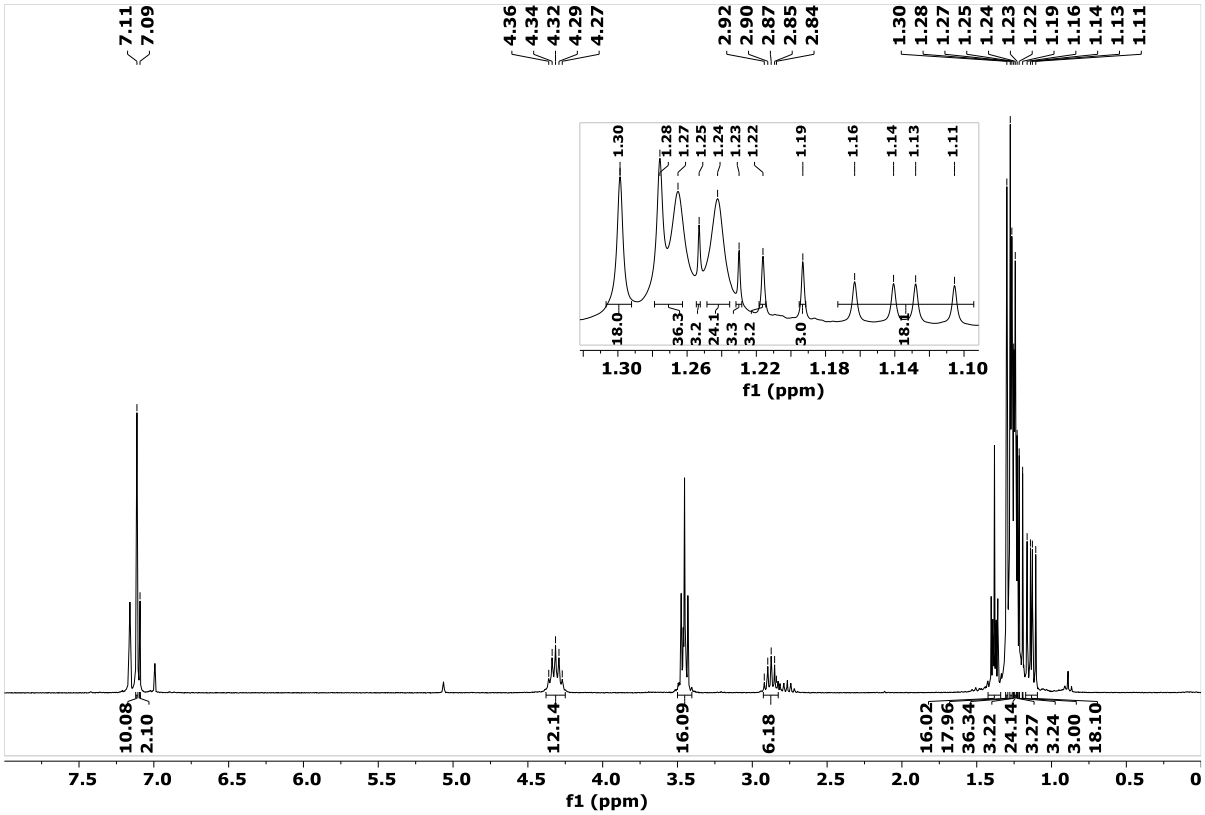

Figure S70: ^{1}H NMR spectrum of complex **6** (298 K, 400 MHz, C_6D_6).

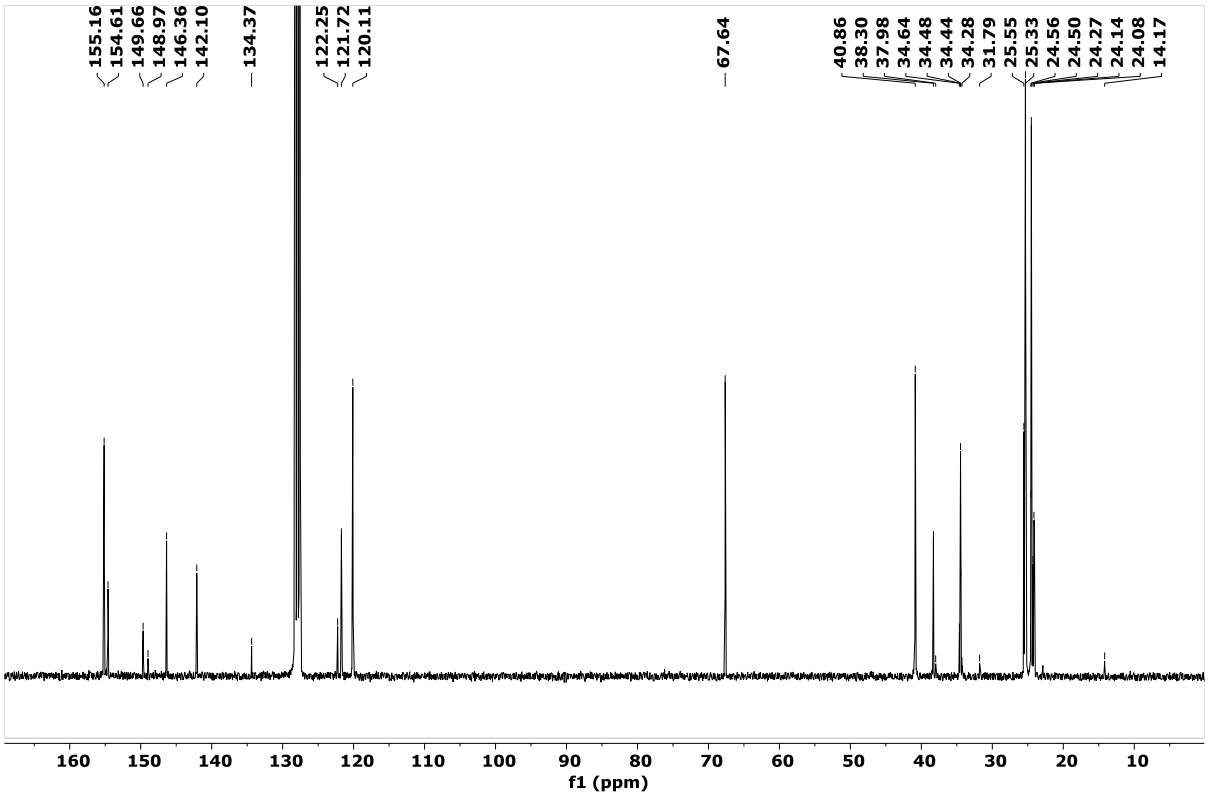

Figure S71: ^{13}C NMR spectrum of complex **6** (298 K, 101 MHz, C_6D_6).

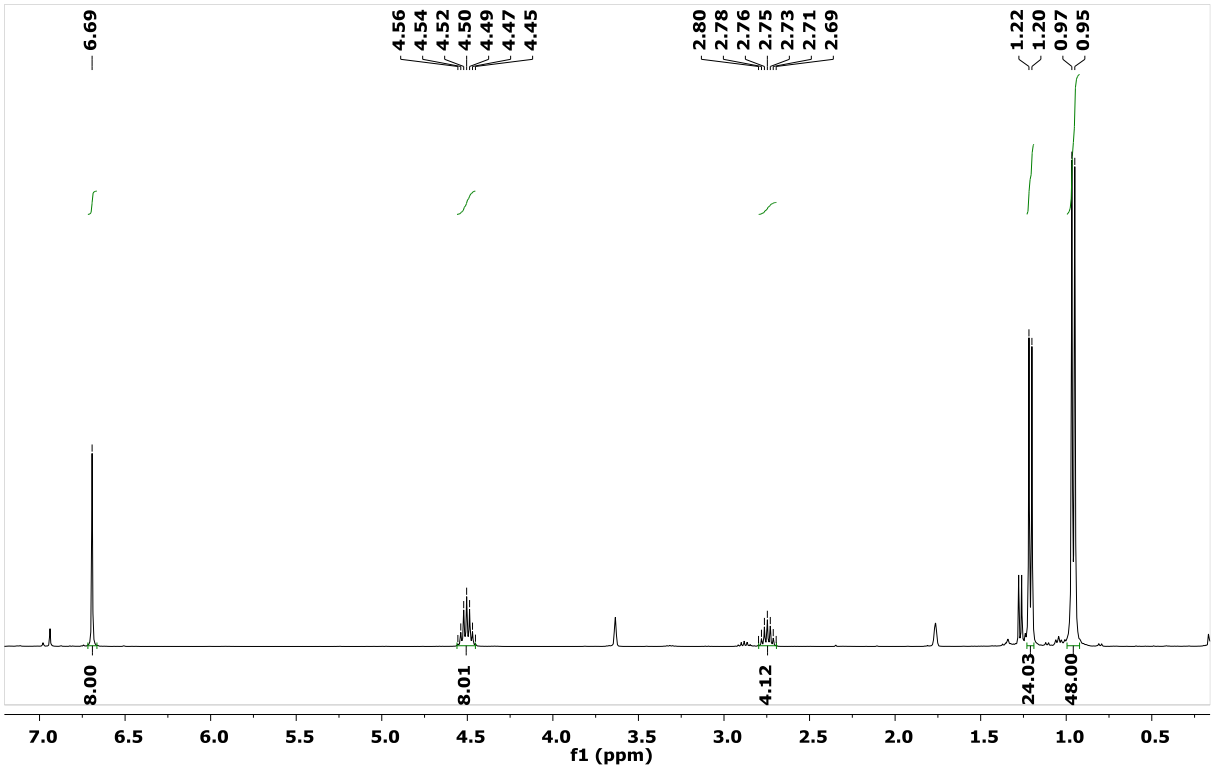

Figure S72. ^{1}H NMR spectra of complex **14** (298 K, 400 MHz, THF-D_8).

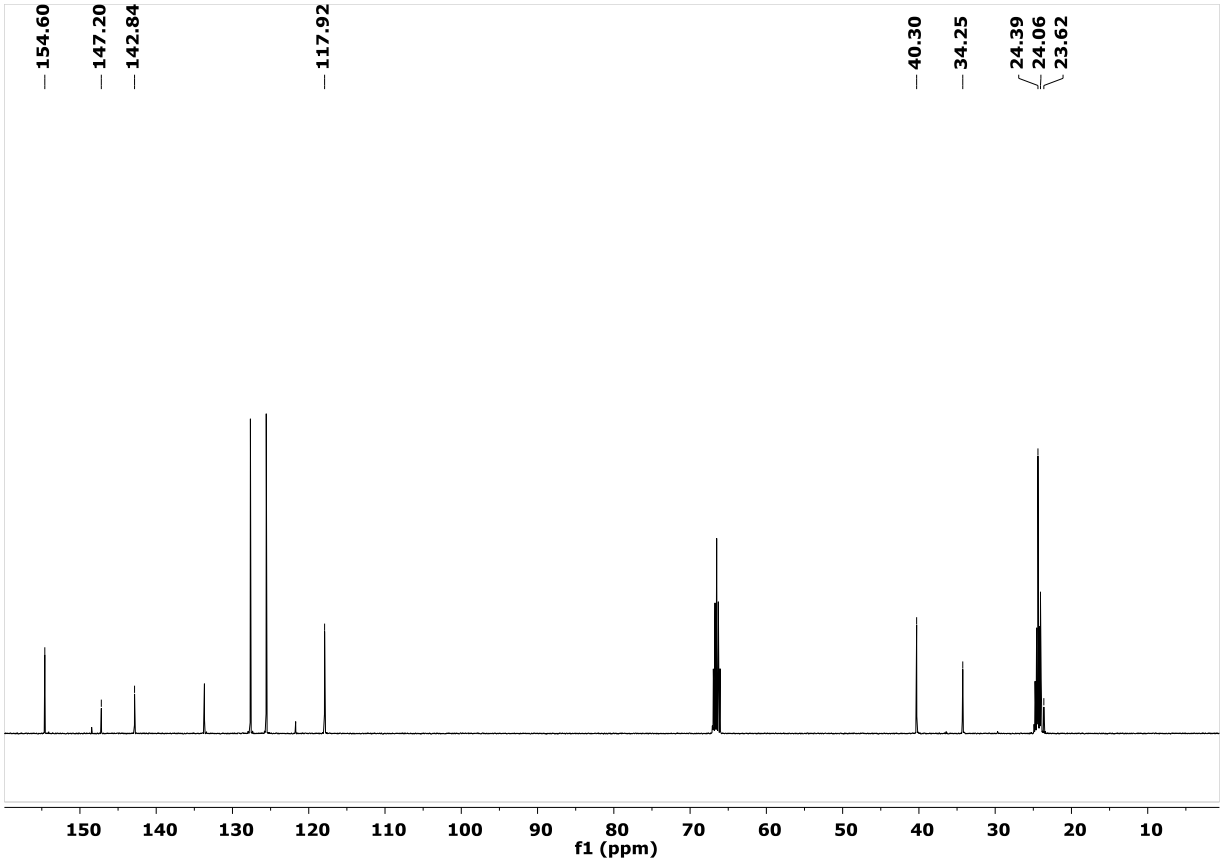

Figure S73. ^{13}C NMR spectra of complex **14** (298 K, 400 MHz, THF-D_8).

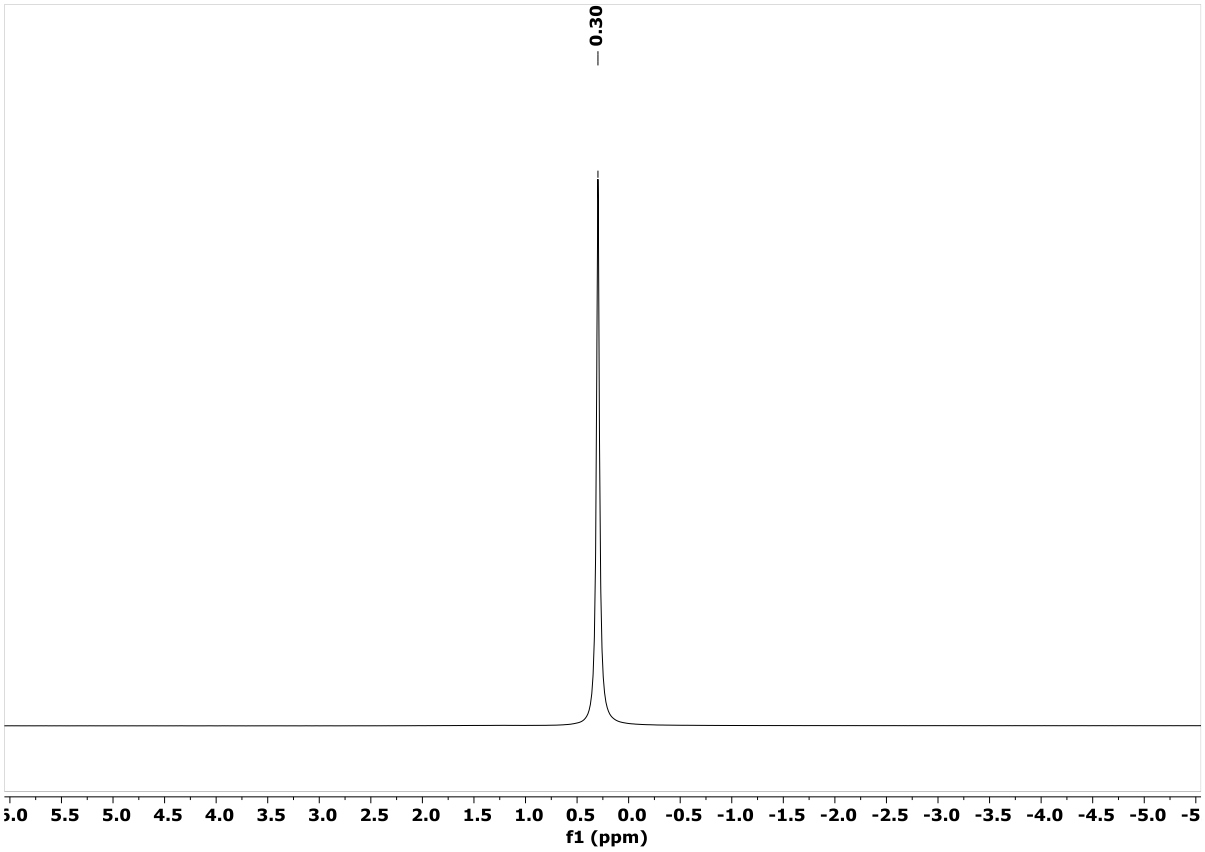

Figure S74. ^{7}Li NMR spectra of complex **14** (298 K, 400 MHz, THF-D_8).

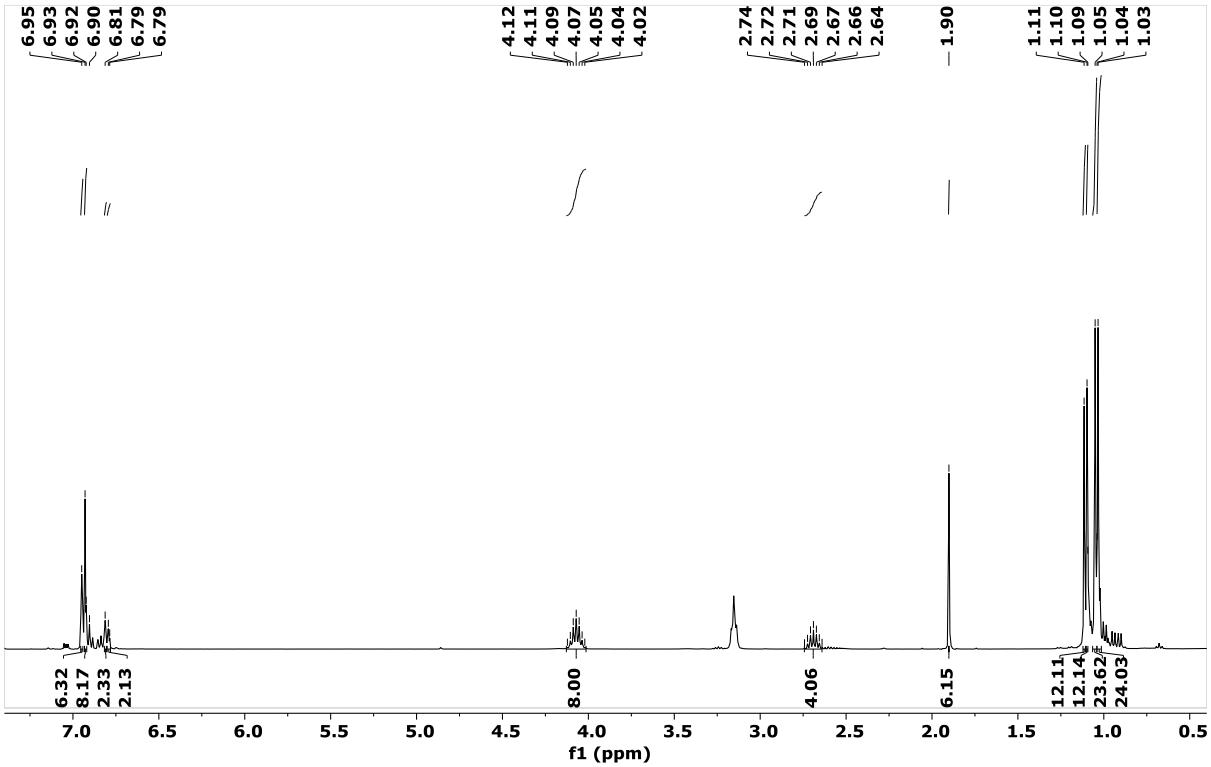

Figure S75: ^{1}H NMR spectrum of complex **15** (298 K, 400 MHz, THF-D_8).

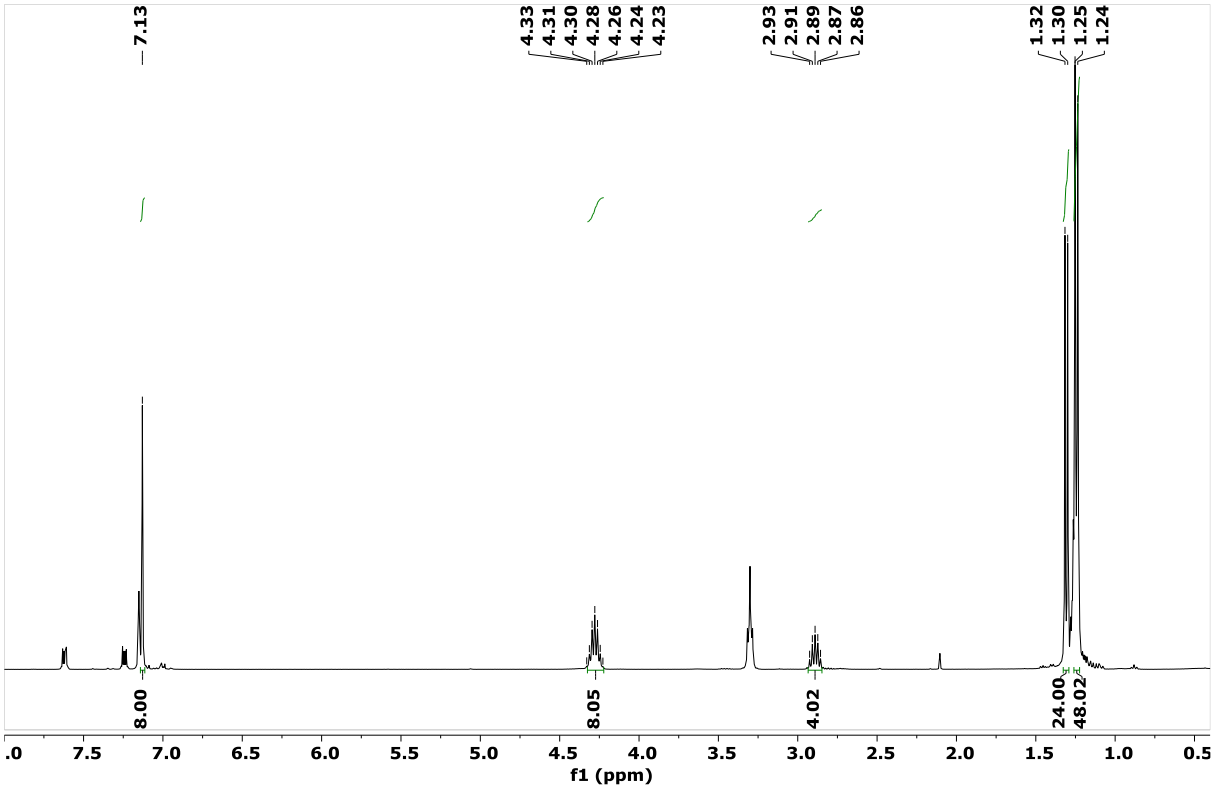

Figure S76: ^{1}H NMR spectrum of pure crystals of complex **15** after 7-10 days of synthesis (298 K, 400 MHz, THF-D_8). This shows the removal of coordinated toluene molecule along with the change in color from dark-red to dark-yellow.

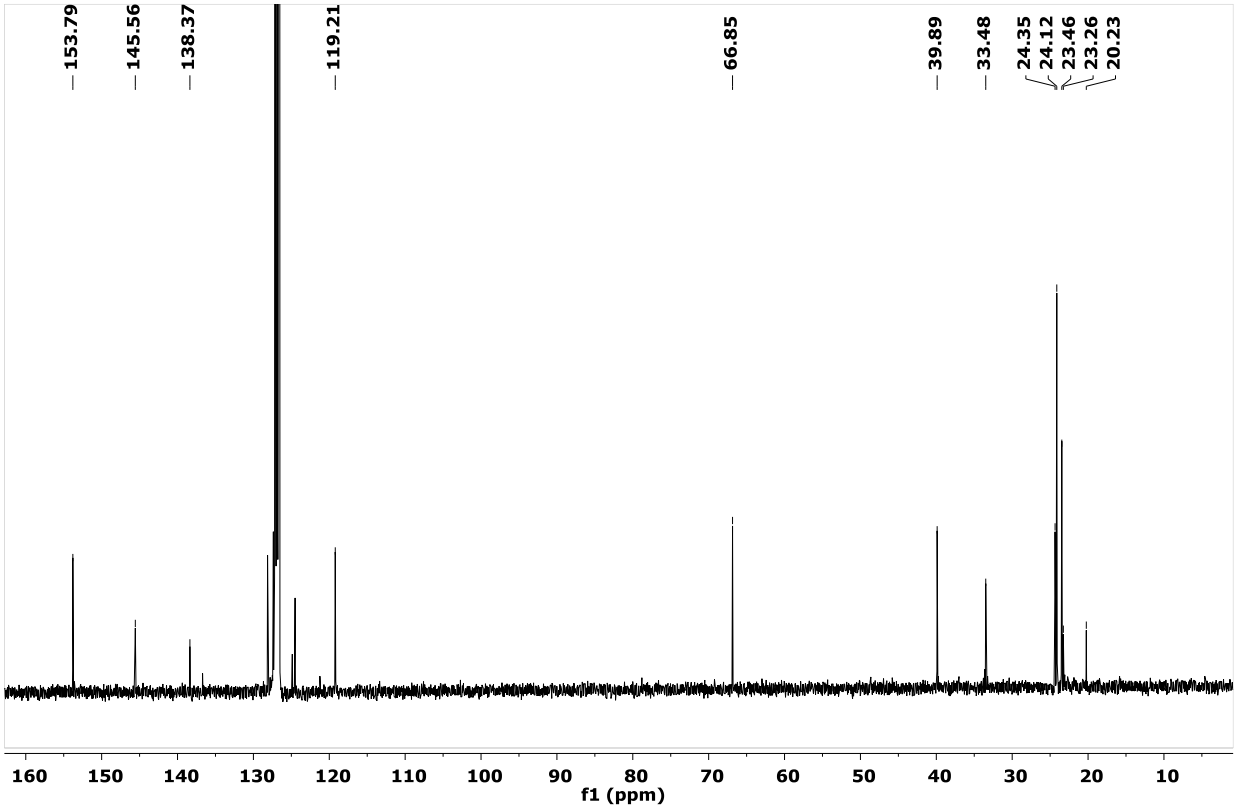

Figure S77: ^{13}C NMR spectrum of complex **15** (298 K, 400 MHz, THF-D_8).

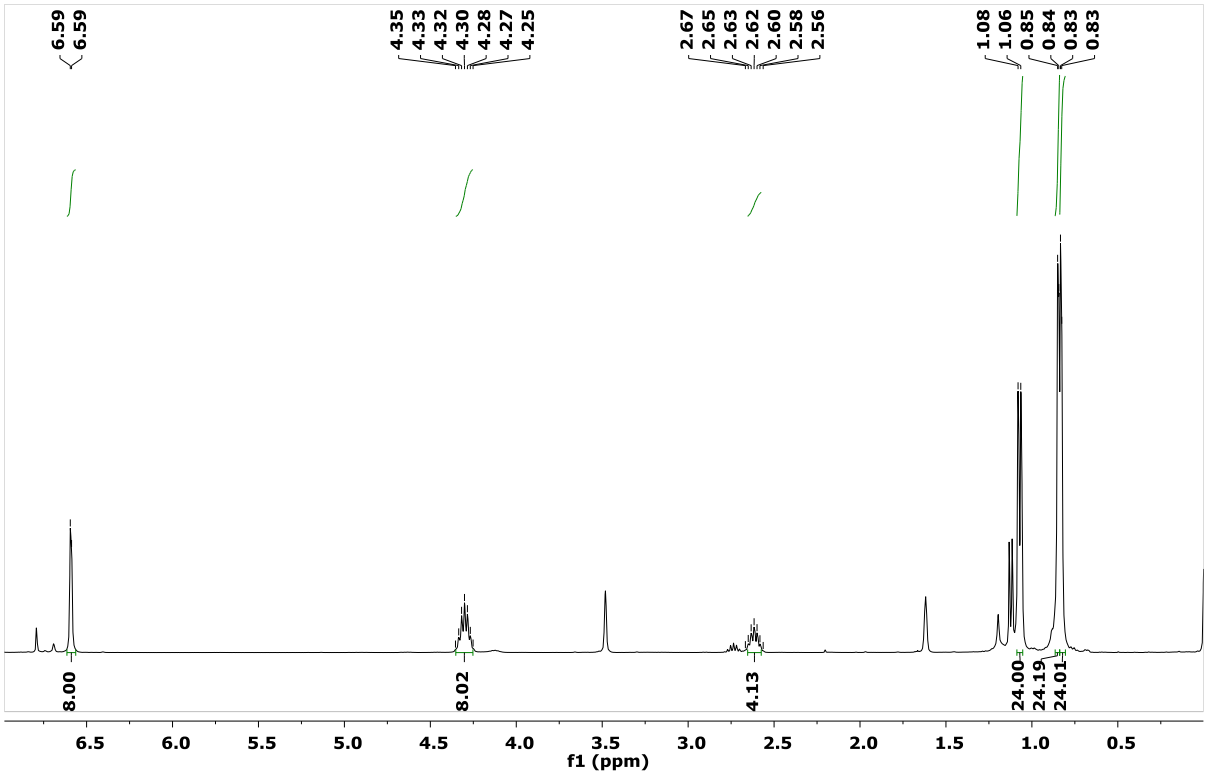

Figure S78: ^{1}H NMR spectrum of **16** (298 K, 400 MHz, THF-D_8).

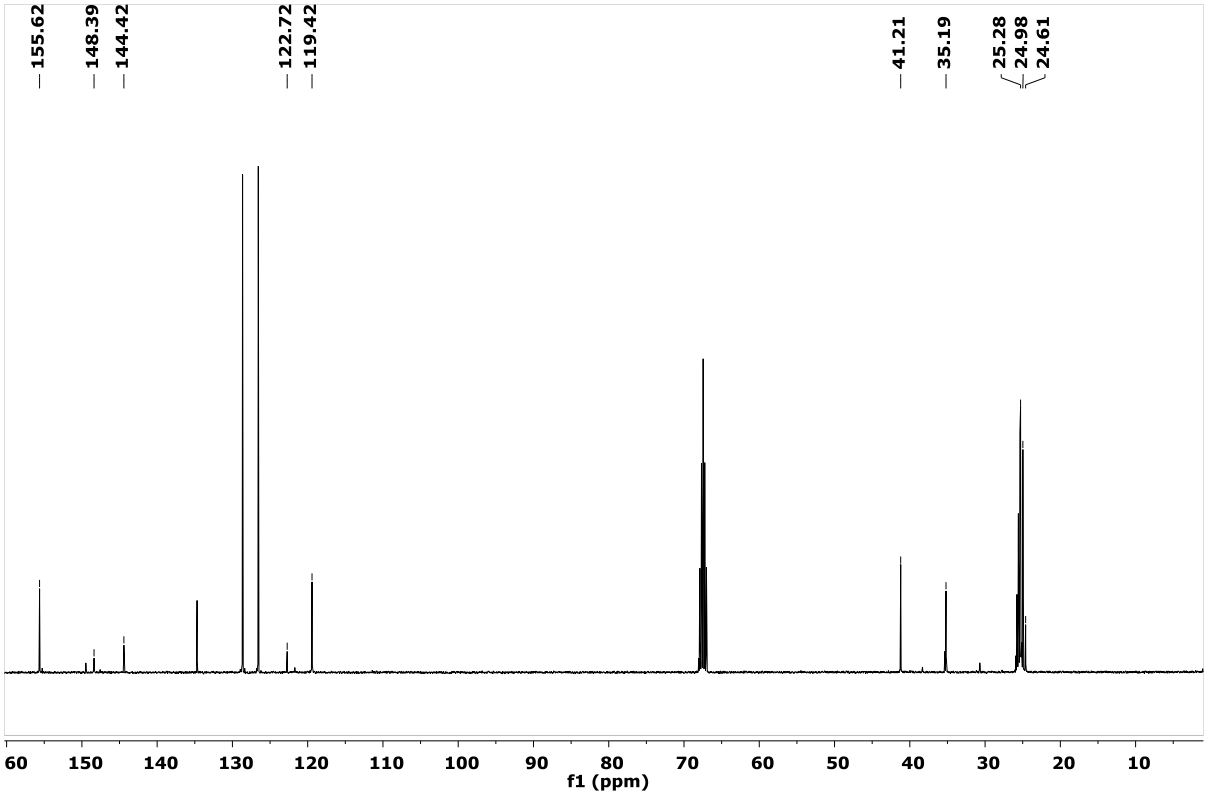

Figure S79: ^{13}C NMR spectrum of **16** (298 K, 400 MHz, THF-D_8).

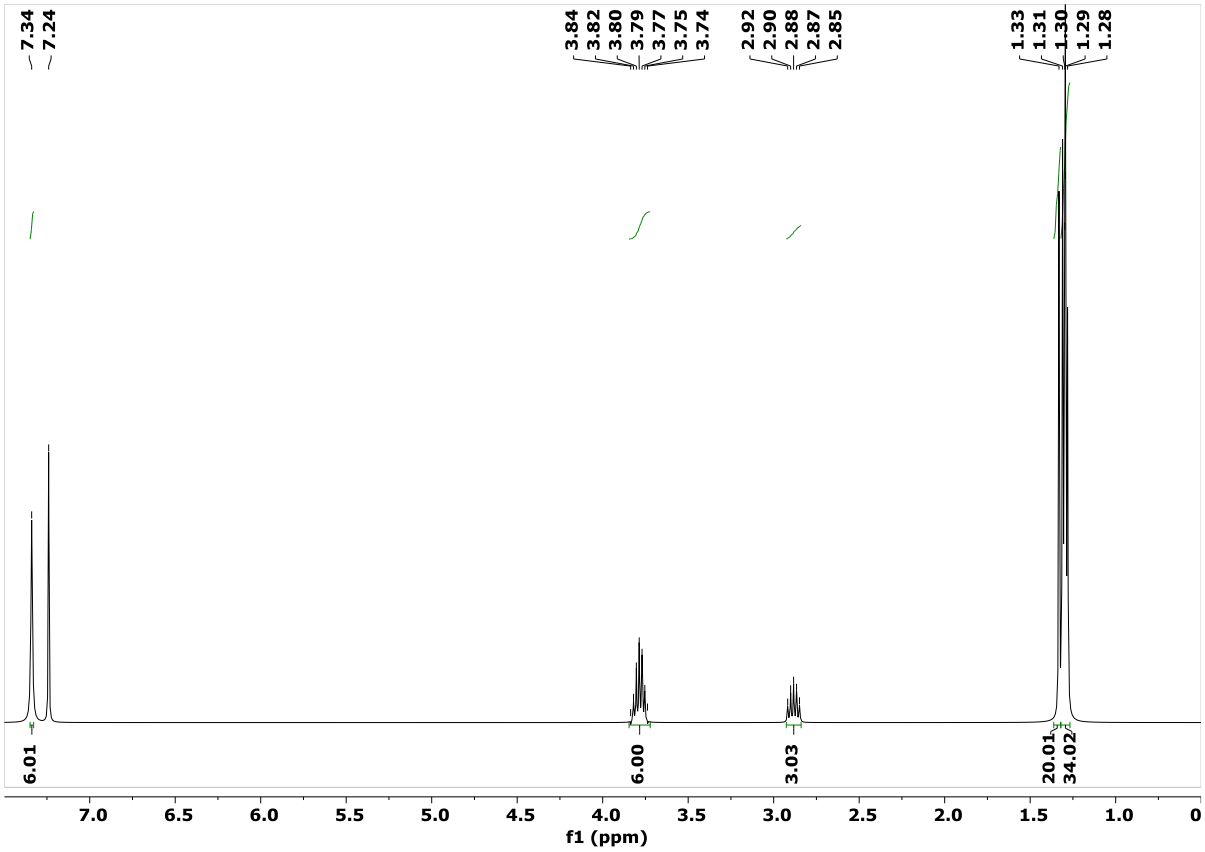

Figure S80: ^{1}H NMR spectrum of compound **17** (298 K, 400 MHz, C_6D_6).

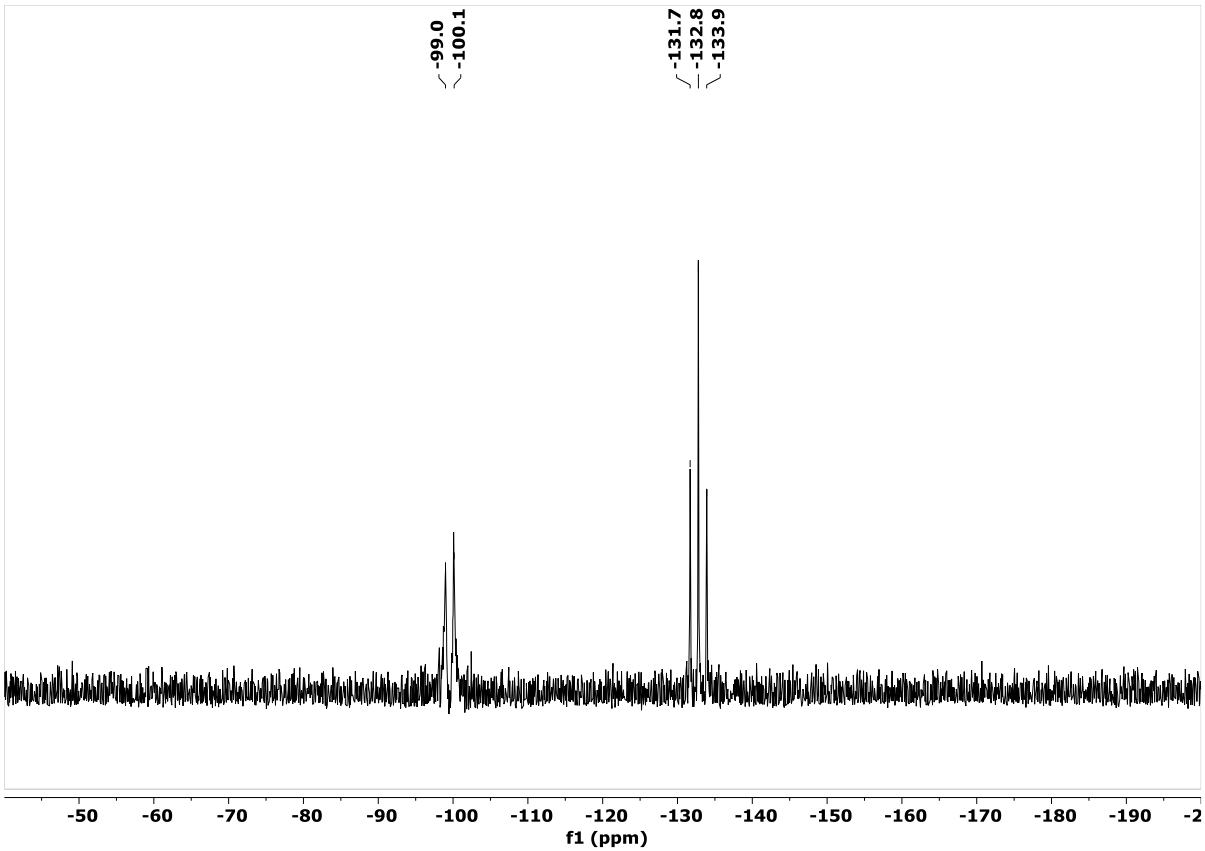

Figure S81: ^{31}P NMR spectrum of compound **17** (298 K, 400 MHz, C_6D_6).

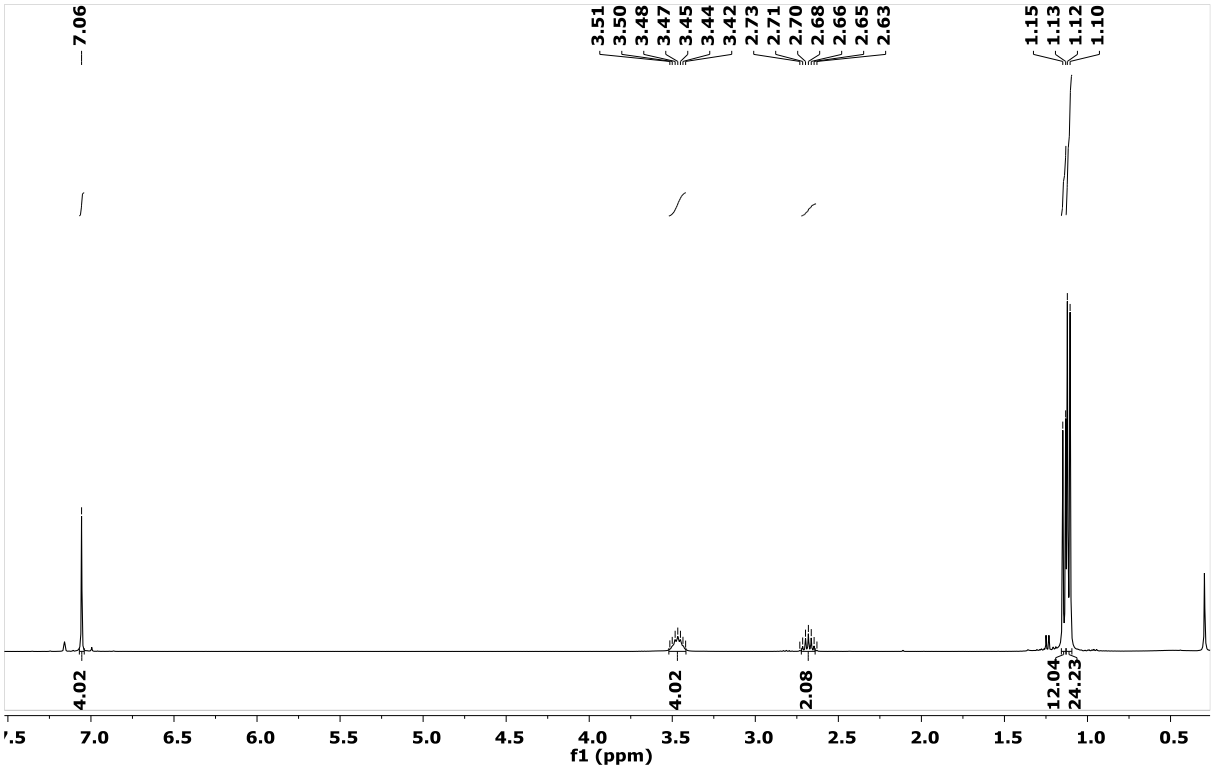

Figure S82: ^{1}H NMR spectrum of cation **19** (298 K, 400 MHz, C_6D_6).

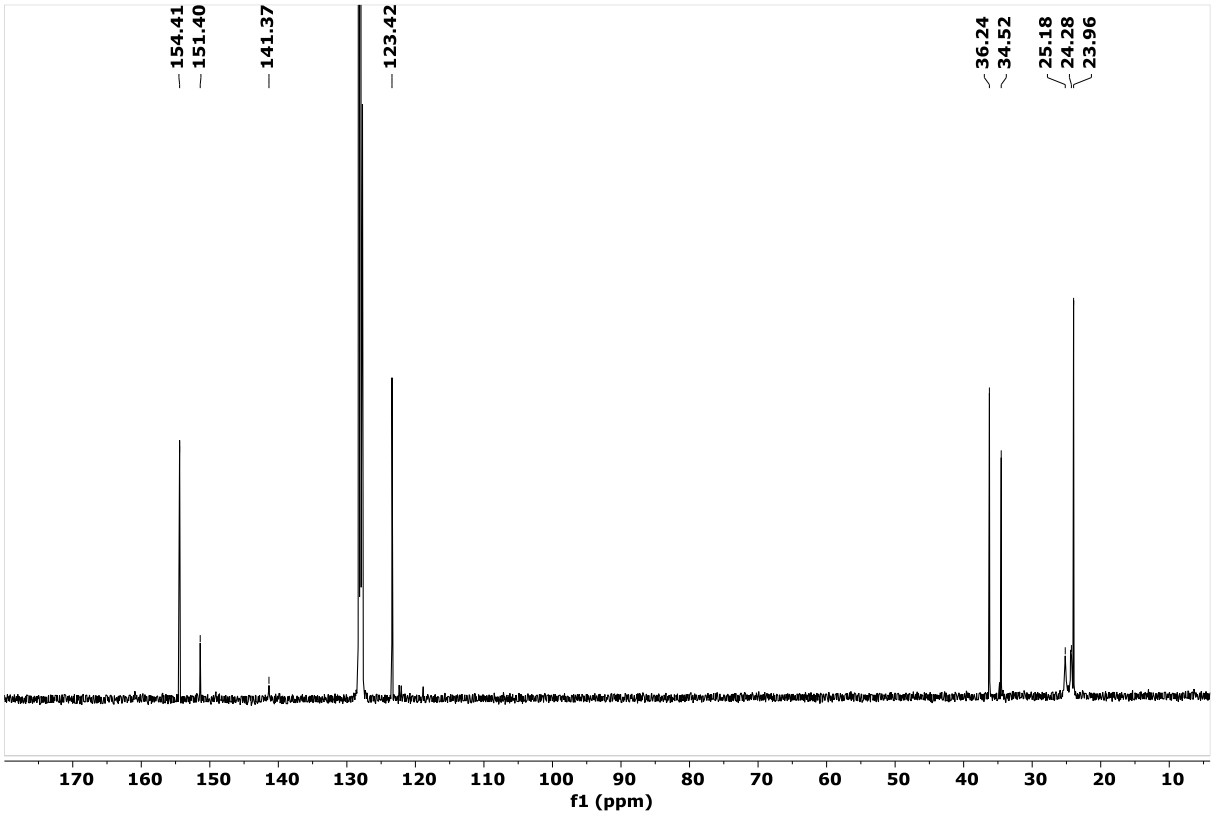

Figure S83: ^{13}C NMR spectrum of the cation **19** (298 K, 101 MHz, C_6D_6).

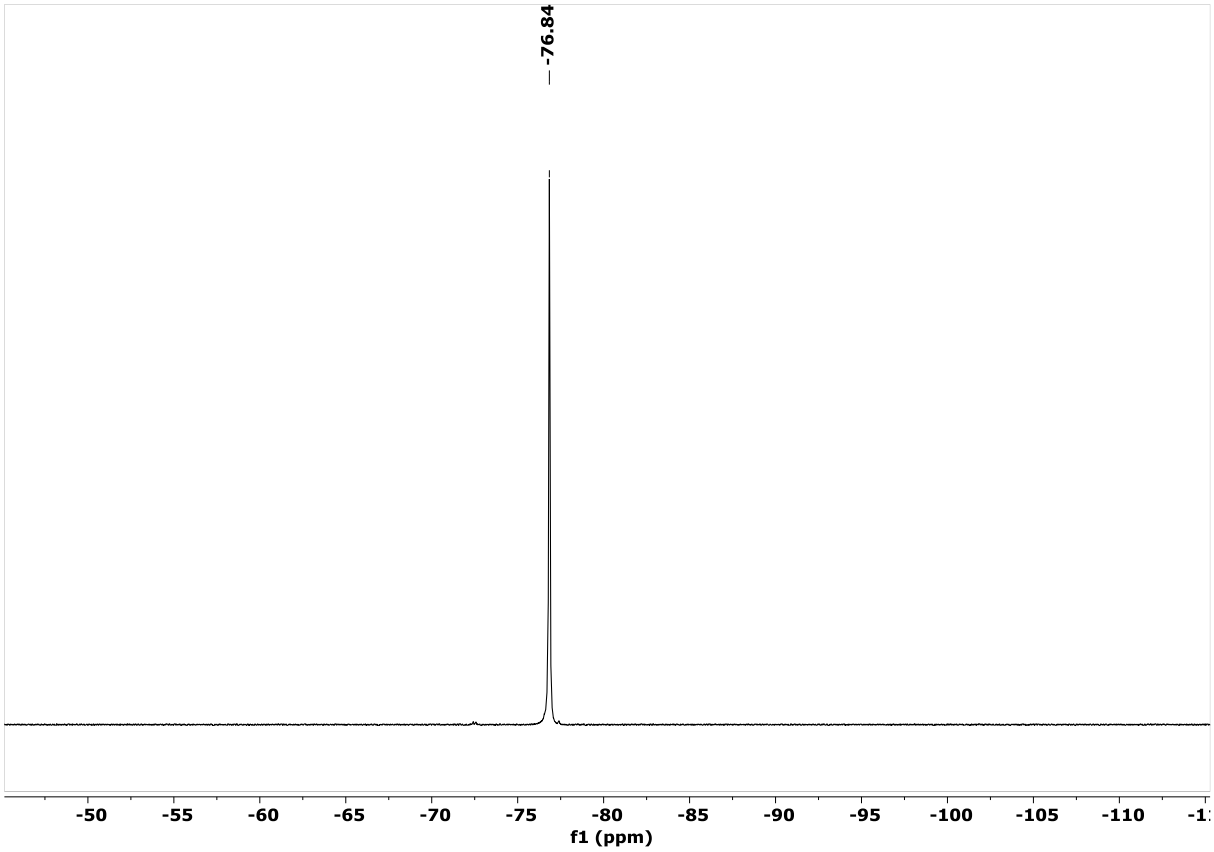

Figure S84: ^{19}F NMR spectrum of the cation **19** (298 K, 377 MHz, C_6D_6).

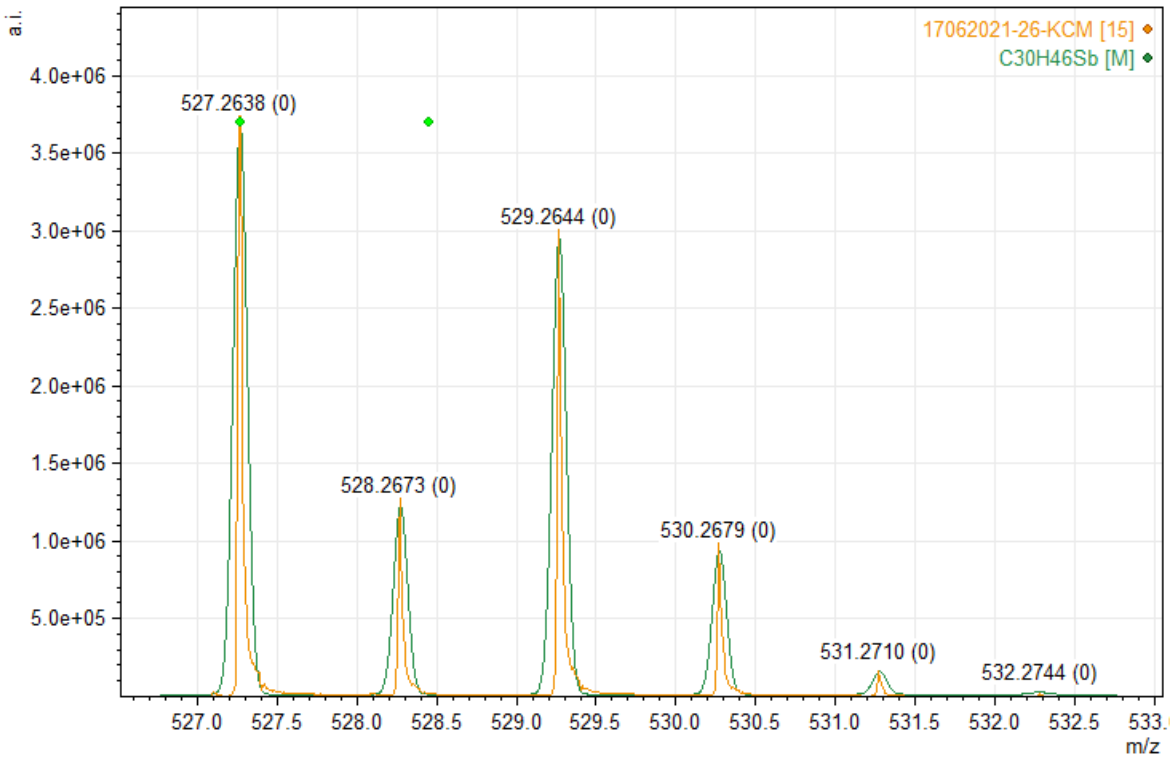

Figure S85: ESI-MS spectrum of $(\mathbf{Tip})_2\mathbf{Sb}^+$ cation. Orange: simulated, green: experimental spectra.

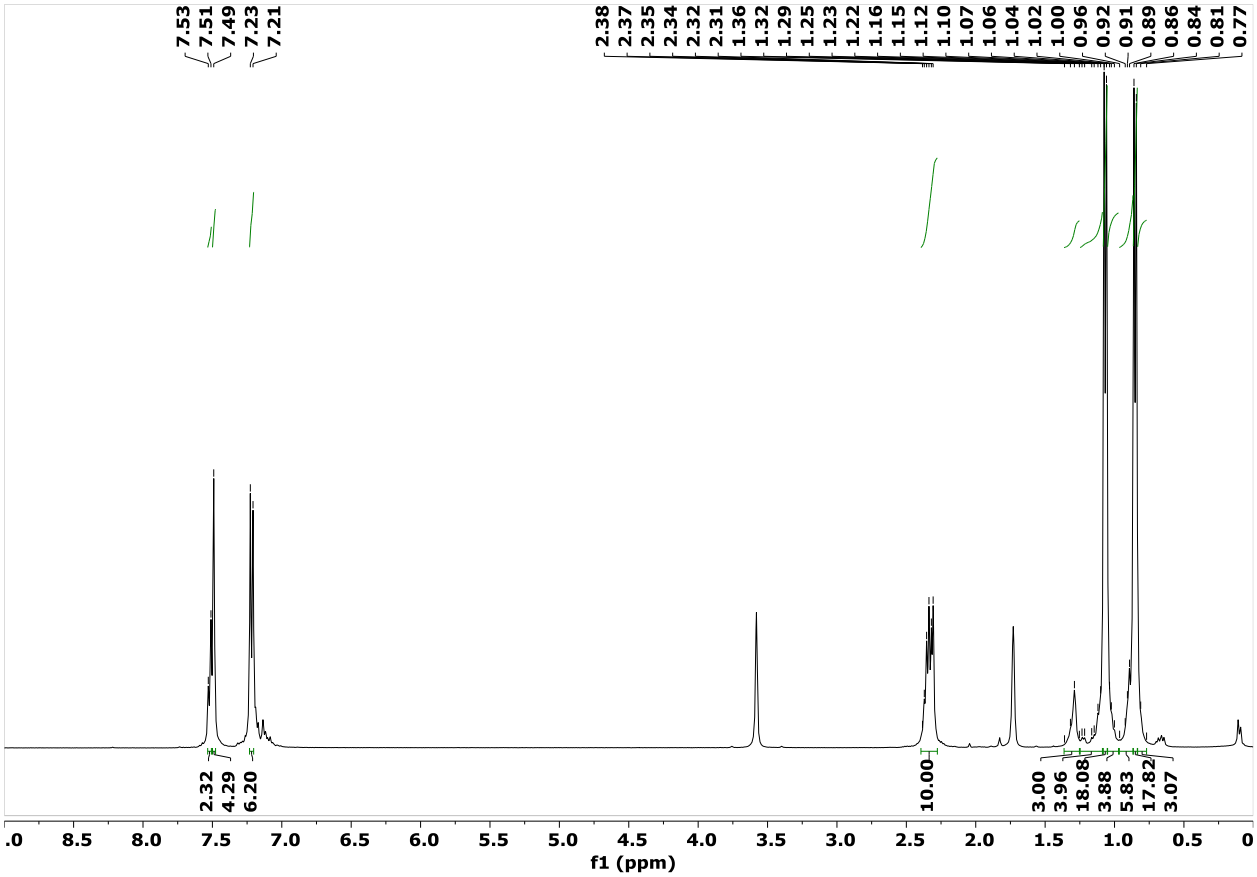

Figure S86: ^{1}H NMR spectrum of the adduct **20** (298 K, 400 MHz, THF-D_8).

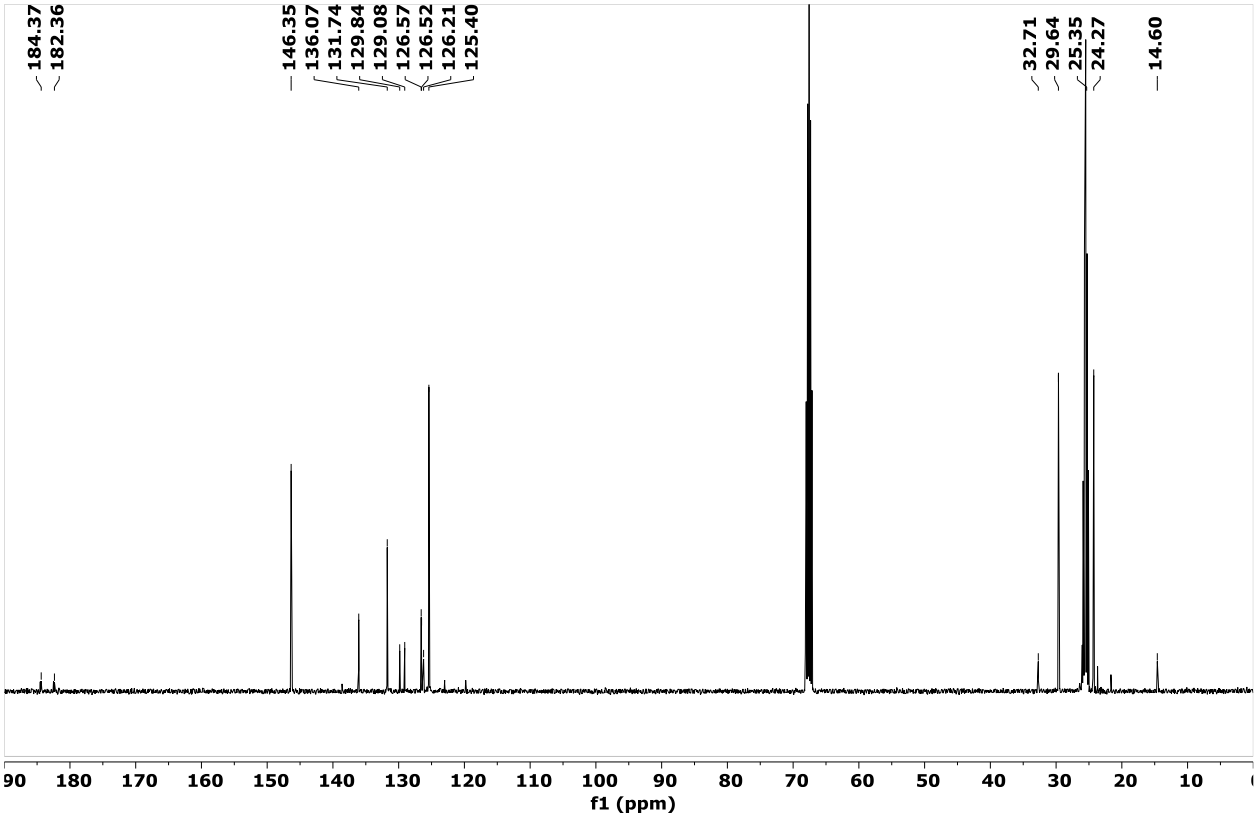

Figure S87: ^{13}C NMR spectrum of the adduct **20** (298 K, 101 MHz, THF-D_8).

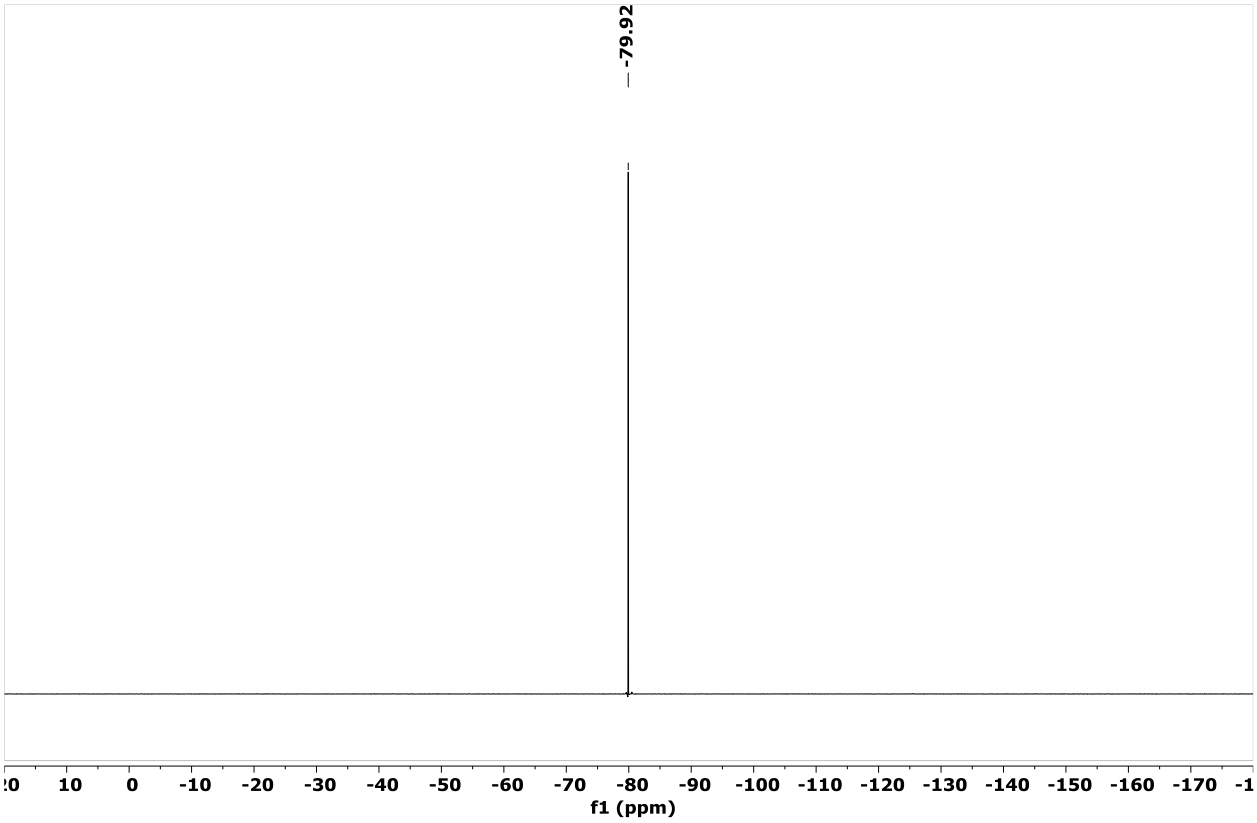

Figure S88: ^{19}F NMR spectrum of the adduct **20** (298 K, 377 MHz, THF-D_8).

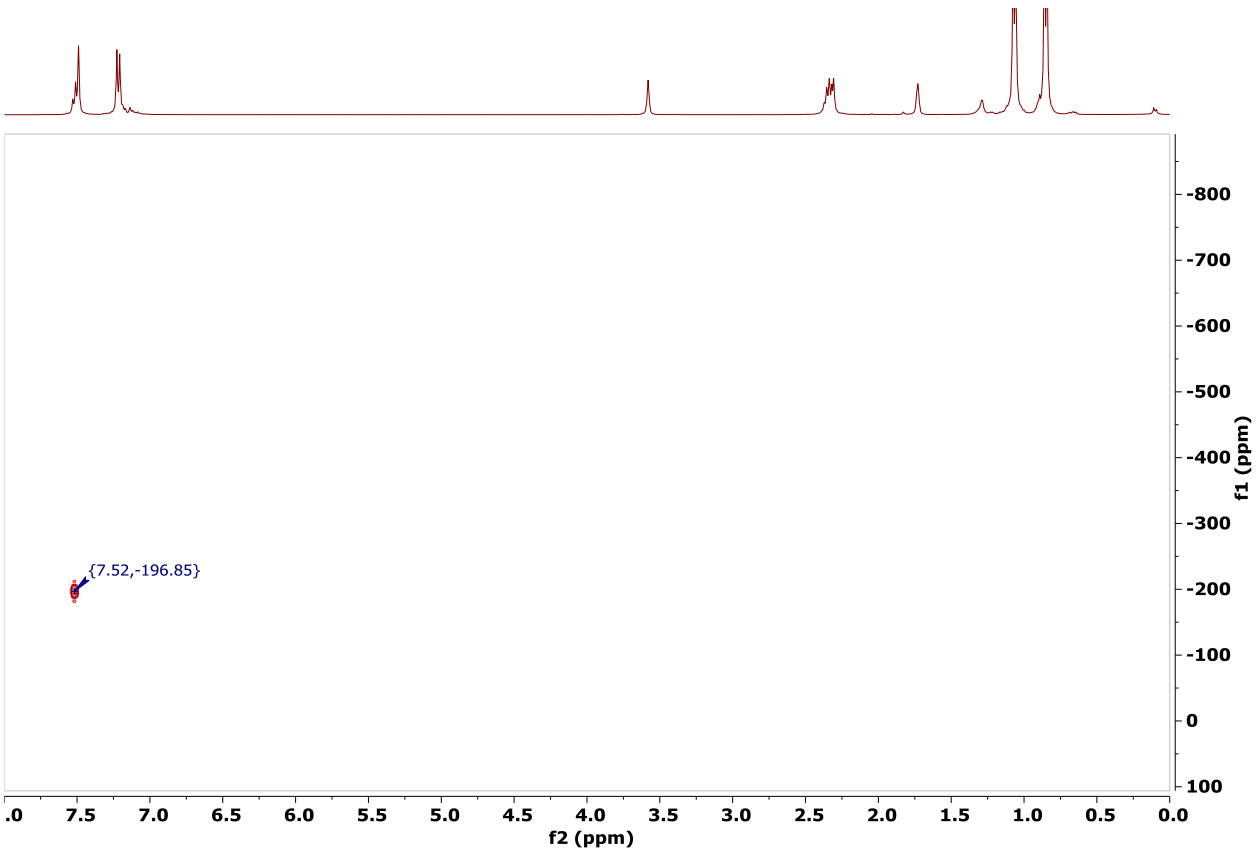

Figure S89: ^{1}H-^{15}N HMBC NMR spectrum of the adduct **20** (298 K, THF-D_8).

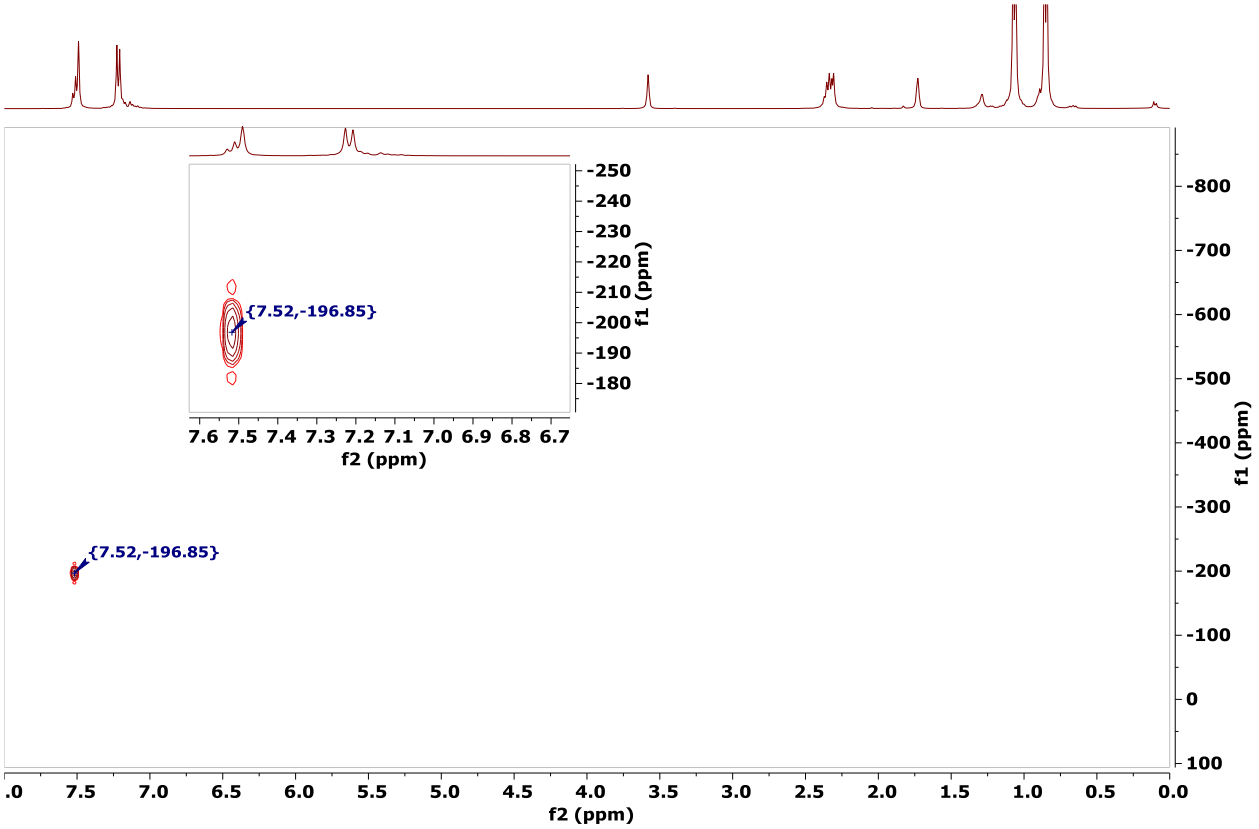

Figure S90: ^{1}H-^{15}N HMBC NMR spectrum of the adduct **20** (298 K, THF-D_8).

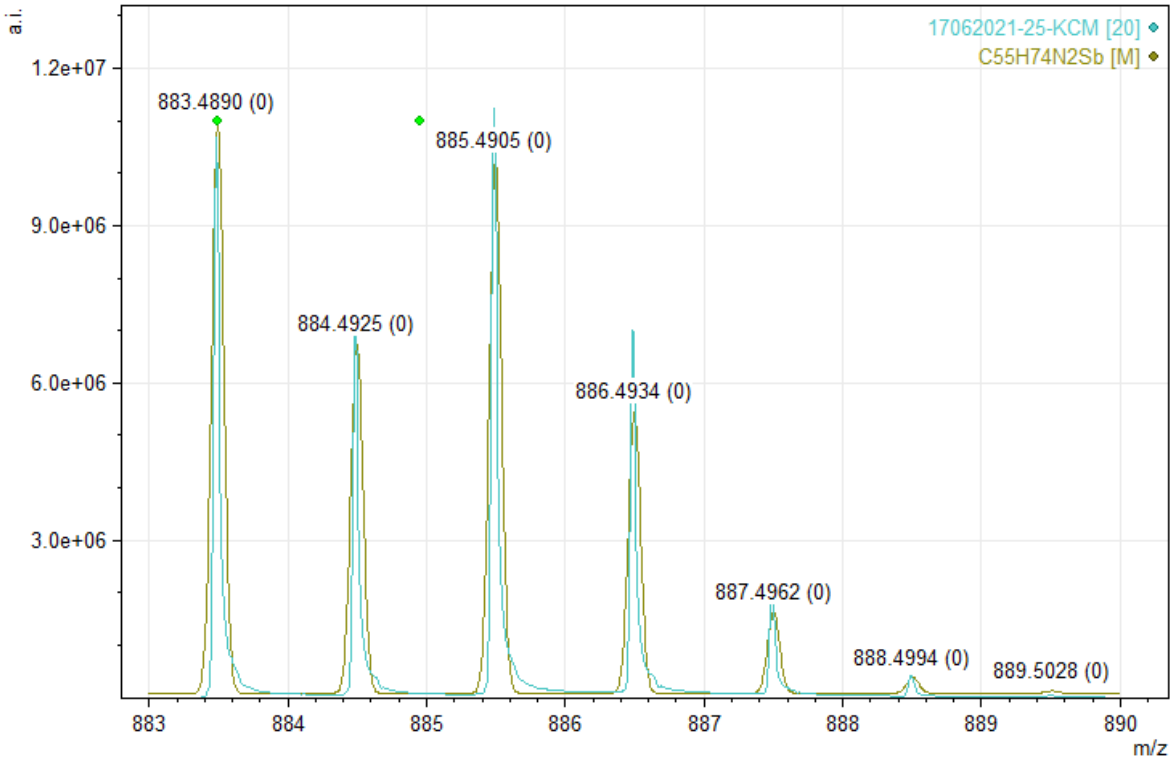

Figure S91: ESI-MS spectrum of the adduct **20**. Green: simulated, pista-green: experimental spectra.

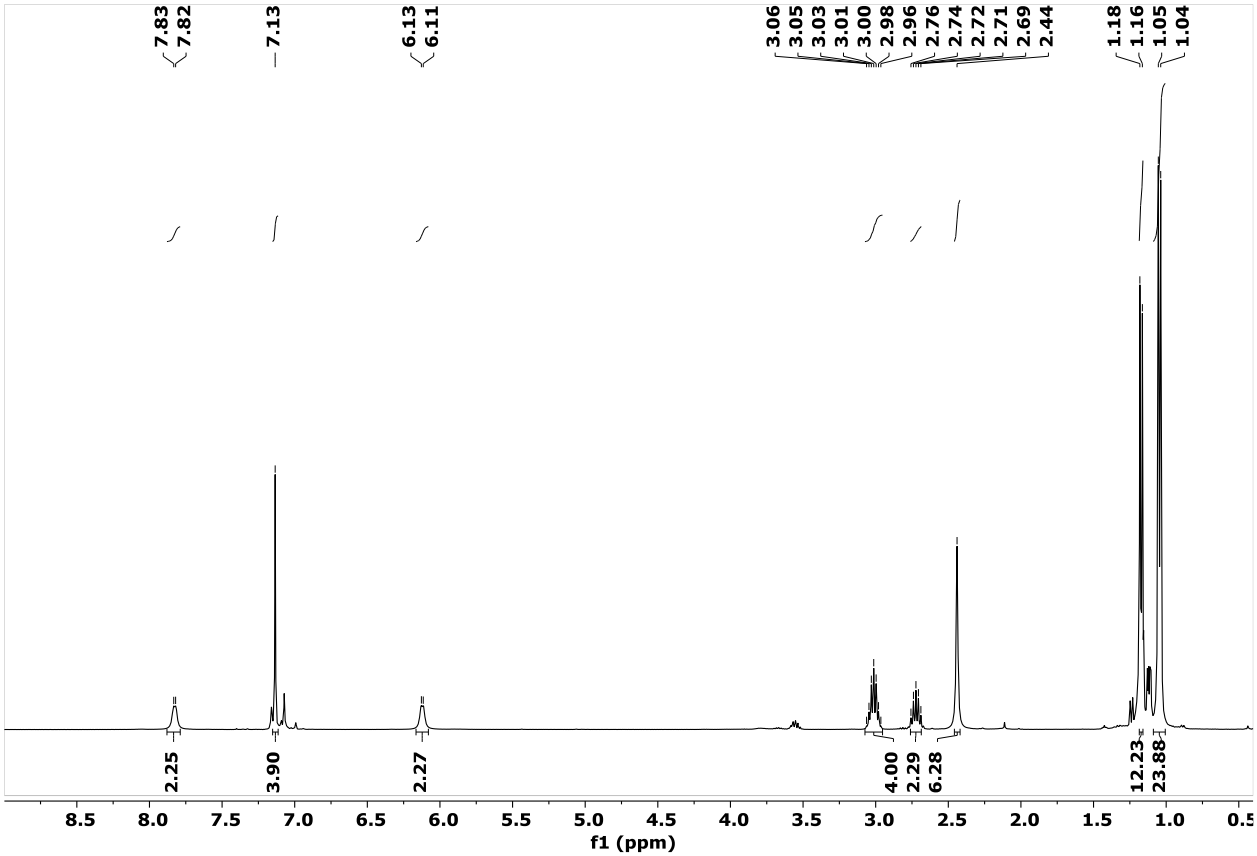

Figure S92: ^{1}H NMR spectrum of the adduct **21** (298 K, 400 MHz, C_6D_6).

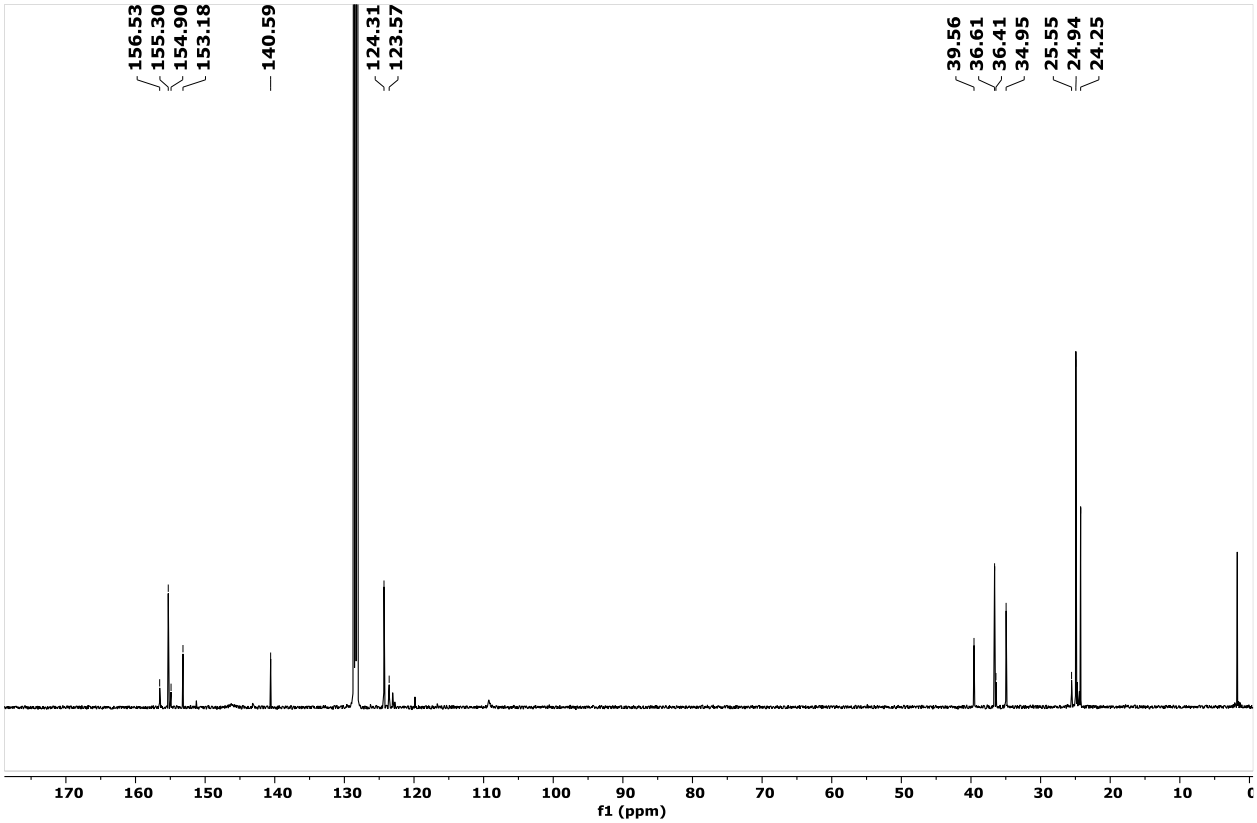

Figure S93: ^{13}C NMR spectrum of the adduct **21** (298 K, 101 MHz, C_6D_6).

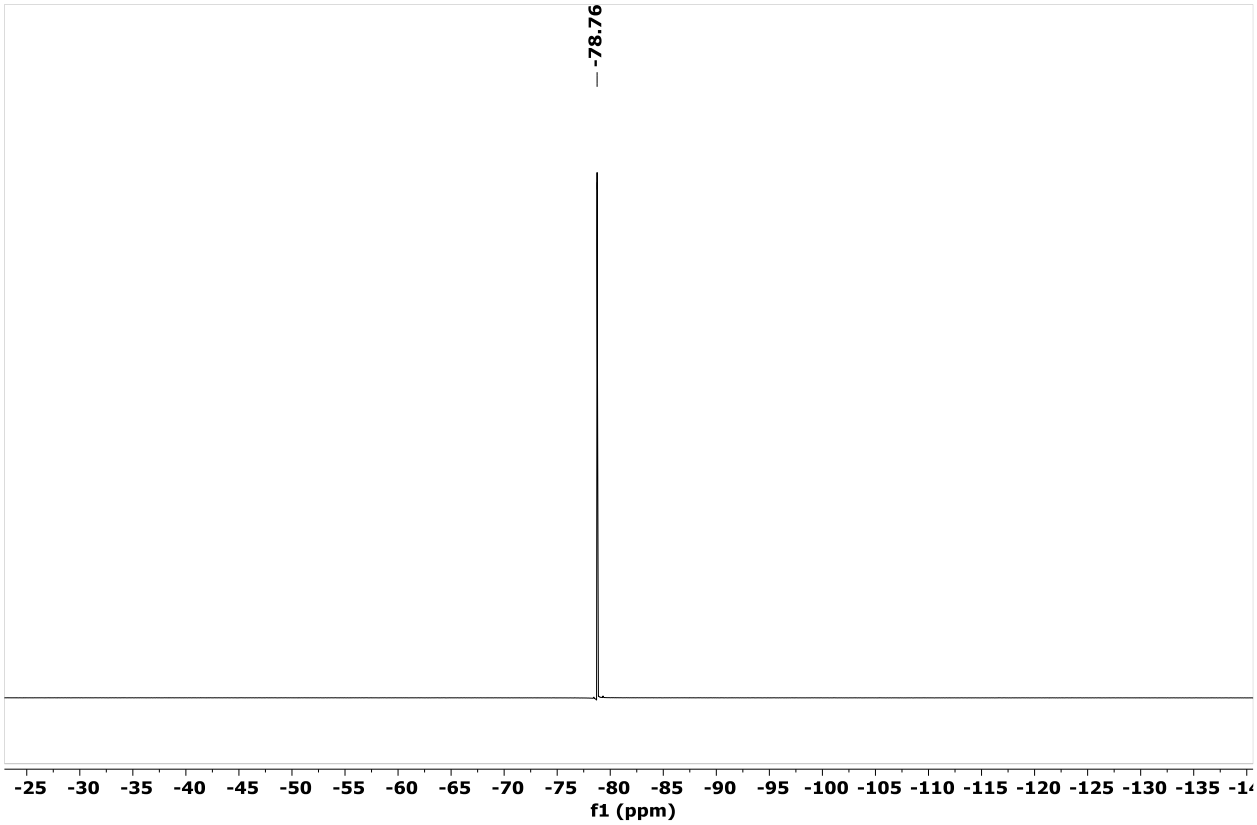

Figure S94: ^{19}F NMR spectrum of the adduct **21** (298 K, 377 MHz, C_6D_6).

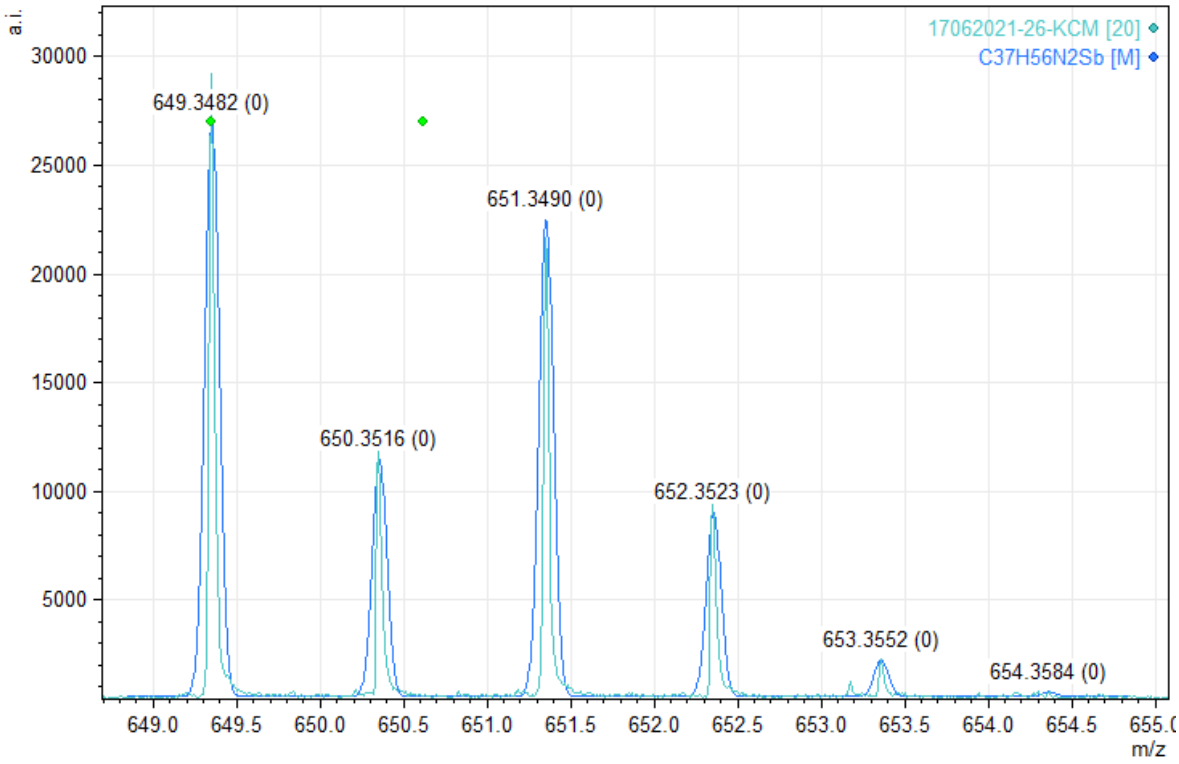

Figure S95: ESI-MS spectrum of the adduct **21**. Green: simulated, blue: experimental spectra.

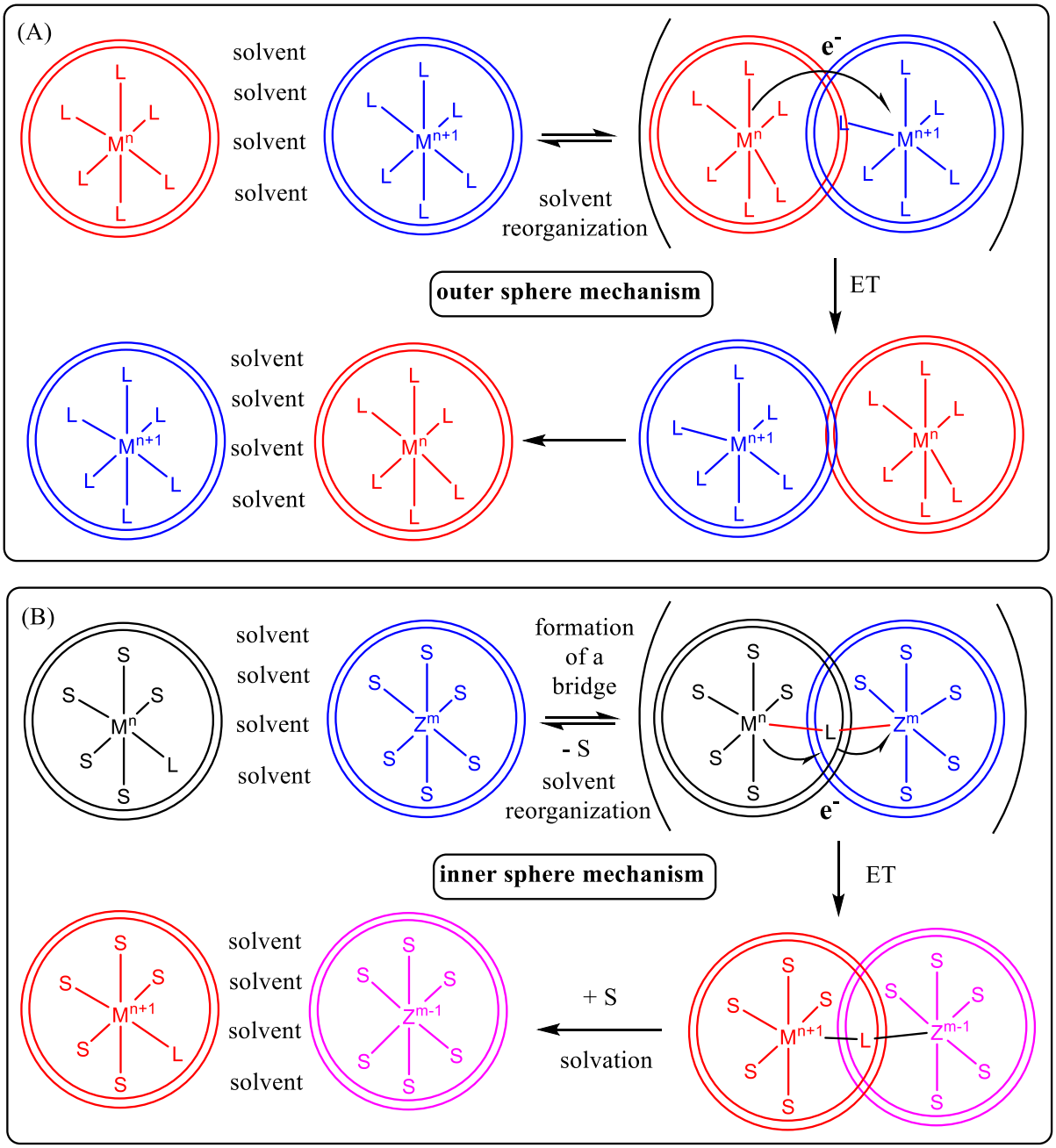

Figure S96: Illustrations of (A) outer sphere and (B) inner sphere ET processes in solution.

S11. References:

1. S. Sasaki, K. Ogawa, M. Watanabe, M. Yoshifuji, *Organometallics* **2010**, *29*, 757.

2. S. Roy, K. C. Mondal, S. Kundu, B. Li, C. J. Schürmann, S. Dutta, D. Koley, R. Herbst-Irmer, D. Stalke, H. W. Roesky, *Chem. Eur. J.* **2017**, *23*, 12153.

3. O. Back, B. Donnadieu, P. Parameswaran, G. Frenking, Guy Bertrand, *Nat. Chem*. **2010**, *2*, 369.

4. Gaussian 09, Revision E.01, M. J. Frisch, G. W. Trucks, H. B. Schlegel, G. E. Scuseria, M. A. Robb, J. R. Cheeseman, G. Scalmani, V. Barone, B. Mennucci, G. A. Petersson, G. H. Nakatsuji, M. Caricato, X. Li, H. P. Hratchian, A. F. Izmaylov, J. Bloino, G. Zheng, J. L. Sonnenberg, M. Hada, M. Ehara, K. Toyota, R. Fukuda, J. Hasegawa, M. Ishida, T. Nakajima, Y. Honda, O. Kitao, H. Nakai, T. Vreven, Jr. J. A. Montgomery, J. E. Peralta, F. Ogliaro, M. Bearpark, J. J. Heyd, E. Brothers, K. N. Kudin, V. N. Staroverov, R. Kobayashi, J. Normand, K. Raghavachari, A. Rendell, J. C. Burant, S. S. Iyengar, J. Tomasi, M. Cossi, N. Rega, J. M. Millam, M. Klene, J. E. Knox, J. B. Cross, V. Bakken, C. Adamo, J. Jaramillo, R. Gomperts, R. E. Stratmann, O. Yazyev, A. J. Austin, R. Cammi, C. Pomelli, J. W. Ochterski, R. L. Martin, K. Morokuma, V. G. Zakrzewski, G. A. Voth, P. Salvador, J. J. Dannenberg, S. Dapprich, A. D. Daniels, Ö. Farkas, J. B. Foresman, J. V. Ortiz, J. Cioslowski, D. J. Fox, Gaussian, Inc., Wallingford CT, **2010**.

5. Y. Zhao, N. E. Schultz, D. G. Truhlar, *J. Chem. Theory and Comput*. **2006**, *2*, 364.

6. R. Krishnan, J. S. Binkley, R. Seeger, J. A. Pople, *J. Chem. Phys.* **1980**, *72*, 650-654.

7. (a) D. Andrae, U. Häussermann, M. Dolg, H. Stoll, H. Preuss, *Theor. Chim. Acta* **1990**, *77*, 123; (b) B. Metz, H. Stoll, M. Dolg, *J. Chem. Phys*. **2000**, 113, 2563; (c) EMSL Basis Set Exchange Software: 1) B. P. Pritchard, D. Altarawy, B. Didier, T. D. Gibson, T. L. Windus. *J. Chem. Inf. Model.* **2019**, *59*(11), 4814-4820; 2) D. Feller, *J. Comp. Chem.* **1996**, *17*(13), 1571-1586; 3) K. L. Schuchardt, B. T. Didier, T. Elsethagen, L. Sun, V. Gurumoorthi, J. Chase, J. Li, T. L. Windus, *J. Chem. Inf. Model.* **2007**, *47(3)*, 1045-1052.

8. a) E. D. Glendening, A. E. Reed, J. E. Carpenter, F. Weinhold, *NBO Version 3.1*; b) A. E. Reed, L. A. Curtiss, F. Weinhold *Chem. Rev.* **1998**, *88*, 899.

9. T. Ziegler, A. Rauk. *Theor. Chim. Acta,* **1977**, *46*, 1.

10. (a) M. Mitoraj, A. Michalak. *Organometallics* **2007**, *26*, 6576; (b) M. Mitoraj, A. Michalak. *J. Mol. Model.* **2008**, *14*, 681.

11. (a) *ADF2017*, SCM, Theoretical Chemistry, Vrije Universiteit, Amsterdam, The Netherlands, http://www.scm.com; (b) G. te Velde, F. M. Bickelhaupt, E. J. Baerends, C. F. Guerra, S. J. A. van Gisbergen, J. G. Snijders, T. Ziegler. *J. Comput. Chem.* **2001**, *22*, 931.

12. (a) E. van Lenthe, E. J. Baerends. *J. Comput. Chem*. **2003**, *24*, 1142; (b) E. van Lenthe, E. J. Baerends, J. G. Snijders. *J. Chem. Phys*. **1993**, *99*, 4597; (c) E. van Lenthe, E. J. Baerends, J. G. Snijders. *J. Chem. Phys*. **1994**, *101*, 9783.

13. (a) G. Frenking, F. M. Bickelhaupt. *The Chemical Bond 1. Fundamental Aspects of Chemical Bonding*, chap. The EDA Perspective of Chemical Bonding, 121. Wiley-VCH: Weinheim, **2014**; (b) L. M. Zhao, von Hopffgarten, D. M. Andrada, G. Frenking. *WIREs Comput. Mol. Sci.* **2018**, *8*, 1345; (c) L. Zhao, M. Hermann, W. H. E. Schwarz, G. Frenking. *Nat. Rev. Chem.* **2019**, *3*, 48; (d) L. Zhao, S. Pan, N. Holzmann, P. Schwerdtfeger, G. Frenking.

Chem. Rev. **2019**, *119*, 8781; (e) J. Andrés, P. W. Ayers, R. A. Boto, R. Carbó-Dorca, H. Chermette, J. Cioslowski, J. Contreras-García, D. L. Cooper, G. Frenking, C. Gatti, F. Heidar-Zadeh, L. Joubert, Á. Martín Pendás, E. Matito, I. Mayer, A. J. Misquitta, Y. Mo, J. Pilmé, P. L. A. Popelier, M. Rahm, E. Ramos-Cordoba, P. Salvador, W. H. E. Schwarz, S. Shahbazian, B. Silvi, M. Solà, K. Szalewicz, V. Tognetti, F. Weinhold, É. L. Zins, *J. Comput. Chem*. **2019**, *40*, 2248; (f) P. Politzer, J. S. Murray, T. Clark, *J. Mol. Model.* **2015**, *21*, 52; (g) W. Yang, K. E. Krantz, L. A. Freeman, D. Dickie, A. Molino, G. Frenking, S. Pan, D. J. D. Wilson, R. J. Gilliard, Jr., *Angew. Chem. Int. Ed.* **2020**, *59*, 3850-3854; (h) G. Deng, S. Pan, G. Wang, L. Zhao, M. Zhou, G. Frenking, *Angew. Chem. Int. Ed*. **2020**, *59*, 10603; (i) S. Pan, G. Frenking, *Angew. Chem. Int. Ed*. **2020**, *59*, 8756; (j) L. Zhao, S. Pan, M. Zhou, G. Frenking. *Science*, **2019**, *365*, eaay5021; (k) R. Saha, S. Pan, P. K. Chattaraj, G. Merino, *Dalton Trans*. **2020**, *49*, 1056.

14. a) J. Andrés et al., *J. Compt. Chem*. **2019**, *40*, 2248; b) P. Politzer, J. S. Murray, T. Clark, *J. Mol. Model*. **2015**, *21*, 52.

15. W. Su, S. Pan, X. Sun, S. Wang, L. Zhao, G. Frenking, C. Zhu, *Nat. Commun*. **2018**, *9*, 1.

16. C. F. Matta, R. J. Boyd, *The Quantum Theory of Atoms in Molecules: From Solid State to DNA and Drug Design* (Eds.:), *Chapter 1*. *An Introduction to the Quantum Theory of Atoms in Molecules*, Wiley, Hoboken, **2007**, 1-34.

17. Bruker AXS Inc., in *Bruker Apex CCD, SAINT v8.40B* (Ed.: Bruker AXS Inst. Inc.), WI, USA, Madison, 2013.

18. Bruker AXS Inc., in *Bruker Apex CCD, SAINT v8.40B* (Ed.: Bruker AXS Inst. Inc.), WI, USA, Madison, 2013.

19. L. Krause, R. Herbst-Irmer, G. M. Sheldrick, D. Stalke, *J. Appl. Crystallogr*. **2015**, *48*, 3-10.

20. G. M. Sheldrick, *Acta Crystallogr.* **2015**, *A71*, 3-8.

21. G. M. Sheldrick, *Acta Crystallogr.* **2015**, *C71*, 3-8.

22. C. B. Hübschle, G. M. Sheldrick, B. Dittrich, *J. Appl. Crystallogr.* **2011**, *44*, 1281-1284.